

12

TECHNICAL REPORT SL-85-4

EFFECTS OF SHEAR STIRRUP DETAILS ON ULTIMATE CAPACITY AND TENSILE MEMBRANE BEHAVIOR OF REINFORCED CONCRETE SLABS

by

Stanley C. Woodson

Structures Laboratory

DEPARTMENT OF THE ARMY
Waterways Experiment Station, Corps of Engineers
PO Box 631, Vicksburg, Mississippi 39180-0631



US Army Corps of Engineers

AD-A161 222



August 1985
Final Report

Approved for Public Release; Distribution Unlimited

DTIC FILE COPY

DTIC
ELECTE
NOV 18 1985
S E D

Federal Emergency Management Agency
Washington, DC 20472



Destroy this report when no longer needed. Do not return
it to the originator.

The findings in this report are not to be construed as an official
Department of the Army position unless so designated
by other authorized documents.

The contents of this report are not to be used for
advertising, publication, or promotional purposes.
Citation of trade names does not constitute an
official endorsement or approval of the use of
such commercial products.

TECHNICAL REPORT SL-85-4

EFFECTS OF SHEAR STIRRUP DETAILS ON ULTIMATE CAPACITY AND TENSILE MEMBRANE BEHAVIOR OF REINFORCED CONCRETE SLABS

by

Stanley C. Woodson

Structures Laboratory

DEPARTMENT OF THE ARMY
Waterways Experiment Station, Corps of Engineers
PO Box 631, Vicksburg, Mississippi 39180-0631



August 1985
Final Report

Approved For Public Release; Distribution Unlimited

This report has been reviewed in the Federal Emergency Management Agency and approved for publication. Approval does not signify that the contents necessarily reflect the views and policies of the Federal Emergency Management Agency.

Prepared for
Federal Emergency Management Agency
Washington, DC 20472

Unclassified

SECURITY CLASSIFICATION OF THIS PAGE (When Data Entered)

REPORT DOCUMENTATION PAGE		READ INSTRUCTIONS BEFORE COMPLETING FORM
1. REPORT NUMBER Technical Report SL-85-4	2. GOVT ACCESSION NO. AD-A161	3. RECIPIENT'S CATALOG NUMBER 222
4. TITLE (and Subtitle) EFFECTS OF SHEAR STIRRUP DETAILS ON ULTIMATE CAPACITY AND TENSILE MEMBRANE BEHAVIOR OF REINFORCED CONCRETE SLABS	5. TYPE OF REPORT & PERIOD COVERED Final report	
	6. PERFORMING ORG. REPORT NUMBER	
7. AUTHOR(s) Stanley C. Woodson	8. CONTRACT OR GRANT NUMBER(s)	
9. PERFORMING ORGANIZATION NAME AND ADDRESS US Army Engineer Waterways Experiment Station Structures Laboratory PO Box 631, Vicksburg, Mississippi 39180-0631	10. PROGRAM ELEMENT, PROJECT, TASK AREA & WORK UNIT NUMBERS	
11. CONTROLLING OFFICE NAME AND ADDRESS Federal Emergency Management Agency Washington, DC 20472	12. REPORT DATE August 1985	
	13. NUMBER OF PAGES 177	
14. MONITORING AGENCY NAME & ADDRESS (if different from Controlling Office)	15. SECURITY CLASS. (of this report) Unclassified	
	15a. DECLASSIFICATION/DOWNGRADING SCHEDULE	
16. DISTRIBUTION STATEMENT (of this Report) Approved for public release; distribution unlimited.		
17. DISTRIBUTION STATEMENT (of the abstract entered in Block 20, if different from Report)		
18. SUPPLEMENTARY NOTES Available from National Technical Information Service, 5285 Port Royal Road, Springfield, Va. 22161. This report is essentially the same as a thesis which was submitted by the author to Mississippi State University in 1984 in partial fulfillment of the requirements for the Master of Science degree.		
19. KEY WORDS (Continue on reverse side if necessary and identify by block number) Blast shelter Reinforced concrete Ultimate capacity Key worker Stirrups One-way slab Tensile membrane		
20. ABSTRACT (Continue on reverse side if necessary and identify by block number) At the time this study was initiated, civil defense planning in the United States called for the evacuation of nonessential personnel to safe host areas when a nuclear attack is probable, requiring the construction of blast shelters to protect the keyworkers remaining in the risk areas. The place- ment of shear stirrups in the one-way reinforced concrete roof slabs of the shelters will contribute significantly to project costs. Ten one-way (Continued)		

DD FORM 1473

EDITION OF 1 NOV 65 IS OBSOLETE

Unclassified

SECURITY CLASSIFICATION OF THIS PAGE (When Data Entered)

Unclassified

SECURITY CLASSIFICATION OF THIS PAGE(When Date Entered)

20. ABSTRACT (Continued).

reinforced concrete slabs were statically and uniformly loaded with water pressure, primarily to investigate the effect of stirrups and stirrup details on the load-response behavior of the slabs. The slabs had clear spans of 24.0 inches, span to effective depth ratios of 12.4, tensile reinforcement of 0.75 percent, and concrete strengths of approximately 5,000 psi.

The test series significantly increased the data base for uniformly loaded one-way slabs. Support rotations between 13.1 and 20.6 degrees were observed. A more ductile behavior was observed in slabs with construction details, implying better concrete confinement due to more confining steel (i.e., closely spaced stirrups, double-leg stirrups, and closely spaced principal reinforcing bars). The parameters investigated did not appear to have a significant effect on ultimate load capacity.

In the case of the Keyworker Shelter, the test series resulted in the recommendation of construction details which reduce construction costs to a level less than the preliminary shelter design.

Unclassified

SECURITY CLASSIFICATION OF THIS PAGE(When Date Entered)

EFFECTS OF SHEAR STIRRUP DETAILS ON ULTIMATE CAPACITY
AND TENSILE MEMBRANE BEHAVIOR OF REINFORCED CONCRETE SLABS

At the time this study was initiated, civil defense planning in the United States called for the evacuation of nonessential personnel to safe host areas when a nuclear attack is probable, requiring the construction of blast shelters to protect the keyworkers remaining in the risk areas. The placement of shear stirrups in the one-way reinforced concrete roof slabs of the shelters will contribute significantly to project costs. Ten one-way reinforced concrete slabs were statically and uniformly loaded with water pressure, primarily to investigate the effect of stirrups and stirrup details on the load-response behavior of the slabs. The slabs had clear spans of 24.0 inches, span to effective depth ratios of 12.4, tensile reinforcement of 0.75 percent, and concrete strengths of approximately 5,000 psi

The test series significantly increased the data base for uniformly loaded one-way slabs. Support rotations between 13.1 and 20.6 degrees were observed. A more ductile behavior was observed in slabs with construction details, implying better concrete confinement due to more confining steel (i.e., closely spaced stirrups, double-leg stirrups, and closely spaced principal reinforcing bars). The parameters investigated did not appear to have a significant effect on ultimate load capacity.

In the case of the Keyworker Shelter, the test series resulted in the recommendation of construction details which reduce construction costs to a level less than the preliminary shelter design.

Accession For	
NTIS GRA&I	<input checked="" type="checkbox"/>
DTIC TAB	<input type="checkbox"/>
Unannounced	<input type="checkbox"/>
Justification	
By _____	
Distribution/	
Availability Codes	
Dist	Avail and/or Special
A-1	



PREFACE

The research reported herein was sponsored by the Federal Emergency Management Agency (FEMA) through the US Army Engineer Huntsville Division (HND) in support of the Keyworker Blast Shelter Test Program.

Construction and testing were conducted by personnel of the Structures Laboratory (SL), US Army Engineer Waterways Experiment Station (WES), under the general supervision of Mr. Bryant Mather, Chief, SL; Mr. J. T. Ballard, Assistant Chief, SL; Dr. J. P. Balsara, Chief, Structural Mechanics Division (SMD), SL; and under the direct supervision of Dr. S. A. Kiger of the Research Group, SMD. This report was prepared by Mr. S. C. Woodson of the Research Group, SMD, and is essentially the same as his thesis which was submitted to Mississippi State University in 1984 in partial fulfillment of the requirements for the Masters of Science Degree.

Commanders and Directors of WES during the investigation and the preparation of this report were COL Tilford C. Creel, CE, and COL Robert C. Lee, CE; Technical Director was Mr. F. R. Brown. Director at the time of publication was COL Allen F. Grum, USA; Technical Director was Dr. Robert W. Whalin.

CONTENTS

	<u>Page</u>
PREFACE	1
CHAPTER 1 INTRODUCTION	6
1.1 BACKGROUND	6
1.2 OBJECTIVES	16
1.3 SCOPE	17
CHAPTER 2 TEST DESCRIPTION	22
2.1 TEST TIME PERIOD, LOCATION, AND GENERAL DESCRIPTION	22
2.2 CONSTRUCTION DETAILS	22
2.3 REACTION STRUCTURE DETAILS	23
2.4 INSTRUMENTATION	23
2.5 PHOTOGRAPHY	24
2.6 TEST PROCEDURE	24
2.7 MATERIAL PROPERTIES	25
CHAPTER 3 TEST RESULTS	35
3.1 STRUCTURAL DAMAGE	35
3.2 PHOTOGRAPHIC DATA	35
3.3 INSTRUMENTATION DATA	36
CHAPTER 4 ANALYSIS	46
4.1 COMPARISON OF STRUCTURAL DAMAGE AND RESPONSE	46
4.2 YIELD-LINE THEORY	47
4.3 COMPRESSIVE MEMBRANE EFFECT	48
4.4 ROTATION CAPACITY	50
4.5 TENSILE MEMBRANE EFFECT	54
CHAPTER 5 SUMMARY, CONCLUSIONS, AND RECOMMENDATIONS	69
5.1 SUMMARY	69
5.2 CONCLUSIONS	70
5.3 RECOMMENDATIONS	70
REFERENCES	72
APPENDIX A: POSTTEST PHOTOGRAPHS AND DATA	77
APPENDIX B: STIRRUP SLAB TEST DATA	83
APPENDIX C: NOTATION	177

LIST OF ILLUSTRATIONS

<u>Figure</u>		<u>Page</u>
1.1	Stirrup details	20
1.2	Temperature steel placement	21
1.3	Principal steel spacing	21
2.1	Principal and transverse reinforcement layout (Slabs 1-8) . .	29
2.2	Principal and transverse reinforcement layout (Slabs 9 and 10)	29
2.3	Stirrup placement, single-leg stirrups	30
2.4	Stirrup placement, double-leg stirrups	30
2.5	Slab 2 construction	31
2.6	Cross section of reaction structure	31
2.7	Reaction structure	32
2.8	Instrumentation gage location	32
2.9	Instrumentation gage location, Slab 4	33
2.10	Four-foot-diameter blast load generator	33
2.11	Membrane in place	34
2.12	Strain gage data	34
3.1	Posttest view of Slab 4	40
3.2	Posttest view of Slab 2	40
3.3	General deformation	41
3.4	Posttest view of undersurface of slabs	41
3.5	Sequence of crack formation, Slab 8	42
3.6	Slab 8 photographic sequence	45
3.7	General load deflection	45
4.1	Formation of three-hinged mechanism	62
4.2	Rotation capacity vs. stirrup spacing	63
4.3	Slab 1 tensile membrane prediction	64
4.4	Slab 2 tensile membrane prediction	64
4.5	Slab 3 tensile membrane prediction	65
4.6	Slab 4 tensile membrane prediction	65
4.7	Slab 5 tensile membrane prediction	66
4.8	Slab 6 tensile membrane prediction	66
4.9	Slab 7 tensile membrane prediction	67
4.10	Slab 8 tensile membrane prediction	67
4.11	Slab 9 tensile membrane prediction	68
4.12	Slab 10 tensile membrane prediction	68

LIST OF TABLES

<u>Table</u>		<u>Page</u>
1.1	Test matrix	19
1.2	Slab characteristics	19
2.1	Results of concrete cylinder tests	27
2.2	Tensile test for steel reinforcement	28
3.1	Structural damage at midspan	37
3.2	Structural damage at supports	37
3.3	Photographic data summary for Slab 8	38
3.4	Load-deflection summary	38
3.5	Residual midspan deflection	39
4.1	Stirrup configuration	58
4.2	Temperature steel placement	58

CONVERSION FACTORS, NON-SI TO SI (METRIC)
UNITS OF MEASUREMENT

Non-SI units of measurement used in this report can be converted to SI (metric) units as follows:

<u>Multiply</u>	<u>By</u>	<u>To Obtain</u>
degrees (angle)	0.01745	radians
feet	0.3048	metres
foot-pounds	1.355818	joules
gallons (US liquid) per minute	3.785412	litres per minute
inches	25.4	millimetres
inch-kips	0.113	kilojoules
kips per square inch	6.894757	megapascals
megatons (nuclear equivalent of TNT)	4.184	gigajoules
microinches per inch	1.0	millionths
pounds (force) per square inch	0.00689475	megapascals

EFFECTS OF SHEAR STIRRUP DETAILS ON ULTIMATE
CAPACITY AND TENSILE MEMBRANE BEHAVIOR
OF REINFORCED CONCRETE SLABS

CHAPTER 1

INTRODUCTION

1.1 BACKGROUND

The Federal Emergency Management Agency (FEMA) has the responsibility of planning an appropriate civil defense program for the United States. At the time this study was initiated, civil defense planning called for the evacuation of nonessential personnel to safe (lower risk) host areas when a nuclear attack is probable. The construction of blast shelters will be required to protect the keyworkers remaining in the risk areas. Both expedient and deliberate types of shelters are planned. The shelters will be designed to resist blast, radiation, and associated effects at the 50-psi¹ peak overpressure level for a 1-MT nuclear weapon. FEMA has tasked the US Army Engineer Huntsville Division (HND) to develop keyworker shelter designs. The US Army Engineer Waterways Experiment Station (WES) is supporting HND with design calculations and structural experiments to verify design calculations.

With the anticipation of the construction of 20,000 to 40,000 of the shelters, economical design requirements are very important. Because of high labor intensity, it is expected that the placement of shear stirrups in the roof slabs of the shelters will contribute significantly to project costs. The primary purpose of the research reported herein is to investigate the effects of stirrups and stirrup details on the moment capacity and ductility of a one-way reinforced concrete slab. This research is a part of the support provided to HND by WES.

In the past, concrete was considered to be a very brittle material. Research by Lee (Reference 1) and Shah (Reference 2) indicates that concrete is not as brittle as once considered. It is relatively more ductile than its constituents, hardened paste or stone. This results from the composite action

¹A table of factors for converting non-SI to SI (metric) units of measurement is presented on page 5.

and slower growth of stable microcracks initiated at the interface between hardened paste and stone. Barnard (Reference 3) concluded that while the internal failure mechanism of concrete may be brittle on the microscopic scale, it is not brittle on the macroscopic or structural scale.

Park and Paulay (Reference 4) state that brittle failure of reinforced concrete members should not occur. In the event of a structure being loaded to failure, it should be capable of undergoing large deflections at near-maximum load-carrying capacity to help prevent total collapse. Depending on the ductility of the members at the critical sections, a moment redistribution can take place. As ultimate load is approached, some sections may reach the ultimate moment capacity before other sections. However, if plastic rotation can occur at these sections, additional load can be carried as the moments elsewhere increase to their ultimate value.

Cohn (Reference 5) and Cohn and Petcu (Reference 6) explain that the rotation capacity of a plastic hinge may be expressed as the total rotation accumulated along a short zone l_p , plastic hinge length, where yield has spread near the support under consideration. The rotation capacity of plastic hinges depends essentially on the inelastic properties of the reinforced concrete sections.

Park and Paulay (Reference 4) also state that if the compression zone of a member is confined by closely spaced transverse reinforcement in the form of closed stirrups, ties, hoops, or spirals, the ductility of the concrete may be greatly improved. At low levels of stress in the concrete, the transverse reinforcement is hardly stressed and the concrete is unconfined. The concrete becomes confined when the transverse strains become very high because of progressive internal cracking and the concrete bears out against the transverse reinforcement which provides passive confinement.

Roy and Sozen (Reference 7) axially loaded 60 prisms with varying tie spacing and amounts of longitudinal reinforcement. It seemed that the square ties did not enhance the load-carrying capacity of the concrete, but did increase the ductility of the concrete in the specimens. In contrast, Chan (Reference 8), Soliman and Yu (Reference 9), Stockl (Reference 10), and Bertero and Felippa (Reference 11) have observed an increase in strength due to closely spaced rectangular hoops.

McDonald (Reference 12) experimentally investigated the effect of confining reinforcement (plane meshes, helices, and closed stirrups) in

112 concrete prisms and 24 simply supported reinforced concrete beams. The beams were tested to failure under two symmetrical line loads applied 6 inches from the beam centerline. Results of the tests clearly demonstrated the ability of confining compressive reinforcement to significantly increase the ductility of reinforced concrete beams using high-strength steel. Uniaxial tests on the prisms demonstrated that concrete properly confined by lateral reinforcement had a considerable load-carrying capacity up to strains in excess of 2 percent, or more than six times the amount of strain usually considered as ultimate for concrete.

Sargin, Ghosh, and Handa (Reference 13) discuss confinement of concrete by rectilinear lateral reinforcement. An experimental investigation was performed in which 63 prisms were tested, with the main variables being:

(1) concrete strength, (2) size, spacing, and grade of lateral reinforcement, (3) strain gradient, and, (4) thickness of cover. Conclusions included:

(1) a laterally reinforced concrete member should be treated as a composite member consisting of a confined core and an unconfined cover, (2) the amount of confinement provided by lateral reinforcement is dependent not only upon the volumetric ratio of lateral reinforcement but also upon the type of lateral reinforcement (discrete square or rectangular ties, spirals, envelopes, etc.); the spacing and grade of reinforcement; and the quality of confined concrete, (3) spacing is the most important parameter because the choices of bar size and qualities of concrete and steel are rather limited in practice. The effect of transverse reinforcement decreases drastically with increasing spacing and becomes negligible for spacings larger than the thickness of the core, and (4) the ductility and hence the rotation capacity of the so-called hinging regions in reinforced concrete members can be improved to a large extent through the use of lateral reinforcement.

Tests indicate that spiral reinforcement is more effective than rectangular hoops in confining concrete. Richart, Brandtzaeg, and Brown (Reference 14) showed that the strength of concrete confined by circular spirals is similar to that confined by fluid pressure. Bertero and Felippa (Reference 11) loaded concrete prisms containing square ties. The effect of ties on the ductility was not as great as in the case of spiral-reinforced cylinders tested by Iyengar, Desayi, and Reddy (Reference 15). Sheikh and Uzumeri (Reference 16) found that for columns with rectilinear reinforcement, the confining pressure is not uniformly applied throughout the volume of the concrete

core, unlike the concrete specimen confined by hydraulic pressure or spiral reinforcement.

Kent and Park (Reference 17) explain that rectangular or square hoops do not confine the concrete as effectively as circular spirals. This is because the confining reaction can only be applied in the corner regions of the hoops, since the bending resistance of the transverse steel between the corners is insufficient to restrain the expansion of the concrete along the whole length of the bar. Since the concrete is only effectively confined in the corner and central regions of the cross section, a disruption of a considerable portion of the core area occurs. However, the rectangular hoops do produce a significant increase in the ductility of the core as a whole.

Base and Read (Reference 18) agree that decreasing the brittleness of the failure of some types of concrete members is an important consideration and that close spacing of rectangular stirrups is one method of containing dilating concrete in the compression zone of a plastic hinge. One-point-loaded, simply supported beams indicated that under-reinforced concrete beams probably have more than adequate plasticity at failure and should not need any special secondary reinforcement at plastic hinge regions. Balanced-section reinforced concrete beams failed in a brittle manner unless the compression zone was "bound". Over-reinforced concrete beams without special secondary reinforcement failed very brittle and failure was terminated by a shear collapse. Closely spaced stirrups completely prevented shear collapse but eventually allowed the compression zone to crush because they deformed outwards under the bursting pressure of the concrete. It was concluded that a combination of helices and close stirrups would be necessary to produce ideal characteristics.

Shah and Rangan (Reference 19) investigated the use of stirrups in reinforced concrete beams. For over-reinforced beams ($\rho > \rho_b$) it was found that: (1) the addition of stirrups does not significantly influence the load-deflection curves up to the maximum load, (2) the addition of stirrups increases ductility, and (3) the addition of stirrups retards internal crack growth of compression concrete. For under-reinforced beams ($\rho < \rho_b$) it was found that: (1) in agreement with Base and Read (Reference 18), the addition of stirrups did not influence the rotation capacities, and (2) no volume dilation of the compression zone was observed and the concrete compressive strains were considerably lower than those for over-reinforced beams.

Shah and Rangan (Reference 19) also studied the relative efficiency of compression reinforcement, rectangular ties, and randomly oriented short steel fibers in improving ductility of compression concrete in flexural members. Rectangular ties were by far the most efficient.

Yamashiro (Reference 20) varied axial load on beam columns. The deflection at ultimate load was quite sensitive to variations in the amounts of transverse and compression reinforcement, whereas the deflection at crushing was not. The deflection at ultimate load was from 2 to 12 times the crushing deflections.

Based on beam data, Keenan and others (Reference 21) state that conventional reinforced concrete members with compression steel can reliably maintain their ultimate moment resistance to maximum support rotations of 4 degrees, provided the compression bars are confined by effective ties and $q \leq 0.14$ where q is the reinforcing index defined by:

$$q = (\rho f_y - \rho' f'_y) / f'_c$$

where:

ρ = tension steel ratio

f_y = yield strength of tension steel

ρ' = compressive steel ratio

f'_y = yield strength of compression steel

f'_c = compressive strength of concrete

The effectiveness of ties depends on the tie spacing, the size of the compression bars, and the applied moment gradient. Without ties but with $q \leq 0.14$, the effectiveness of compression reinforcement is less reliable.

Mattock (Reference 22) tested 37 beams, demonstrating that the rotational capacity of a part of a beam under loading producing a moment gradient is greater than that of a similar beam under loading producing constant moment (zero shear). A method was proposed to calculate the rotational capacity of a hinging region in reinforced concrete beams. Mattock states that if calculations are to be made of the total inelastic or plastic rotations, a knowledge of moment-curvature relationships for the reinforced concrete sections is necessary. It was shown that close estimates of moments and safe limiting estimates of curvatures and rotations can be derived from well-known principles of equilibrium of forces and compatibility of strains, provided that strain

hardening of the reinforcement and variation of maximum concrete compressive strain are taken into account. Mattock also found that maximum apparent concrete strain is often considerably in excess of the commonly assumed value of 0.0030 and that it increases as the shear span decreases.

Based upon tests on two beams and two columns, Sinha and Rane (Reference 23) concluded that the use of an ultimate concrete strain value of 0.0030 and the determination of the position of the neutral axis assuming linear strain distribution provides a very conservative basis for determining the total curvature developed in a reinforced concrete member. The data obtained from the experiments showed that a concrete strain value of 0.0050 to 0.0060 for beams reinforced in tension and compression yields better results.

Mattock (Reference 22) points out that in the past, considerable effort has been made to determine moment-curvature relationships experimentally and to devise calculational methods. Curvature measurements have usually been taken in the constant-moment region of a simply supported beam loaded at two points. Rotations have been predicted with reasonable accuracy except for plastic rotation calculations of the region adjacent to a support in a continuous beam, in which calculated rotational capacity is less than the observed rotation in the continuous beam.

Mattock did not investigate confinement of concrete in the beam tests. Corley (Reference 24) tested 40 beams as an extension of Mattock's tests to investigate the effects of specimen size and confinement of the concrete in compression. Corley also studied the effects of moment gradient, percentage of tensile reinforcement, and size of loaded area. All 40 beams had rectangular stirrups and were under-reinforced. Failure occurred due to crushing of the concrete after the tension reinforcement had yielded. Corley concluded that the direct effect of size of model on rotational capacity is not significant, and that beams with a large number of closely spaced stirrups exhibit considerably more rotational capacity than beams with few stirrups.

Taylor, Maher, and Haynes (Reference 25) used axial test data on reinforced concrete cylinders to conclude that confinement is found to be effective only when the pitch of the ties is less than the least lateral dimension of the confined specimen.

Bachman (Reference 26) tested two groups of five symmetrical two-span beams and observed two types of plastic hinges: (1) flexural crack hinges and (2) shear crack hinges. Flexural crack hinges develop in a beam zone in which

the bending moment is predominant. The shear stress is small and only vertical flexural cracks occur. When the plastic deformations are concentrated mainly to one or a few cracks, the rotational capacity of such a flexural crack hinge may be very small. At a shear crack hinge, diagonal flexural-shear cracks are produced due to a relatively large shear stress accompanied by a bending moment, improving the behavior of the hinge. It was shown that the plastic deformations in a shear crack hinge occur over a much wider zone than with flexural crack hinges, allowing a much greater rotational capacity.

Bachman stated that in flexural crack hinges with ultimate failure due to the rupture of the reinforcement, the ultimate rotations are found to decrease with: (1) better bond properties, (2) smaller bar diameter, (3) less strain-hardening, (4) smaller permanent steel strain, (5) greater crack spacing, and (6) greater shear force.

Cohn and Ghosh (Reference 27) recognize ductility as a factor governing the rotation capacity of hinging zones and the redistribution of moments in a structure. The researchers state that members are sufficiently ductile, for all practical purposes, when they resist only transverse loads, are moderately reinforced in tension, moderately to heavily reinforced in compression and shear, use mild- or intermediate-grade steels, and use high-grade concretes. Cohn and Ghosh believe that ductility can be increased somewhat by reducing the spacing and increasing the diameter of the ties. They also believe that ductility decreases with increasing amounts of tension steel, but can be improved considerably by the addition of suitable amounts of compression steel.

Srinivasa Rao, Kannan, and Subrahmanyam (Reference 28) and Burnett (Reference 29) point out that several authors including Corley (Reference 24), Mattock (Reference 22), and Baker and Amarakone (Reference 30) disagree even on the basic definition of what is to be taken as plastic rotation capacity. Baker and Amarakone suggest that the rotation capacity under a concentrated load acting at beam midspan increases with length of the beam. In contrast, Mattock and Corley predict that rotation capacity will be larger in short beams. Srinivasa Rao, Kannan, and Subrahmanyam loaded simply supported beams with a concentrated load at midspan, varying span length. It was concluded that plastic rotation capacity increased as the spread of plasticity increased with larger beam spans.

Burnett states that if research priorities are to be established, it is

evident that the support critical section is particularly important.

In any study investigating the effect of a parameter (for example, the variation of shear stirrup shape and placement) on the load-response behavior of reinforced concrete slabs, an understanding of the effects of boundary conditions and loading conditions on the load-response behavior of slabs is beneficial. In 1955, Ockleston (Reference 31) tested a slab in a dental hospital building and found that the interior panel of the under-reinforced floor system, acting as a restrained slab, carried more than double the load predicted by Johansen's yield-line theory (Reference 32).

In 1958, Ockleston (Reference 33) explained that the unexpected results of his test in 1955 were not due to reinforcement strain hardening, tensile strength of concrete, or catenary actions. It was concluded that the increase in load capacity was due to the development of inplane compressive forces, termed "arching" or "dome action."

Experimental research using uniformly loaded beams or one-way slabs is very limited. Burnett (Reference 34) considered that the effect of applying a uniformly distributed load rather than a point load to a simply supported beam would alter the moment distribution, the curvature distribution, and the moment-rotation relation. Burnett concluded that the parameters involved in the behavior of a member as a whole are many more than those affecting the behavior of an individual section within that member. Corley (Reference 24) acknowledged that uniform loading was not investigated as a part of his extension of Mattock's work. Corley stated that although no significant change in the results of tests with uniform loading should be anticipated, this respect still remains to be studied. Iqbal and Derecho (Reference 35) stated that no data are available for one-way slabs tested under uniformly distributed load.

During the same year that Iqbal and Derecho reported their work (1969), Keenan (Reference 36) tested four laced reinforced concrete one-way slabs to failure under a uniformly distributed load. All slabs spanned one direction with ends clamped and longitudinally restrained to prevent rotation and longitudinal movement at their supports. One slab was tested to the point of failure with an increasing static load applied by water pressure. The other three slabs were subjected to two or more short-duration dynamic loads. Principal tension and compression reinforcement were placed to the interior of the transverse reinforcement, and diagonal lacing bars were bent around the exterior face of the transverse reinforcement in a grid system. The lacing

bars distributed the load, resisted diagonal tension stresses, and confined both the flexural steel and concrete separating the two layers of reinforcement. The experimental rotation capacity of Keenan's slabs at the supports was greater than 9.2 degrees.

Keenan (Reference 37) developed a theory for predicting the thrust, deflection, and ultimate flexural resistance of uniformly loaded square slabs. He then applied this theory to the tested one-way slabs (Reference 36) and found good correlation between the theoretical and experimental resistance, deflection, and steel stresses at stages of ultimate flexure and initial tensile membrane action.

Keenan's theory considers that a slab spanning one direction is subjected to combined bending and direct stress if the ends are restrained against longitudinal movement. Deflections of the slab induce thrust on sections along hinge lines which increases the moment resistance of sections along the hinge lines, thereby significantly increasing the stiffness and ultimate flexural resistance of the slab.

Park and Gamble (Reference 38) explain that Johansen's yield-line theory only considers the presence of moments and shear forces at the yield lines in the slab. Park and Gamble agree with Keenan that if the edges of slabs are restrained against lateral movement by stiff boundary elements, inplane (compressive membrane) forces are induced as the slab deflects and changes of geometry cause the slab edges to tend to move outward and to react against the bounding elements. The compressive membrane forces enhance the flexural strength of the slab sections at the yield lines, which causes the ultimate load of the slab to be greater than the ultimate load calculated using Johansen's yield-line theory.

Kiger, Eagles, and Baylot (Reference 39) tested five one-way slabs primarily to investigate the effects of soil cover on the static and dynamic capacity of earth-covered reinforced concrete slabs. One slab was loaded surface flush with a slowly increasing uniform load. Compressive membrane forces acted to almost triple the slab capacity predicted for the slab under unrestrained conditions.

Roberts (Reference 40) tested 36 strips representing restrained one-way slabs loaded by several point forces to simulate uniformly distributed loading. The ratio of peak load to that given by Johansen's yield-line theory varied from approximately 17 for strips with high concrete strength and a low

percentage of reinforcement to approximately 3 for beams with low concrete strength and a high percentage of reinforcement. Roberts concluded that the deflection at maximum load is not a fixed proportion of the slab thickness, and that it is not necessary for the restraint to have enormous stiffness to develop enhanced peak loads.

Wood (Reference 41), Park (Reference 42), and Morley (Reference 43) assume the central deflection at ultimate load to be 0.5 times the slab thickness for fully restrained slabs. Hung and Nawy (Reference 44) use experimental values of deflection at ultimate load and note that the ultimate load is not always reached at a deflection equal to 0.5 times the slab thickness. Instead, values ranging from approximately 0.4 to 1.0 times the slab thickness are considered.

Work by Isaza (Reference 45) indicates that the maximum compressive membrane effect occurs at a central deflection equal to approximately one-sixth of the slab thickness.

Hopkins (Reference 46) points out that the absence of top steel at the edges of laterally restrained slabs has little effect on the ultimate load. The complete omission of top steel is not considered wise, but its length could be reduced in slabs subjected to compressive membrane forces.

Brotchie, Jacobson, and Okubo (Reference 47) tested 45 two-way square slabs in a highly rigid steel frame. It was observed that at small deformations, the compressive strength of the concrete governs and if the plate is restrained, arching or compressive membrane behavior occurs. However, at large deformations, the concrete crushes, leaving only the tensile strength of the reinforcement to resist loading. If the edge of the slab is restrained against inward displacement, the full strength of the reinforcement may be developed as a tensile net. It was also observed that tensile cracks increase in number but decrease in width with the number of reinforcing bars.

Park (Reference 48) and Park and Gamble (Reference 38) discuss the tensile net development known as tensile membrane behavior. After ultimate load has been reached in a reinforced concrete slab, the supported load decreases rapidly with further deflection. Eventually, membrane forces in the central region of the slab change from compression to tension and the slab boundary restraints begin resisting inward movement. Cracks in the central region penetrate the whole thickness of the concrete and yielding of the steel spreads throughout the region. The reinforcement may begin acting as a

tensile membrane with load-carrying capacity increasing with further deflection until the reinforcement fractures.

From tests by Park (Reference 48), it was evident that pure tensile membrane action did not occur in lightly reinforced two-way slabs, since the cracking present at the end of the tests was little more than the cracking which developed with the yield-line pattern at the ultimate flexural load. Therefore, the load was carried by a stronger combined bending and tensile membrane action. Heavily reinforced slabs cracked over much of their area and therefore approached pure tensile membrane action.

1.2 OBJECTIVES

In considering the use of stirrups in one-way reinforced concrete slabs, it is important to understand the benefits which will be gained through the use of the stirrups. Also, the effects which specific physical details will have on the efficiency of the stirrups should be understood. Figure 1.1 shows three possible stirrup configurations. Figure 1.1a shows a double-leg stirrup (Type I) which might be expected to provide better confinement of concrete and principal steel than the single-leg stirrup (Type II) in Figure 1.1b. The 135-degree bends on both ends of the Type II single-leg stirrup might be expected to confine concrete and principal steel better than the Type III single-leg stirrup, shown in Figure 1.1c which has a 90-degree bend on one end. It is obvious that installation of both single-leg stirrups would be labor-saving when compared to the installation of the Type I stirrup. The Type III stirrup is also easier to install than the Type II stirrup, but the question arises as to whether the 90-degree bend is as effective as the 135-degree bend against pullout. Type III stirrups used by Slawson (Reference 49) fractured under large slab deflection, indicating that pullout may not be a problem. In conjunction with specific details, the placement and quantity of the stirrups required to achieve the desired benefits must be known. This leads to an investigation of stirrup spacing.

Another important parameter to be considered is the interaction of the stirrups with other reinforcement in the slab (for example, the transverse reinforcement or temperature steel). Much of the work explained above concerned the use of closed rectangular hoops. The presence of stirrups and temperature steel at the same location forms a closed hoop resembling a continuous rectangular tie. Keenan and others (Reference 21) indicated that in order to

assure adequate confinement of concrete rubble under large deflections of a slab, the principal steel bar spacing should not exceed the effective depth. The interaction of this parameter with the presence of stirrups should be understood to insure that stirrups are not used ineffectively due to excessive principal steel bar spacing.

Specifically, the objectives of this study were to investigate the effects of the following parameters on the ultimate load capacity and tensile membrane behavior of a one-way reinforced concrete slab: (1) stirrup configurations as presented in Figure 1.1; (2) stirrup spacing; (3) the interaction of the stirrups with the transverse reinforcement (temperature steel) under the two placement conditions shown in Figure 1.2; and (4) the interaction of the stirrups with the two principal reinforcement bar spacings shown in Figure 1.3.

1.3 SCOPE

Ten one-way reinforced concrete slabs were statically (slowly) loaded with water pressure in the WES 4-foot-diameter blast load generator. Huff (Reference 50) gives a detailed description of the test device, which is capable of developing static loads up to 500 psi. The slabs had a span-to-effective-depth (L/d) ratio of 12.4 with a clear span length of 24 inches. Principal steel ratios were about 0.0075 and 0.0085 for the tension face and compression face, respectively. Grade-60 reinforcement steel was used, and the concrete had an average test-day compressive strength of 4,790 psi. The slabs were supported in a reaction structure and were restrained at the ends.

Table 1.1 presents a test matrix demonstrating the variations of the parameters required to accomplish the stated objectives. Each of the three stirrup configurations was separately tested in three different slabs. An analysis based upon three empirical relations developed by Baker and Amarakone (Reference 30), Corley (Reference 24), and Mattock (Reference 51) was used to determine the stirrup spacings to be investigated. Stirrup spacings of 0.75, 1.5, and 3.0 inches were selected with the anticipation that the behavior of the slabs with the 0.75-inch spacings would be considerably different from slabs with the 1.5- or 3.0-inch spacings.

The temperature steel was spaced at 3.0 inches on center in both faces in all slabs, giving a ratio of total temperature steel to total concrete area of 0.00326. Placing the temperature steel in the interior and the exterior

regions of the slab cross section, as shown in Figure 1.2, allows a variation in the area of concrete confined between the temperature steel. Therefore, two slabs were constructed with the temperature steel placed in the exterior regions.

Two principal steel spacings, 1.75 and 3.75 inches, were used in the slabs. The 3.75-inch spacing was used in order to allow correlation with tests being performed by Slawson (Reference 52) on 1/4-scale box elements representing the HND-proposed roof slab design. The 1.75-inch spacing was used to investigate the effect of the criteria given by Keenan and others (Reference 21) maintaining the bar spacing to a value less than the effective depth, 1.9375 inches.

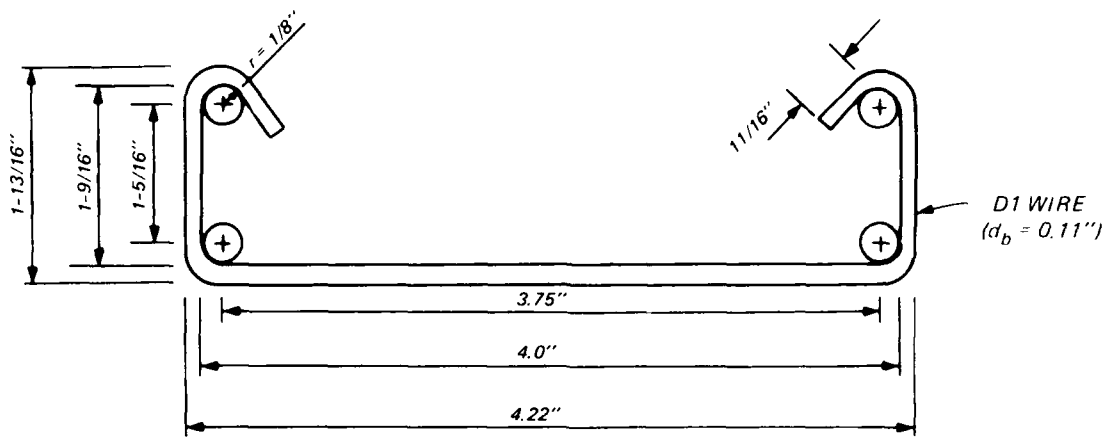
Table 1.2 presents a more detailed description of each of the ten slabs.

Table 1.1. Test matrix.

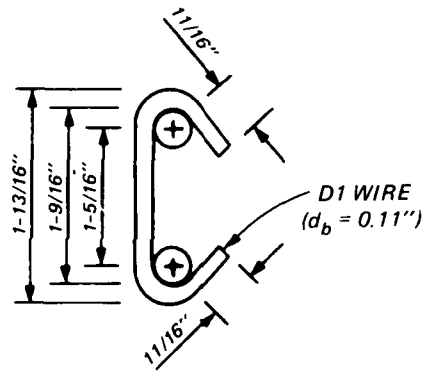
Stirrup Config- uration	Number of Spacings to be Tested with Temperature Steel in		Spacing of Principal Steel, in	Number of Spacings, Interior and Exterior
	Interior Region	Exterior Region		
Type I	1	--	3.75	1
Type II	3	1	3.75	4
Type II	2	--	1.75	2
Type III	1	1	3.75	2
No Stirrups	1	--	3.75	1
Total Number of Tests				10

Table 1.2. Slab characteristics.

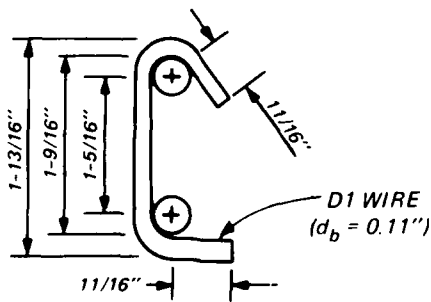
Slab	Stirrup Configuration Type	Stirrup Spacing in	Principal Steel Spacing in	Temperature Steel Placement
1	No Stirrups	--	3.75	Interior
2	II	0.75	3.75	Interior
3	II	1.5	3.75	Interior
4	II	3.0	3.75	Interior
5	II	1.5	3.75	Exterior
6	III	1.5	3.75	Interior
7	III	1.5	3.75	Exterior
8	I	1.5	3.75	Interior
9	II	1.5	1.75	Interior
10	II	0.75	1.75	Interior



a. TYPE 1

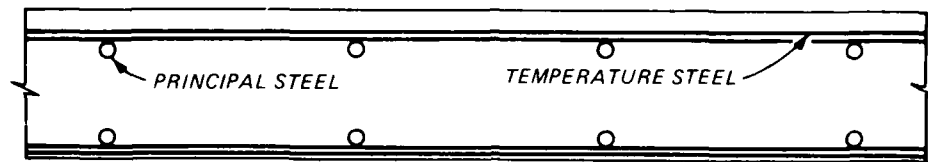


b. TYPE 2

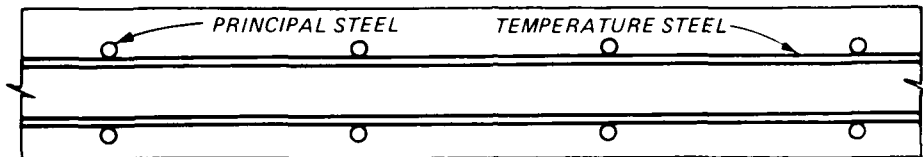


c. TYPE 3

Figure 1.1. Stirrup details.

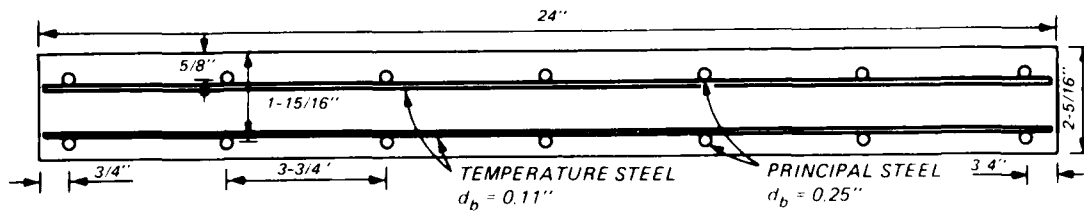


a. Temperature steel outside principal steel.

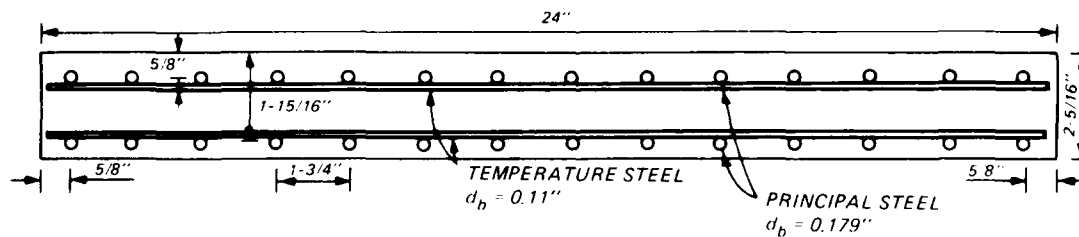


b. Temperature steel inside principal steel.

Figure 1.2. Temperature steel placement.



a. 3-3/4-inch spacing.



b. 1-3/4-inch spacing.

Figure 1.3. Principal steel spacing.

CHAPTER 2

TEST DESCRIPTION

2.1 TEST TIME PERIOD, LOCATION, AND GENERAL DESCRIPTION

Ten one-way reinforced concrete slabs were statically tested by WES in Vicksburg, Mississippi, between 30 November 1983 and 3 February 1984.

The following sections describe test slab construction details, reaction structure details, instrumentation, photography, test procedure, and material properties.

2.2 CONSTRUCTION DETAILS

Eight of the ten slabs (Slabs 1 through 8) were constructed of 0.25-inch-diameter deformed wire (principal reinforcement) and D1 deformed wire (temperature reinforcement). Slabs 2 through 8 were also reinforced with D1 deformed wire stirrups. Figure 2.1 shows a plan view of Slabs 1 through 8 without stirrups. The total area of reinforcement in the compression face was equal to the total area of reinforcement in the tension face. Due to the different thickness of concrete cover on compression and tension reinforcement, compression and tension reinforcement ratios were not equal. The effective depth used in calculating the ratios was measured from the extreme tension face for the compression reinforcement and from the compression face for the tension reinforcement. Principal reinforcement percentages for Slabs 1 through 8 were 0.72 percent and 0.83 percent for the tension face and compression face, respectively.

Slabs 9 and 10 were constructed of D2.5 deformed wire (principal reinforcement) and D1 deformed wire (temperature reinforcement). Figure 2.2 is a plan view of Slabs 9 and 10 without stirrups. Stirrups in these two slabs were made from 0.080-inch-diameter smooth wire. Principal reinforcement percentages for Slabs 9 and 10 were 0.75 percent and 0.86 percent for the tension face and compression face, respectively.

The temperature steel was spaced at 3.0 inches on center in both faces in all slabs, giving a ratio of total temperature steel to total concrete area of 0.00326. The effective depth (d) in each slab was 1.9375 inches, and the span-to-effective depth (L/d) ratio was 12.4.

As discussed in Chapter 1 and shown in Figure 1.2, two temperature reinforcement placement conditions were investigated. Slabs 5 and 7 were constructed using the "exterior" placement condition presented in Figure 1.2a. The remaining eight slabs were constructed using the "interior" placement condition presented in Figure 1.2b.

Each slab, except Slab 1, contained stirrups as presented in Table 1.2. Figure 2.3 shows typical placement details for slabs having single-leg (Type I or Type II) stirrups. Figure 2.4 shows stirrup placement details for the slab (Slab 8) containing double-leg stirrups. The stirrup spacing utilized in Figures 2.3 and 2.4 is 1.50 inches. The double-leg stirrups were staggered to place only one leg at any location along the principal reinforcement, simulating the spacing of single-leg stirrups.

The slabs were constructed and cast at the Structures Laboratory of WES. Figure 2.5 documents the steel reinforcement placement of Slab 2 (bottom side up) prior to placement of concrete.

2.3 REACTION STRUCTURE DETAILS

The reaction structure used by Kiger, Eagles, and Baylot (Reference 39) at the WES Structures Laboratory in a previous test program was utilized in the test series under discussion. Figure 2.6 shows a cross-sectional view of the reaction structure. The reaction structure was modified with a removable door to allow access as shown in Figure 2.7. Placement of a 36- by 24-inch slab in the reaction structure allowed 6 inches of the slab at each end to be clamped by a steel plate bolted into position, thereby leaving a 24- by 24-inch one-way restrained slab for testing.

2.4 INSTRUMENTATION

Each slab was instrumented for strain, displacement, and pressure measurement. The data were recorded on a Sangamo Sabre III FM magnetic tape recorder, and digitized and plotted by computer. Figure 2.8 shows the instrumentation gage layout for a typical slab with stirrups. Two displacement transducers were used in each test to measure vertical displacement of the slab, one at one-eighth span (D1) and one at midspan (D2). The transducers used were Trans-Tek Model 0246-0000, having a working range of 6.00 inches.

Two single-axis, metal-film, 0.125-inch-long, 350-ohm, strain gage pairs were installed on principal reinforcement in each slab. Each pair consisted

of a strain gage on a top bar and one on a bottom bar directly below. One pair was located at one-fourth span (ST1, SB1) and one was located at midspan (ST2, SB2). The gages used were Micro-Measurements Model EA-06-125 BZ-350.

Strain gages were also installed on three stirrups in each of Slabs 2 through 10. The strain gages were located at mid-height of total stirrup height. One instrumented stirrup was placed at 1.50 inches from the support (S3), one at one-fourth span (S4), and one at midspan (S5). Figure 2.9 shows that Slab 4 is an exception, with Gages S4 and S5 placed at 7.50 and 10.50 inches from the support, respectively.

One Kulite Model HKM-S375, 500-psi-range pressure gage (P1) was mounted in the bonnet of the test chamber in order to measure the water pressure applied to the slab.

2.5 PHOTOGRAPHY

Photographic coverage was provided during construction of the slabs and during posttest examination of each slab. The photographs helped document the structural damage for comparative purposes.

Photographic coverage was also provided during the testing procedure. A Cannon AE-1 35-mm camera was placed inside the reaction structure beneath the slab and was remotely controlled. Therefore, photographs of the undersurface of the slab were obtained at several levels of damage.

2.6 TEST PROCEDURE

The 4-foot-diameter blast load generator (Figure 2.10) was used to statically load the slab with water pressure. The reaction structure was placed inside the test chamber and surrounded with compacted sand as shown in Figure 2.7. The slab was then placed on the reaction structure. The wire leads from the instrumentation gages and transducers were connected, and the camera was placed into position. After placing the removable door in position, the sand backfill was completed on the door side. A 1/4-inch-thick neoprene rubber membrane was placed over the slab, and 1/2- by 24-inch steel plates were bolted into position as shown in Figure 2.11. Prior to the bolting of the plates, Aqua Seal putty was placed between the rubber membrane and the steel plates to seal gaps around the bolts and to prevent loss of water pressure during testing. A torque wrench was used to achieve approximately 50 foot-pounds on each bolt, and a consistent sequence of tightening the bolts

was used for each slab. The bonnet was bolted into position with forty 1-1/8-inch-diameter bolts tightened with a pneumatic wrench. A commercial waterline was diverted to the chamber's bonnet. The data tape recorder was started immediately preceding the opening of the waterline valve. A time of approximately 18 minutes was required to fill the bonnet volume of the test chamber. A relief plug in the top of the bonnet indicated when the bonnet had been filled. At that time the waterline valve was closed to allow closing of the relief plug. The waterline valve was again opened slowly, allowing a flow of approximately 1.0 gal/min through the 1/4-inch-diameter waterline and inducing a slowly increasing load to the slab's surface. A pneumatic water pump was connected to the waterline to facilitate water pressure loading in the case that commercial line pressure was not great enough to reach ultimate resistance of the slab in any particular test. Only tests of Slabs 9 and 10 required use of the pump due to the lack of sufficient commercial waterline pressure. Monitoring of the pressure gage and the deflection gage located at midspan of the slab indicated the behavior of the slab during the test and enabled the engineer to make a decision for test termination by closing the waterline valve. Following test termination, the bonnet was drained and removed. Detailed measurements and photographs of the slab were taken after removal of the rubber membrane. Finally, the damaged slab was removed and the reaction structure was prepared for another slab test.

2.7 MATERIAL PROPERTIES

The 10 slabs were cast of concrete from one batch which was proportioned for a 28-day design strength of 4,000 psi. The concrete was composed of Type I portland cement and 3/8-inch-maximum-diameter pea gravel. The mix proportion, by weight, given as cement:fine aggregate:coarse aggregate was 1:3.26:3.14. The water-cement ratio, by weight, was 0.67.

One test cylinder was cast for each slab and two cylinders were cast from the batch for 28-day compression tests. The one cylinder per slab was tested on test day for that particular slab. Results of the concrete cylinder tests are presented in Table 2.1.

Five of the concrete cylinders were instrumented with strain gages. Figure 2.12 is a typical plot of the strain gage data for a cylinder. The average values of modulus of elasticity E and Poisson's ratio ν for the five instrumented cylinders were 4.4×10^6 psi and 0.22, respectively.

Deformed wire was used as reinforcement in the slabs. The wire was heat-treated in an oven at WES, producing a definite yield point at a yield stress of approximately 60,000 psi. Before heat treatment, the wire had an approximate yield stress of 90,000 psi. Numerous trials with various oven temperatures were required before satisfactory results were obtained. Table 2.2 presents results of tensile tests performed on specimens from heat-treated batches used in construction.

Table 2.1. Results of concrete cylinder tests.

<u>Concrete Batch</u>	<u>Age days</u>	<u>Compressive Strength, psi</u>	<u>Corresponding Slab Test</u>
1	28	4,120	--
1	28	3,960	--
1	103	4,860	4
1	118	5,060	3
1	124	4,920	2
1	140	4,850 ^a	6
1	144	5,110 ^a	8
1	154	5,020 ^a	7
1	158	5,060 ^a	5
1	163	4,700 ^a	9
1	166	4,930	10
1	168	4,830	1

^aStrain-gaged cylinder.

Table 2.2. Tensile test for steel reinforcement
(deformed wire).

Wire Diameter in	Yield Stress psi	Ultimate Stress psi
0.11	68,500	69,400
Temperature steel, all slabs	57,760	61,580
Stirrup steel, Slabs 1 through 8	65,040	67,650
	57,310	61,130
0.247	64,300	66,700
Principal steel, Slabs 1 through 8	58,000	65,500
	59,290	65,570
	57,620	65,990
	59,490	60,960
	61,200	68,480
	58,460	64,930
0.174	66,400	71,200
Principal steel, Slabs 9 and 10	65,600	72,000
	66,200	77,400
	58,000	72,400
	55,600	79,200
0.080	63,360	81,470
Stirrup steel, Slabs 9 and 10	64,360	82,040
	63,650	80,620
	62,660	80,600

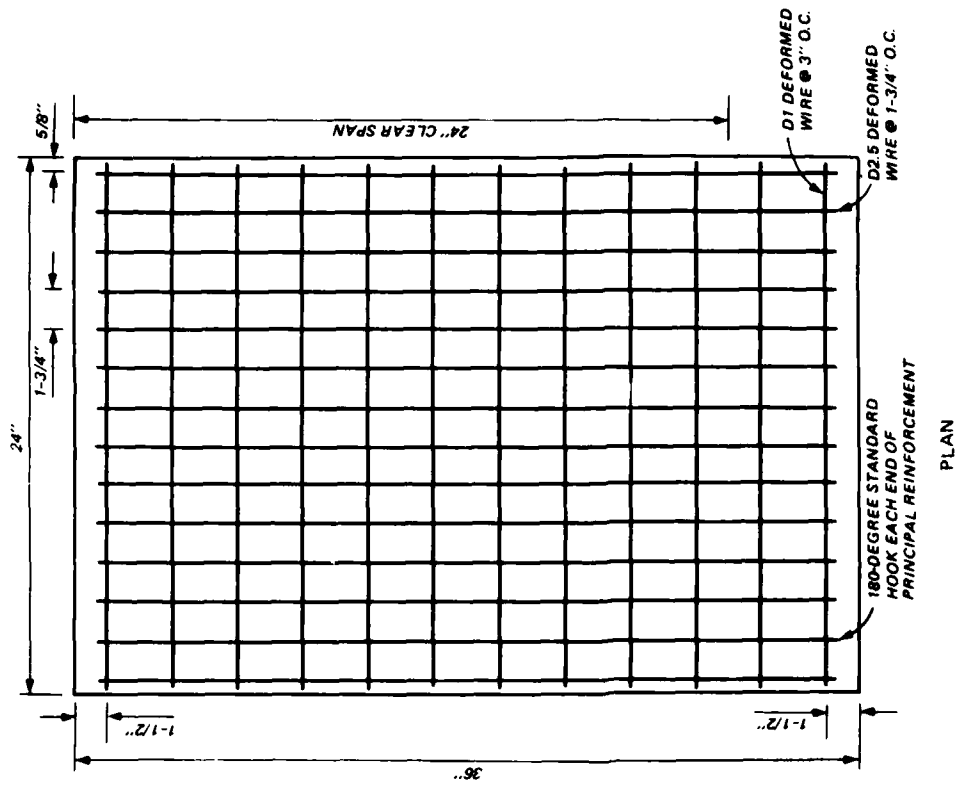


Figure 2.1. Principal and transverse reinforcement layout (Slabs 1-8).

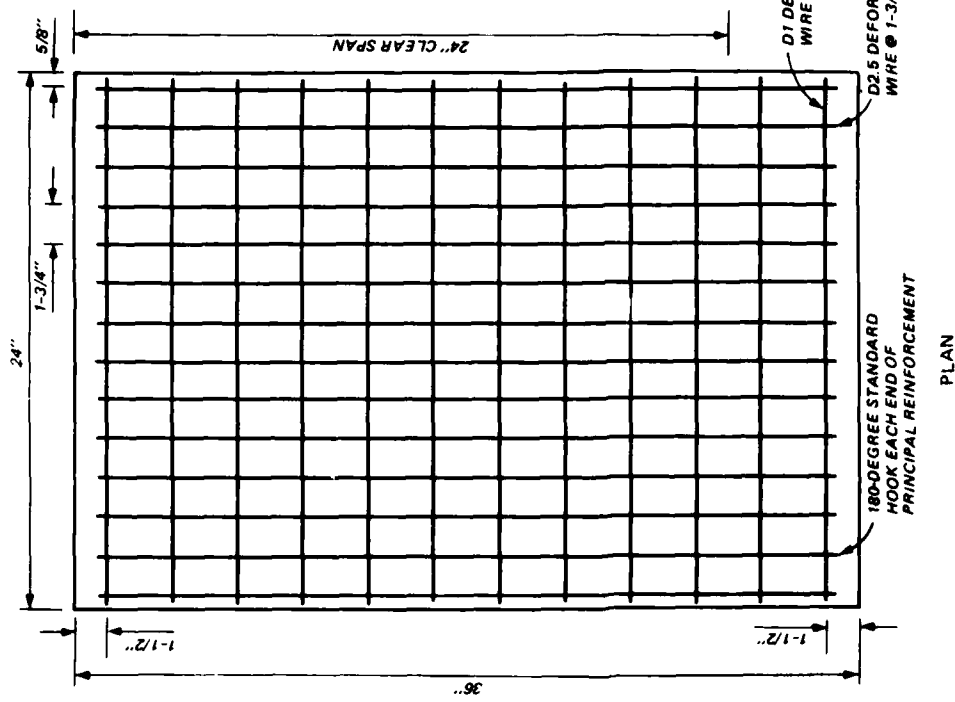
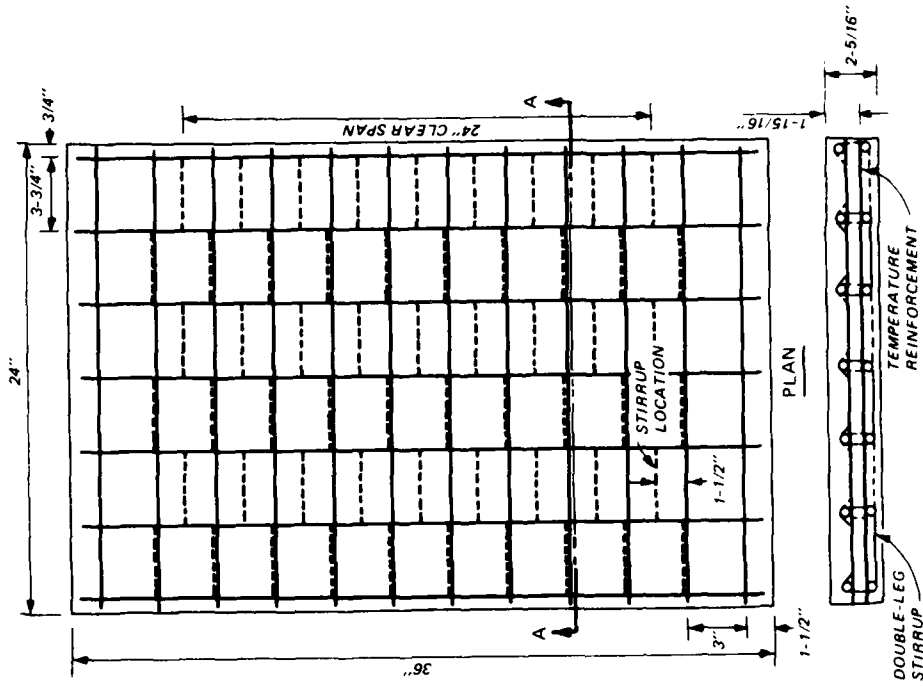
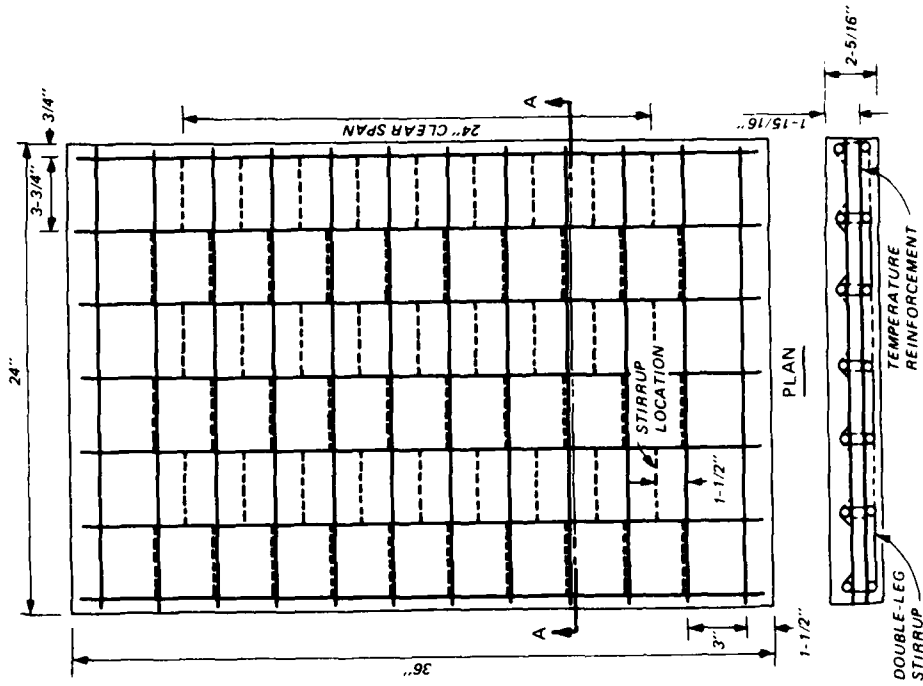


Figure 2.2. Principal and transverse reinforcement layout (Slabs 9 and 10).



SECTION A-A

Figure 2.3. Stirrup placement, single-leg stirrups.



SECTION A-A

Figure 2.4. Stirrup placement, double-leg stirrups.



Figure 2.5. Slab 2 construction.

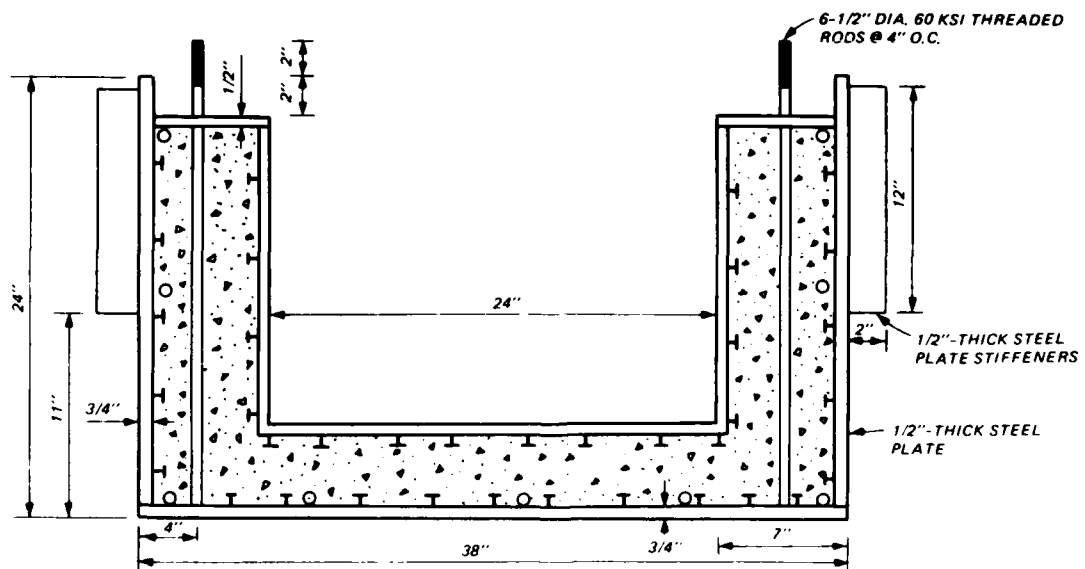


Figure 2.6. Cross section of reaction structure.

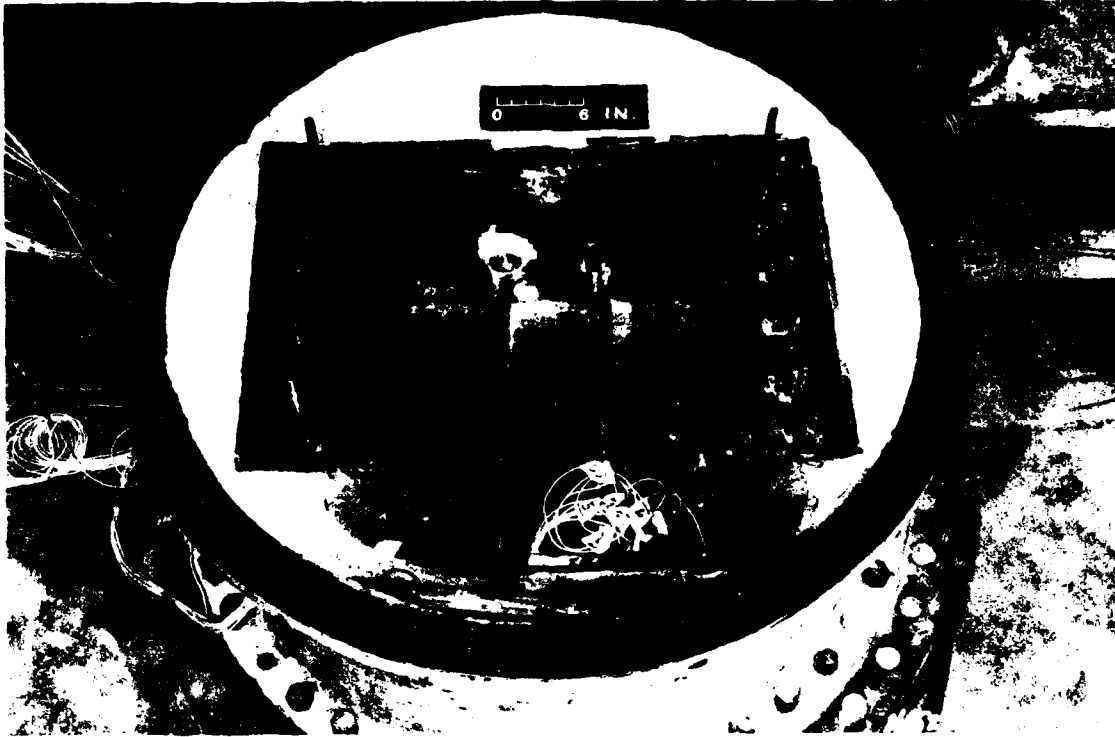


Figure 2.7. Reaction structure.

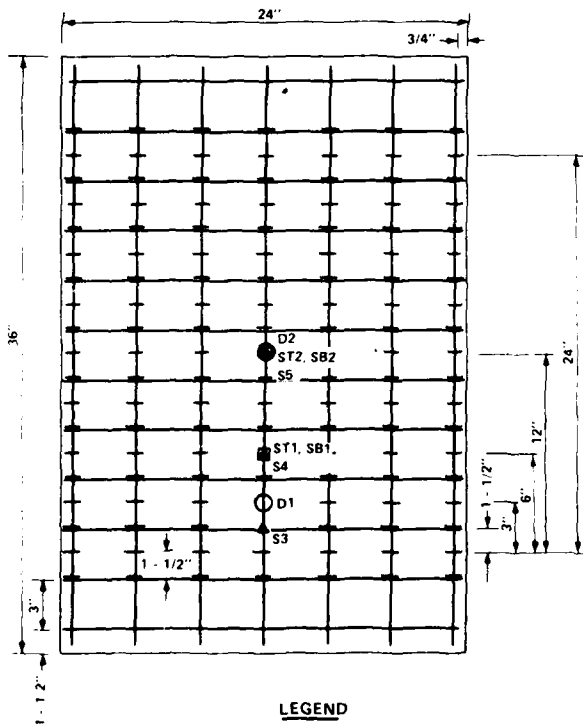
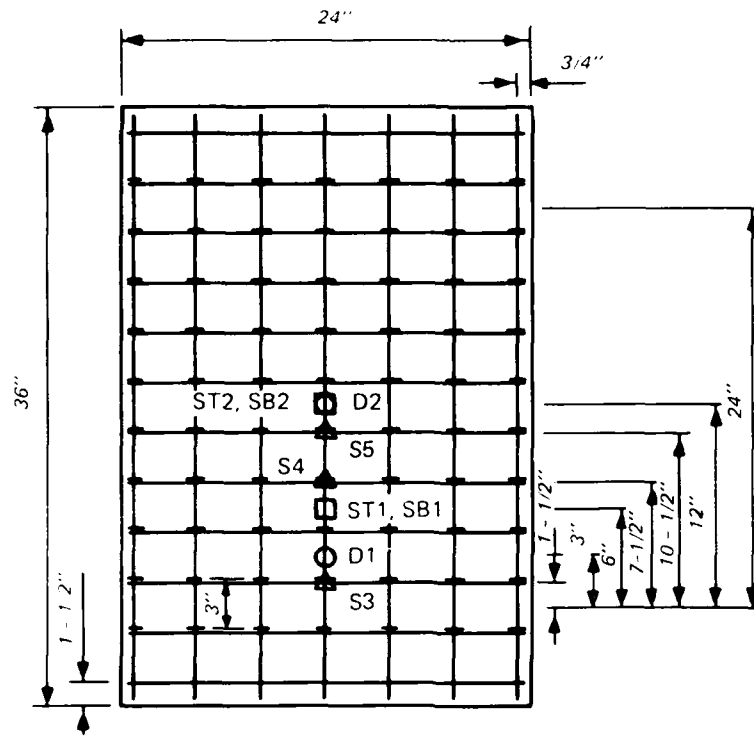


Figure 2.8. Instrumentation gage location.

- LEGEND**
- STRAIN GAGE ON TOP AND BOTTOM PRINCIPLE REINFORCED BARS
 - ▲ STRAIN GAGE ON STIRRUP
 - DISPLACEMENT GAGE BENEATH SLAB



LEGEND

- STRAIN GAGE ON TOP AND BOTTOM PRINCIPLE REINFORCEMENT BARS
- △ STRAIN GAGE ON STIRRUP
- DEFLECTION GAGE BENEATH SLAB

Figure 2.9. Instrumentation gage location, Slab 4.

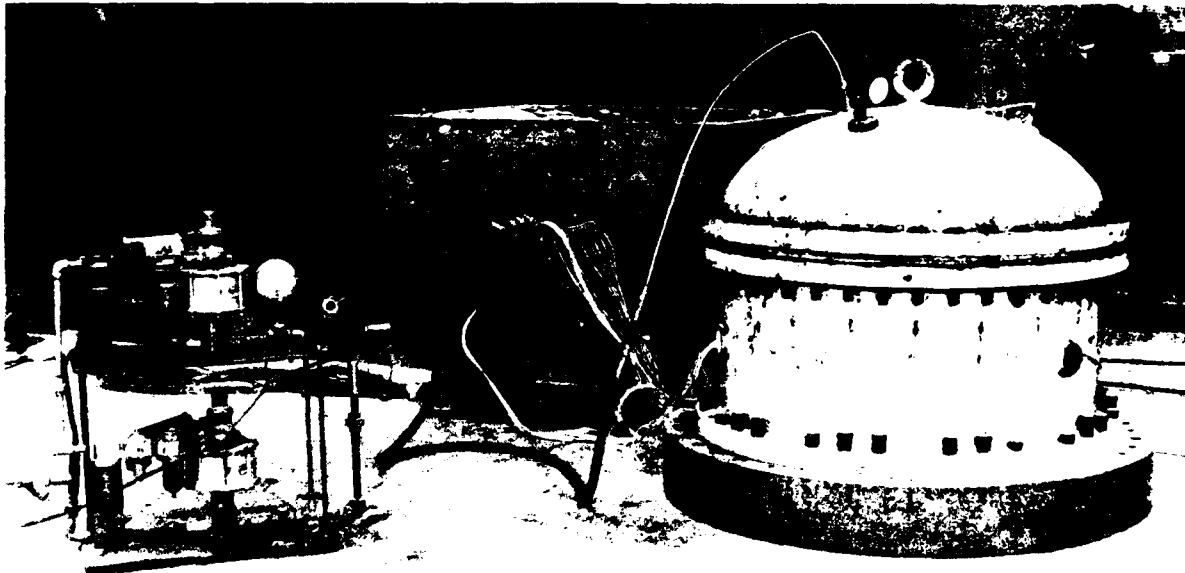


Figure 2.10. Four-foot-diameter blast load generator.



Figure 2.11. Membrane in place.

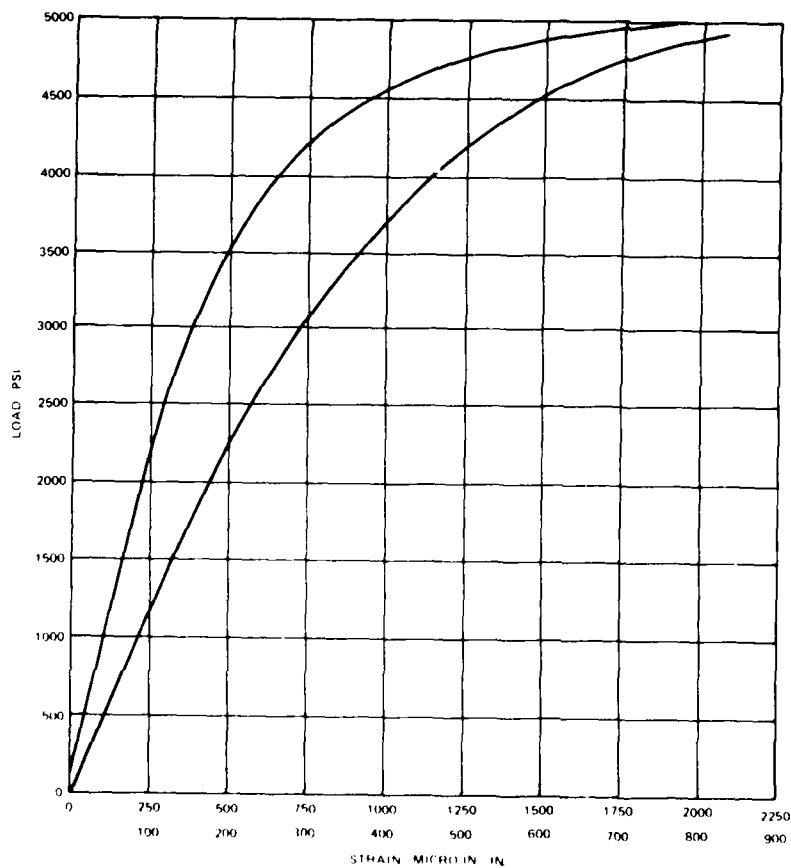


Figure 2.12. Strain gage data.

CHAPTER 3

TEST RESULTS

3.1 STRUCTURAL DAMAGE

Detailed posttest measurements and inspection provided a data check and damage assessment of each slab prior to removal from the test device. Figures 3.1 and 3.2 show overviews of two of the slabs representing the range of damage experienced in this test series. Similar views of each of the remaining eight slabs are presented in Figures A.1 through A.8 in Appendix A. The cracks were darkened with black ink markers for photographic purposes.

Figure 3.3 is a side view schematic of the general three-hinged mechanism that was formed in each slab. The measured posttest midspan deflection represented by the variable Δ is also given in Figure 3.3 for each slab. Posttest measurements also documented damage at the critical hinge regions of the three-hinged mechanism. Tables 3.1 and 3.2 present the posttest data measured at midspan and at the supports, respectively.

3.2 PHOTOGRAPHIC DATA

Figure 3.4 shows the underside of all 10 slabs after removal from the test device. It is evident that all slabs underwent the same general form of response, but variations in the pattern of the smaller cracks are obvious.

Photography during the application of load resulted in documentation of crack formation on the undersurface of eight slabs at several pressure levels. Malfunctions of camera equipment prohibited the collection of photographic data during tests on Slabs 4 and 7. Figure 3.5 consists of photographs taken during the testing of Slab 8, showing the crack formation sequence typical of most of the slabs. The general view of the photographs is from near the support (top of photograph) to slightly past midspan. The displacement gage probe mounted to the undersurface of the slab indicates the location of midspan, and the black dashed line is at the one-fourth span of the one-way slab.

Figure 3.6 shows the pressure and midspan displacement at the time each of the photographs was taken. Points labeled 1 through 11 correspond to Figure 3.5, a through k, respectively. Table 3.3 summarizes the data shown in Figure 3.6.

3.3 INSTRUMENTATION DATA

The electronically recorded data are presented in Appendix B. A summary of the data is presented in this section, and a more detailed analysis is presented in Chapter 4.

Due to a water leak and pressure loss during the first loading of Slab 5 at a pressure of about 55 psi, the slab was reloaded (Test 5B). Data for Test 5B are shown on pages 121 through 130.

In general, the quality of the recovered data was very good. Gages SB2 and S3 in Slab 7 and Gages D1 and S5 in Slab 10 failed to operate properly, resulting in a 96-percent data recovery for the test series.

Figure 3.7 shows the general shape of the midspan load-deflection curve for the slabs as measured with Gages P1 and D2. Values of load and deflection at points A through D in Figure 3.7 are given in Table 3.4. During the testing procedure, the decision to terminate a test depended upon the trend of the monitored load-deflection curve; therefore, the deflection at test termination varied among slabs.

Maximum deflections measured at midspan (as presented in Figure 3.3) differ from those in Table 3.4. Values presented in Figure 3.3 were physically measured after each test while those in Table 3.4 were electronically recorded during each test. The data presented in Appendix B indicate a rebound in most of the slabs following pressure relief at test termination. A comparison of the electronically recorded residual deflections with the post-test measured deflections is presented in Table 3.5.

The posttest measured deflection was greater than or equal to the electronically recorded residual deflection for each slab. The discrepancies were due to kinking of the displacement transducer probe at large slab deflections. The R/M ratio given in Table 3.5 is an indication of the discrepancies in recorded and measured maximum deflections at midspan. In general, the recorded strain gage data appeared to be good. The gages on principal reinforcement indicated yielding and rupture of steel, and the gages on stirrups indicated strains below yield.

Table 3.1. Structural damage at midspan.

Slab	Measured Midspan Deflection in	Bottom Bars Broken percent	Top Bars Broken percent	Width of Crushed Area in	Width of Crack on Undersurface in
1	3.5	86	0	3 to 9	1.5 to 2.0
2	4.5	100	43	1.75 to 10	1.25 to 2.5
3	3.0	100	0	0.5 to 4	0.25 to 2.0
4	2.8	100	0	1 to 4	0.5 to 1.5
5	3.25	86	0	2 to 8	1.25 to 1.5
6	3.0	71	0	1.25 to 6	0.5 to 1.0
7	3.1	86	0	1.5 to 8	1.0 to 1.5
8	3.0	71	0	1 to 7	1.0 to 2.5
9	3.5	100	0	1.5 to 4	0.5 to 1.25
10	4.0	100	57	2 to 7	1.5 to 4.0

Table 3.2. Structural damage at supports.

Slab	Top Crack Width in	Measurable Top Crack Depth in	Top Bars Broken percent
1	0.5 to 1	2.00	50
2	0.5 to 2	1.75	64
3	0.1 to 0.5	0.90	43
4	0.1 to 0.75	0.90	29
5	0.1 to 0.6	1.25	14
6	0.25 to 0.5	1.00	14
7	0.1 to 0.6	1.10	14
8	0.1 to 0.5	0.75	14
9	0.1 to 1	1.50	39
10	0.1 to 1	1.50	71

Table 3.3. Photographic data summary for Slab 8.

<u>Point Labeled (Figure 3.6)</u>	<u>Corresponding Figure</u>	<u>Pressure psi</u>	<u>Displacement in</u>
1	3.5a	23	0.12
2	3.5b	40	0.20
3	3.5c	53	0.37
4	3.5d	69	0.85
5	3.5e	65	1.20
6	3.5f	53	1.90
7	3.5g	58	2.30
8	3.5h	54	3.10
9	3.5i	38	3.10
10	3.5j	12	2.90
11	3.5k	0	2.80

Table 3.4. Load-deflection summary.

<u>Slab</u>	<u>Load-Deflection</u>							
	<u>P_A psi</u>	<u>Δ_A in</u>	<u>P_B psi</u>	<u>Δ_B in</u>	<u>P_C psi</u>	<u>Δ_C in</u>	<u>P_D psi</u>	<u>Δ_D in</u>
1	59.7	0.75	42	1.8	35	3.1	43	3.7
2	66.1	0.75	39	2.1	41	3.1	66	4.1
3	71.6	0.75	32	1.7	45	3.0	a	a
4	76.0	0.75	52	1.7	45	2.8	a	a
5	75.2	0.65	47	1.6	47	2.4	67	3.2
6	66.6	1.1	55	1.8	49	3.1	a	a
7	65.5	0.85	42	1.8	42	2.7	55	3.4
8	69.5	0.80	51	2.0	48	2.8	54	3.1
9	71.0	0.75	41	1.6	37	2.9	56	3.4
10	77.4	0.90	42	1.7	42	2.8	85	3.4

^aNo increase in load-carrying capacity experienced.

Table 3.5. Residual midspan deflection.

Slab	Posttest Measured (M) in	Electronically Recorded (R) in	R/M
1	3.5	3.5	1.0
2	4.5	4.0	0.89
3	3.0	2.7	0.90
4	2.8	2.5	0.89
5	3.3	3.0	0.91
6	3.0	2.8	0.93
7	3.1	3.1	1.0
8	3.0	2.8	0.93
9	3.5	3.4	0.97
10	4.0	3.4	0.85

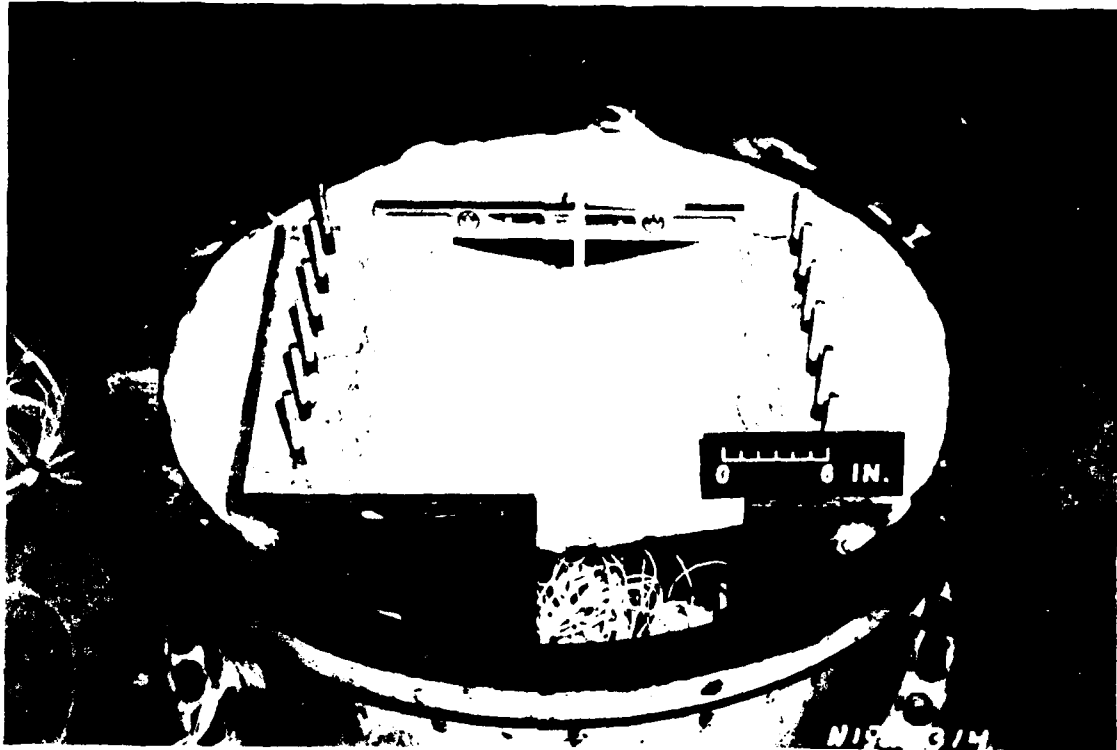


Figure 3.1. Posttest view of Slab 4.

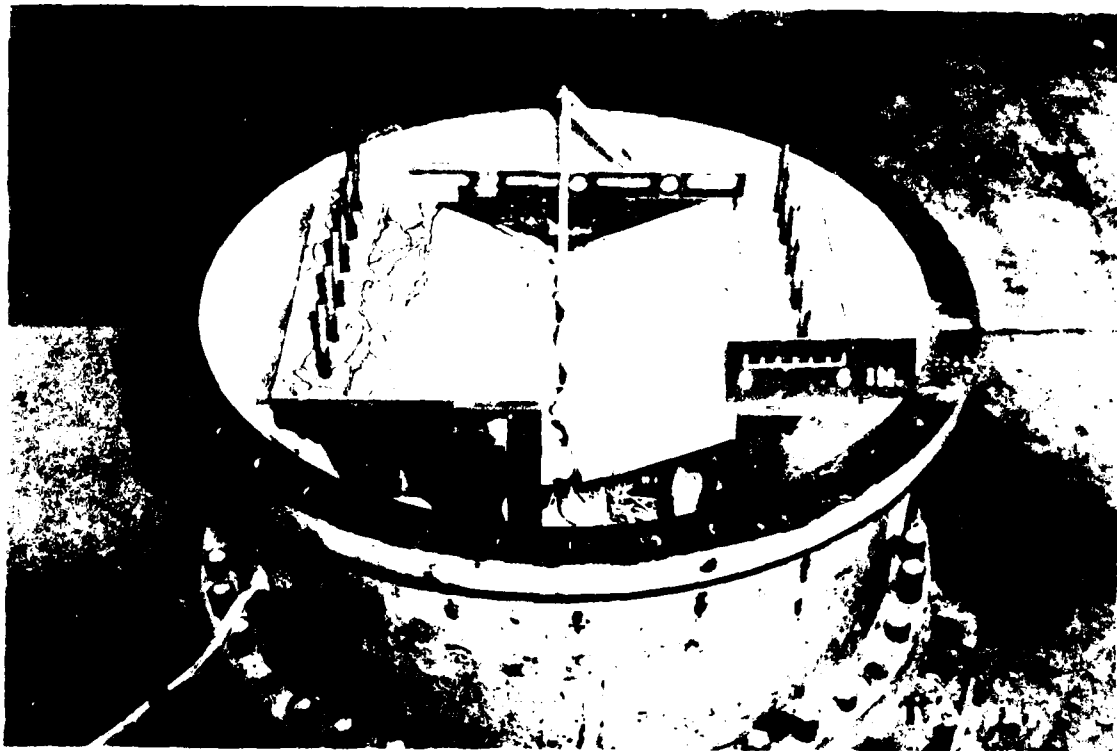


Figure 3.2. Posttest view of Slab 2.

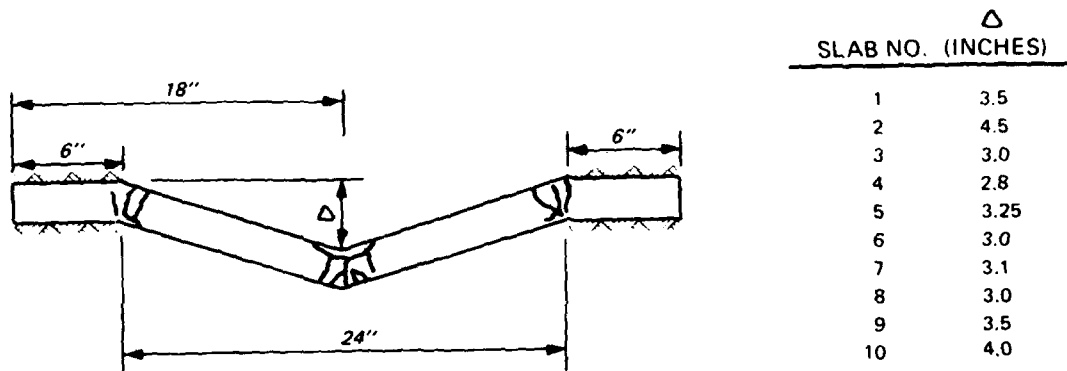
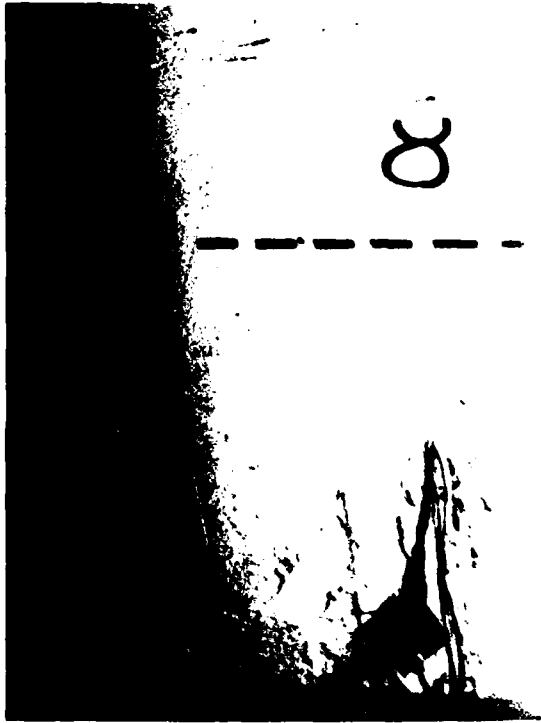


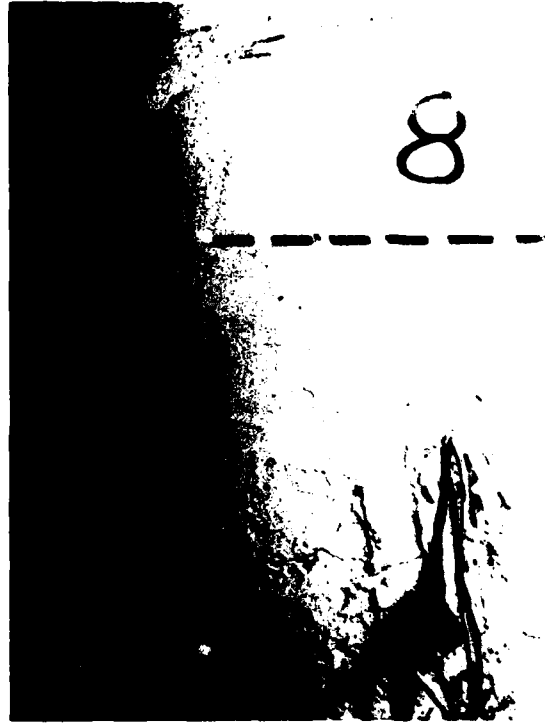
Figure 3.3. General deformation.



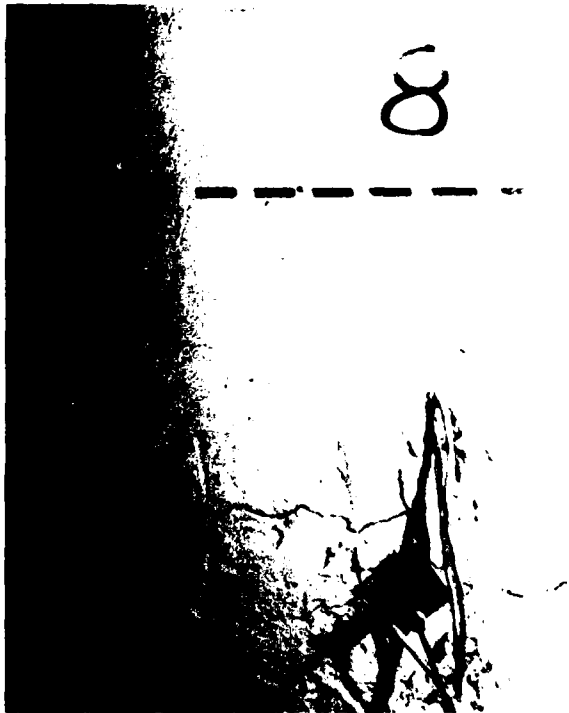
Figure 3.4. Posttest view of underside of slabs.



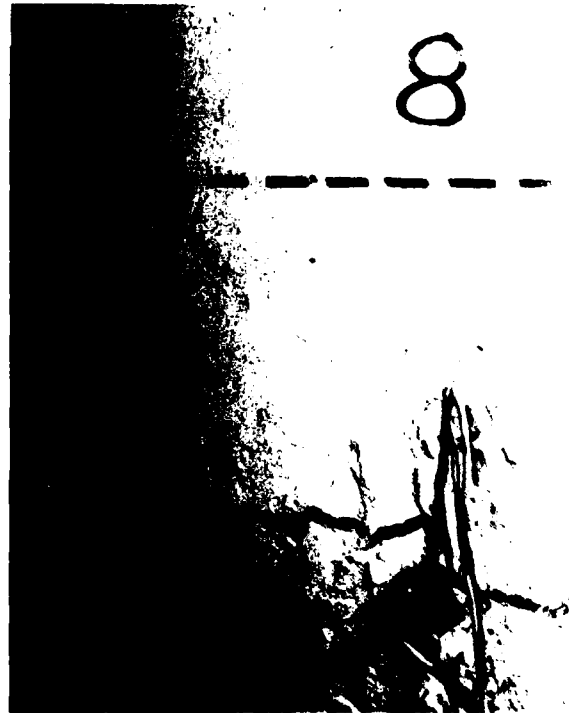
a. 23 psi, 0.12 inch.



b. 40 psi, 0.20 inch.



c. 53 psi, 0.37 inch.

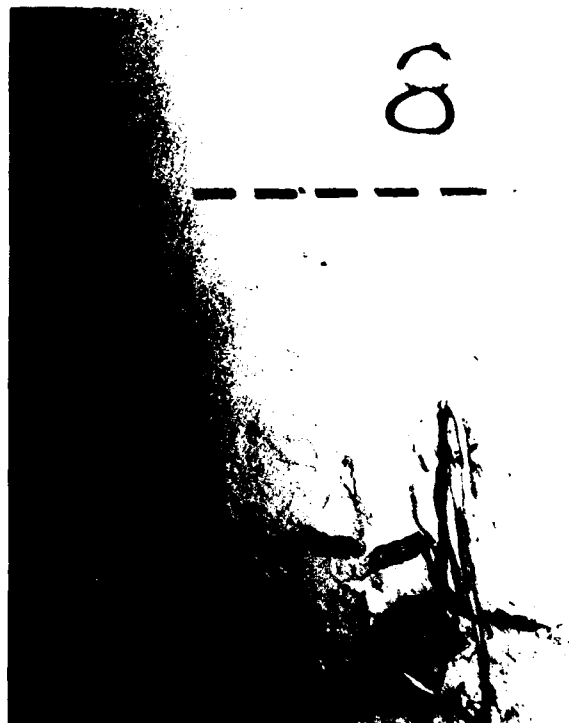


d. 69 psi, 0.85 inch.

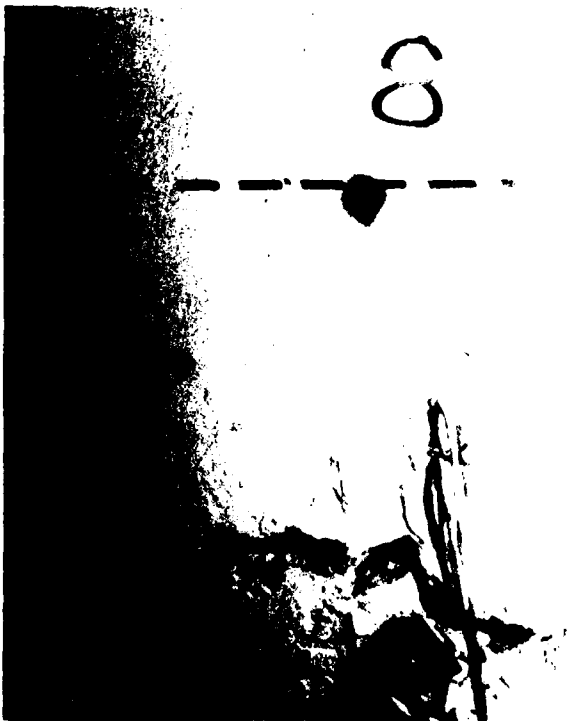
Figure 3.5. Sequence of crack formation, Slab 8 (Sheet 1 of 3).



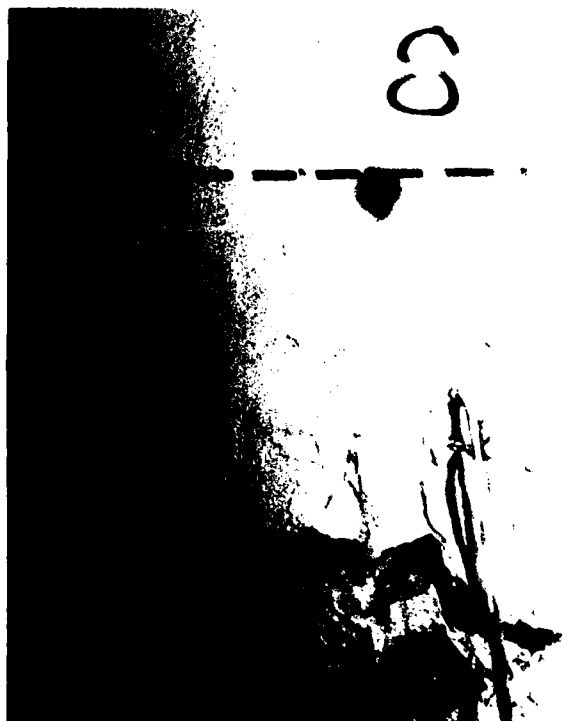
e. 65 psi, 1.20 inches.



f. 53 psi, 1.90 inches.



g. 58 psi, 2.30 inches.



h. 54 psi, 3.10 inches.

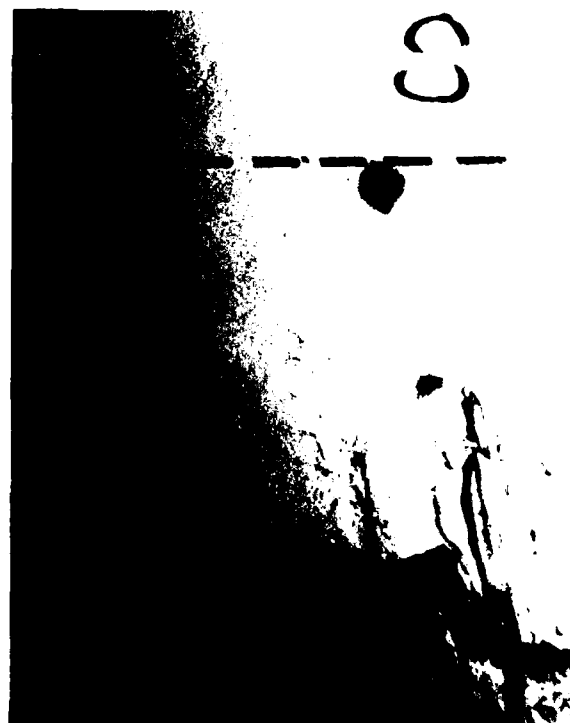
Figure 3.5. (Sheet 2 of 3).



i. 38 psi, 3.10 inches.



j. 12 psi, 2.90 inches.



k. 0 psi, 2.80 inches.

Figure 3.5. (Sheet 3 of 3).

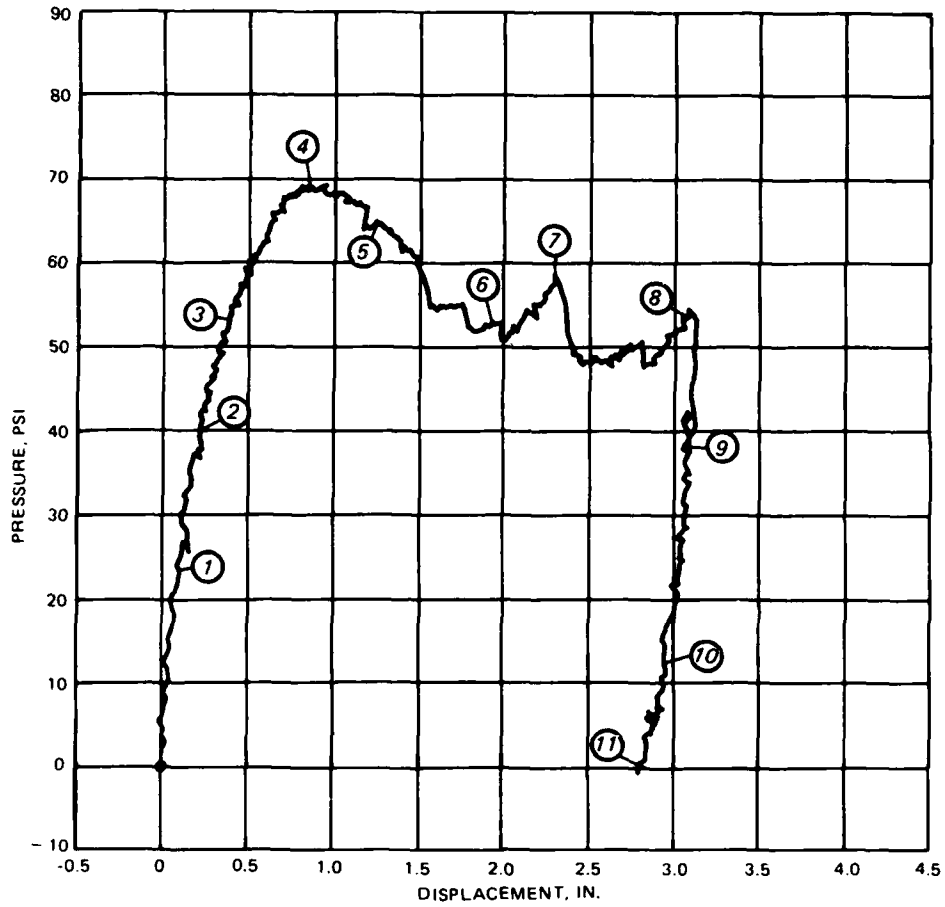


Figure 3.6. Slab 8 photographic sequence. Note: See Table 3.3. for data summary.

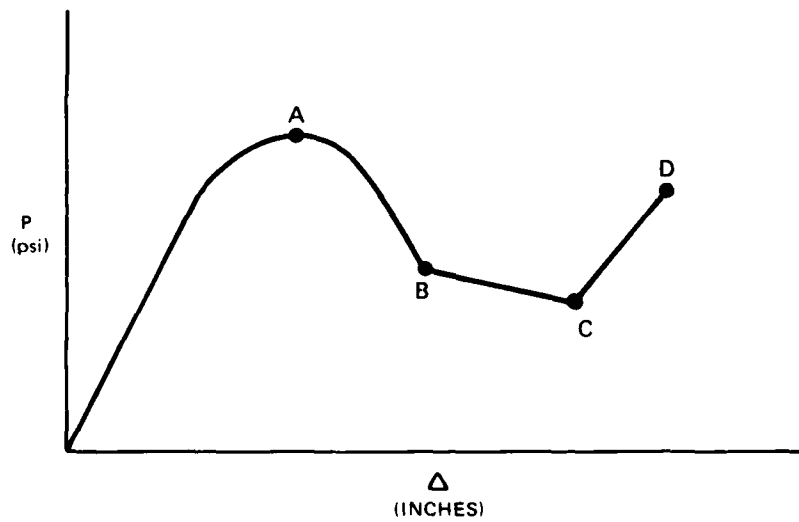


Figure 3.7. General load deflection.

CHAPTER 4

ANALYSIS

4.1 COMPARISON OF STRUCTURAL DAMAGE AND RESPONSE

Table 3.4 presents a load-deflection summary of the 10 slabs. In order to compare slab response and satisfy stated objectives, it is convenient to categorize the data in Table 3.4 by parameter investigated. The following discussion refers to points on the curve presented in Figure 3.7. Table 4.1 compares the results of tests on Slabs 3, 6, and 8 which were used to investigate the effects of the three stirrup configurations presented in Figure 1.1.

Ultimate load capacity (P_A) of Slab 6 was approximately 93 percent of that for Slab 3. Slab 8 had an ultimate load capacity that was approximately 97 percent of that for Slab 3. The load-deflection responses of the three slabs were similar except that a small increase in load-carrying capacity from Point C to Point D was experienced by Slab 8 but not by Slabs 3 and 6.

Although Slabs 5 and 7 were primarily tested to investigate the effects of temperature steel placement, they also provided data on the effects of stirrup Types II and III. As was the case for Slabs 3 and 6, the slab with Type III stirrups (Slab 7) had an ultimate load capacity less than the Type II stirrup slab (Slab 5). Data for Slabs 5 and 7 are shown in Table 4.2.

Table 4.3 shows that Slabs 1, 2, 3, and 4 were used to investigate stirrup spacing. The load capacity of Slab 2 at Point A was 8 percent and 13 percent less than Slabs 3 and 4, respectively. At Point B, the load capacity was 25 percent and 11 percent less than that of Slabs 3 and 4, respectively. Slab 1 had no stirrups (simulating a very large spacing) and the lowest value of P_A . Slab 1 had a slightly higher capacity at Point B than did Slab 2, but it had the lowest value at Point C. Slabs 2, 3, and 4 had relatively similar values for P_C . Slab 2 (the closest stirrup spacing) was the only slab of this group having P_D approximately equal to P_A . Slab 1 did show an increase in load capacity from Point C to Point D, but P_D was approximately equal to P_B (not P_A).

Slabs 3 and 4 behaved similarly, having almost identical load-deflection values at Point C.

Inconsistencies in the ultimate load capacity indicate scatter in the data. The ultimate load capacity decreased as stirrup spacing decreased from

3.0 inches to 0.75 inch; however, the slab with the largest spacing (no stirrups) had the lowest value of P_A instead of the highest.

Table 4.2 presents data for the two pairs of slabs used to investigate the effects of the two temperature steel placement conditions shown in Figure 1.2. Slabs 3 and 5 investigate the parameter, as do Slabs 6 and 7. The region of the load-deflection curve affected by the steel placement was at large deflections. Slabs 5 and 7 experienced an increase in load resistance from Point C to Point D, whereas Slabs 3 and 6 were constructed with the interior placement condition and experienced no significant increase in load resistance beyond Point B.

Table 4.4 shows that two pairs of slabs were used to investigate the effects of the principal steel spacings shown in Figure 1.3. Slabs 2 and 10 constituted one pair used to investigate the parameter, and the other pair consisted of Slabs 3 and 9.

Slabs 3 and 9 in Table 4.4 had stirrups spaced at 1.5 inches. Slab 9 had a closer spacing of principal steel and exhibited an increase in load resistance from Point C to Point D ($P_D \approx 0.79 P_A$), whereas Slab 3 did not. Slab 10 had a stirrup spacing of 0.75 inch and the closer principal steel spacing of 1.75 inches. It was observed from Table 4.3 that Slab 2 with a 0.75-inch stirrup spacing was the only slab of that group with a significant increase in load resistance at Point D ($P_D \approx P_A$). Slab 10 exhibited a greater increase in load resistance ($P_D = 1.10 P_A$) at large deflections than any of the slabs in the test series. It is not clear whether the closer principal reinforcing is totally responsible for the increased resistance, since the testing of Slab 3 was terminated at a deflection of about 3.0 inches (the deflection at which Slab 9 began increasing in load resistance).

4.2 YIELD-LINE THEORY

The method of limit analysis of reinforced concrete slabs known as the yield-line theory was developed by Johansen (Reference 32). An assumed collapse mechanism consistent with boundary conditions is used to estimate the ultimate load capacity of the slab. Considering the moments of the plastic hinge lines as the ultimate moments of resistance, the ultimate load is determined using the principle of virtual work or the equations of equilibrium. As Park and Gamble (Reference 38) point out, Johansen's yield criterion is for the case where in-plane (membrane) forces do not exist in the slab. The

yield-line theory assumes that the slab has sufficient shear strength to insure a flexural collapse mode of failure.

The results of applying the yield-line theory to the slabs in this study are presented in Table 4.5 along with the experimental values of ultimate load resistance. An average test-day concrete compressive strength of 4,790 was used in the yield-line calculations. The yield-line theory predicts from approximately 57.8 to 73.5 percent of the experimental values for this test series. The greater percentage (73.5) was for Slab 1, which was the only slab without stirrups.

The predicted yield-line values were based upon nominal moment capacities of the slabs calculated in accordance with the ultimate strength method of the 1983 ACI Code (Reference 53). Slabs 1 through 8 had nominal moment capacities of approximately 42.5 and 33.3 inch-kips at the midspan and the supports, respectively. Slabs 9 and 10 had nominal moment capacities of approximately 43.6 and 34.3 inch-kips at the midspan and the supports, respectively. Slabs 9 and 10 differed from Slabs 1 through 8 in this calculation due to the use of $f_y = 62.4$ ksi rather than 60.0 ksi.

The virtual-work method was used, whereby the work performed by the external loads during the displacement is equated to the internal work absorbed by the hinges. The ultimate load W for a uniformly loaded fixed beam or one-way slab may be expressed as

$$W = 8 \frac{(M_s + M_m)}{L^2} \quad (4.1)$$

where:

- W = uniform load
- M_s = moment capacity at the support
- M_m = moment capacity at midspan
- L = length of beam

4.3 COMPRESSIVE MEMBRANE EFFECT

As discussed in Chapter 1, compressive membrane forces are induced in slabs whose edges are restrained against lateral movement. As the slab deflects, changes of geometry cause the slab edges to tend to move outward and to react against the stiff boundary elements. The membrane forces enhance the

flexural strength of the slab sections at the yield lines.

Table 4.6 presents the results of applying compressive membrane theory to the slabs at ultimate resistance along with the experimental values. An average test-day concrete compressive strength of 4,790 psi was used.

The approach utilized for compressive membrane theory was that developed by Park (Reference 42) and discussed by Park and Gamble (Reference 38). A fixed-end strip with plastic hinges and full restraint against rotation and vertical translation is assumed by the theory. The ends of the strip are considered to be partially restrained against lateral displacement. Other assumptions include: (1) the tension steel has yielded at each plastic hinge, (2) the compressed concrete has reached its strength with the stress distribution as defined by the 1983 ACI Code (Reference 53), (3) the tensile strength of the concrete can be neglected, (4) the top steel at opposite supports has the same area per unit width, (5) the bottom steel is constant along the length of the strip, but the top and bottom steel may be different, (6) the portions of the strip between plastic hinge sections remain straight, and (7) the sum of the elastic creep and shrinkage axial strain have a constant value along the length of the strip.

The compressive membrane values in Table 4.6 were calculated through the use of a computer program at WES which utilizes Park's theory. The deflection-thickness, $(\Delta/t)_{ult}$ values in Table 4.6 are the experimental ratios of midspan deflection at ultimate resistance to slab thickness. Wood (Reference 41), Park (Reference 42), and Morley (Reference 43) assume a ratio of 0.5. Hung and Nawy (Reference 44) use experimental values to conclude that ratios ranging between about 0.4 and 1.0 should be considered. Work by Isaza (Reference 45) indicates a ratio of about 0.17.

Table 4.7 shows that compressive membrane theory is sensitive to the $(\Delta/t)_{ult}$ ratio. Deflection-thickness ratios suggested by the above researchers are applied, resulting in considerable variation in predicted load resistance. Experimental ultimate load resistance values are given for comparison.

Predicted resistance, assuming $(\Delta/t)_{ult}$ of 0.5, corresponds more closely to the predicted yield-line theory values of Table 4.5 than to the experimental values. The trend observed from Table 4.7 is that predicted ultimate resistance increases with decreasing $(\Delta/t)_{ult}$ ratios. This trend is also indicated in the experimental data. Slabs 1 through 8 had similar

principal steel spacings, although there were some differences among the slabs. Of that group, Slabs 3, 5, 6, 7, and 8 had stirrup spacings of 1.5 inches, but did vary in stirrup type and temperature steel placement. Table 4.8 lists the five slabs by order of increasing experimental $(\Delta/t)_{ult}$ ratios. Slab 6 had a slightly higher ultimate resistance than Slab 7, causing an inconsistency in the trend.

It is evident from Table 4.7 that the compressive membrane theory closely approximates the experimental ultimate resistance for 60 percent of the slabs (2, 3, 6, 7, 8, and 9) when a $(\Delta/t)_{ult}$ ratio of 0.3 is used. Thirty percent (Slabs 4, 5, and 10) are approximated by the criteria of $(\Delta/t)_{ult}$ equal to 0.17, and the remaining slab (Slab 1) is approximated using a ratio of 0.4. No correlation of the varying parameters of this investigation with the $(\Delta/t)_{ult}$ ratio was apparent, except that only the slab without stirrups had an ultimate resistance more closely approximated by the use of a $(\Delta/t)_{ult}$ ratio of 0.4.

Roberts (Reference 40) concluded that the deflection of maximum load is not a fixed proportion of the slab thickness. Two slab strips in that study had tensile steel percentages and compressive concrete strengths very similar to that of the current study, and a $(\Delta/t)_{ult}$ ratio of about 0.275 was observed. The 0.275 value is similar to the approximate value of 0.3 observed in the majority of slab tests in this study.

4.4 ROTATION CAPACITY

Figure 4.1 shows the idealized behavior of a beam or one-way slab under uniform loading. The structure initially undergoes elastic deflection. Under continued loading, plastic hinges first form at the supports and later at mid-span. The rotational capacity of the plastic hinges is directly related to the ductility of the slab. The inelastic rotation that can occur in the vicinity of the plastic hinge (critical section) may be expressed as

$$\theta_p = (\phi_u - \phi_y)l_p \quad (4.2)$$

where:

θ_p = plastic hinge rotation to one side of the critical section

ϕ_u = ultimate curvature of the section

ϕ_y = yield curvature of the section

l_p = equivalent plastic hinge length

as discussed by Park and Paulay (Reference 4).

Corley (Reference 24), Mattock (Reference 22), and Baker and Amarakone (Reference 30) have proposed empirical expressions for λ_p and the maximum concrete strain (ϵ_c) at ultimate curvature. Based on tests on simply supported beams, Corley proposed:

$$\begin{aligned} \lambda_p &= 0.5d + 0.2\sqrt{d} \frac{Z}{d} \\ \epsilon_c &= 0.003 + 0.02 \frac{b}{Z} + \left(\frac{\rho_s f_y}{20} \right)^2 \end{aligned} \quad (4.3)$$

where:

d = effective depth of beam

Z = distance from the critical section to the point of contraflexure

b = width of beam

ρ_s = ratio of volume of confining steel (including compression steel) to volume of concrete core

f_y = yield strength of the confining steel in kips per square inch.

Mattock modified Corley's work and suggested the following expressions:

$$\begin{aligned} \lambda_p &= 0.5d + 0.05Z \\ \epsilon_c &= 0.003 + 0.02 \frac{b}{Z} + 0.2\rho_s \end{aligned} \quad (4.4)$$

where Z , B , d , and ρ_s are defined as in Equation 4.2.

For members confined by transverse steel, Baker proposes the following:

$$\begin{aligned} \lambda_p &= 0.8 k_1 k_3 \left(\frac{Z}{d} \right) c \\ \epsilon_c &= 0.0015 \left[1 + 150\rho_s + (0.7 - 10\rho_s) \frac{d}{c} \right] \leq 0.01 \end{aligned} \quad (4.5)$$

where:

k_1 = 0.7 for mild steel or 0.9 for cold-worked steel

k_3 = 0.6 when $f'_c = 5,000$ psi or 0.9 when $f'_c = 1,700$ psi,
assuming $f'_c = 0.85 \times$ cube strength of concrete

c = neutral axis depth at the ultimate moment

ρ_s = ratio of volume of the transverse confining reinforcement to the volume of the concrete core

The effect of stirrup spacing on rotation capacity in the slabs in this study was investigated using the expressions by Corley, Mattock, and Baker. Values for curvature, strains, and neutral axis depth used in the calculations were obtained by use of a computer program developed by Mahin and Bertero called Reinforced Concrete Column Analysis (RCCOLA) (Reference 54). The RCCOLA program evaluates general flexural characteristics of reinforced concrete cross sections subjected to axial forces and uniaxial bending moments. The stress-strain relationship for concrete utilized by the program was that proposed by Kent and Park (Reference 17) for concrete confined by rectangular hoops.

The results of the calculations are presented in Figure 4.2 for the plastic hinge rotation to one side of the critical section at midspan. Similar results were obtained at the support critical sections. Figure 4.2 shows that discrepancies pertaining to rotation capacity exist among researchers. The significance of Figure 4.2 is that it shows an increase in rotation capacity when close stirrup spacings are used.

The vertical dashed lines in Figure 4.2 indicate the spacings used in this test series (0.75, 1.5, and 3.0 inches). The predicted increase in rotation capacity induced by the 0.75-inch spacing compared to the 3.0-inch spacing is slightly greater than 0.01 radian when using Corley's criterion. The predicted enhancement is less when using Mattock's or Baker's criterion. The predicted enhancement due to the 1.5-inch spacing is less than one-half of that due to the 0.75-inch spacing. At the 3.0-inch spacing, an increase of only about 0.0015 radian is predicted by Corley's criterion when compared to a larger spacing of 6.0 inches. The slopes of all three curves in Figure 4.2 approach zero beyond the 6.0-inch spacing.

It should be noted that the empirical expressions are for design purposes and tend to be conservative. Considering the evaluation of rotation capacity, the results may be questionable. In fact, Burnett (Reference 29) discusses that both the concept and use of curvature are unrealistic for postyield response. Table 4.2 indicates that the stirrup spacing had no significant effect on the behavior of the slabs until the region of large deflections (2 to 4 inches). Having similar load-deflection curves up to ultimate load, Slabs 1 through 4 all reached ultimate load capacity at a midspan deflection of 0.75 inch.

Using the support plastic hinge rotation capacities determined from the

Corley, Mattock, and Baker criteria, midspan deflections at the predicted rotations were computed for Slabs 2, 3, and 4, and are presented in Table 4.9. The theory implies that the ductility of the slabs should be adequate to maintain the ultimate load capacity to the deflections in Table 4.9. Close examination of the experimental load-deflection curves shows that Slabs 2, 3, and 4 experienced sharp drops in load resistance of several pounds per square inch at midspan deflections of about 1.25, 1.25, and 1.2, respectively. The load resistances immediately prior to the sudden drops were 97, 92, and 89 percent, respectively, of the ultimate load capacities for Slabs 2, 3, and 4. Deflections derived from Corley's criterion most accurately predict experimental deflections incurred prior to sharp decreases in load resistance. The validity of this comparison is questionable since, as mentioned in the discussion comparing structural damage and response, there appear to be inconsistencies in the ultimate load capacities for Slabs 1 through 4. Also, the calculations based on Corley's criterion do not account for in-plane compressive membrane thrusts. Slab 1 experienced a more gradual decline in load resistance past the ultimate load and did not incur a sudden drop in resistance until a deflection of about 1.6 inches was reached.

Based on beam test data, Keenan and others (Reference 21) state that reinforced concrete members with compression steel can reliably maintain their ultimate moment resistance to support rotations of up to 4 degrees, provided the compression bars are confined by effective ties and $q \leq 0.14$ where q is the reinforcing index defined by:

$$q = \frac{(\rho f_y - \rho' f'_y)}{f'_c} \quad (4.6)$$

The slabs in this test series meet Keenan's criterion assuming the stirrups act as effective ties. A support rotation of 4 degrees implies a midspan deflection of approximately 0.84 inch, which is 84 to 88 percent of that predicted using Corley's criterion for Slabs 2, 3, and 4.

The rotational capacity of a plastic hinge, particularly for design purposes, is limited to situations in which one of the following actions occurs:

1. Tension steel fractures.
2. The concrete compression block crushes.

3. Compression steel buckles.

4. Ties fracture in tension.

In the case of the slabs in this study, a redistribution of forces at the critical hinge sections allowed the slabs to continue carrying some load after one or more of the above failure modes had occurred in portions of the critical sections. Considering the formation of a three-hinge mechanism, the rotation of the hinges at the supports when the tests were terminated (anticipated incipient collapse) are presented in Table 4.10. Table 4.10 also gives the percentage ratio of maximum attained midspan deflection (Δ_{\max}) to the clear span length (L).

4.5 TENSILE MEMBRANE EFFECT

It is generally known (Reference 38) that after the ultimate load resistance has been reached in a reinforced concrete slab, the supported load decreases until membrane forces in the central region of the slab change from compression to tension. In pure tensile membrane behavior, cracks penetrate the whole slab thickness, and yielding of the steel spreads throughout the central region of the slab. The load is carried mainly by the reinforcing bars acting as a tensile net or membrane.

Park (Reference 48) concluded that pure tensile membrane action did not occur in lightly reinforced two-way slabs, since the cracking present at the end of the tests was little more than the cracking which developed with the yield-line pattern at the ultimate flexural load. Therefore, the load was carried by a combined bending and tensile membrane action. Similarly, Figure 3.5, d. and k. show little change in the crack pattern during testing of Slab 8. The dominant cracks became larger in width and depth, but significant spreading of the crack pattern was not evident. Table 3.4 shows that Slabs 2 and 10 exhibited the most significant increases in load resistance in the tensile membrane region. Figure 3.4 shows that Slabs 2 and 10 also experienced the greatest spread in crack patterns.

Park (Reference 48) gives criteria for predicting the slab response in the tensile membrane region. For uniformly loaded one-way slabs, the relationship between the load and the midspan deflection is approximated as:

$$\Delta = \frac{WL^2}{8T} \quad (4.7)$$

where T = yield force of the reinforcement per unit width. Figures 4.3 through 4.12 show the linear regression proposed by Park plotted on the experimental load-deflection curves of Slabs 1 through 10, respectively. Most of the slabs exhibited the tendency for an increase in load resistance at a midspan deflection between 1.75 and 2.0 inches ($d = 1.9375$ inches). The curves for Slabs 1, 4, 5, 7, and 8 clearly indicate a transition into the tensile membrane region near the intersection of the load-deflection curve and the predicted regression. The slopes of the experimental curves also appear to be similar to the predicted slope, particularly for Slabs 5 and 8. Though not as obvious as in the case of these slabs, the curve for Slab 10 also has a slight tendency to follow the predicted slope during initial stages of tensile membrane behavior.

Keenan (Reference 37) shows that the slab resistance just prior to tensile membrane behavior should nearly equal the computed yield-line resistance corresponding to zero thrust in the plane of the slab (Johansen's yield-line value). The yield-line resistance has been shown to be approximately 44 psi for Slabs 1 through 8 and 45 psi for Slabs 9 and 10. The transition into the tensile membrane region occurred at load resistances between about 42 and 45 psi for Slabs 1, 2, 4, 5, 7, 9, and 10, but the resistances of Slabs 3, 6, and 8 were around 50 to 52 psi. Slabs 3 and 6 never indicated strong tendencies for tensile membrane behavior, but rather gradually decayed in resistance from the ultimate load to nearly equal the yield-line value at a midspan deflection of about 3.0 inches.

Pure tensile membrane behavior did not occur in any of the slabs. Fracture of the tensile reinforcement (bottom steel at midspan and top steel at supports) weakens the tensile membrane effect.

Table 3.1 shows that large percentages of bottom bars at midspan and top bars at supports fractured. Only Slabs 2 and 10 experienced rupture of top bars at midspan. Table 3.2 shows that Slabs 2 and 10 also had the largest percentage of steel to fracture at the supports.

Slabs 1 through 4 investigated the effects of stirrup spacing, and all but Slab 1 incurred fracture of 100 percent of the bottom steel at midspan. Slab 1 had one unbroken bar remaining. All five slabs also experienced fracture of some top reinforcing at the supports.

Only the load-deflection curve for Slab 2 showed a steady increase in load resistance past a midspan deflection of about 2.5 inches.

A significant difference in the behavior of Slabs 3 and 5 was observed in the tensile membrane region. At a midspan deflection of 3.0 inches, the load resistance of Slab 5 had climbed from the yield-line resistance of approximately 45 to 60 psi. The load resistance of Slab 3 gradually decayed from ultimate load and was approximately equal to the yield-line resistance at the midspan deflection of 3.0 inches. Slabs 3 and 5 investigated the effects of temperature reinforcement placement in the "interior" and "exterior" conditions, respectively. Slabs 6 and 7 also investigated the parameter of temperature steel placement and yielded results similar to Slabs 3 and 5 but to a lesser degree.

Slabs 3, 5, 6, and 7 were all constructed with Type II or Type III single-leg stirrups spaced at 1.5 inches. Slab 8 was constructed with the Type I double-leg stirrup and temperature steel placed in the interior placement condition. Unlike Slabs 3 and 6, Slab 8 exhibited strong tendencies for increasing load resistance in the tensile membrane region. However, Slab 8 could not maintain a steady climb in load resistance.

Slabs 9 and 10 were constructed with a close principal steel spacing of 1.75 inches and experienced a sharper decay in load resistance after ultimate loading than Slabs 1 through 8. After the decay, the load resistances of Slabs 9 and 10 remained at or below the yield-line resistance until a deflection of about 3.0 inches was reached. A sharp increase in load resistance was then experienced in Slabs 9 and 10. The testing of Slab 9 was terminated at a lower pressure than Slab 10. It appears that the variation in stirrup spacing in the slabs having close principal reinforcement had little effect on the load-deflection behavior in the tensile membrane region.

The loading of Slabs 9 and 10 beyond a midspan deflection of 3.0 inches revealed that at very large displacements under slowly applied load, the tension loading of the top steel at midspan induces an increase in load resistance. It is not clear that this behavior would not have occurred in Slabs 3, 4, 6, and 8 since testing of these slabs was terminated at a midspan deflection of about 3.0 inches. Slab 1 had no stirrups and was tested to a midspan deflection of about 3.75 inches. Slab 1 did exhibit an increase in load resistance past the 3.0-inch deflection; however, the increase at the 3.75-inch deflection was significantly less than that in Slabs 9 and 10 at a deflection less than 3.5 inches.

Table 4.1. Stirrup configuration.

Slab	Stirrup Type	Stirrup Spacing in	P _A psi	Δ _A in	P _B psi	Δ _B in	P _C psi	Δ _C in	P _D psi	Δ _D in
8	I	1.5	69.5	0.80	51	2.0	48	2.8	54	3.1
3	II	1.5	71.6	0.75	52	1.7	45	3.0	a	a
6	III	1.5	66.6	1.1	55	1.8	49	3.1	a	a

^aTest was terminated due to large deflections and decreasing load-carrying capacity.

Table 4.2. Temperature steel placement.

Slab	Temperature Steel Placement	Stirrup Type	Stirrup Spacing in	P _A psi	Δ _A in	P _B psi	Δ _B in	P _C psi	Δ _C in	P _D psi	Δ _D in
3	Interior	II	1.5	71.6	0.75	52	1.7	45	3.0	a	a
5	Exterior	II	1.5	75.2	0.65	47	1.6	47	2.4	67	3.2
6	Interior	III	1.5	66.6	1.1	55	1.8	49	3.1	a	a
7	Exterior	III	1.5	65.5	0.85	42	1.8	42	2.7	55	3.4

^aTest was terminated due to large deflections and decreasing load-carrying capacity.

Table 4.3. Stirrup spacing.

Slab	Stirrup Type	Stirrup Spacing in	P _A psi	Δ _A in	P _B psi	Δ _B in	P _C psi	Δ _C in	P _D psi	Δ _D in
1	No stirrups	--	59.7	0.75	42	1.8	35	3.1	43	3.7
2	II	0.75	66.1	0.75	39	2.1	41	3.1	66	4.1
3	II	1.5	71.6	0.75	52	1.7	45	3.0	a	a
4	II	3.0	76.0	0.75	44	1.7	45	2.8	a	a

^aTest was terminated due to large deflections and decreasing load-carrying capacity.

Table 4.4. Principal steel spacing.

Slab	Principal Steel Spacing in.	Stirrup Type	Stirrup Spacing in	P _A psi	Δ _A in	P _B psi	Δ _B in	P _C psi	Δ _C in	P _D psi	Δ _D in
2	3.75	II	0.75	66.1	0.75	39	2.1	41	3.1	66	4.1
10	1.75	II	0.75	77.4	0.90	42	1.7	42	2.8	85	3.4
3	3.75	II	1.5	71.6	0.75	52	1.7	45	3.0	a	a
9	1.75	II	1.5	71.0	0.75	41	1.6	37	2.9	56	3.4

^aTest was terminated due to large deflections and decreasing load-carrying capacity.

Table 4.5. Yield-line theory versus experimental ultimate load resistance.

Slab	Yield-Line (YL) psi	Experimental (E) psi	YL/E percent
1	43.9	59.7	73.5
2	43.9	66.1	66.4
3	43.9	71.6	61.3
4	43.9	76.0	57.8
5	43.9	75.2	58.4
6	43.9	66.6	65.9
7	43.9	65.5	67.0
8	43.9	69.5	63.2
9	45.1	71.0	63.5
10	45.1	77.4	58.3

Table 4.6. Compressive membrane theory versus experimental ultimate load resistance.

Slab	Compressive Membrane CM psi	Δ/t	Experimental (E) psi	CM/E percent
1	66.6	0.32	59.7	111.6
2	66.6	0.32	66.1	100.8
3	66.6	0.32	71.6	93.0
4	66.6	0.32	76.0	87.6
5	70.5	0.28	75.2	93.8
6	52.5	0.48	66.6	78.8
7	61.9	0.37	65.5	94.5
8	63.7	0.35	69.5	91.7
9	69.1	0.32	71.0	97.3
10	62.6	0.39	77.4	80.9

Table 4.7. Ultimate resistance versus $(\Delta/t)_{ult}$

Slab	Experimental Resistance (E) psi	Predicted Resistance due to Compressive Membrane Theory for $(\Delta/t)_{ult} =$							
		(a)	(b)	(c)	(d)	a/E	b/E	c/E	d/E
		0.17 psi	0.3 psi	0.4 psi	0.5 psi	%	%	%	%
1	59.7	80.7	67.1	57.5	48.9	135.2	112.4	96.3	81.9
2	66.1	80.7	67.1	57.5	48.9	122.1	101.5	87.0	74.0
3	71.6	80.7	67.1	57.5	48.9	112.7	93.7	80.3	68.3
4	76.0	80.7	67.1	57.5	48.9	106.2	88.3	75.7	64.3
5	75.2	80.7	67.1	57.5	48.9	107.3	89.2	76.5	65.0
6	66.6	80.7	67.1	57.5	48.9	121.2	100.8	86.3	73.4
7	65.5	80.7	67.1	57.5	48.9	123.3	102.4	87.8	74.6
8	69.5	30.7	67.1	57.5	48.9	116.1	96.5	82.7	70.4
9	71.0	82.8	69.3	59.7	51.2	116.6	97.6	84.1	72.1
10	77.4	82.8	69.3	59.7	51.2	107.0	89.5	77.1	66.1

Table 4.8. Increasing $(\Delta/t)_{ult}$.

<u>Slab</u>	<u>$(\Delta/t)_{ult}$</u>	<u>Experimental Ultimate Resistance, psi</u>
5	0.28	75.2
3	0.32	71.6
8	0.35	69.5
7	0.37	65.5
6	0.48	66.6

Table 4.9. Predicted midspan deflection.

<u>Slab</u>	<u>Stirrup Spacing in</u>	<u>Midspan Deflection, in</u>		
		<u>Corley</u>	<u>Mattock</u>	<u>Baker</u>
2	0.75	1.0	0.62	0.11
3	1.5	0.95	0.61	0.10
4	3.0	0.95	0.60	0.094

Table 4.10. Maximum support rotations.

<u>Slab</u>	<u>Rotation degrees</u>	<u>$\frac{\Delta_{max}}{L}$ percent</u>
1	16.3	14.6
2	20.6	18.8
3	14.0	12.5
4	13.1	11.7
5	15.4	13.8
6	14.0	12.5
7	14.5	12.9
8	14.0	12.5
9	16.3	14.6
10	18.4	16.7

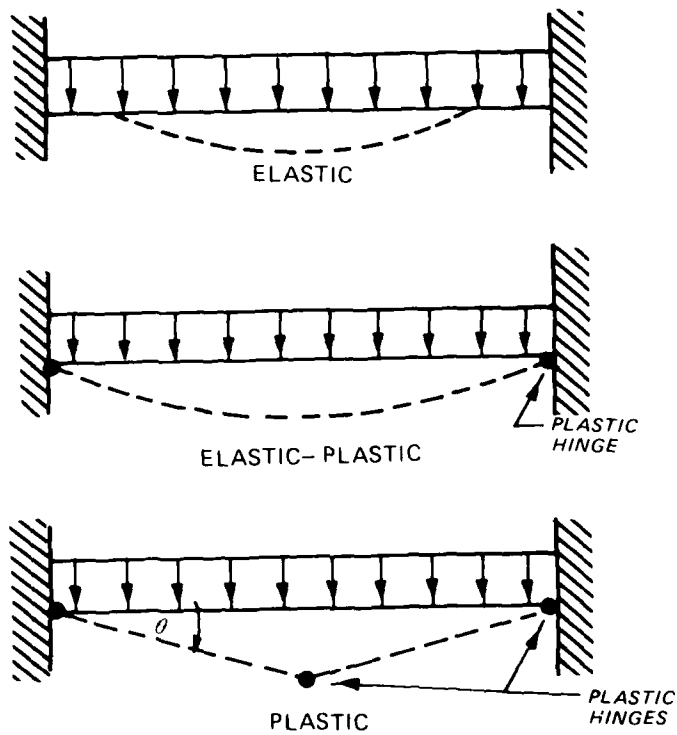


Figure 4.1. Formation of three-hinged mechanism.

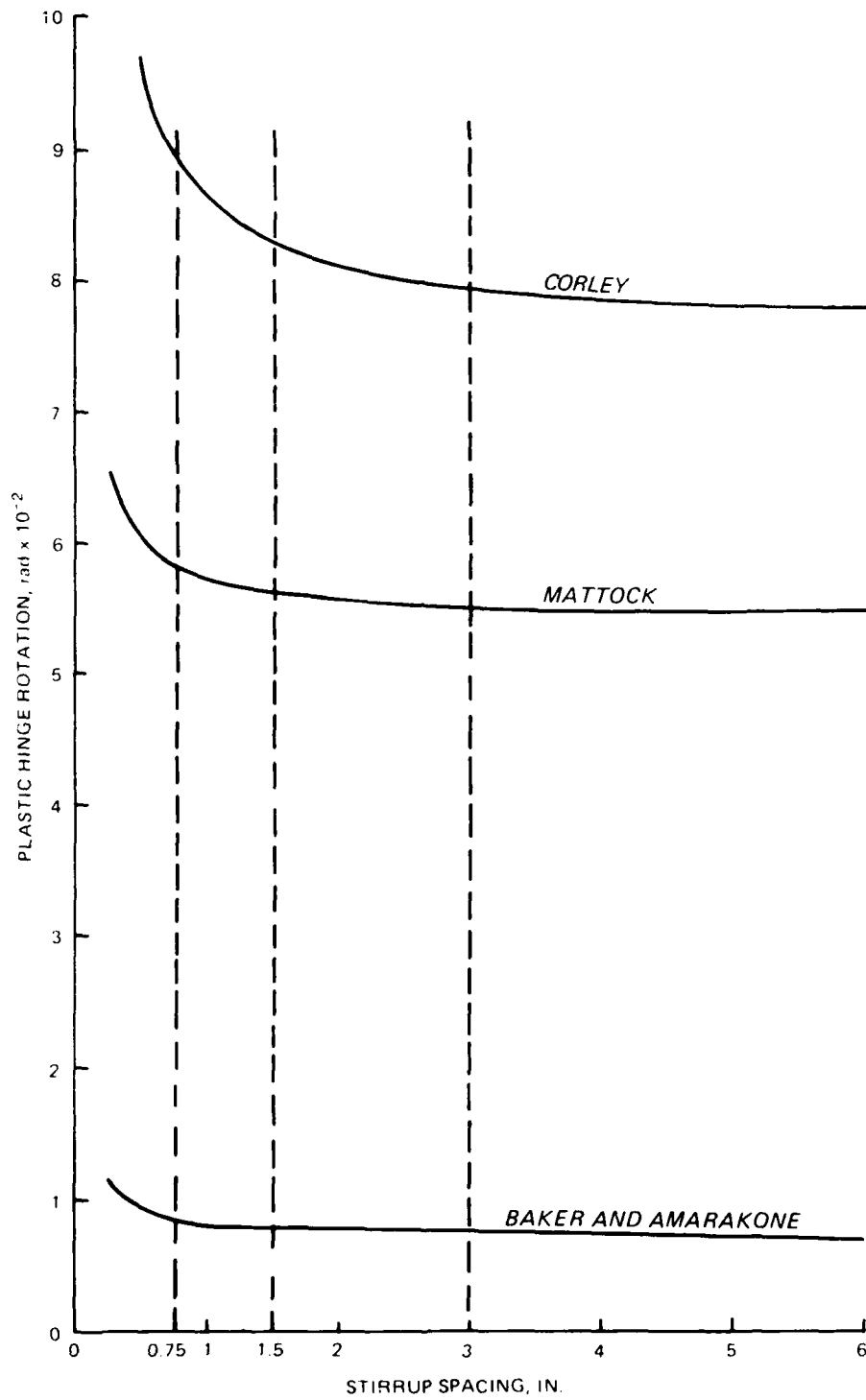


Figure 4.2. Rotation capacity versus stirrup spacing.

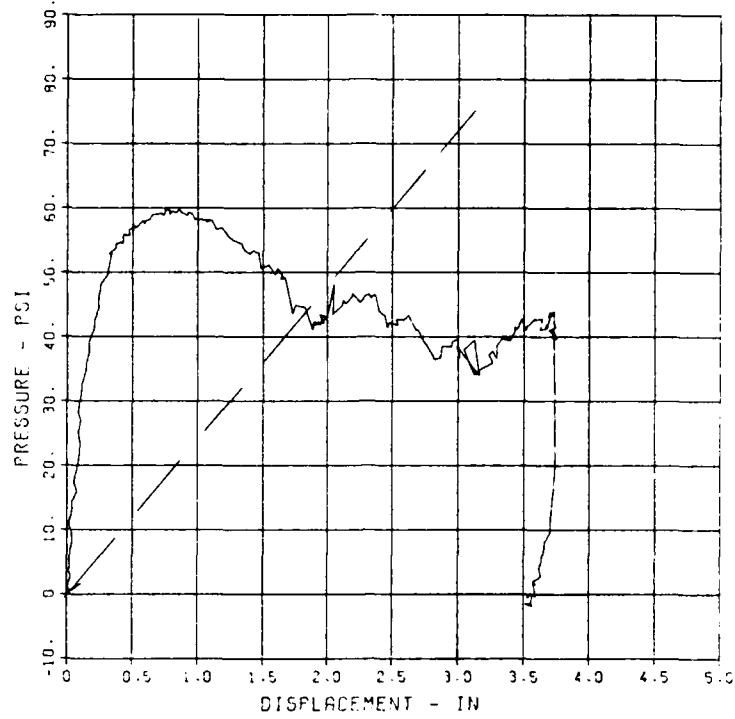


Figure 4.3. Slab 1 tensile membrane prediction.

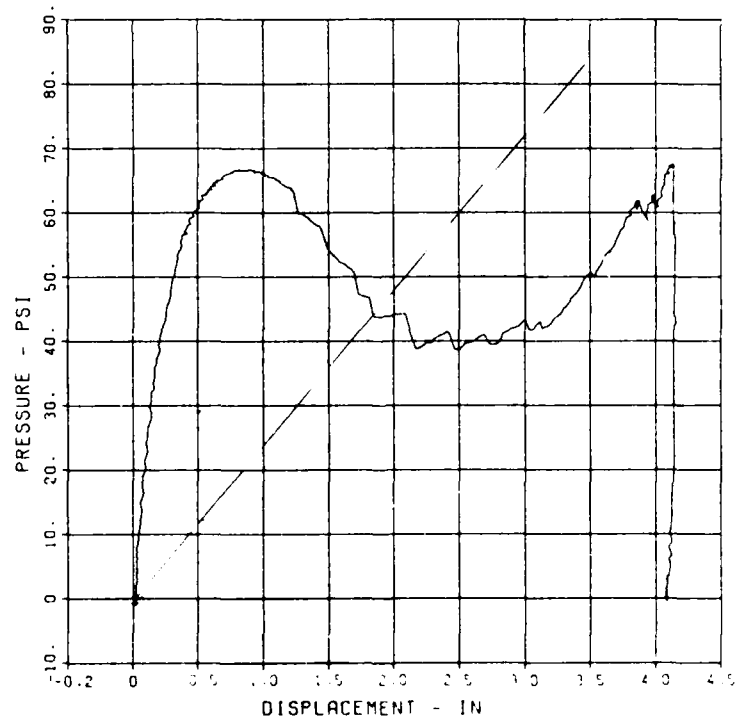


Figure 4.4. Slab 2 tensile membrane prediction.

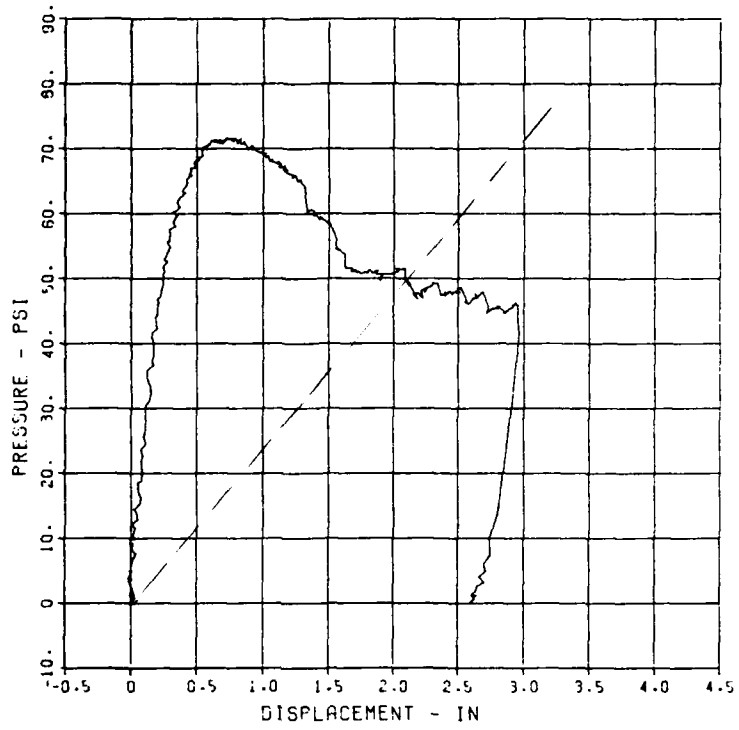


Figure 4.5. Slab 3 tensile membrane prediction.

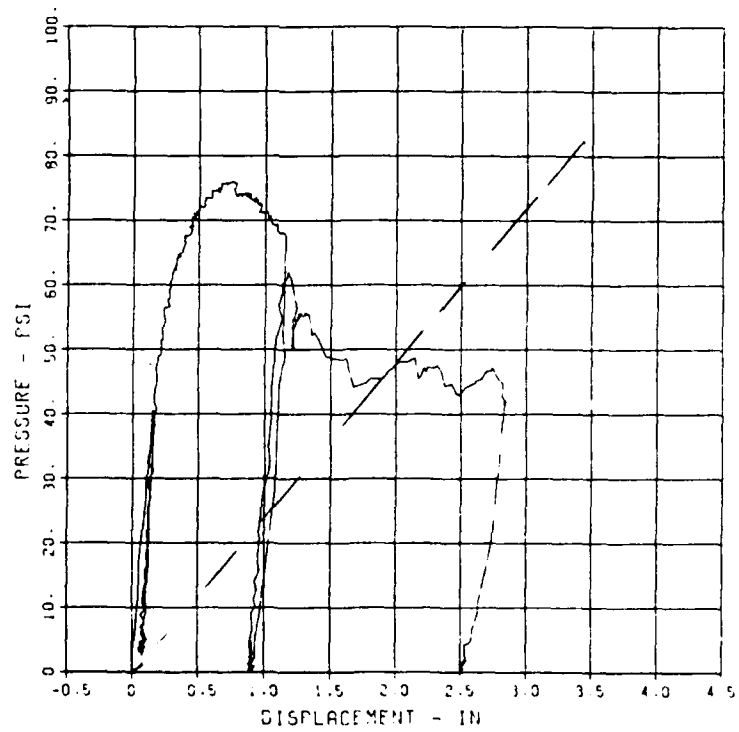


Figure 4.6. Slab 4 tensile membrane prediction.

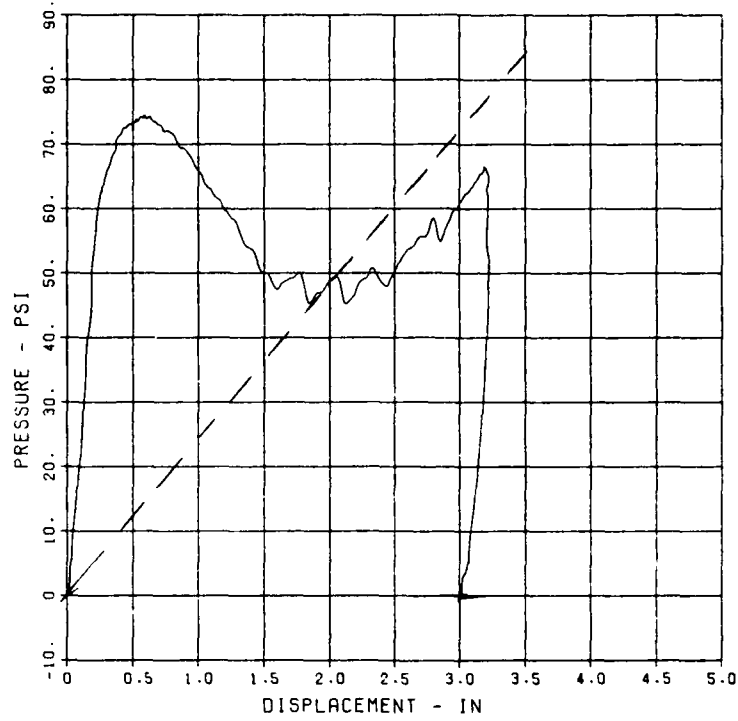


Figure 4.7. Slab 5 tensile membrane prediction.

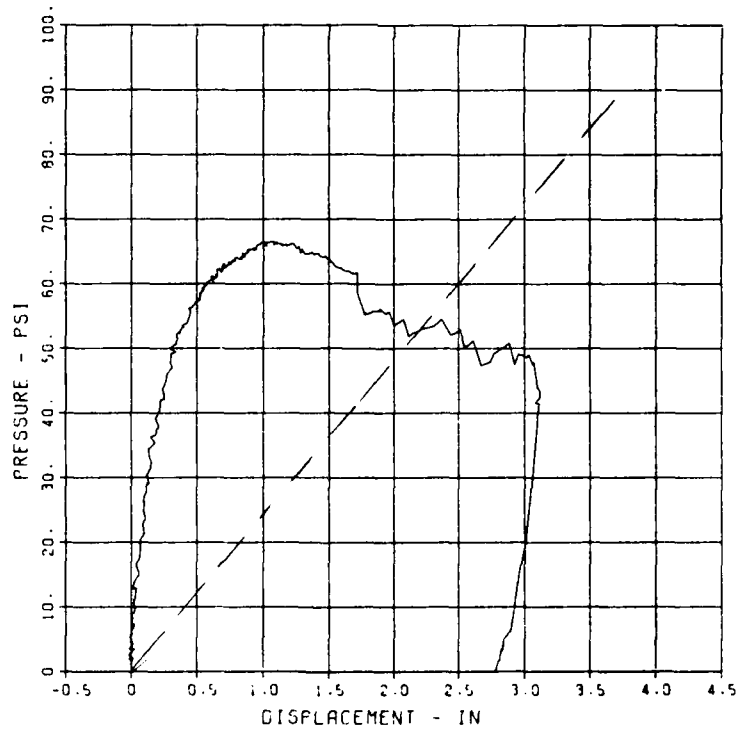


Figure 4.8. Slab 6 tensile membrane prediction.

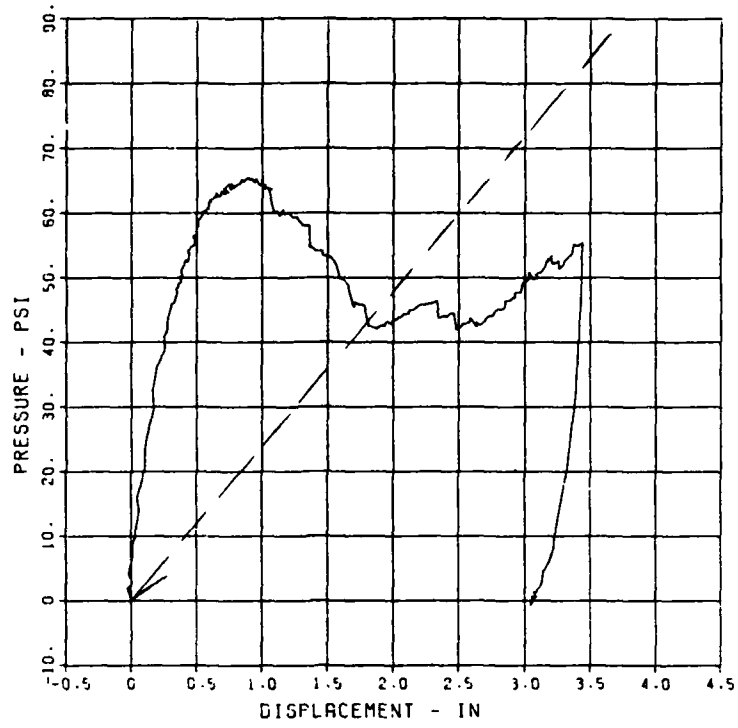


Figure 4.9. Slab 7 tensile membrane prediction.

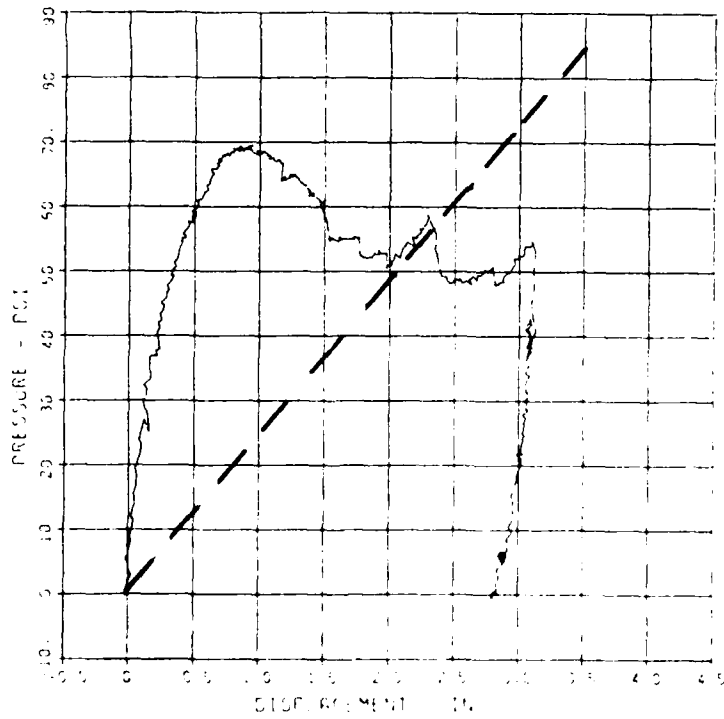


Figure 4.10. Slab 8 tensile membrane prediction.

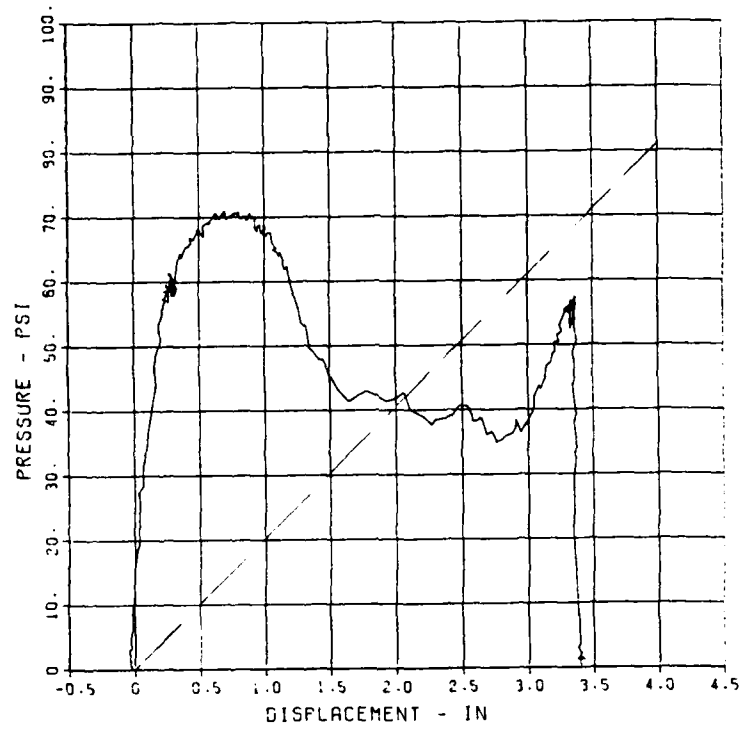


Figure 4.11. Slab 9 tensile membrane prediction.

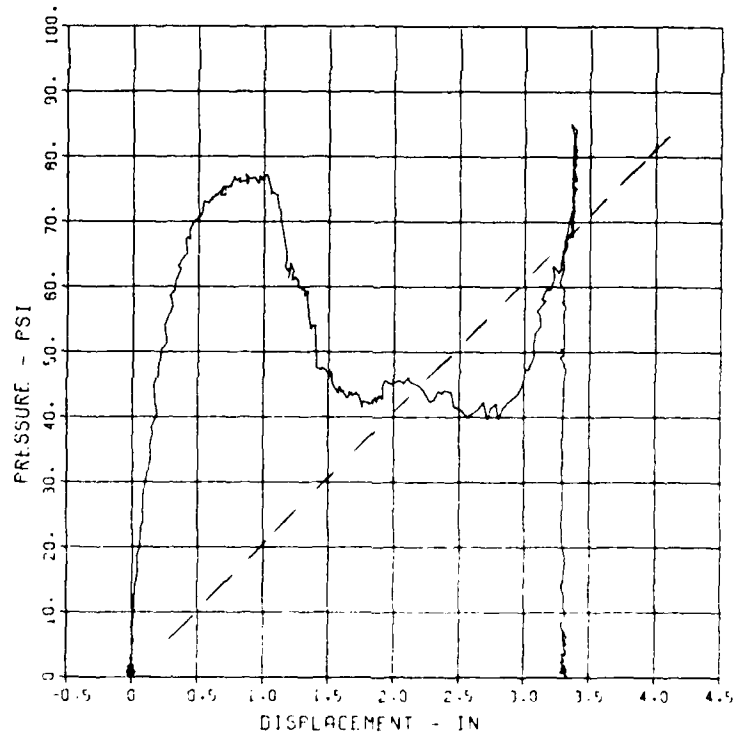


Figure 4.12. Slab 10 tensile membrane prediction.

CHAPTER 5

SUMMARY, CONCLUSIONS, AND RECOMMENDATIONS

5.1 SUMMARY

Ten one-way reinforced concrete slabs were statically tested under a uniform load to large deflections to investigate the use of stirrups in the key-worker shelter. These data significantly increase the current data base on the large deflection behavior of one-way slabs under uniform loads.

The ultimate load resistance of the laterally restrained slabs in this test series was approximately 1.4 to 1.7 times the yield-line value computed from theory developed by Johansen (Reference 32). The experimentally attained midspan-deflection-to-slab-thickness $(\Delta/t)_{ult}$ ratios varied from about 0.32 to 0.48. Compressive membrane theory by Park (Reference 42) closely predicts the ultimate load resistance of the slabs when a Δ/t ratio between about 0.2 and 0.4 is used (0.3 is applicable to the majority of the slabs).

The following two observations were made pertaining to the effects of the varied parameters on the ultimate load resistance:

(1) The lowest ultimate load capacity occurred in the slab having no stirrups, and (2) slabs constructed with the Type III stirrups experienced ultimate resistances 88 to 93 percent of those for slabs having Type I or II stirrups.

Rotation capacity calculations based on criteria from Corley (Reference 24), Mattock (Reference 22), and Baker and Amarakone (Reference 30) indicate an enhancement in ductility in the slab having the closest stirrup spacing (Slab 2). Support rotations between 13.1 and 20.6 degrees were observed. The rotations correspond to maximum attained midspan-deflection-to-clear span ratios (Δ_{max}/L) between 11.7 and 18.8 percent. The greatest support rotation of 20.6 degrees was experienced by Slab 2 and appeared to be very near the incipient collapse support rotation.

A three-hinged mechanism was formed in each slab, and significant spreading of the cracking pattern on the underface of the slabs did not occur. The greatest spreading of cracking was observed in Slab 2 which experienced a significant increase in load resistance at large deflections.

Park (Reference 48) approximated the midspan deflection (approximately equal to the effective depth of the slab) and the load resistance

(approximately equal to the yield-line value) at which the slabs exhibited initial tensile membrane tendencies. Fracture of reinforcement in these under-reinforced slabs ($\rho < \rho_b$) prohibited extensive load resistance enhancement in the tensile membrane region.

5.2 CONCLUSIONS

Conclusions for this test series are given below.

1. Slabs with a large number of closely spaced (spacing $\leq d/2$) stirrups exhibit increasing load resistance at large deflections.

2. Slabs with stirrups spaced at 1-1/2 inches ($d/2 < \text{spacing} < d$) behaved similar to those with stirrups spaced at 3.0 inches or without stirrups at large deflections. The 1-1/2-inch stirrup spacing represented the preliminary keyworker shelter design.

3. Slabs with temperature steel placed "exterior" to the principal reinforcement experience better tensile membrane behavior than do slabs having temperature steel placed "interior" to the principal reinforcement.

4. Slabs containing Type I double-leg stirrups have greater tendencies toward tensile membrane behavior than do slabs containing the Type II or Type III single-leg stirrup.

5. Slabs containing the Type III stirrup with a 90-degree bend at one end have load response behavior similar to those containing the Type II stirrup (up to at least the midspan deflections yielding a Δ_{\max}/L ratio of about 12.5 percent), except for a slight reduction in resistance at the ultimate load.

6. The load-response behavior of slabs having a principal reinforcing bar spacing slightly less than the effective depth (d) is not significantly affected by close stirrup spacings.

In summary, ductile behavior is increased by construction details which imply better confinement due to more confining steel (i.e., closely spaced stirrups, Type I stirrups, and closely spaced principal reinforcing bars) or a larger area of the confined core (i.e., exterior placement of temperature reinforcing). The effects of the same construction details on ultimate load capacity are not apparent from the data for these under-reinforced one-way slabs.

5.3 RECOMMENDATIONS

The slabs tested in this series are among the very few one-way slabs that have been tested under uniform loading conditions. An extension of the data base is necessary to support the findings of these tests.

Parameters similar to those varied in this series should be investigated for over-reinforced slabs ($\rho > \rho_b$). Also, the effects of these parameters on slabs that have different span-to-thickness ratios, principal reinforcing details, and end restraints remain to be investigated. In general, the large number of investigations that have been performed on beams (usually simply supported under concentrated loads) should be extended to the uniformly loaded one-way slab.

Based upon these tests, recommendations to HND pertaining to the deliberate-type Keyworker Blast Shelter roof design are given below.

1. The omission of stirrups is recommended unless the sustaining of a reserve capacity (increasing load resistance at large deflections) is deemed a criterion significant enough to justify the expense of a large number of stirrups spaced at $d/2$ or less. The omission of stirrups in the roof and floor of the keyworker shelter decreases the construction costs of the preliminary design by 3.5 to 4 percent.

2. Consideration should be given to the development of alternate principal reinforcement designs which may economically provide a reserve capacity.

3. If stirrups are included, the Type III stirrup should be used to provide economical benefits without significantly decreasing roof load capacity.

4. The placement of the transverse reinforcement (temperature steel) should be in the "exterior" condition when stirrups are used, and should probably have the same bar diameter as the stirrups in order to maintain concrete cover. In the absence of stirrups, benefits from the exterior placement may not be observed since a reduction in the principal reinforcement effective depth would occur for a given slab thickness and concrete cover.

5. It is not clear that the closer spacing (less than d) of the principal steel is responsible for an enhancement in load resistance at very large deflections, but it has been suggested by other researchers (Keenan and others, Reference 21) as a means to confine concrete rubble. Closer spacing should be considered, particularly if the recommended amount of attention is given to alternate principal reinforcing details.

REFERENCES

1. C. H. Lee; "Ductility of Reinforced Concrete Under Repeated and Tensile Loading"; 1969; thesis presented to Department of Material Engineering, University of Illinois, Chicago, Ill.
2. S. P. Shah; "Micromechanics of Concrete and Fiber Reinforced Concrete"; Proceedings, International Conference on Structure, Solid Mechanics and Design in Civil Engineering, April 1969; University of Southampton, England.
3. P. R. Barnard; "The Collapse of Reinforced Concrete Beams"; Proceedings, International Symposium on Flexural Mechanics of Reinforced Concrete, November 1964, Pages 501-520; American Society of Civil Engineers and American Concrete Institute.
4. R. Park and T. Paulay; "Reinforced Concrete Structures"; 1975; John Wiley & Sons, New York.
5. M. Z. Cohn; "Rotation Compatibility in the Limit Design of Reinforced Concrete Continuous Slabs"; Flexural Mechanics of Reinforced Concrete, November 1964, Pages 359-382; American Society of Civil Engineers and American Concrete Institute.
6. M. A. Cohn and V.A. Petcu; "Moment Redistribution and Rotation Capacity of Plastic Hinges in Redundant Reinforced Concrete Beams"; The Indian Concrete Journal, August 1963, Vol. 37, No. 8, Pages 282-290.
7. H. E. H. Roy and M. A. Sozen; "Ductility of Concrete"; Flexural Mechanics of Reinforced Concrete, November 1964, Pages 213-236; American Society of Civil Engineers and American Concrete Institute.
8. W. L. Chan; "The Ultimate Strength of Deformation of Plastic Hinges in Reinforced Concrete Frameworks"; Magazine of Concrete Research, November 1955, Vol. 7, No. 2, Pages 121-132.
9. M. T. M. Soliman and C. W. Yu; "The Flexural Stress-Strain Relationship of Concrete Confined by Rectangular Transverse Reinforcement"; Magazine of Concrete Research, December 1967, Vol. 19, No. 61, Pages 233-238.
10. S. Stockl; Discussion of "Ductility of Concrete," by H. E. H. Roy and M. A. Sozen; Proceedings, International Symposium on Flexural Mechanics of Reinforced Concrete, November 1964, Pages 225-227; American Society of Civil Engineers and American Concrete Institute.
11. V. V. Bertero and C. Felippa; Discussion of "Ductility of Concrete," by H. E. H. Roy and M. A. Sozen; Proceedings, International Symposium on Flexural Mechanics of Reinforced Concrete, November 1964, Pages 227-234; American Society of Civil Engineers and American Concrete Institute.
12. J. E. McDonald; "The Effect of Confining Reinforcement on the Ductility of Reinforced Concrete Beams"; Technical Report C-69-5, March 1969; US Army Engineer Waterways Experiment Station, Vicksburg, Miss.
13. M. Sargin, S. K. Ghosh, and V. K. Handa; "Effects of Lateral Reinforcement Upon the Strength and Deformation Properties of Concrete"; Magazine of Concrete Research, June-September 1971, Vol. 23, No. 75-76, Pages 99-110.

14. F. E. Richart, Z. Brandtzaeg, and R. L. Brown; "The Failure of Plain and Spirally Reinforced Concrete in Compression"; Engineering Experiment Station Bulletin No. 190, 1929; University of Illinois, Urbana, Ill.
15. K. T. R. J. Iyengar, P. Desayi, and K. N. Reddy; "Stress-Strain Characteristics of Concrete Confined in Steel Binders"; Magazine of Concrete Research, September 1970, Vol. 22, No. 72, Pages 173-284.
16. S. A. Sheikh and S. M. Uzumeri; "Analytical Model for Concrete Confinement in Tied Columns"; Journal, American Concrete Institute, December 1982, No. ST12, Pages 2703-2722.
17. D. C. Kent and R. Park; "Flexural Members with Confined Concrete"; Journal Structural Division, American Society of Civil Engineers, July 1971, Vol. 97, No. ST7, Pages 1969-1990.
18. G. D. Base and J. B. Read; "Effectiveness of Helical Binding in the Compression Zone of Concrete Beams"; Journal, American Concrete Institute, July 1965, Vol. 62, No. 7, Pages 763-780.
19. S. P. Shah and B. V. Rangan; "Effects of Reinforcements on Ductility of Concrete"; Journal, Structural Division, American Society of Civil Engineers, June 1970, Vol. 96, No. ST6, Pages 1167-1184.
20. R. Yamashiro; "Moment-Rotation Characteristics of Reinforced Concrete Members Subjected to Bending, Shear, and Axial Load"; November 1962; thesis submitted to Department of Civil Engineering, University of Illinois, Urbana, Ill.
21. W. Keenan and others; "Structures to Resist the Effects of Accidental Explosions" (Revision in preparation); Department of the Army Technical Manual TM 5-1300, Department of the Navy Publication NAVFAC P-397, Department of the Air Force Manual AFM 88-22; Departments of the Army, the Navy, and the Air Force, Washington, DC.
22. A. H. Mattock; "Rotational Capacity of Hinging Regions in Reinforced Concrete Beams"; Proceedings, International Symposium on Flexural Mechanics of Reinforced Concrete, November 1964, Pages 227-234; American Society of Civil Engineers and American Concrete Institute.
23. N. C. Sinha and V. S. Rane; "Computation of Curvature and Deflection in Reinforced Concrete"; Journal, Institution of Engineers, India, July 1965, Vol. 45, No. 11, Pages 826-836.
24. W. G. Corley; "Rotational Capacity of Reinforced Concrete Beams"; Journal, Structural Division, American Society of Civil Engineers, October 1966, Vol. 92, No. ST5, Pages 121-146.
25. R. Taylor, D. R. H. Maher, and B. Haynes; "Effect of the Arrangement of Reinforcement on the Behavior of Reinforced Concrete Slabs"; Magazine of Concrete Research, June 1966, Vol. 18, No. 55, Pages 85-94.
26. H. Bachman; "Influence of Shear and Bond on Rotational Capacity of Reinforced Concrete Beams"; International Association for Bridge and Structural Engineering, Zurich, Vol. 30, Part II, Pages 11-28.
27. M. Z. Cohn and S. K. Ghosh; "Ductility of Reinforced Concrete Sections in Bending"; Symposium on Inelasticity and Non-Linearity in Structural Concrete, January-June 1972, Pages 111-146; University of Waterloo, Waterloo, Ontario, Canada.

28. P. Srinivasa Rao, P. R. Kannan, and B. V. Subrahmanyam; "Influence on Span Length and Application of Load on the Rotation Capacity of Plastic Hinges"; Journal, American Concrete Institute, 1971, Vol. 68, No. 6, Pages 468-471.
29. E. P. Burnett; "Rotation Capacity of Reinforced Concrete Flexural Elements"; Symposium on Inelasticity and Non-Linearity in Structural Concrete, January-June 1972, Pages 181-209; University of Waterloo, Waterloo, Ontario, Canada.
30. A. L. L. Baker and A. M. N. Amarakone; "Inelastic Hyperstatic Frame Analysis"; Flexural Mechanics of Reinforced Concrete, 1965, SP-12, Pages 85-142; American Society of Civil Engineers and American Concrete Institute.
31. A. J. Ockleston; "Load Tests on a Three-Story Reinforced Building in Johannesburg"; Structural Engineer, October 1955, Vol. 33, No. 10, Pages 304-322.
32. K. W. Johansen; "Brudinie Teorier" ("Yield-Line Theory"); 1943; Gjellerups Forlag, Copenhagen; Page 191; Translated by Cement and Concrete Association, London, 1962, page 181.
33. A. J. Ockleston; "Arching Action in Reinforced Concrete Slabs"; Structural Engineer, June 1958, Vol. 36, No. 6, Pages 197-201.
34. E. Burnett; "Flexural Rigidity, Curvature and Rotation and Their Significance in Reinforced Concrete Design"; Magazine of Concrete Research, March-December 1964, Vol. 16, No. 46-49, Pages 67-72.
35. M. Iqbal and A. T. Derecho; "Design Criteria for Deflection Capacity of Conventionally Reinforced Concrete Slabs--Phase I"; January-August 1979; Construction Technology Laboratories, Skokie, Ill.
36. W. A. Keenan; "Strength and Behavior of Laced Reinforced Concrete Slabs Under Static and Dynamic Load"; R620, April 1969; US Naval Civil Engineering Laboratory, Port Hueneme, Calif.
37. W. A. Keenan; "Strength and Behavior of Restrained Reinforced Concrete Slabs Under Static and Dynamic Loading"; R621, April 1969; US Naval Civil Engineering Laboratory, Port Hueneme, Calif.
38. R. Park and W. L. Gamble; "Reinforced Concrete Slabs"; 1980; John Wiley & Sons, New York; Pages 562-609.
39. S. A. Kiger, P. S. Eagles, and J. T. Baylot; "Response of Earth-Covered Slabs in Clay and Sand Backfills"; Technical Report SL-84-18, October 1984; US Army Engineer Waterways Experiment Station, Vicksburg, Miss.
40. E. H. Roberts; "Load-Carrying Capacity of Slab Strips Restrained Against Longitudinal Expansion"; Concrete, 1969, Vol. 3, Pages 369-378.
41. R. H. Wood; "Plastic and Elastic Design of Slabs and Plates"; 1961; Thames & Hudson, London, England; Pages 225-261.
42. R. Park; "Ultimate Strength of Rectangular Concrete Slabs Under Short-Term Uniform Loading with Edges Restrained Against Lateral Movement"; Proceedings, Institution of Civil Engineers, June 1964, Vol. 28, Pages 125-150.

43. C. T. Morley; "Yield Line Theory for Reinforced Concrete Slabs at Moderately Large Deflections"; Magazine of Concrete Research, December 1967, Vol. 19, No. 61, Pages 211-222.
44. T. Y. Hung and E. G. Nawy; "Limit Strength and Serviceability Factor in Uniformly Loaded, Isotropically Reinforced Two-Way Slabs"; Cracking, Deflection and Ultimate Load of Concrete Slab Systems, 1971, Special Publication 30, Pages 301-324; American Concrete Institute, Detroit, Mich.
45. E. C. Isaza; "Manual of Extensibility of Reinforcement for Catenary Action"; August 1972; Concrete Structures Technology, Civil Engineering Department, London, England.
46. D. C. Hopkins; "Effects of Membrane Action on the Ultimate Strength of Reinforced Concrete Slabs"; December 1969; thesis presented to the Department of Civil Engineering, University of Canterbury, Christchurch, New Zealand.
47. J. F. Botchie, A. Jacobson, and S. Okubo; "Effect of Membrane Action on Slab Behavior"; R-65-25, August 1965; US Naval Civil Engineering Laboratory, Port Hueneme, Calif.
48. R. Park; "Tensile Membrane Behavior of Uniformly Loaded Rectangular Reinforced Concrete Slabs with Fully Restrained Edges"; Magazine of Concrete Research, March 1964, Vol. 16, No. 46, Pages 39-44.
49. T. R. Slawson; "Dynamic Shear Failure of Shallow-Buried Flat-Roofed Reinforced Concrete Structures Subjected to Blast Loads"; December 1983; thesis presented to the Department of Civil Engineering, Mississippi State University, Mississippi State, Miss.
50. W. L. Huff; "Test Devices Blast Load Generator Facility"; Miscellaneous Paper N-69-1, April 1969; US Army Engineer Waterways Experiment Station, Vicksburg, Miss.
51. A. H. Mattock; Discussion of "Rotational Capacity of Reinforced Concrete Beams", by W. G. Corley; Journal, Structural Division, American Society of Civil Engineers, April 1967, Vol. 93, No. ST2, Pages 519-522.
52. T. R. Slawson; "Structural Element Tests in Support of the Keyworker Blast Shelter Program" (in preparation); US Army Engineer Waterways Experiment Station, Vicksburg, Miss.
53. American Concrete Institute; "Building Code Requirements for Reinforced Concrete"; ACI 318-83, November 1983; Detroit, Mich.
54. S. A. Mahin and V. V. Bertero; "RCCOLA (A Computer Program for Reinforced Concrete Column Analysis), User's Manual and Documentation"; August 1977; Department of Civil Engineering, University of California, Berkeley, Calif.

APPENDIX A
POSTTEST PHOTOGRAPHS AND DATA

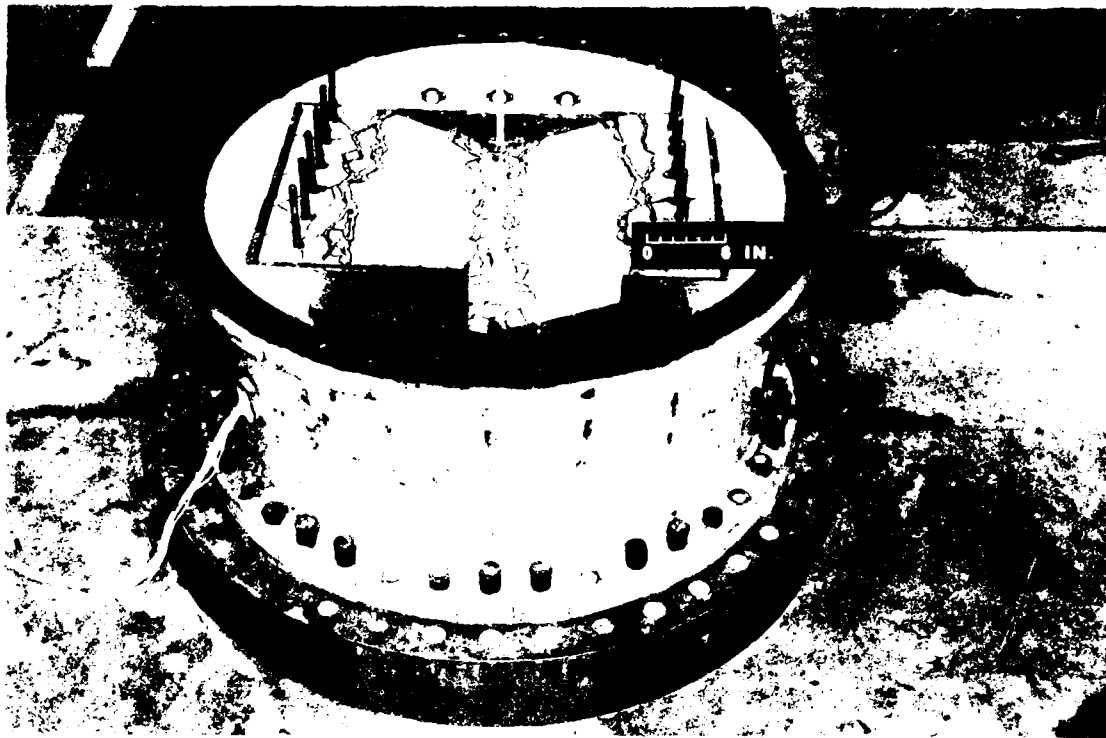


Figure A.1. Slab 1 posttest.

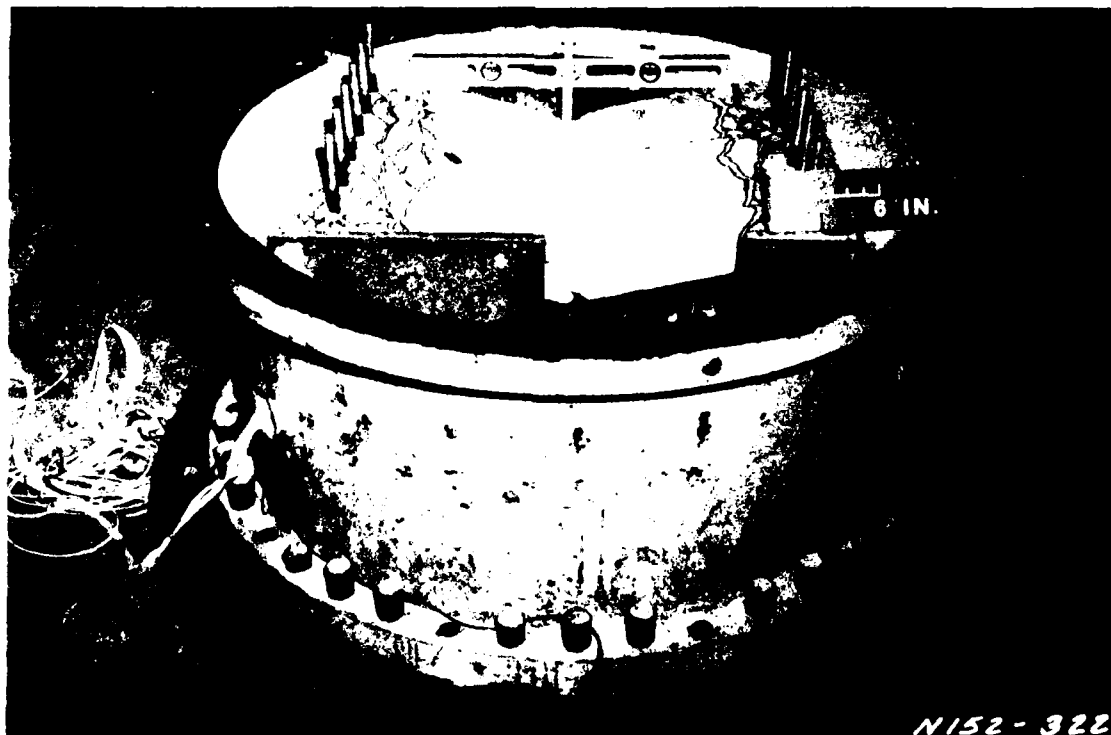


Figure A.2. Slab 3 posttest.

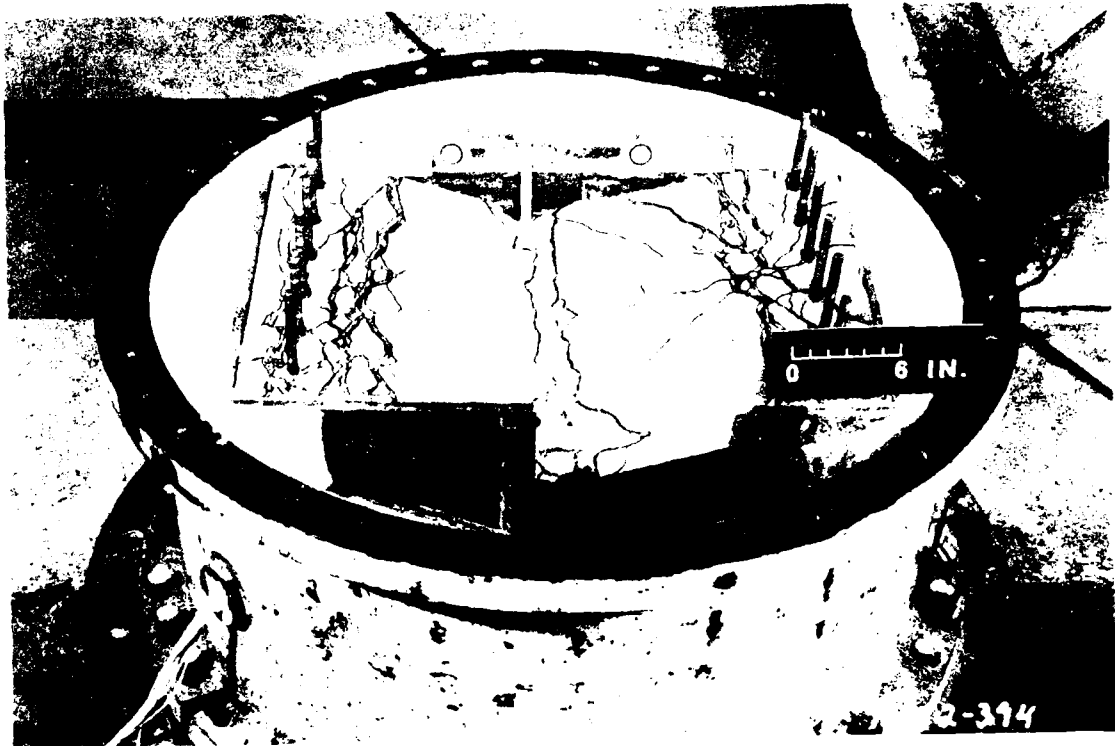


Figure A.3. Slab 5 posttest.

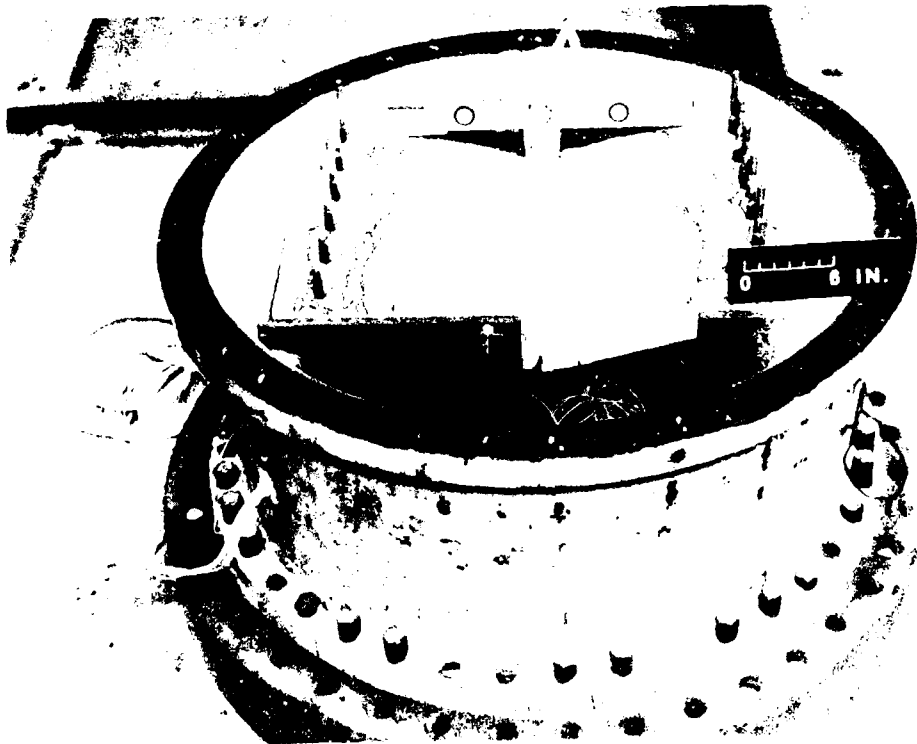


Figure A.4. Slab 6 posttest.

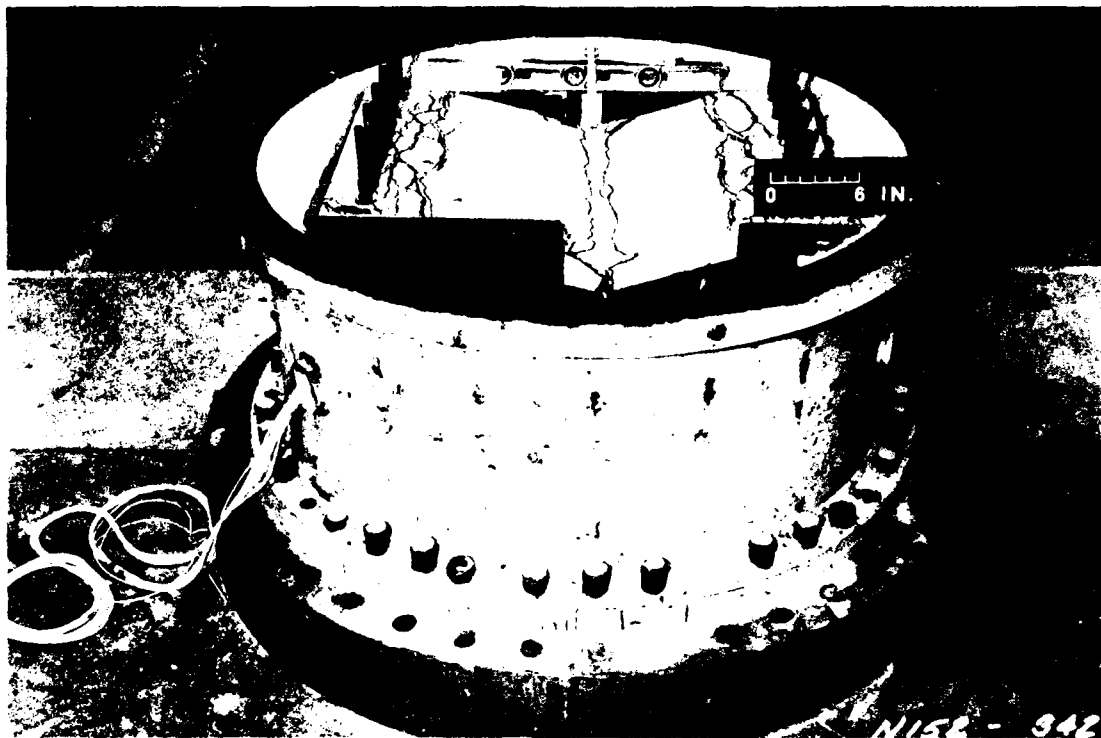


Figure A.5. Slab 7 posttest.

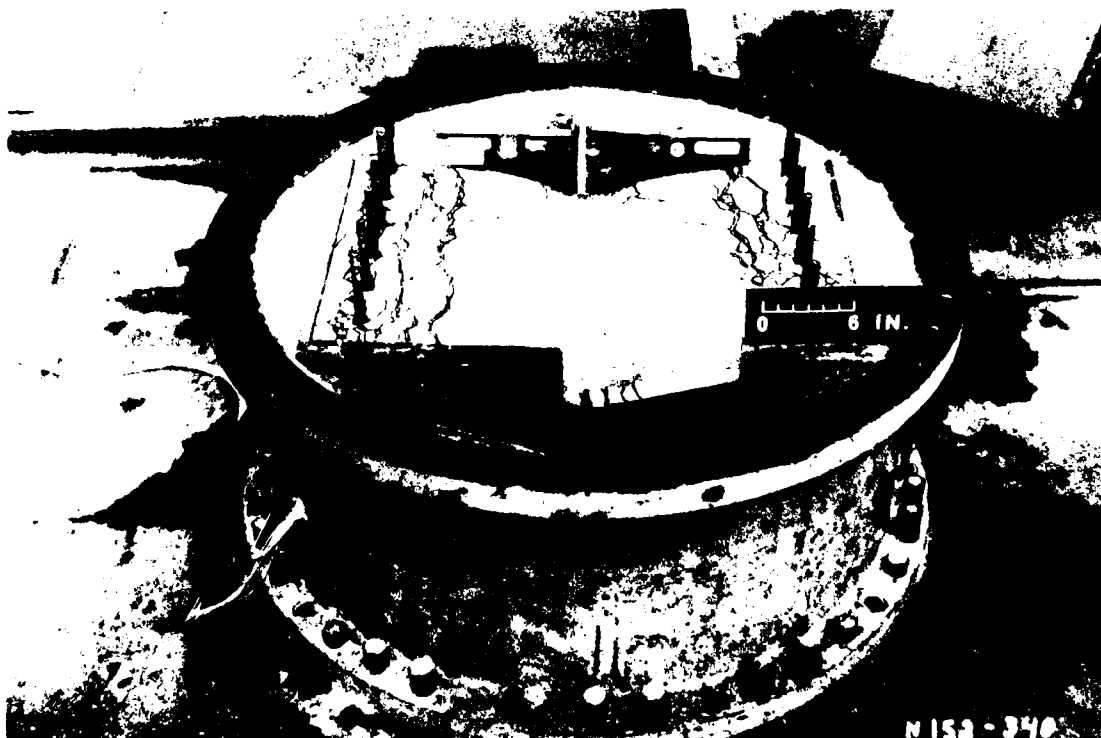


Figure A.6. Slab 8 posttest.

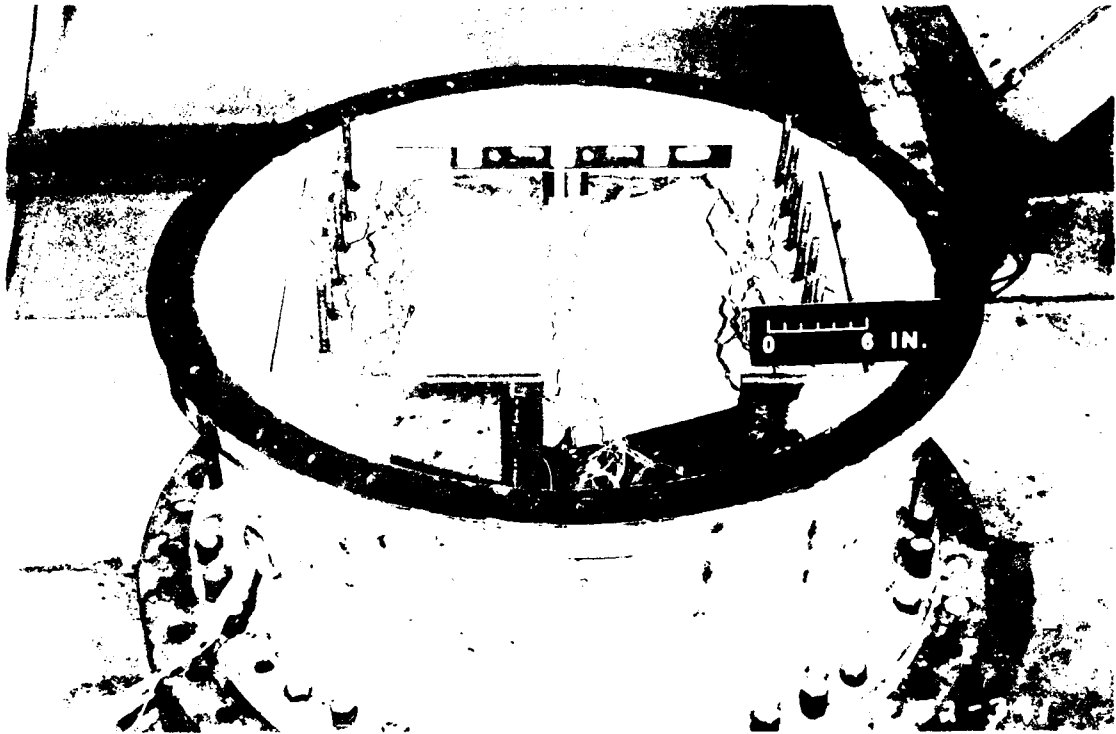


Figure A.7. Slab 9 posttest.

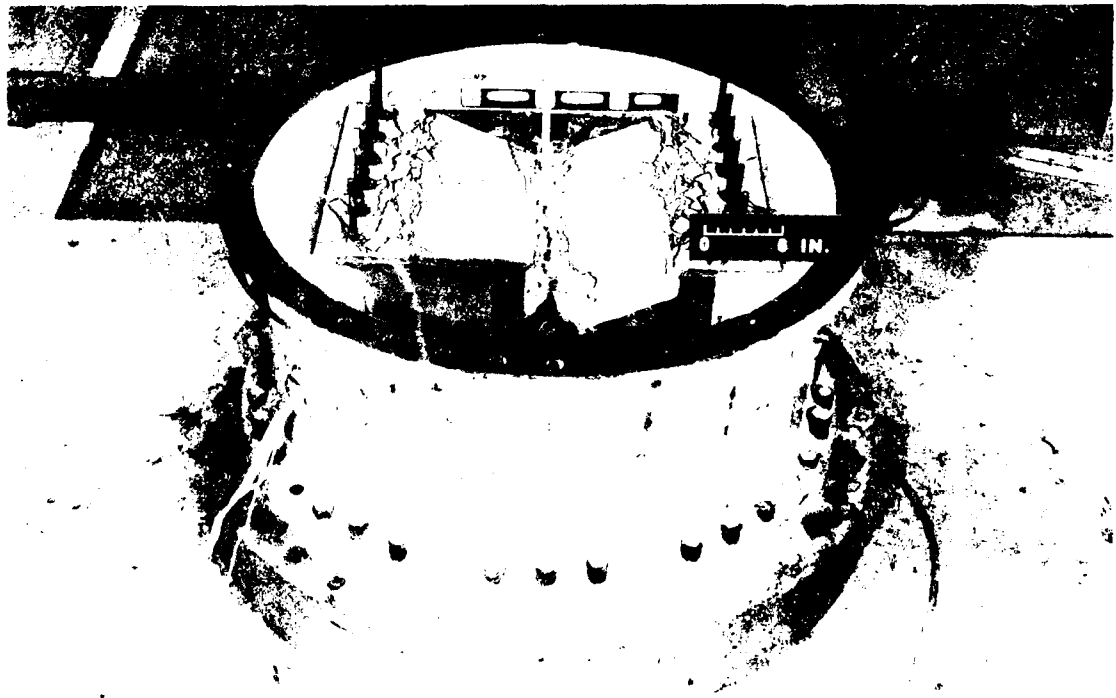


Figure A.8. Slab 10 posttest.

APPENDIX B
STIRRUP SLAB TEST DATA

FEMA STIRRUP SLAB 1

P-1

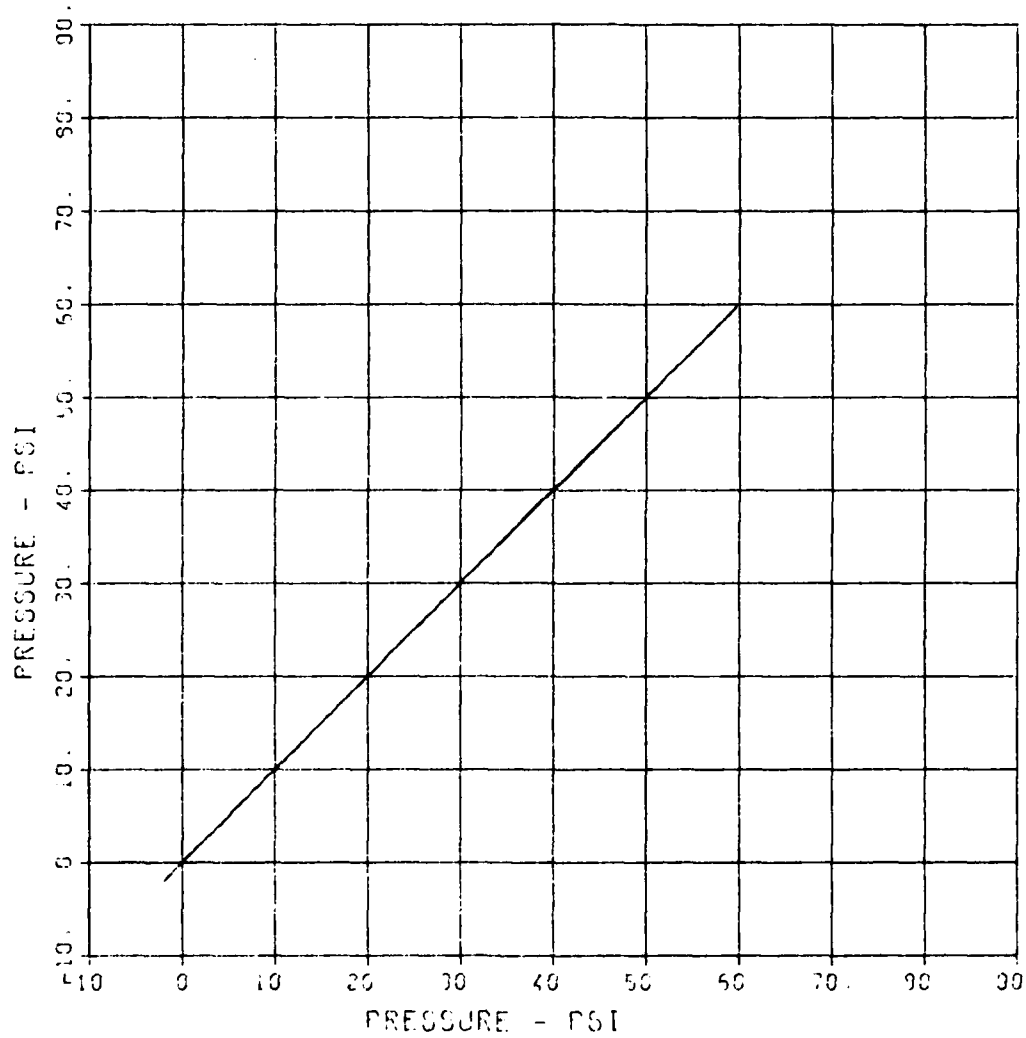
MAXIMUM
53.7134

SIGMA CAL
2.5271

CAL VAL
135.0

CHANNEL NO 20053 1

05/04/94 R0517



FEMA STIRRUP SLAB 1

D-1

MAXIMUM
0.1472

SIGMA CAL
2.3227

CAL VAL
1.1

CHANNEL NO

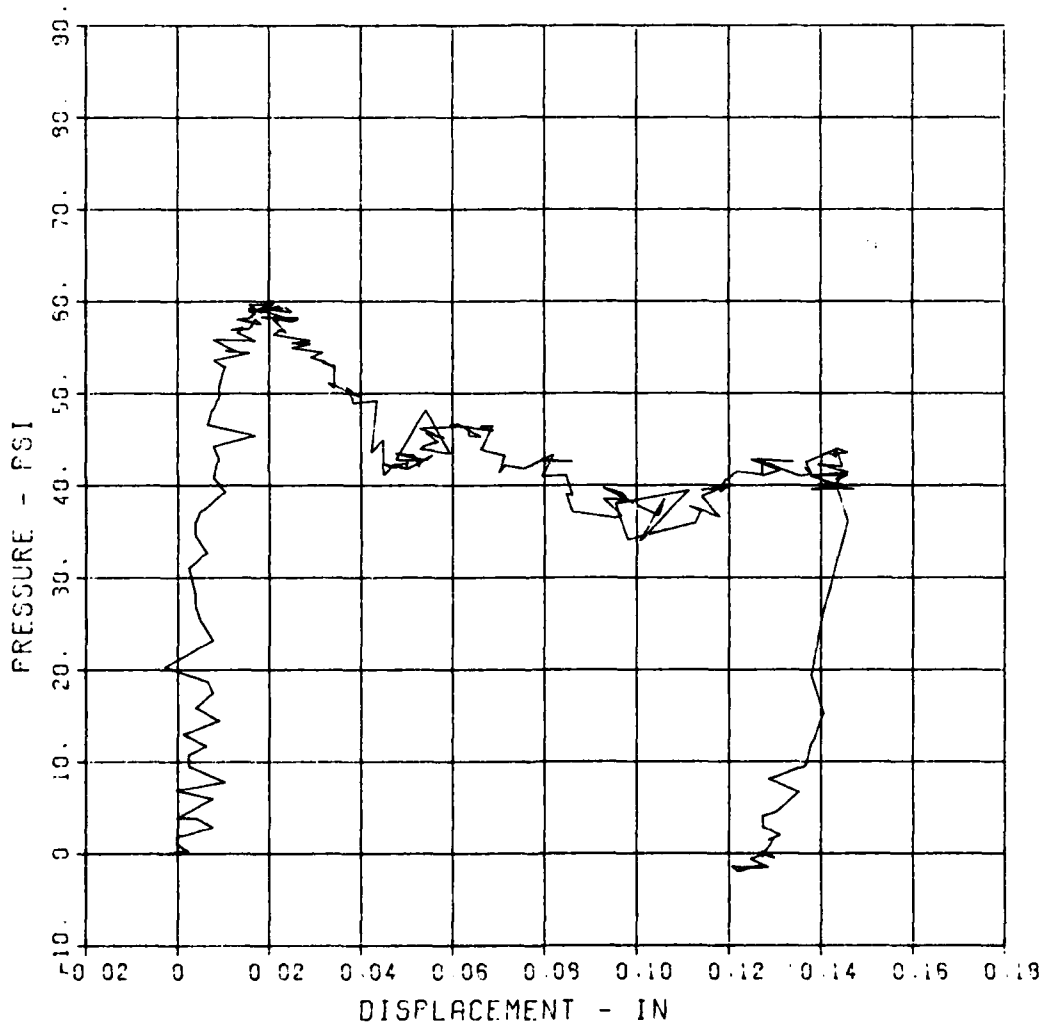
2

20053

1

05/04/94

R0517



FEMA STIRRUP SLAB 1

D-2

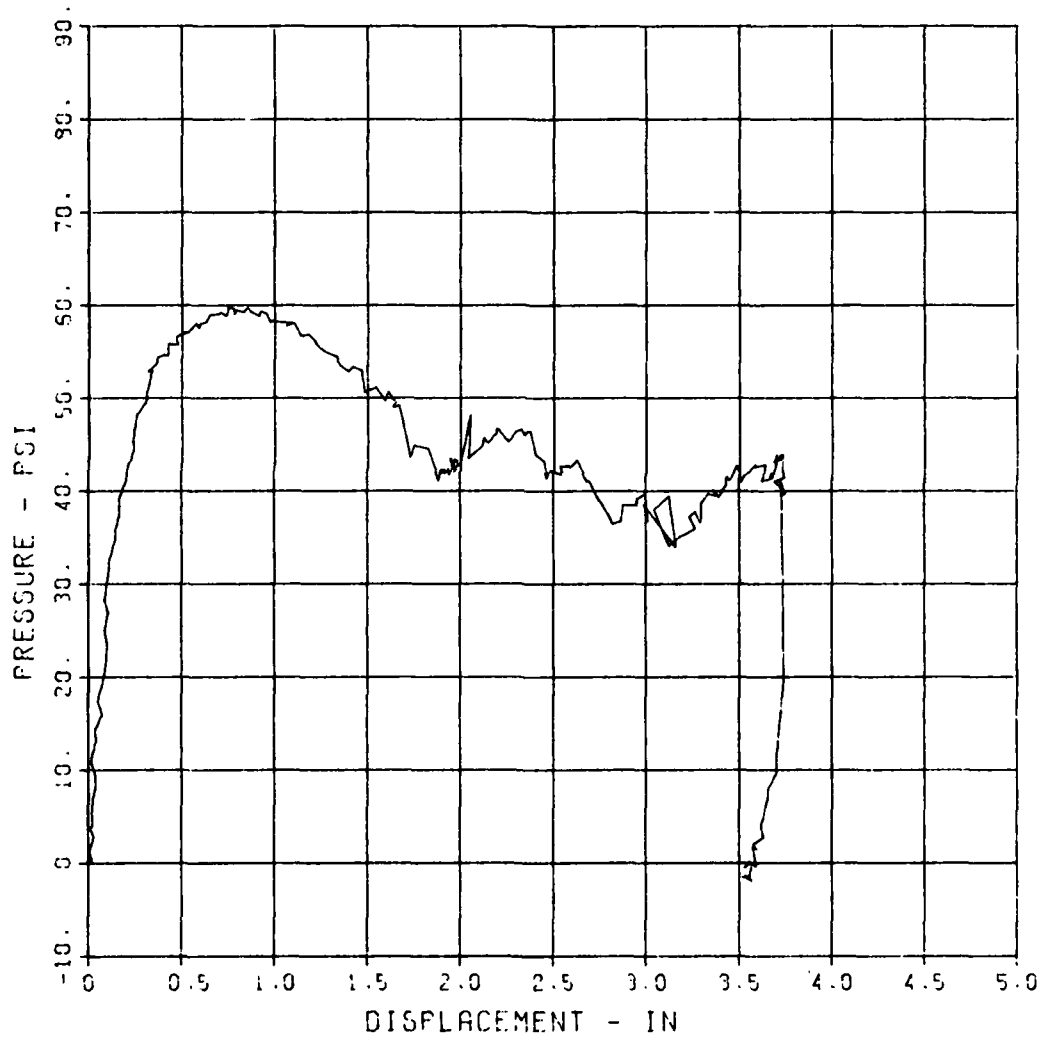
MAXIMUM
3.7510

SIGMA CAL
2.8252

CAL VAL
5.2

CHANNEL NO 3 20353 1

05/04/84 R0617



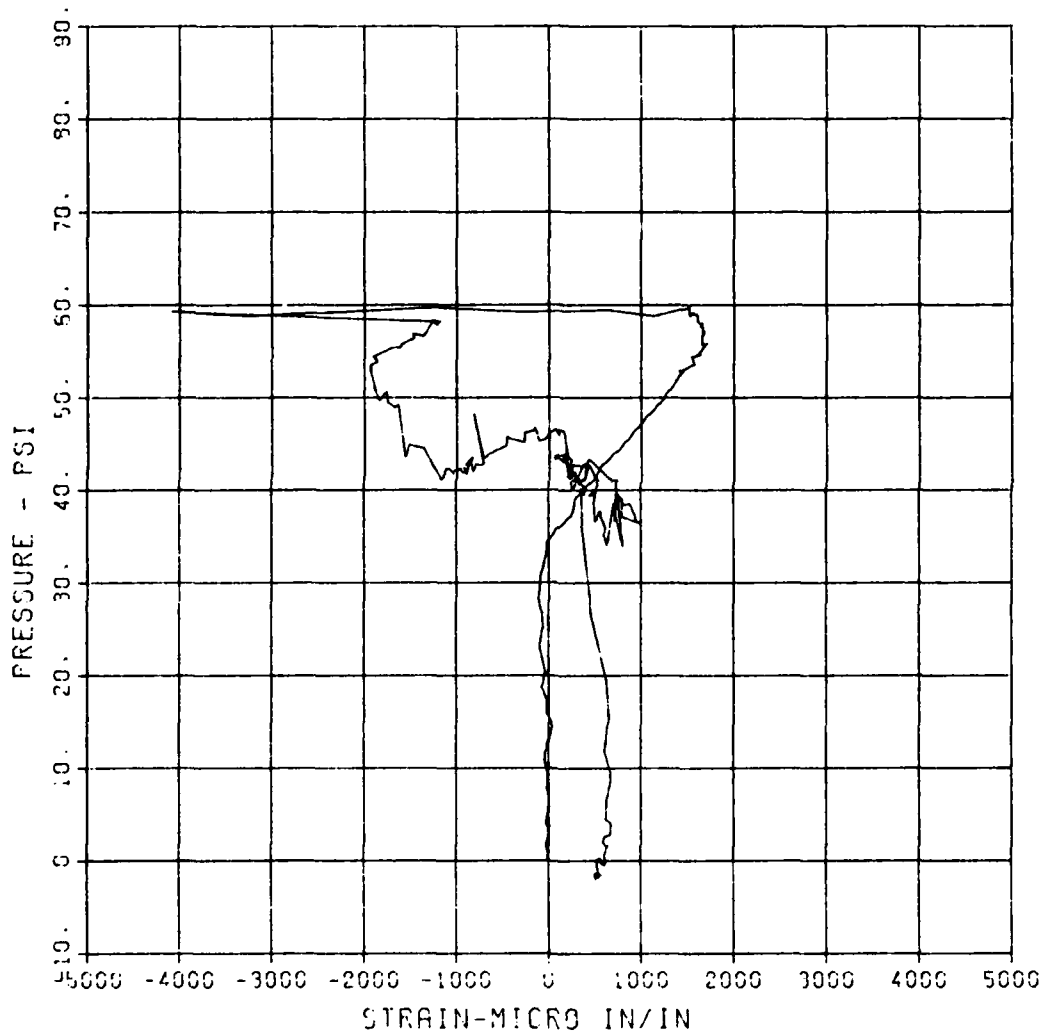
FEMA STIRRUP SLAB 1

ST-1

MAXIMUM SIGMA_CAL CAL_VAL
-4095.0456 2.4150 11655.7

CHANNEL NO. 4 20963 1

05/04/94 R0617



FEMA STIRRUP SLAB 1

SB-1

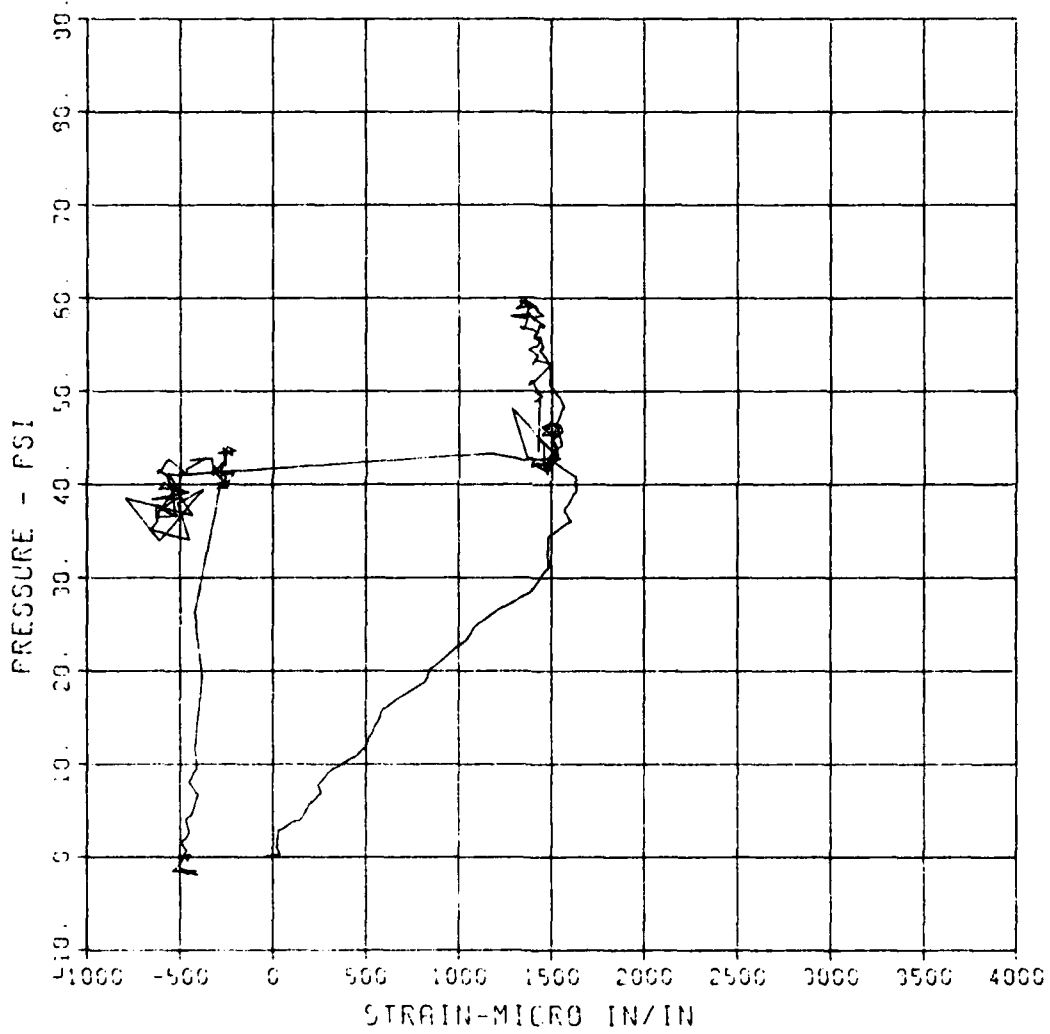
MAXIMUM
1637.5021

SICMA CAL
2.6347

CAL VAL
11655.7

CHANNEL NO 5 20963 1

05/04/94 R0517



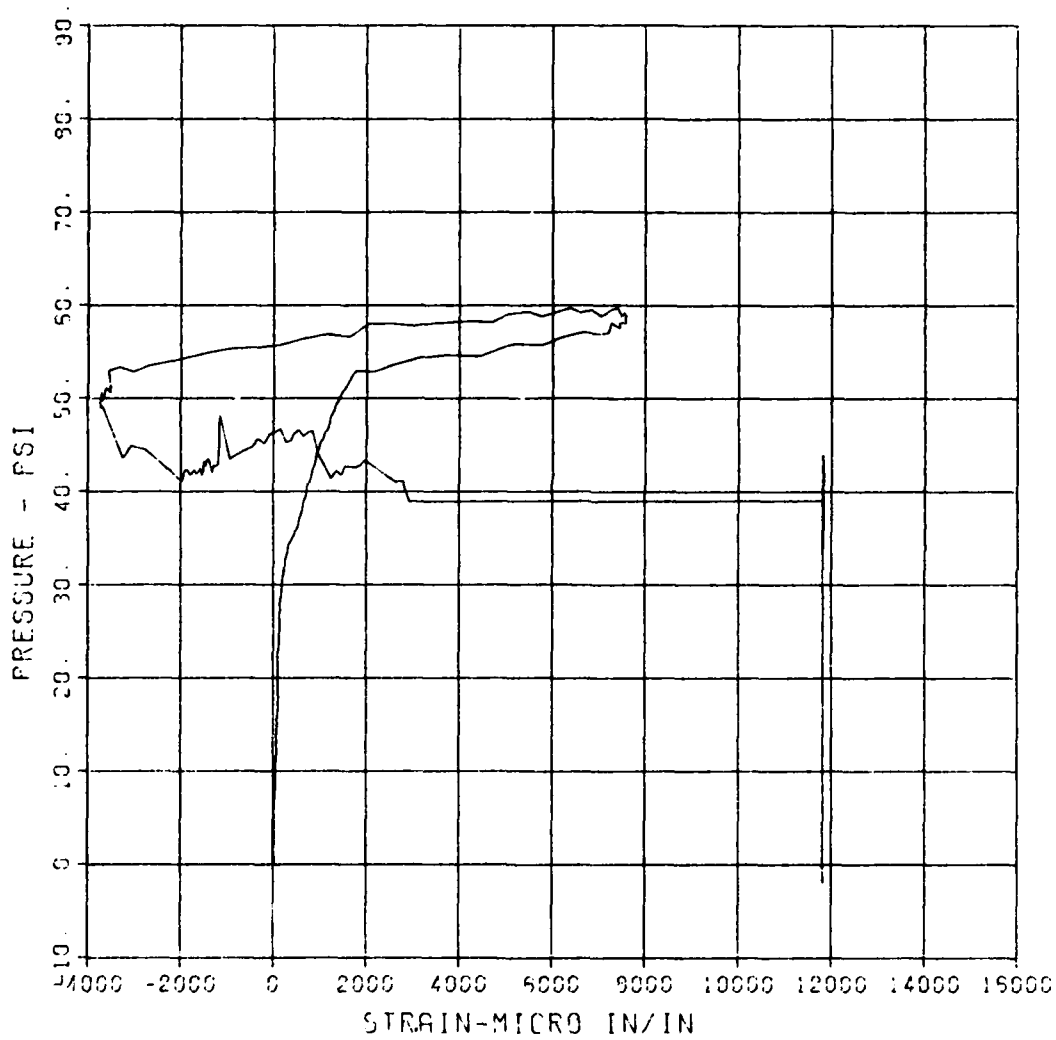
FEMA STIRRUP SLAB 1

ST-2

MAXIMUM 11913.3551 SIGMA CAL 2.7202 CAL VAL 5765.1

CHANNEL NO. 6 20953 1

05/04/94 R0517



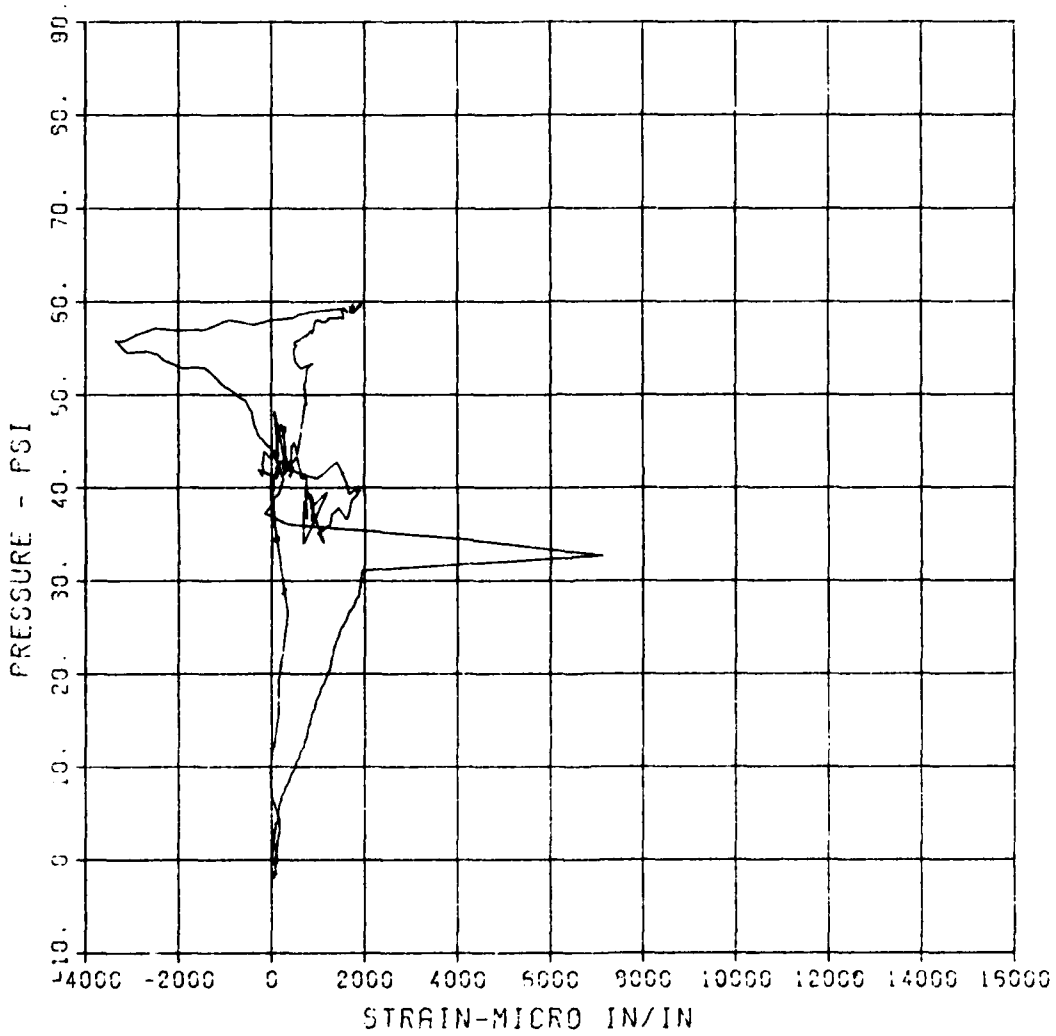
FEMA STIRRUP SLAB 1

SB-2

MAXIMUM SIGMA CAL CAL VAL
7124.5357 2.3593 5755.1

CHANNEL NO. 7 20063 1

05/04/84 R0617



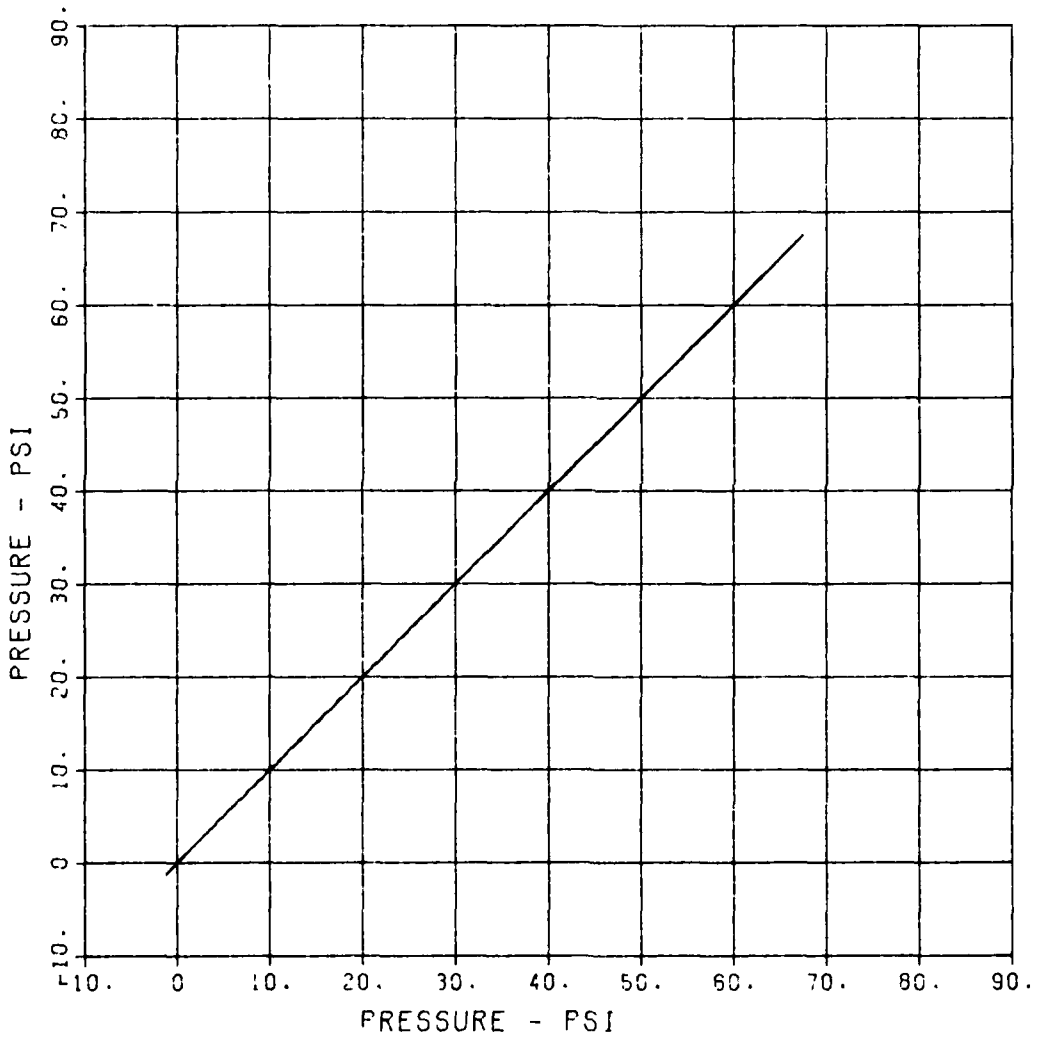
FEMA STIRRUP SLAB 2

P-1

MAXIMUM	SIGMA CAL	CAL VAL
67.5286	1.1281	135.9

CHANNEL NO. : 13092 1

06/12/84 R0342



FEMA STIRRUP SLAB 2

D-1

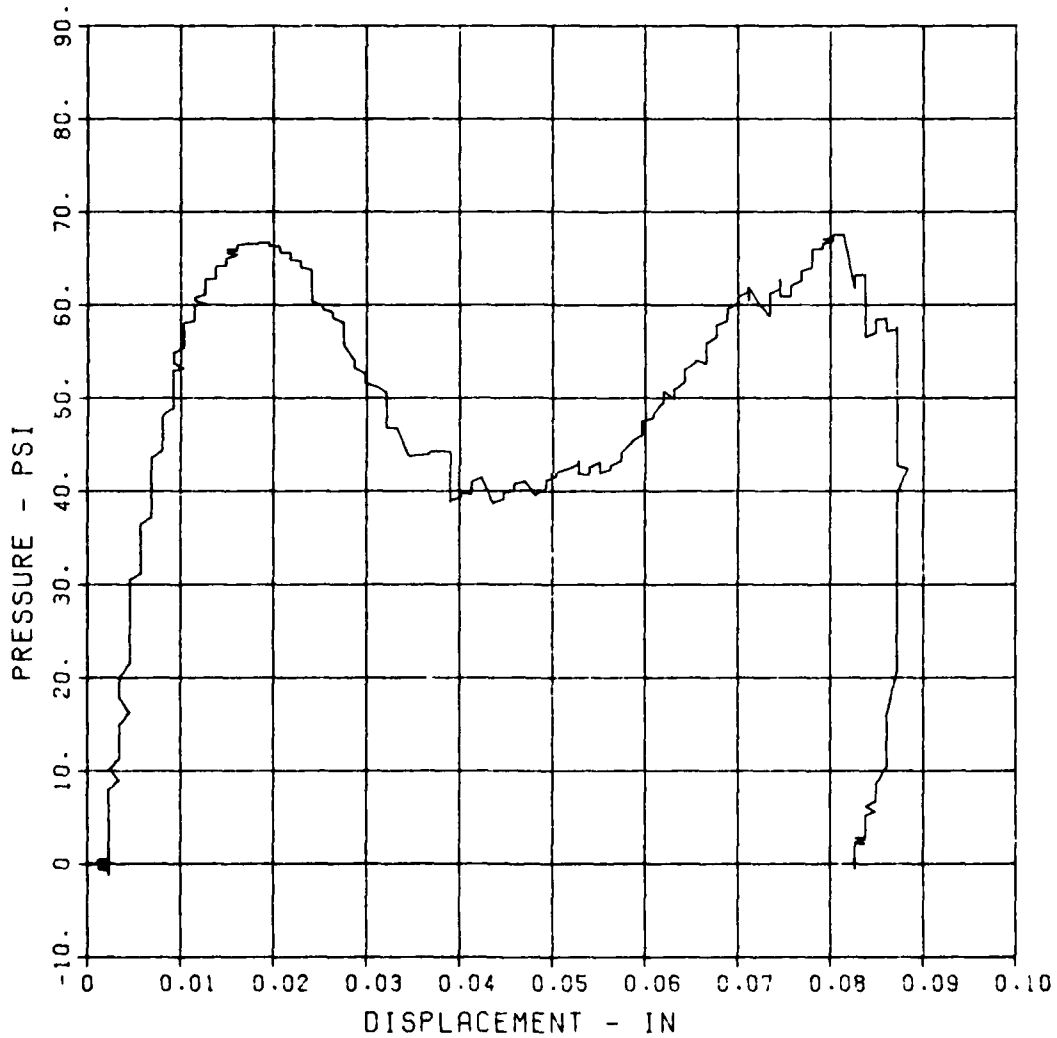
MAXIMUM
0.0884

SIGMA CAL
0.9772

CAL. VAL
1.1

CHANNEL NO. 2 13092 1

06/12/84 R0342



FEMA STIRRUP SLAB 2

D-2

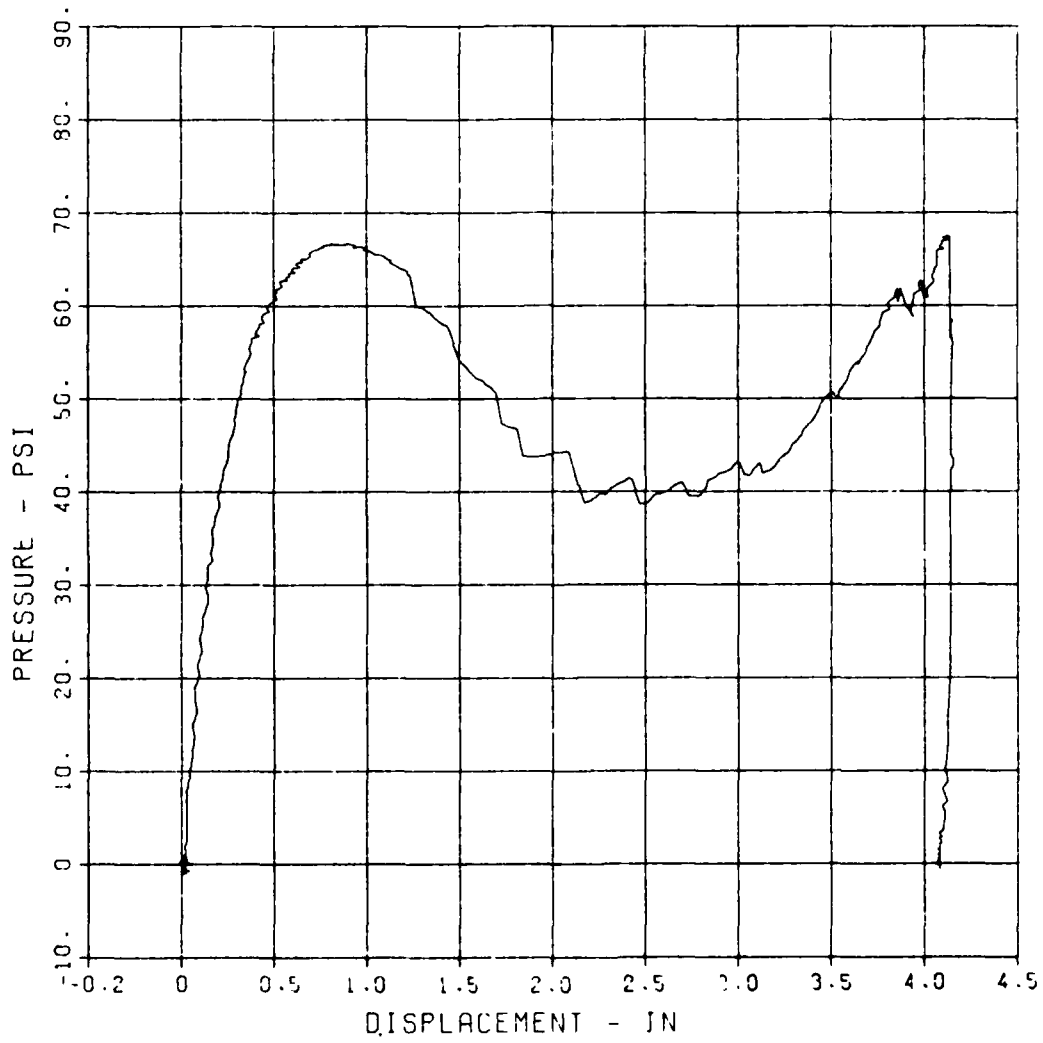
MAXIMUM
1.6610

SIGMA CAL
1.8505

CAL VAL
5.3

CHANNEL NO. 4 13092 1

06/12/84 R0342



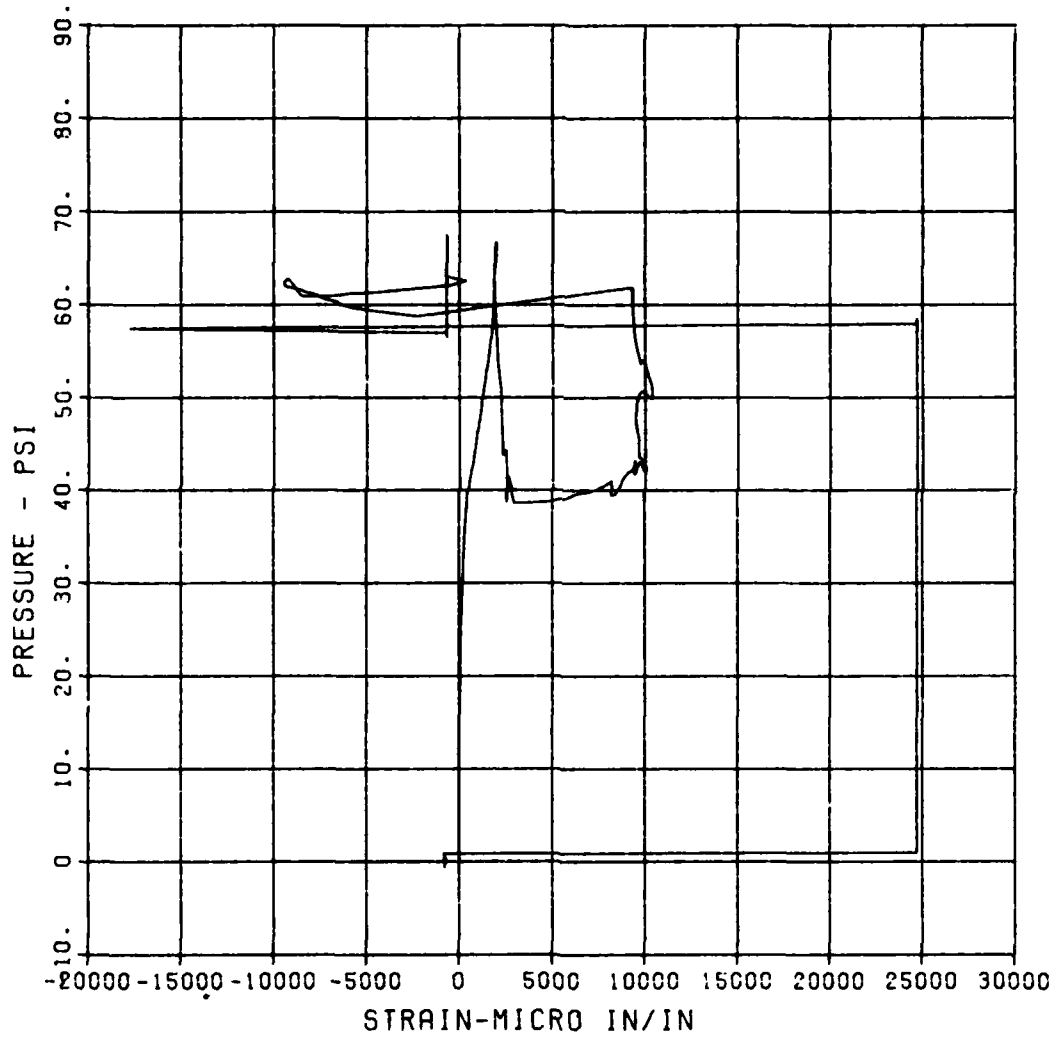
FEMA STIRRUP SLAB 2

ST-1

MAXIMUM	SIGMA CAL	CAL VAL
24714.6999	1.0935	11666.7

CHANNEL NO. 5 13092 1

06/12/84 R0342



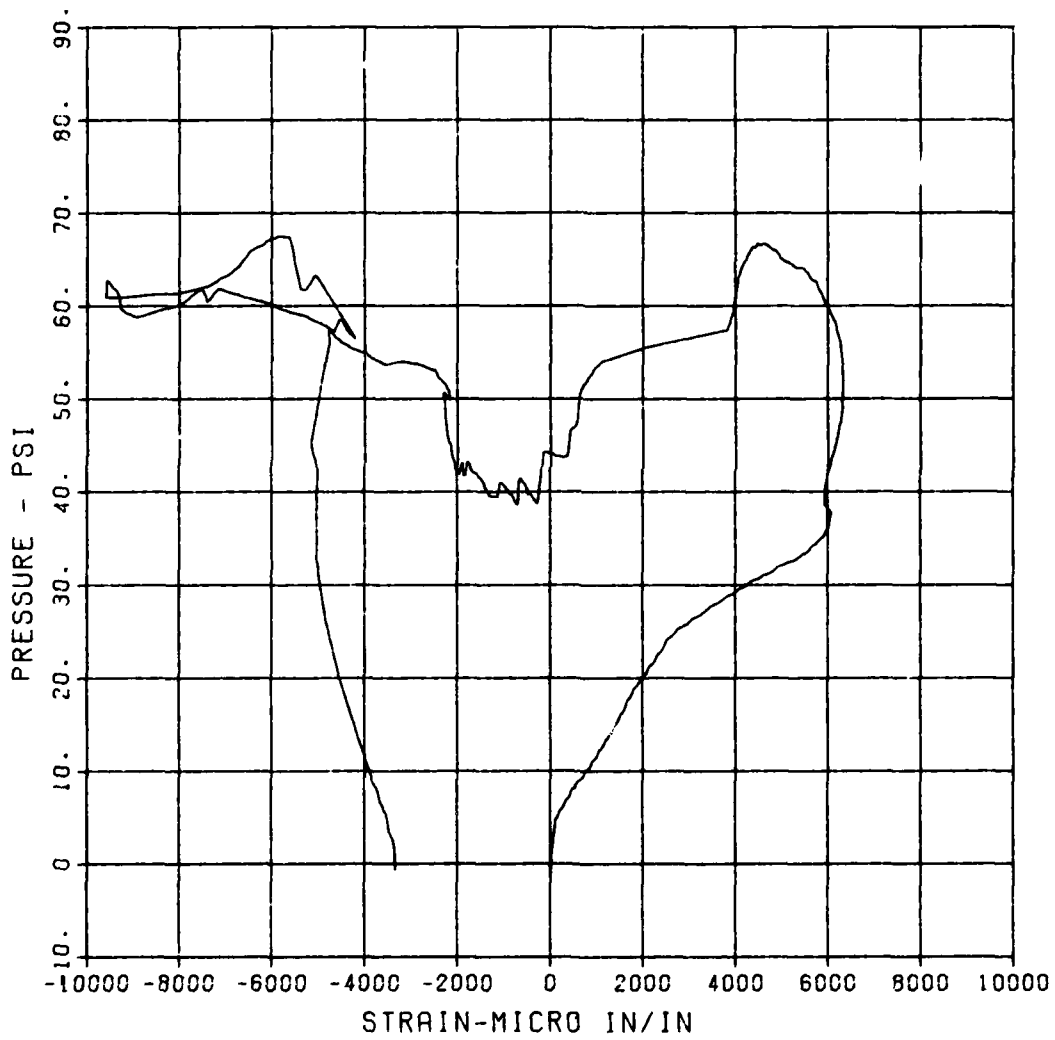
FEMA STIRRUP SLAB 2

SB-1

MAXIMUM	SIGMA CAL	CAL VAL
-9591.3249	1.1550	11666.7

CHANNEL NO. 7 13092 1

06/12/84 R0342



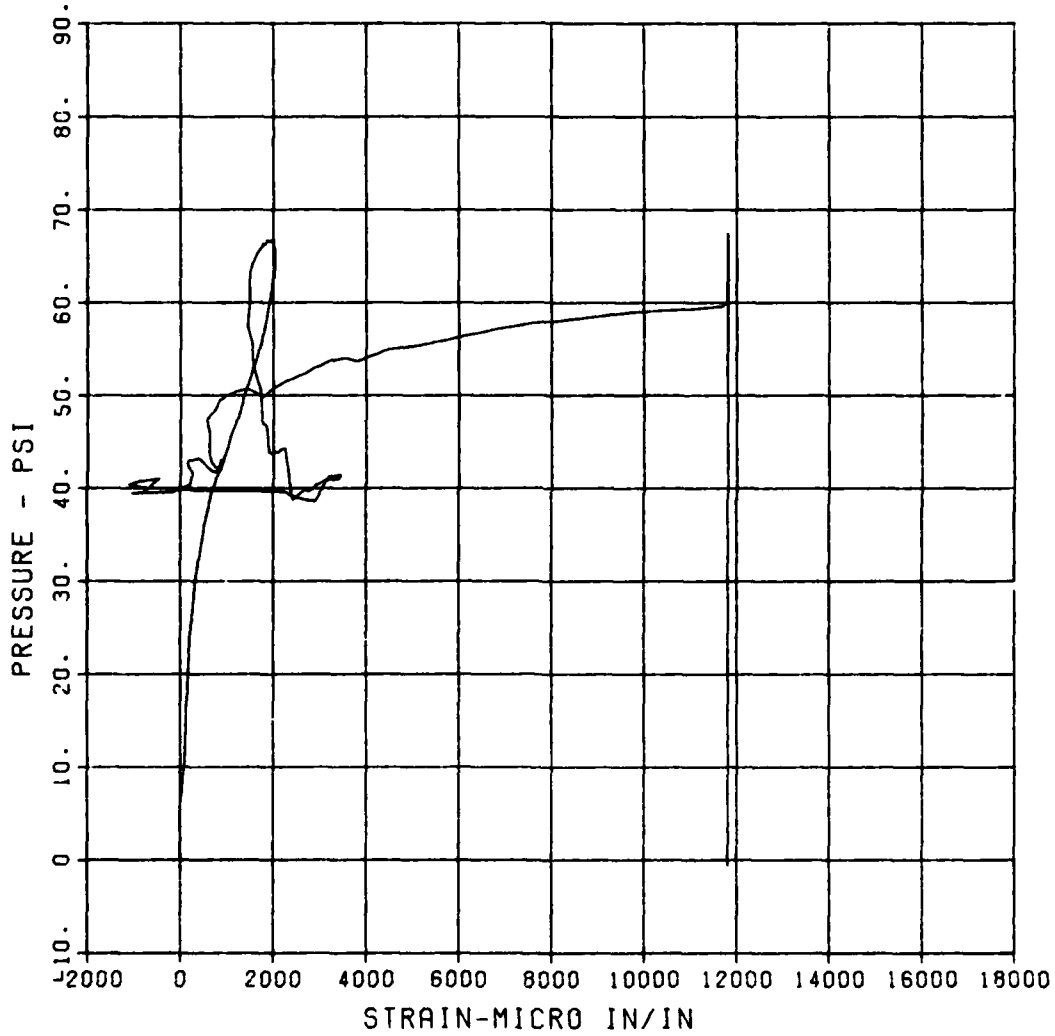
FEMA STIRRUP SLAB 2

ST-2

MAXIMUM	SIGMA CAL	CAL VAL
11811.3975	1.1069	5766.1

CHANNEL NO. 8 13092 1

06/12/84 R0342



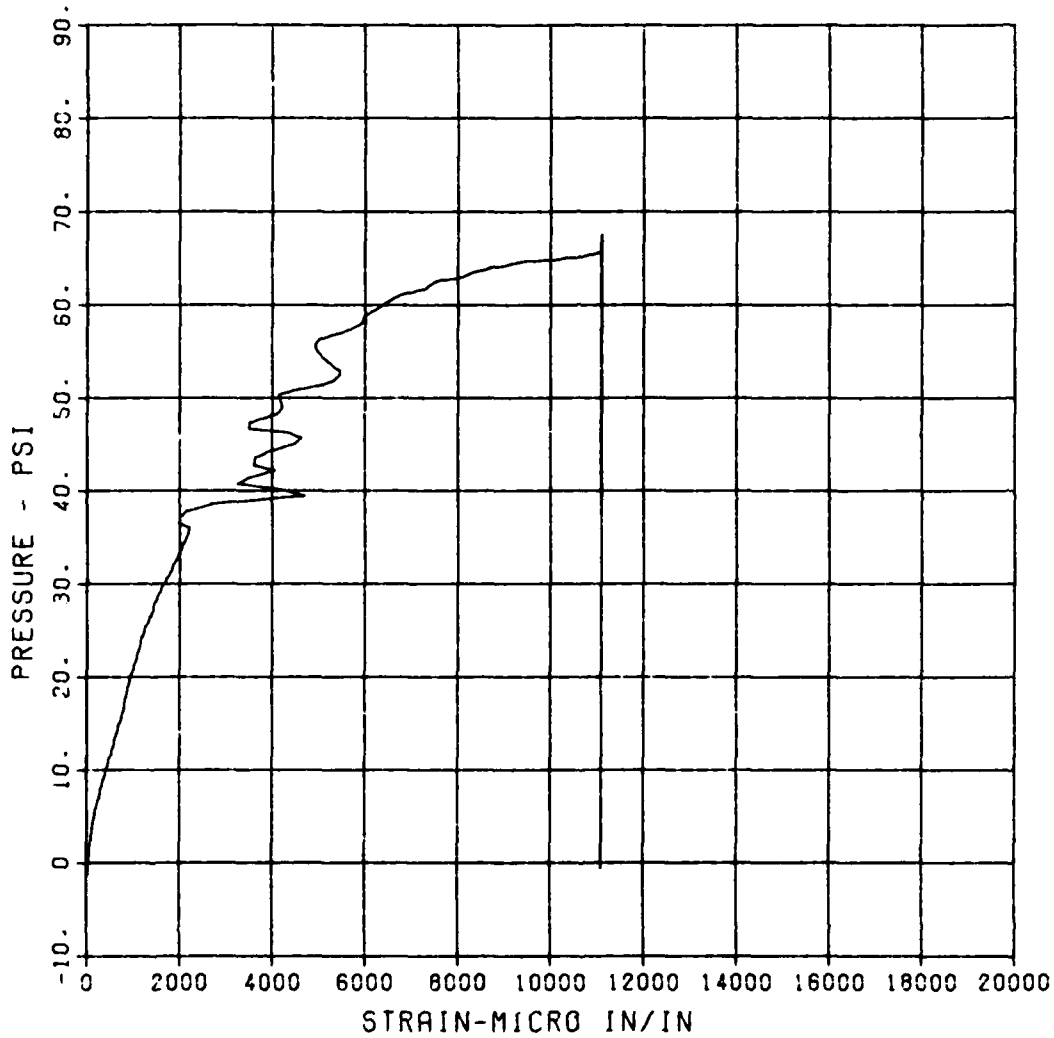
FEMA STIRRUP SLAB 2

SB-2

MAXIMUM 11096.0516 SIGMA CAL 1.5889 CAL VAL 5766.1

CHANNEL NO 9 13092 1

06/12/84 R0342



FEMA STIRRUP SLAB 2

S-3

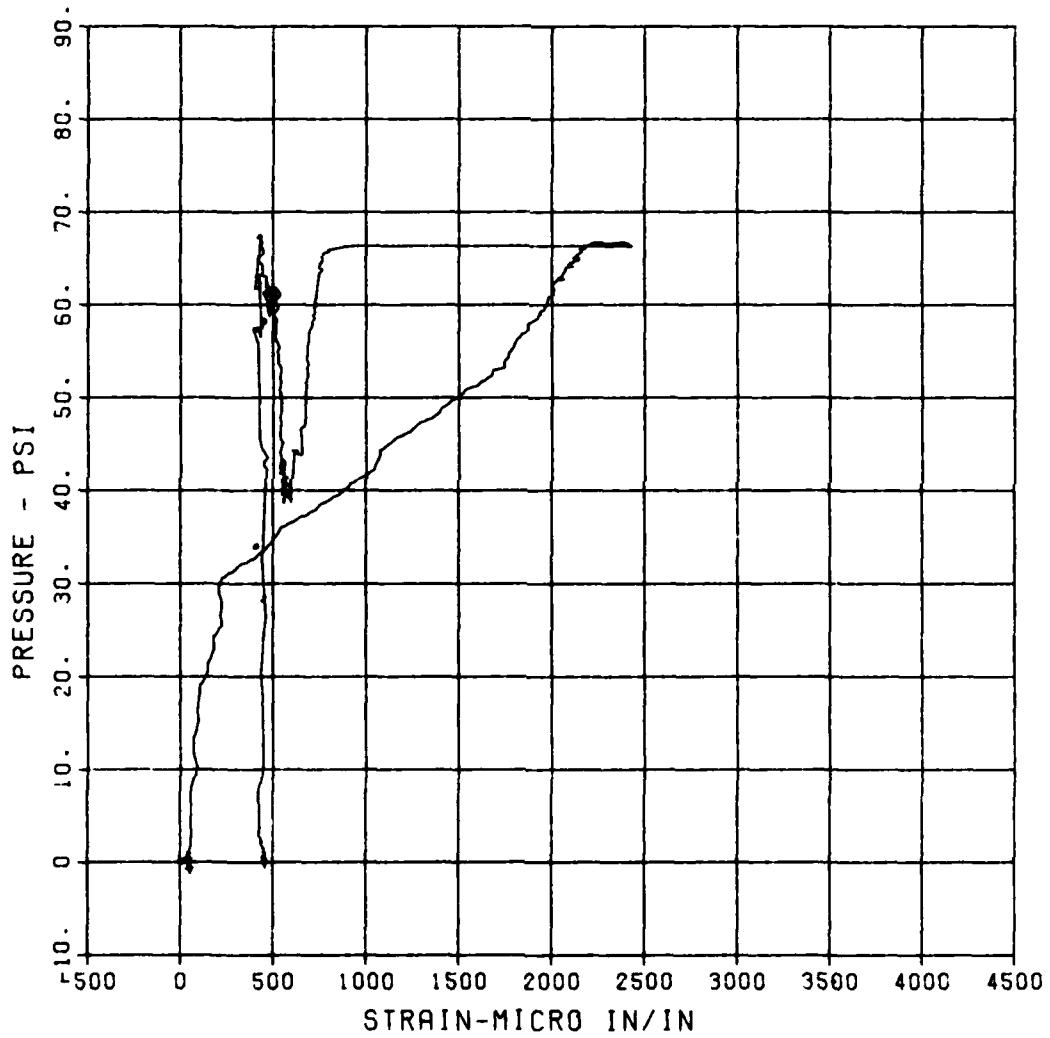
MAXIMUM
2432.6618

SIGMA_CAL
4.0873

CAL_VAL
5766.1

CHANNEL NO. 10 13092 1

06/12/84 R0342



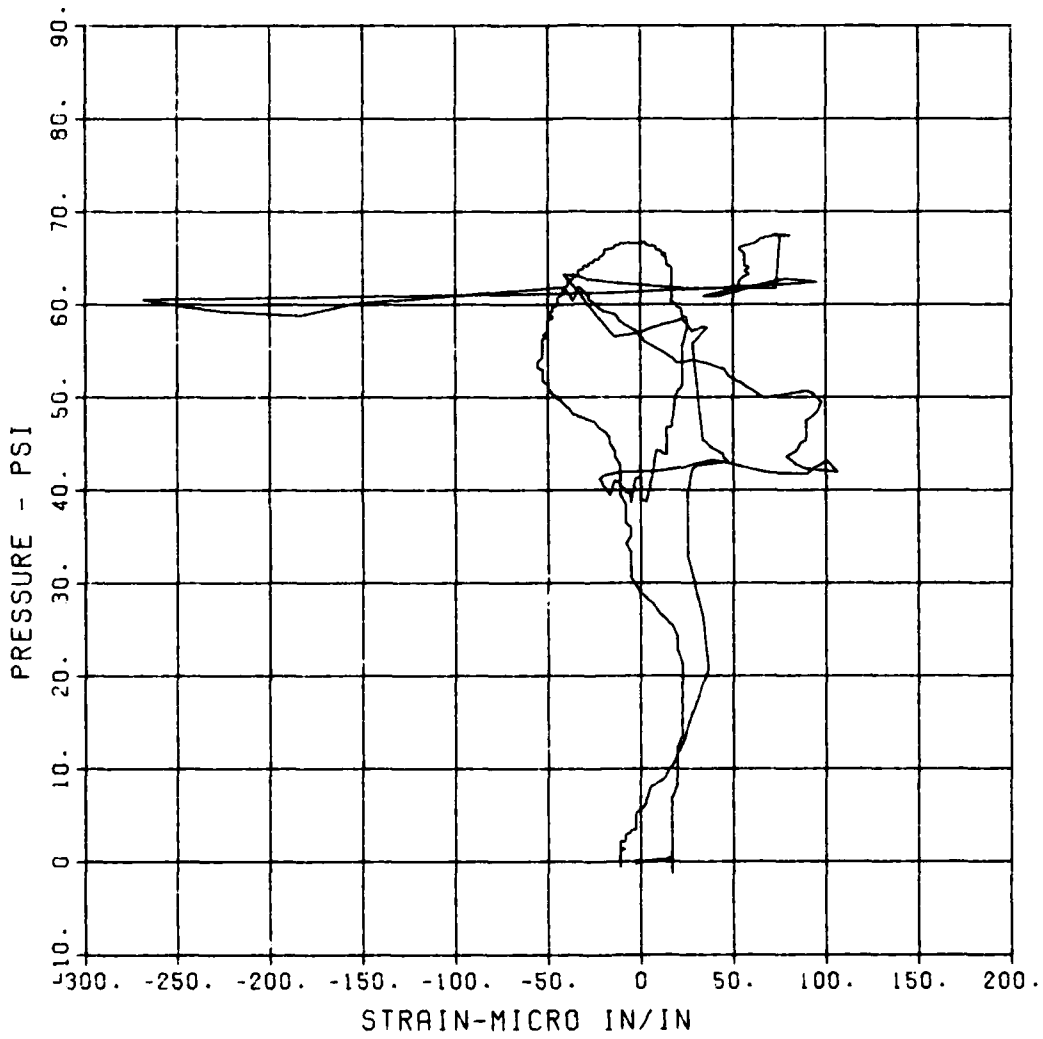
FEMA STIRRUP SLAB 2

S-4

MAXIMUM	SIGMA CAL	CAL VAL
-268.4668	1.3558	2899.8

CHANNEL NO. 11 13092 1

06/12/84 R0342



FEMA STIRRUP SLAB 2

S-5

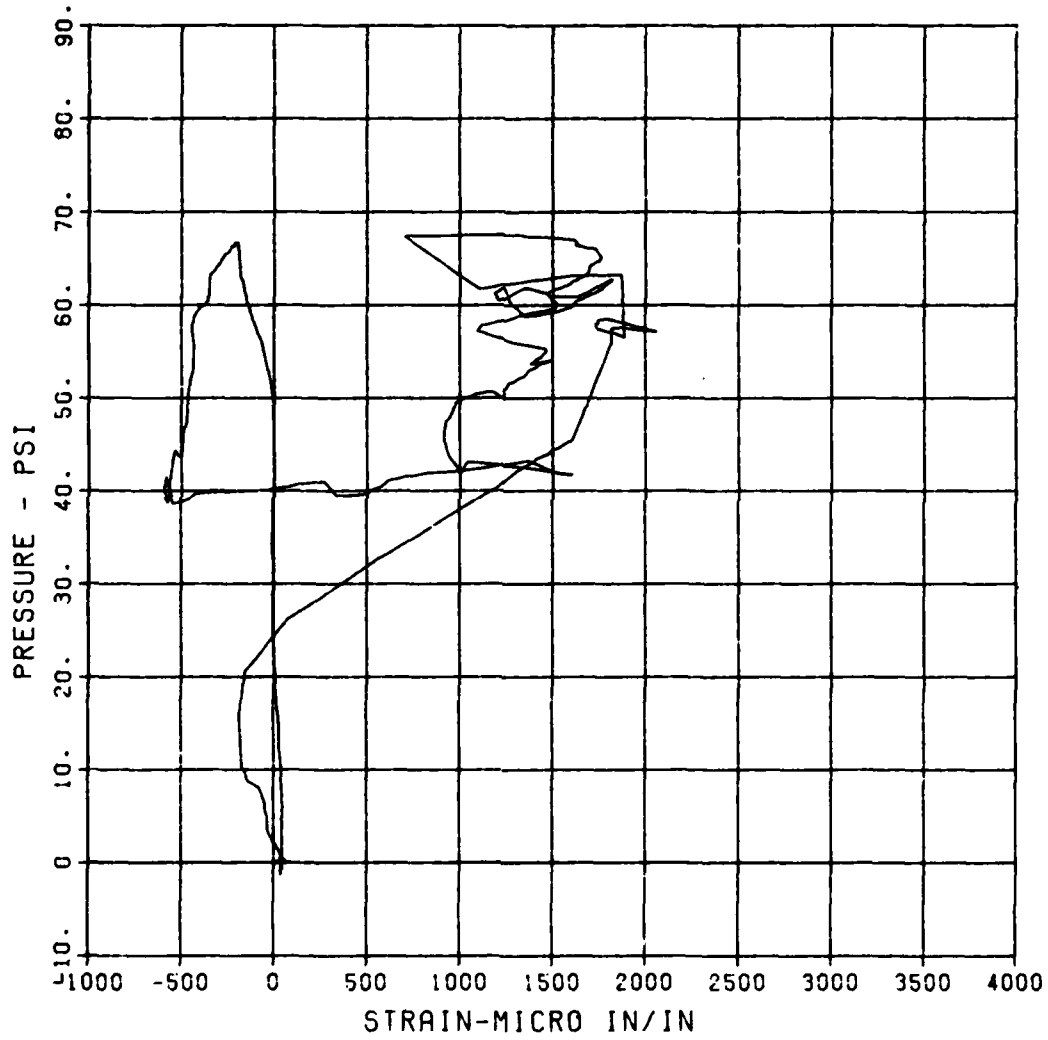
MAXIMUM
2062.2923

SIGMA CAL
1.2231

CAL VAL
5766.1

CHANNEL NO. 12 13092 1

06/12/84 R0342



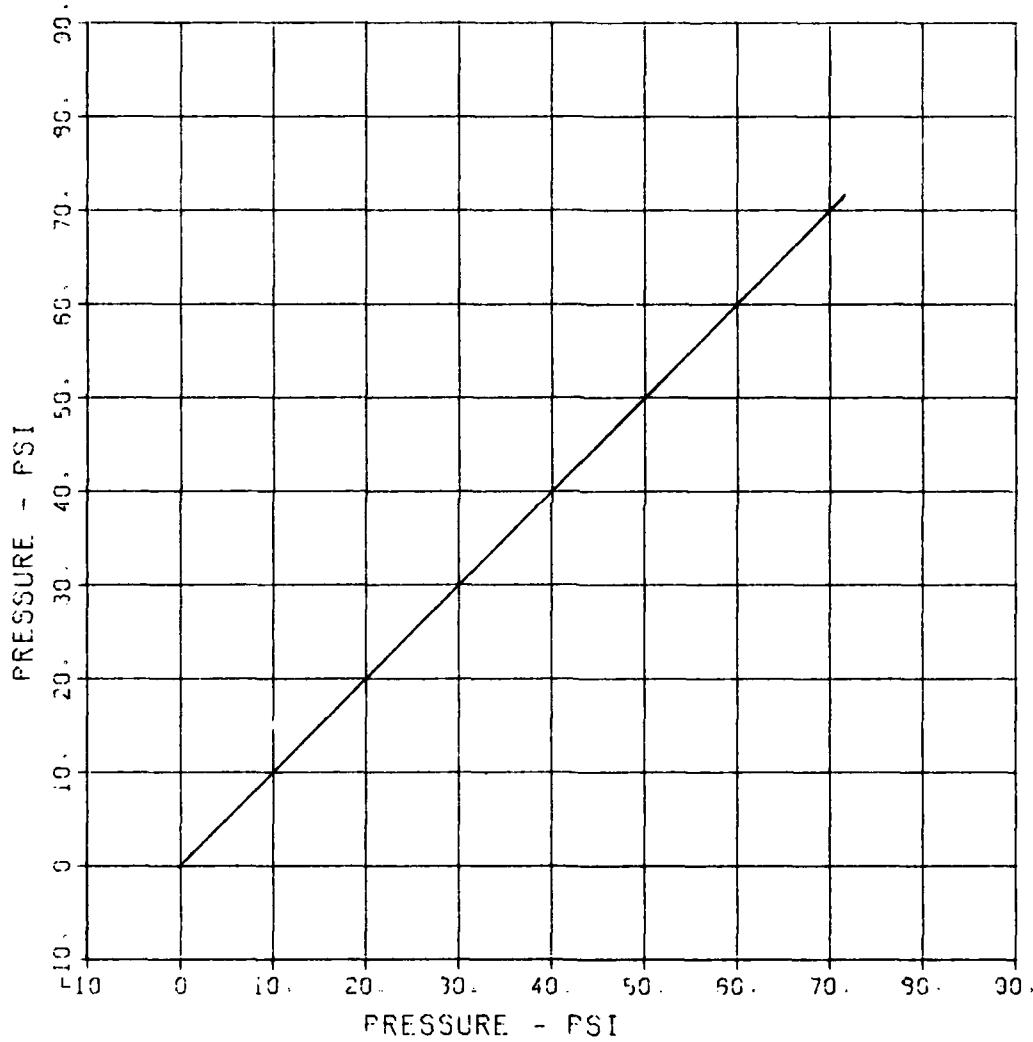
FEMA STIRRUP SLAB 3

P-1

MAXIMUM	SIGMA CAL	CAL VAL
71.5079	2.7533	135.9

CHANNEL NO. i 13437 1

04/25/84 R0434



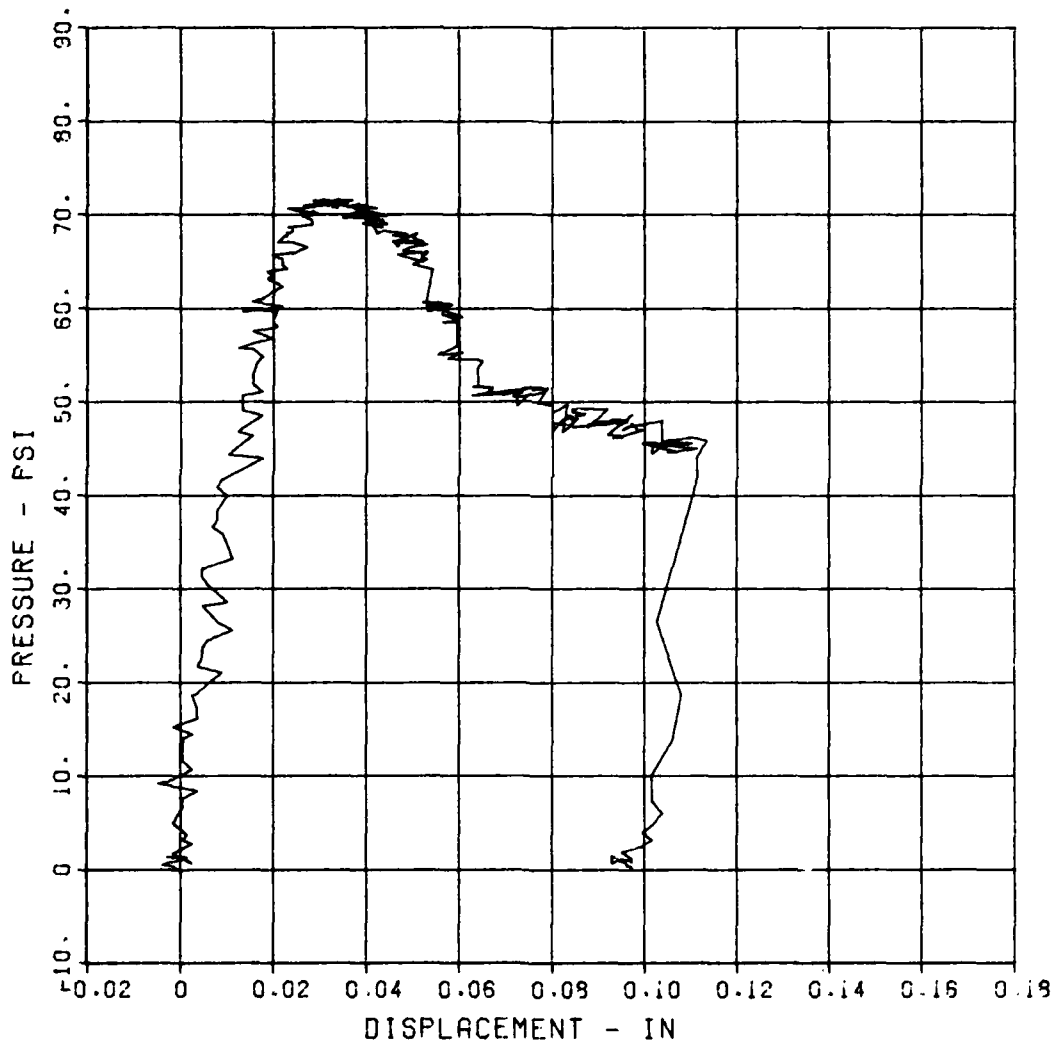
FEMA STIRRUP SLAB 3

D-1

MAXIMUM	SIGMA CAL	CAL VAL
0.1134	2.8919	1.1

CHANNEL NO. 2 13437 1

04/25/94 R0434



FEMA STIRRUP SLAB 3

D-2

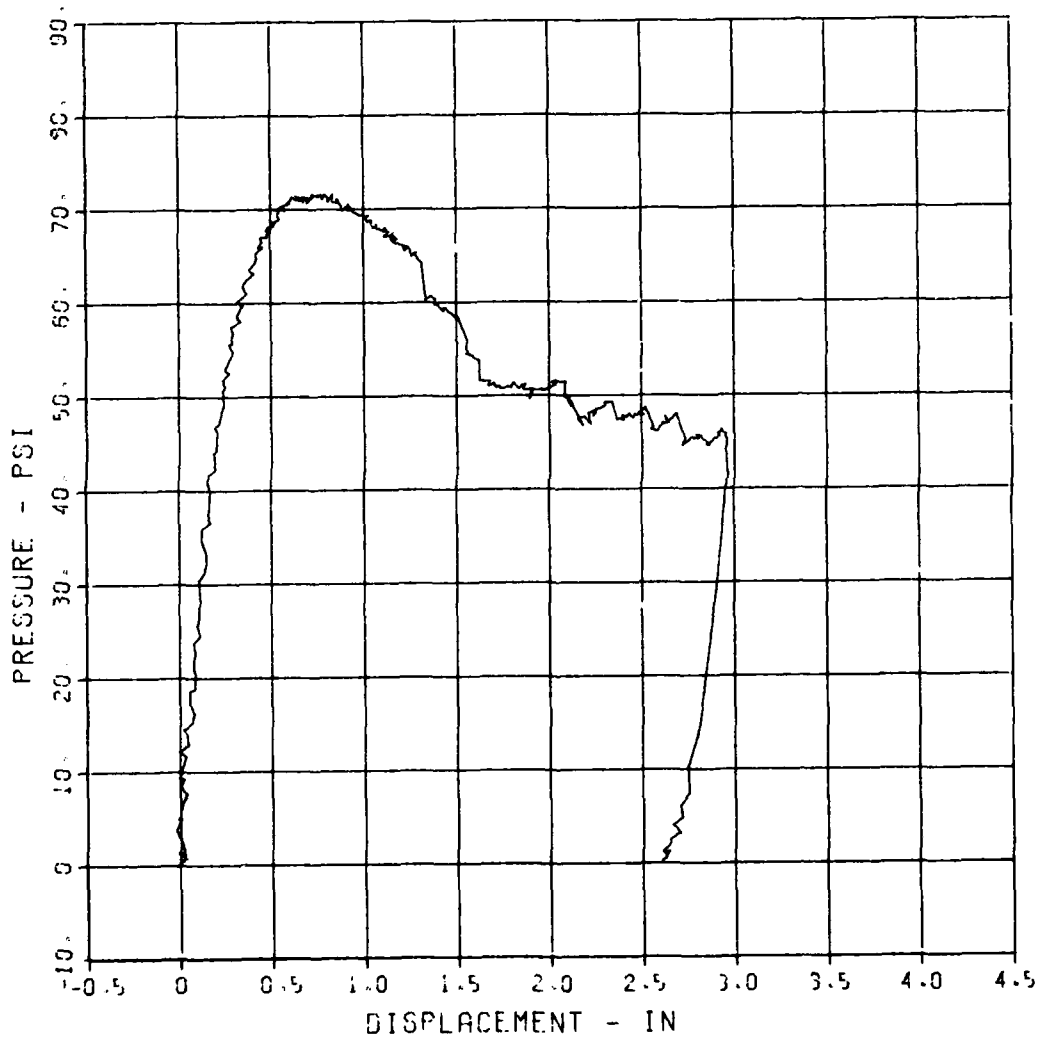
MAXIMUM
2.9645

SIGMA CAL
2.5995

CAL VAL
5.3

CHANNEL NO. 4 13437 i

04/23/94 R0335



FEMA STIRRUP SLAB 3

ST-1

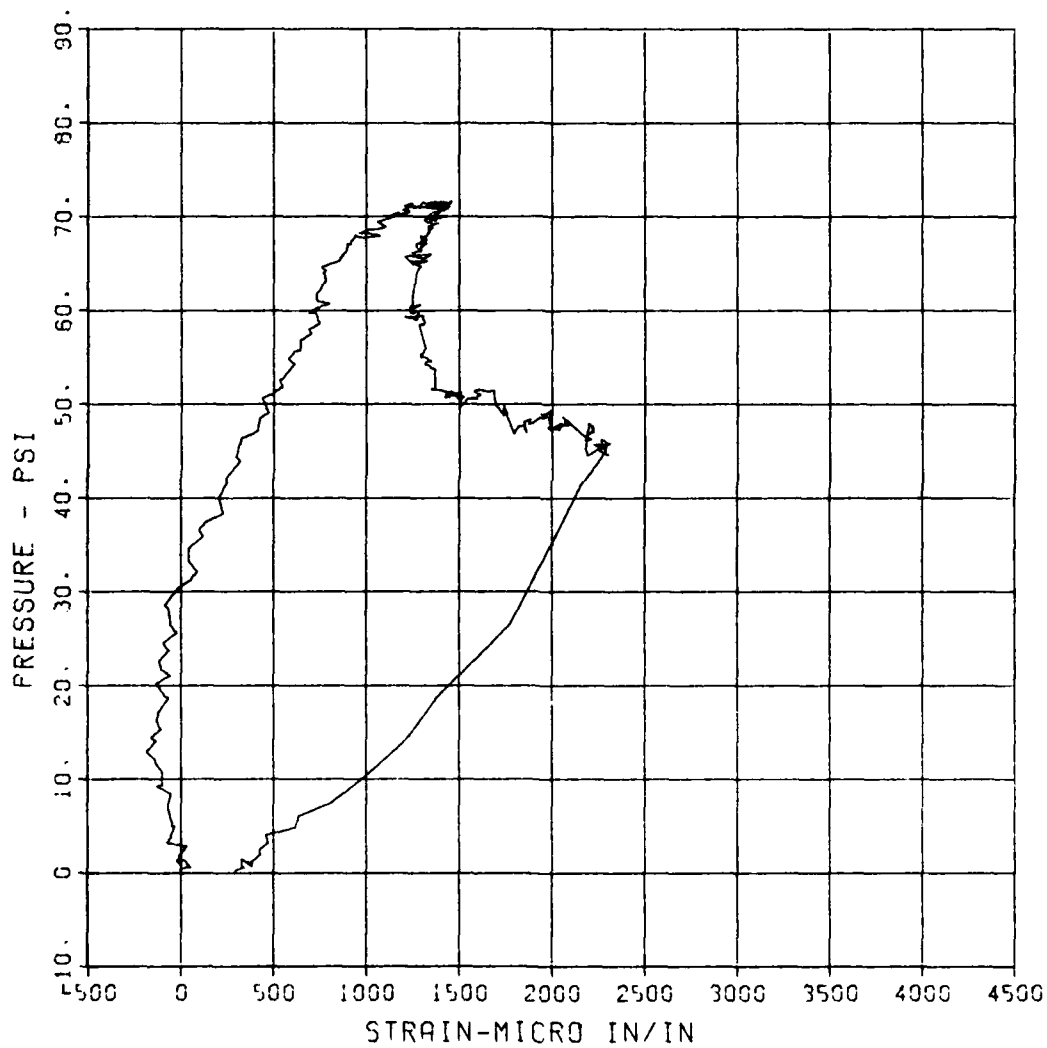
MAXIMUM
2311.0539

SIGMA CAL
3.1963

CAL VAL
11666.7

CHANNEL NO. 5 13437 1

04/25/94 R0434



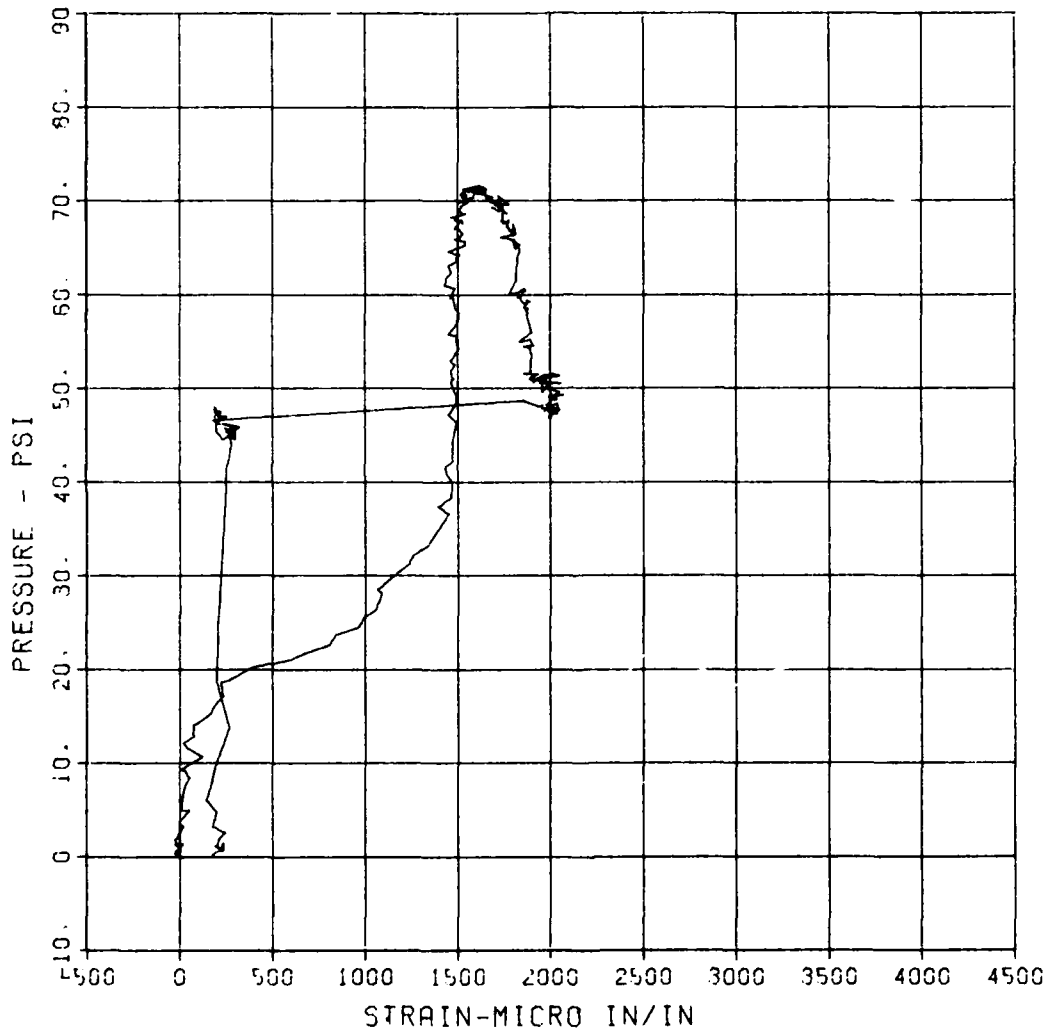
FEMA STIRRUP SLAB 3

SB-1

MAXIMUM	SIGMA_CAL	CAL_VAL
2070.4158	3.0372	11656.7

CHANNEL NO. 7 13437 1

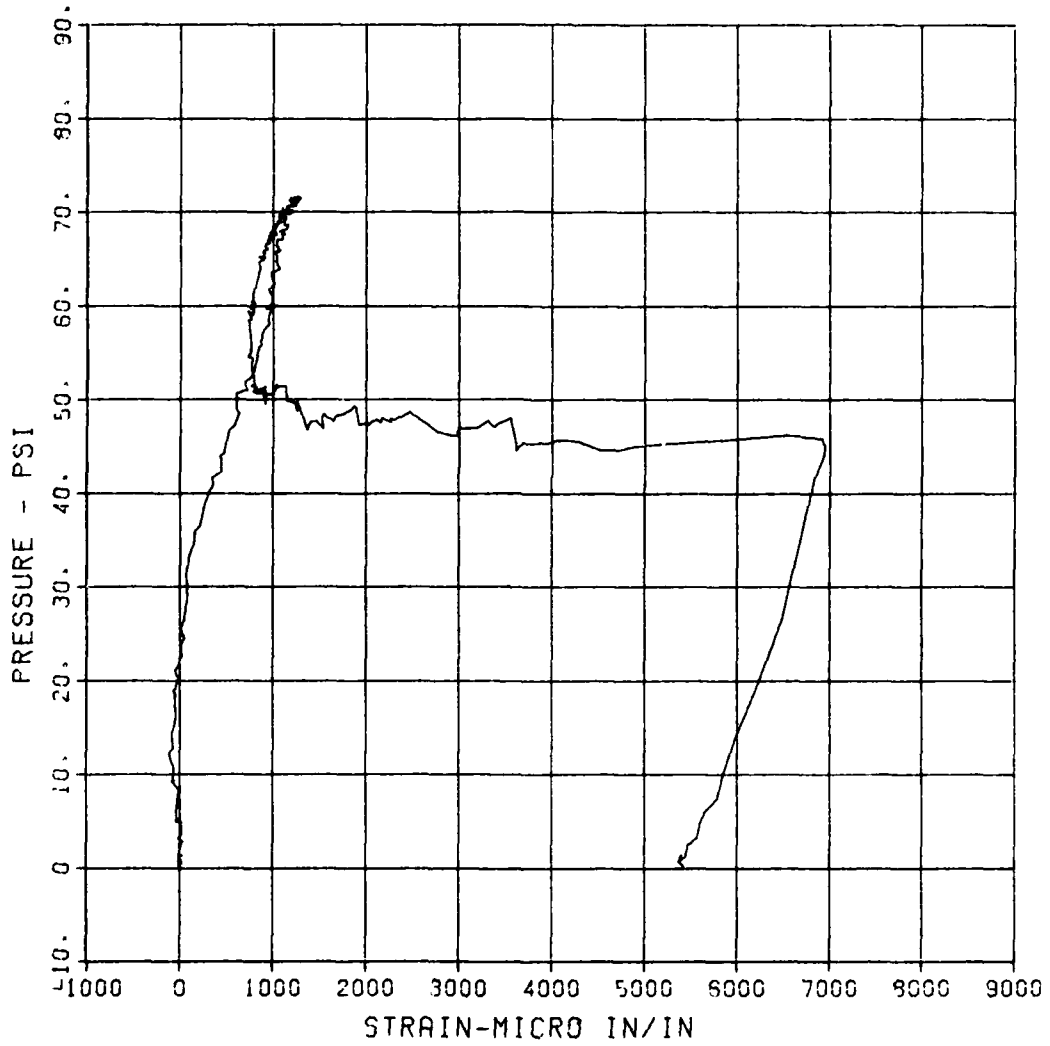
04/25/84 R0434



FEMA STIRRUP SLAB 3
ST-2

MAXIMUM 6947.1936 SIGMA CAL 5.1005 CAL VAL 5799.1

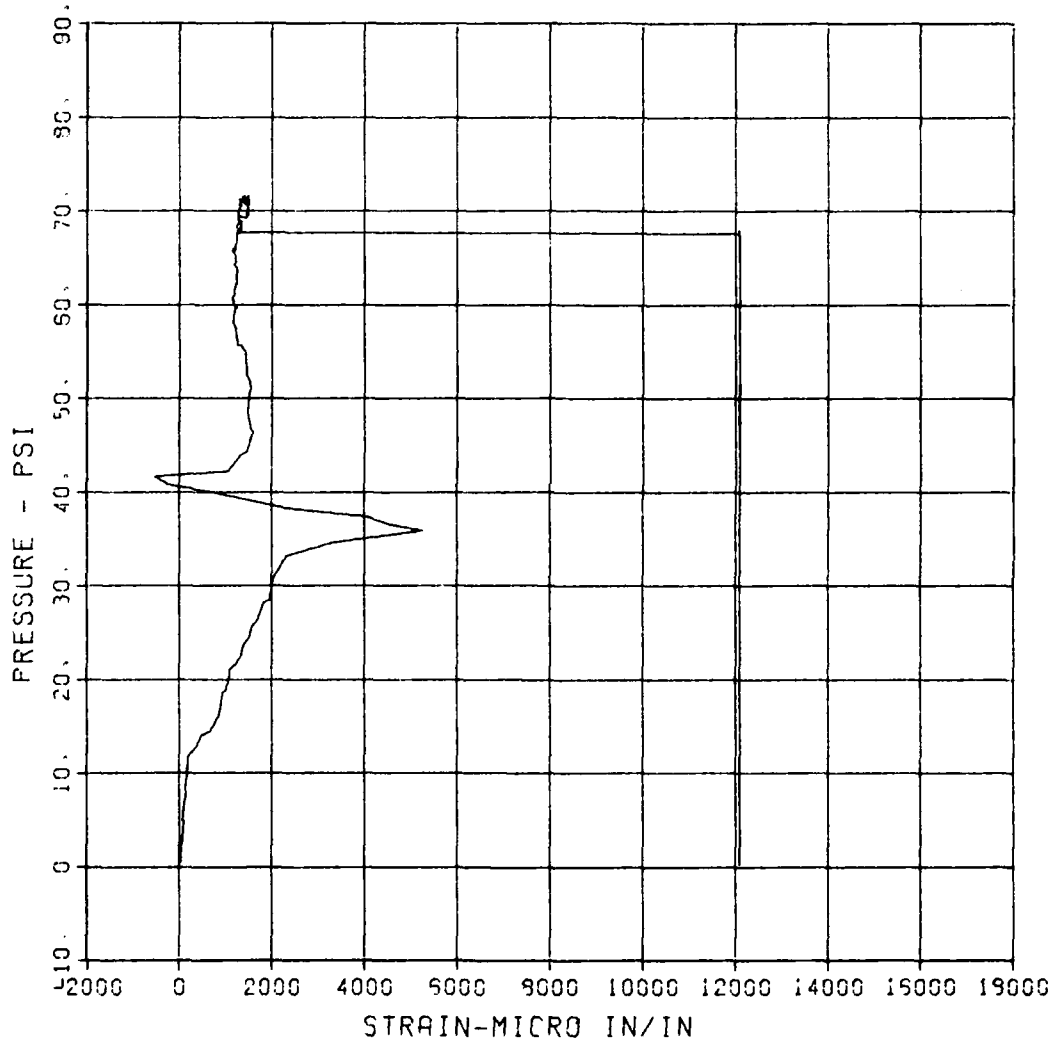
CHANNEL NO. 9 13437 1
04/25/94 R0434



FEMA STIRRUP SLAB 3
SB-2

MAXIMUM 12090.7947 SIGMA CAL 4.4195 CAL_VAL 5755.1

CHANNEL NO. 9 13437 1
04/25/94 R0434



FEMA STIRRUP SLAB 3

S-3

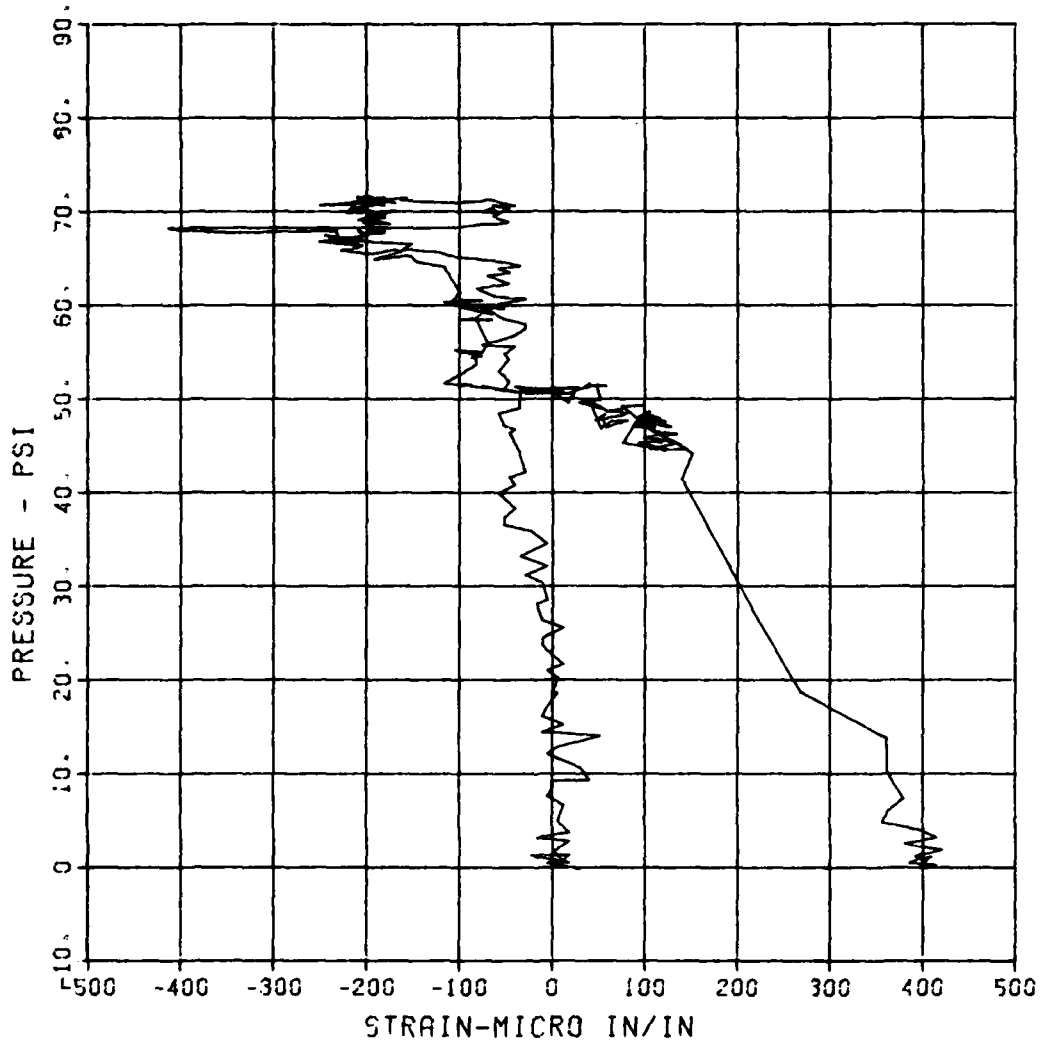
MAXIMUM
420.4322

SIGMA CAL
2.9928

CAL VAL
5766.1

CHANNEL NO. 10 13437 i

04/23/84 R0335



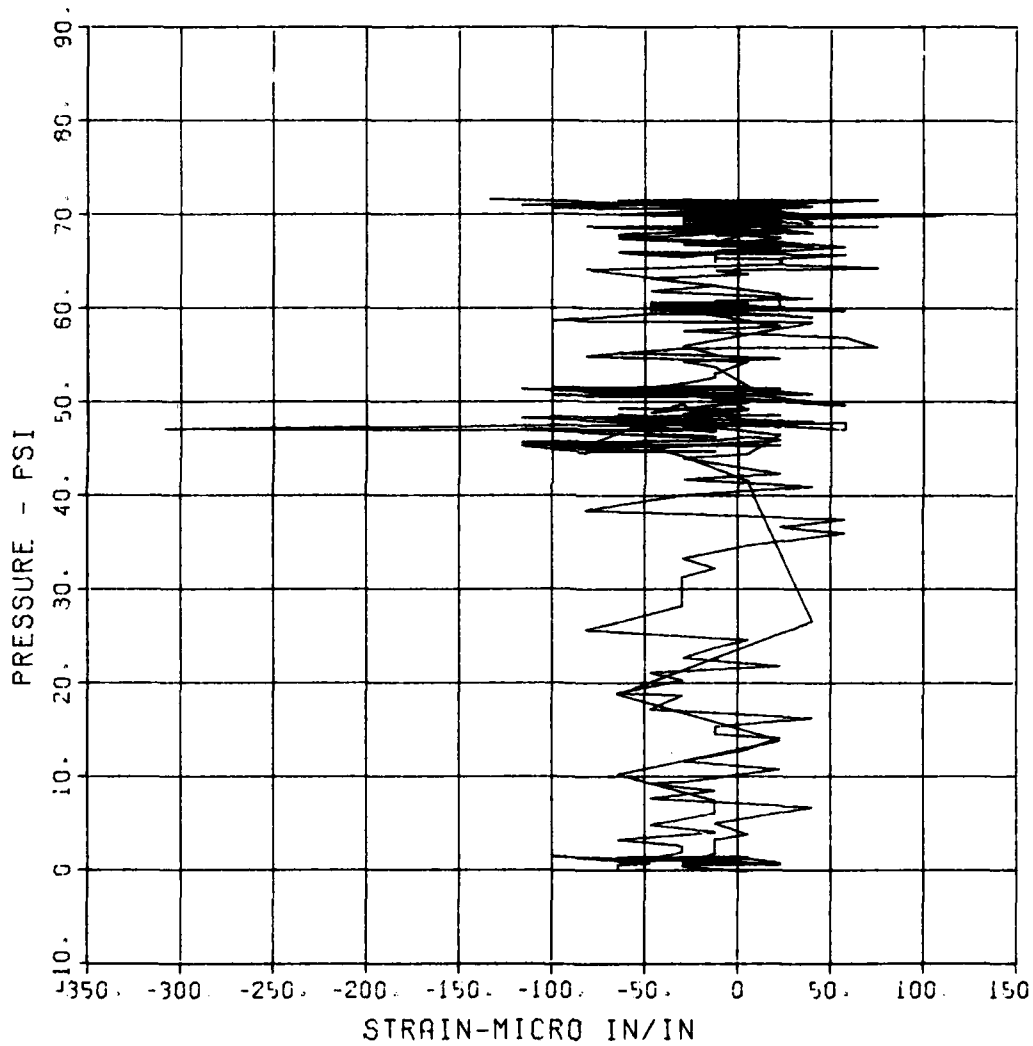
FEMA STIRRUP SLAB 3

S-4

MAXIMUM	SIGMA CAL	CAL VAL
-309.2492	2.5140	2999.9

CHANNEL NO. 11 13437 1

04/25/84 R0434



FEMA STIRRUP SLAB 3

S-5

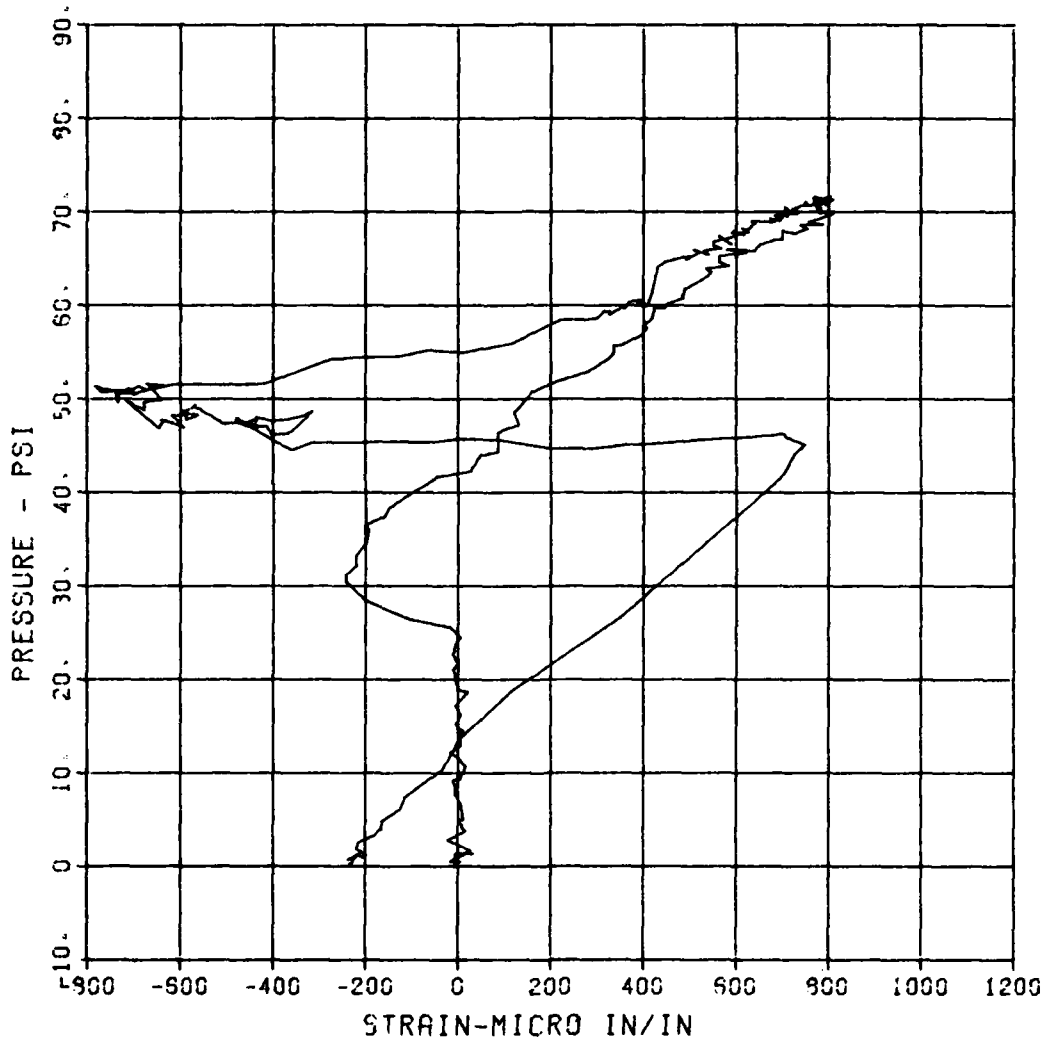
MAXIMUM
910.370i

SIGMA CAL
2.45i2

CAL VAL
5765.1

CHANNEL NO. 12 13437 i

04/23/94 R0395



FEMA STIRRUP SLAB 4

P-1

MAXIMUM
75.029

SIGMA CAL
2.6142

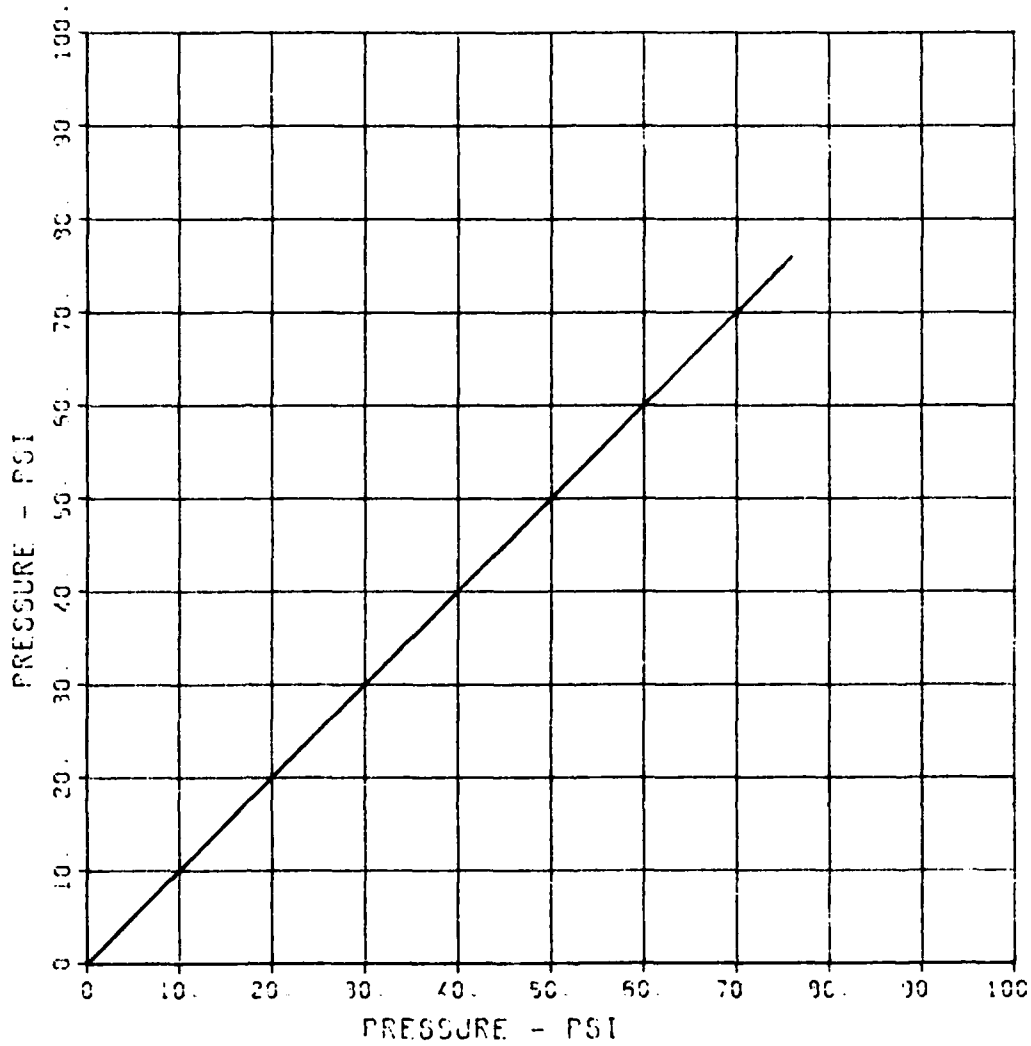
CAL VAL
135.0

CHANNEL NO

3492 :

05/04/94

50515



FEMA STIRRUP SLAB 4

D-1

MAXIMUM
0.7822

SIGMA CAL
2.5265

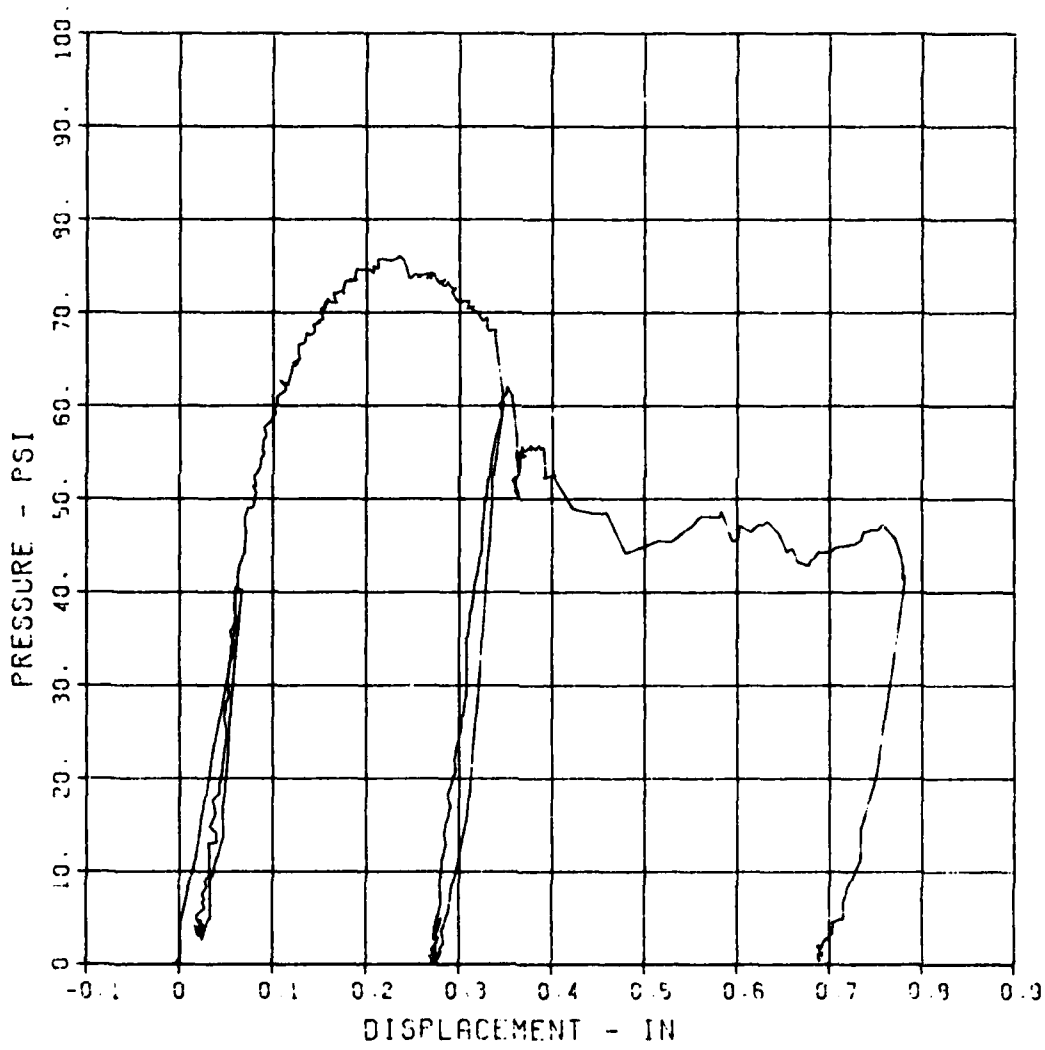
CAL VAL
1.1

CHANNEL NO. 2

3462 1

05/04/84

R0516



FEMA STIRRUP SLAB 4

D-2

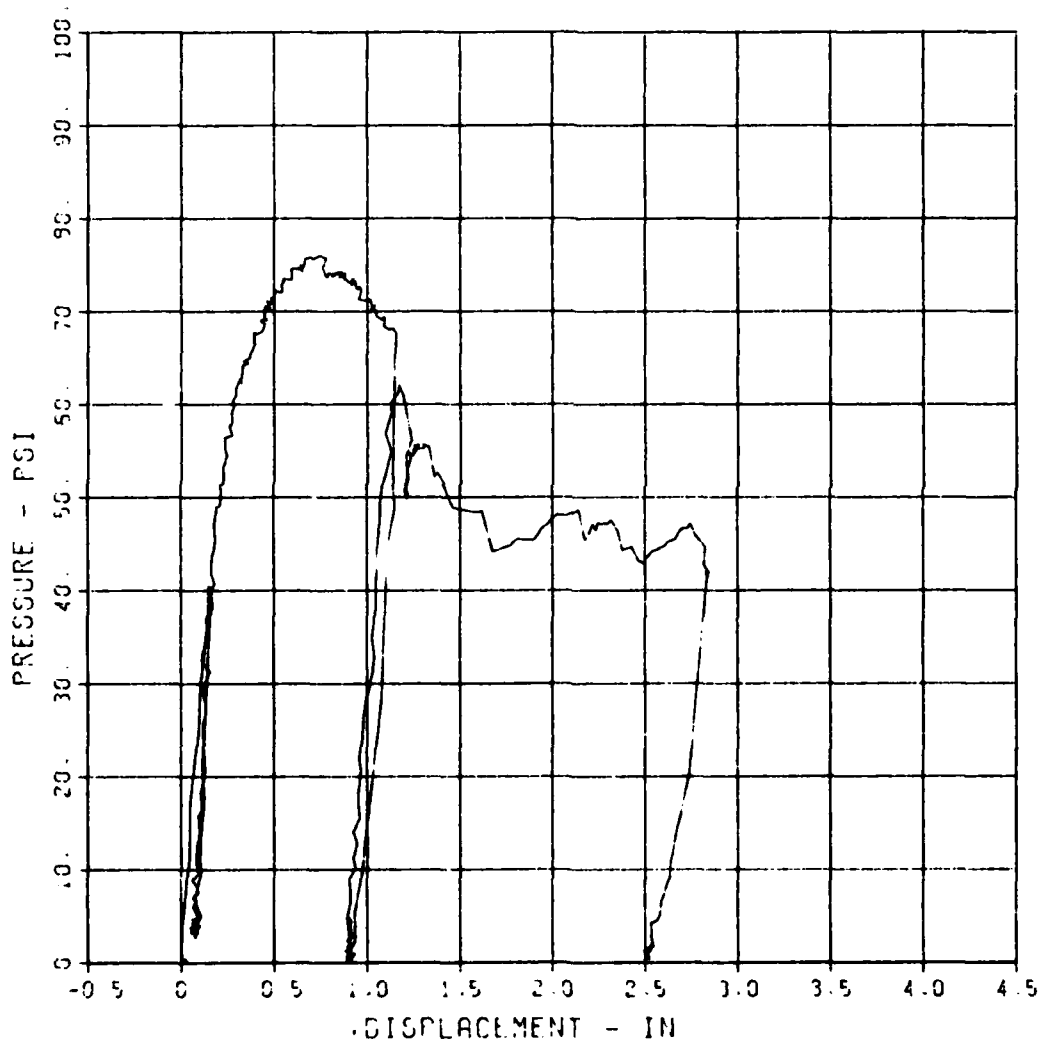
MAXIMUM
2.9459

SIGMA CAL
3.1365

CAL VAL
5.3

CHANNEL NO 4 3452 1

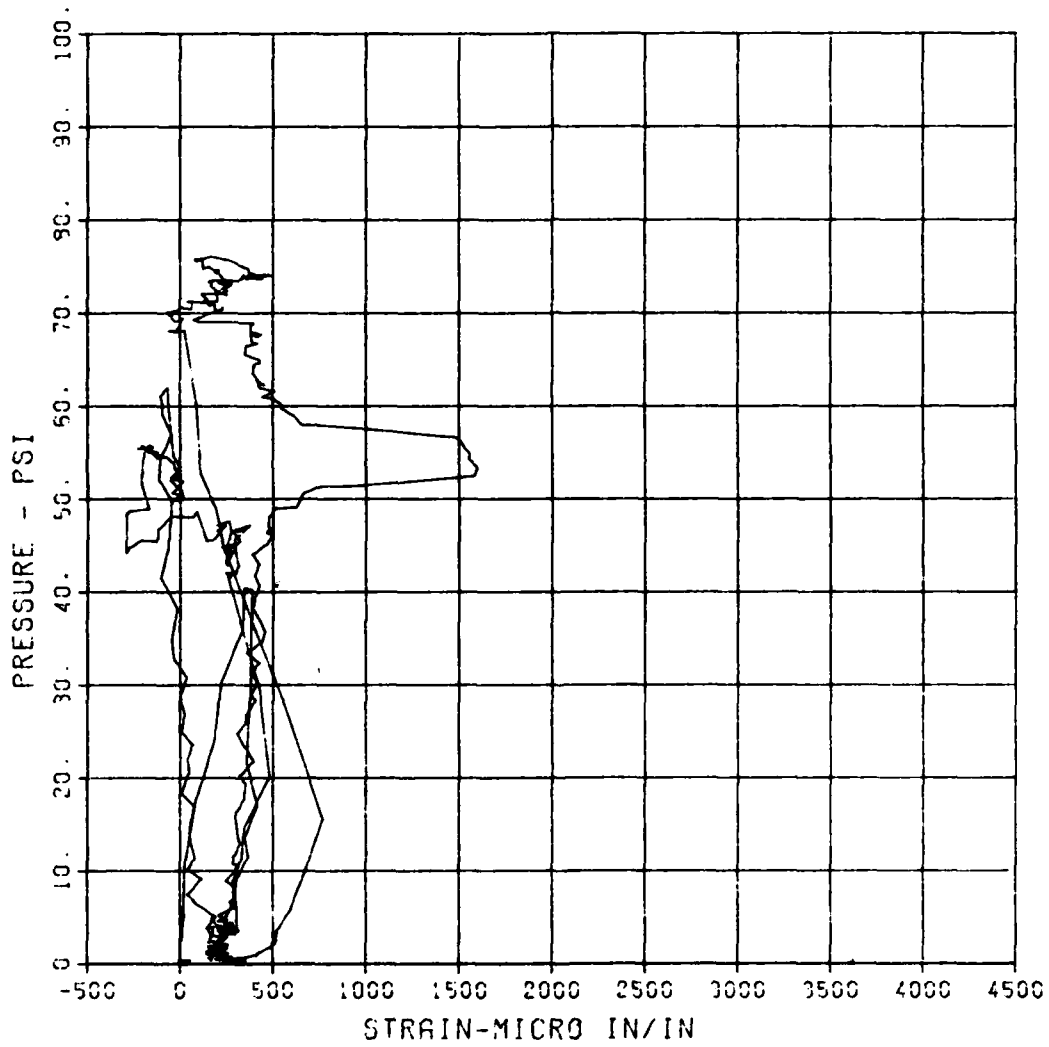
05/04/84 R0515



FEMA STIRRUP SLAB 4
ST-1

MAXIMUM 1900 5959 SIGMA CAL 2.3333 CAL VAL 11655.7

CHANNEL NO. 5 3462
05/04/84 R0516



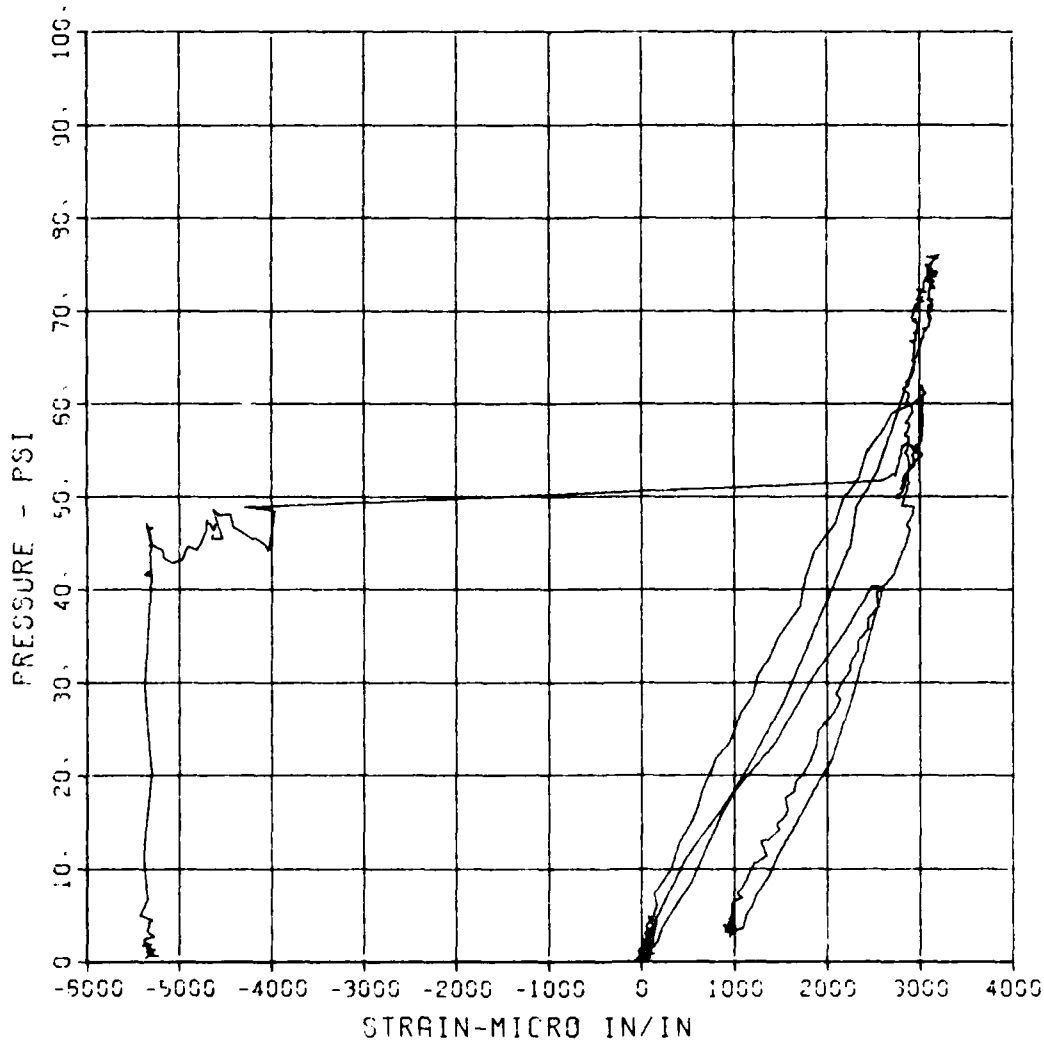
FEMA STIRRUP SLAB 4

SB-1

MAXIMUM -5431.3500 SIGMA CAL 4.0524 CAL VAL 11555.7

CHANNEL NO. 7 3452 1

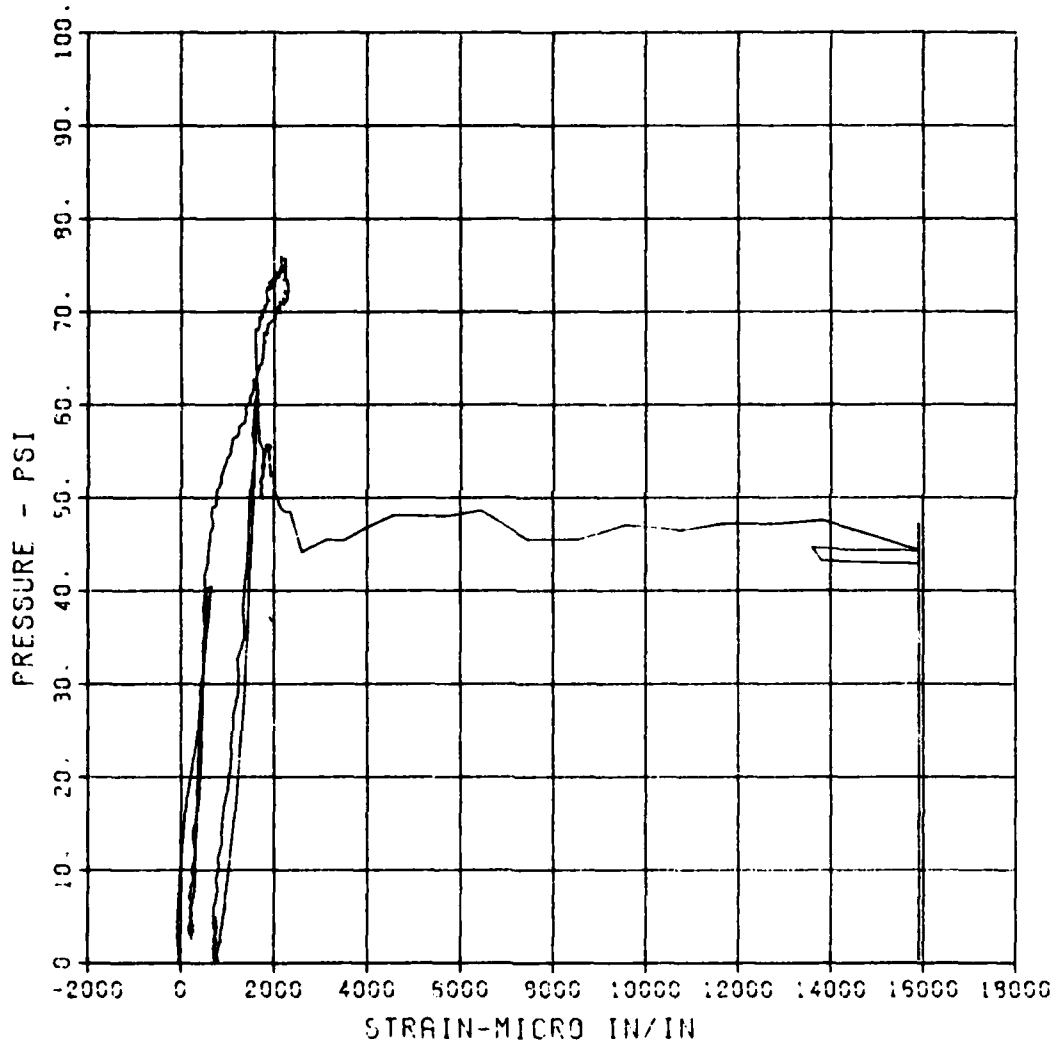
05/11/94 R0731



FEMA STIRRUP SLAB 4
ST-2

MAXIMUM 19303.0733 SIGMA CAL 3.4160 CAL VAL 5766.1

CHANNEL NO. 9 3462 1
05/04/94 R0515



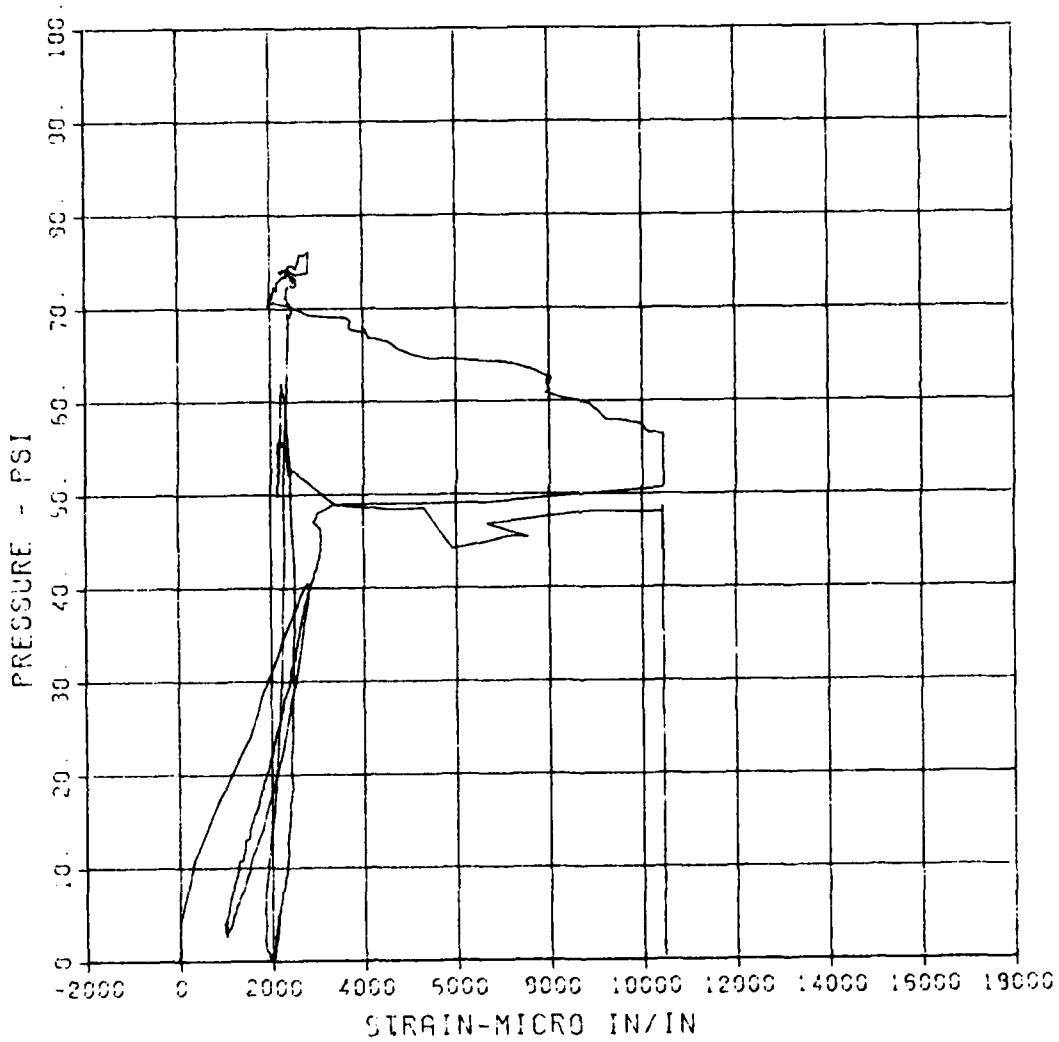
FEMA STIRRUP SLAB 4

SB-2

MAXIMUM 10442.7230 SIGMA CAL 3.0331 CAL VOL 5755

CHANNEL NO 0 3452

05/04/94 R0619



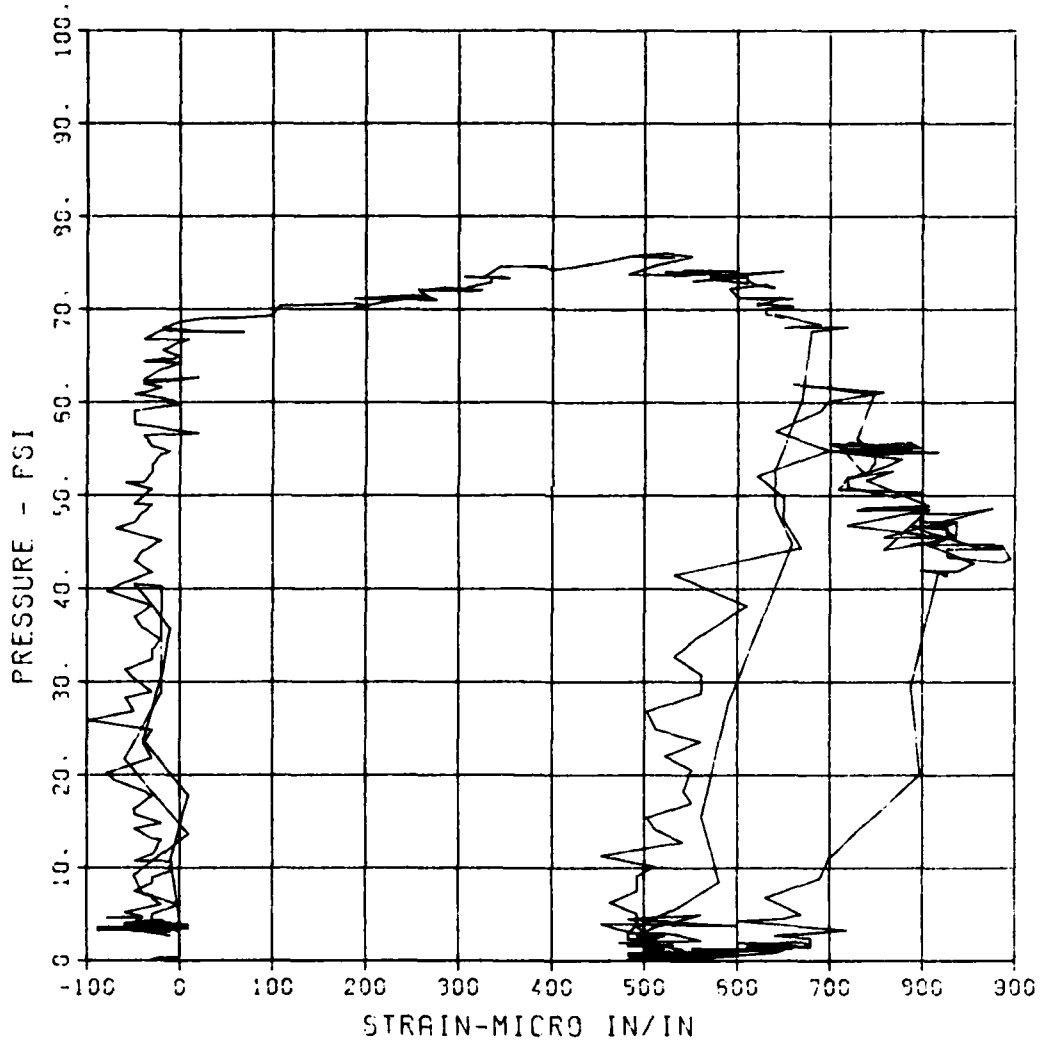
FEMA STIRRUP SLAB 4

S-3

MAXIMUM	SIGMA CAL	CAL VAL
995.9792	2.5712	5765.1

CHANNEL NO. 10 3452 1

05/04/84 R06:5



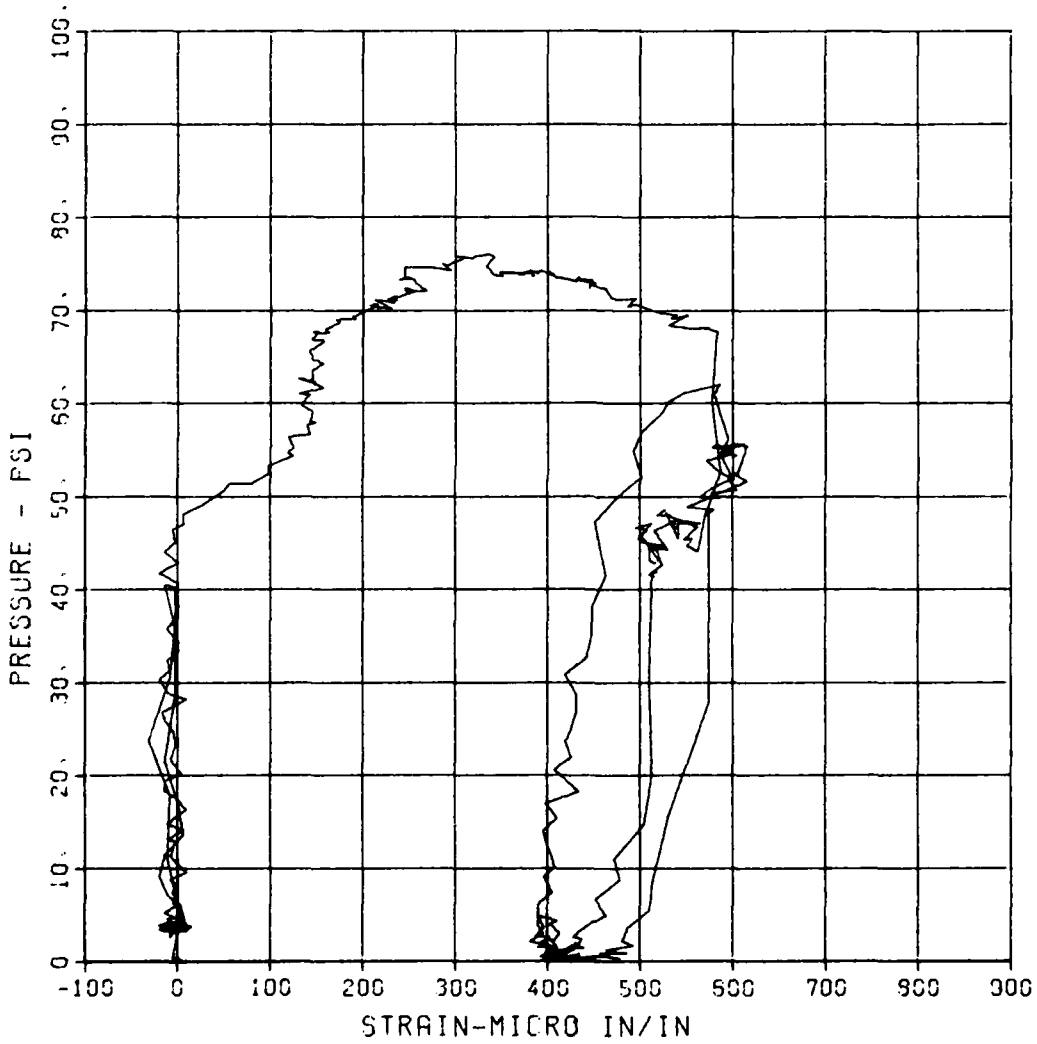
FEMA STIRRUP SLAB 4

S-4

MAXIMUM	SIGMA CAL	CAL VAL
515.3542	3.9145	2990.3

CHANNEL NO. 11 3462 1

05/11/94 R073i



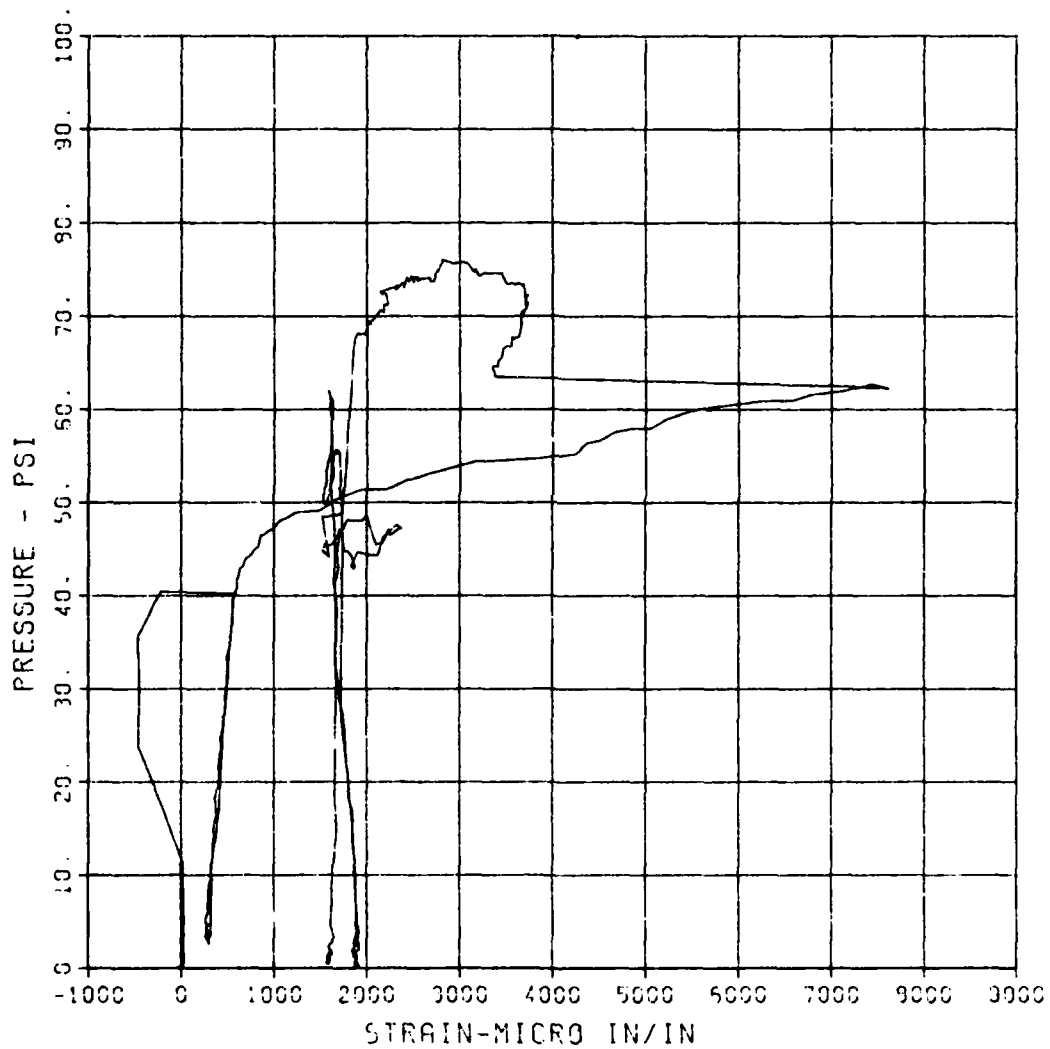
FEMA STIRRUP SLAB 4

S-5

MAXIMUM	SIGMA CAL	CAL VAL
7515.5470	2.7424	5755.1

CHANNEL NO. 12 3452 1

05/04/84 R0515



STIRRUP SLAB 5B

P-1

MAXIMUM
74.5348

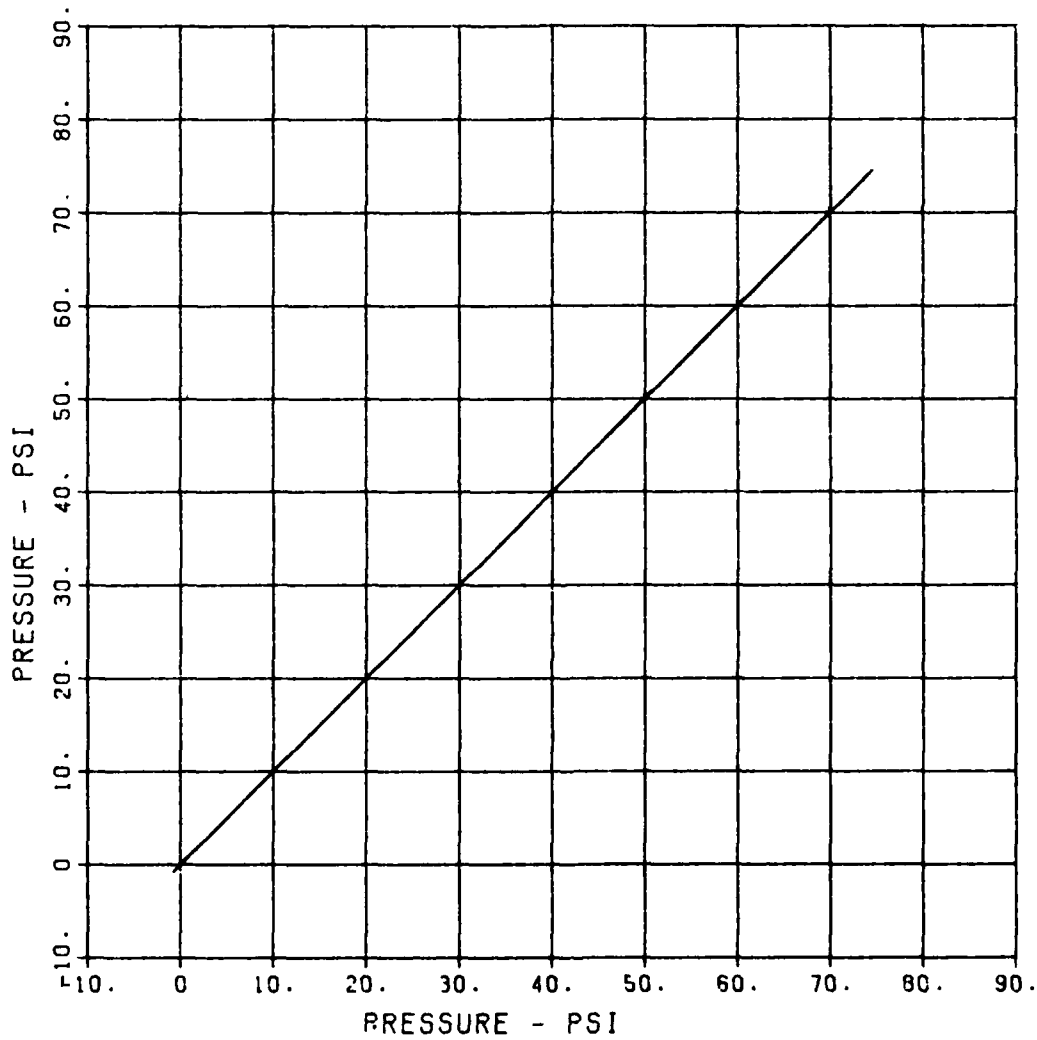
SICMA CAL
4.7394

CAL VAL
135.9

F2

CHANNEL NO. 1 13701 1

08/17/84 R0181



STIRRUP SLAB 5B

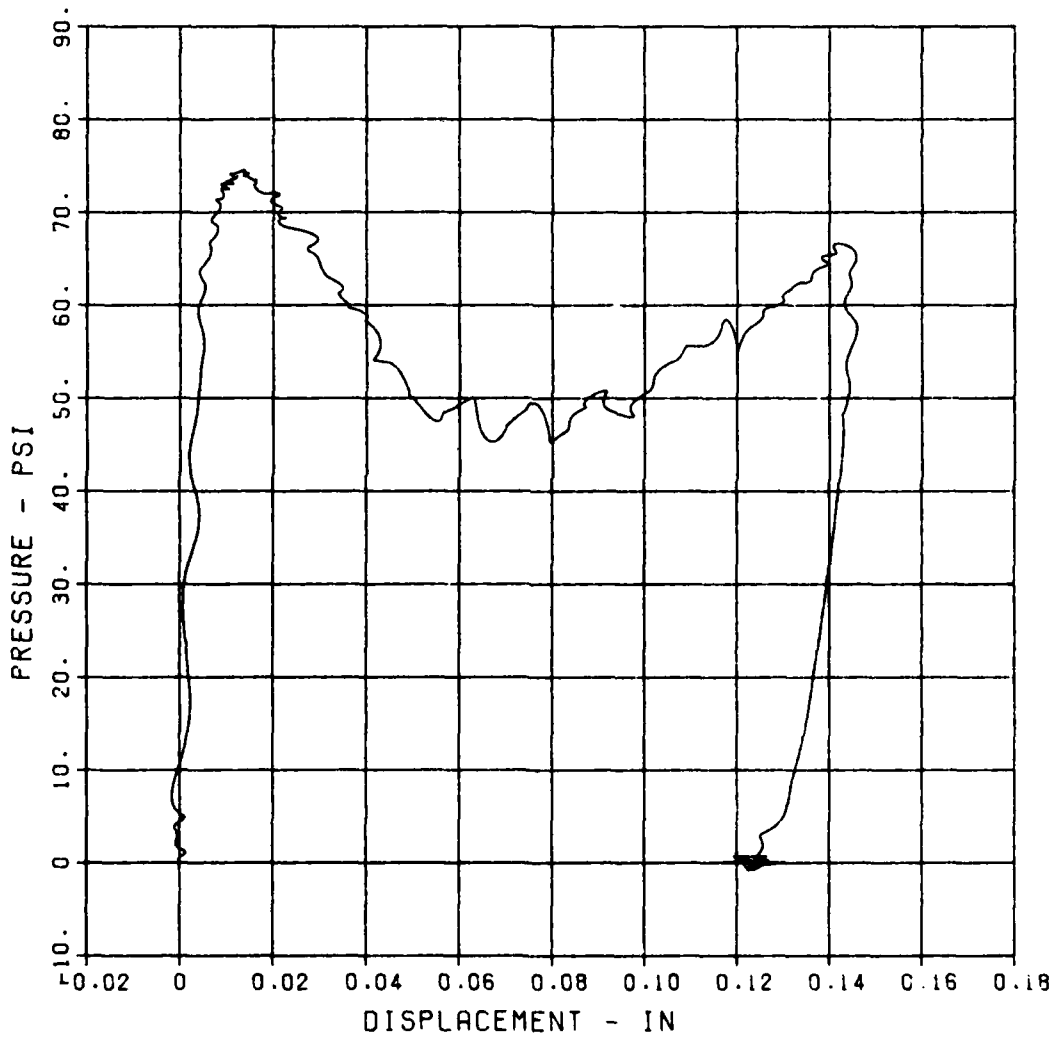
D-1

MAXIMUM	SIGMA CAL	CAL VAL
0.1461	2.7534	1.1

F2

CHANNEL NO.	2	13701	1
-------------	---	-------	---

08/17/84	RO181
----------	-------



STIRRUP SLAB 5B

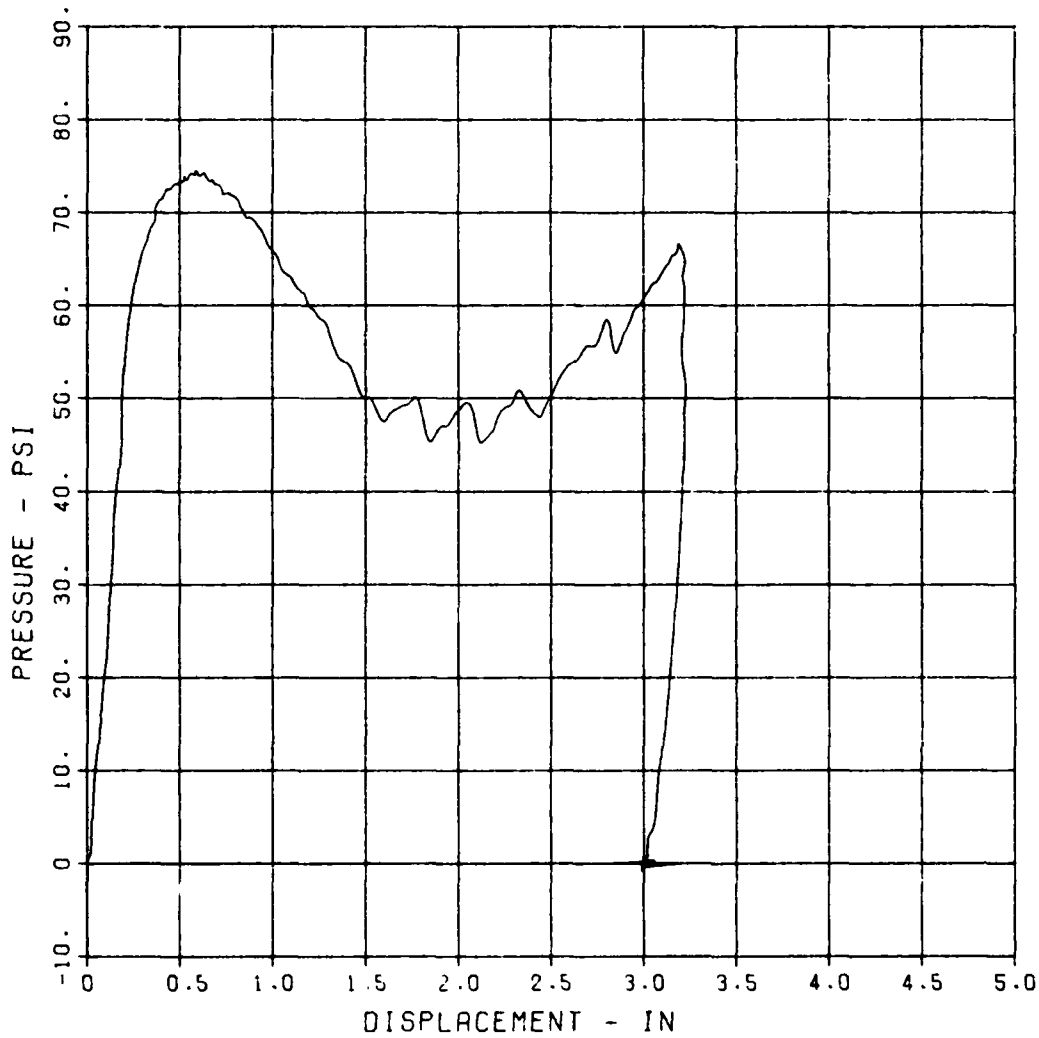
D-2

MAXIMUM	SIGMA CAL	CAL VAL
3.2265	2.3787	5.2

F2

CHANNEL NO.	3	13701	1
-------------	---	-------	---

08/17/84	R0181
----------	-------



STIRRUP SLAB 5B

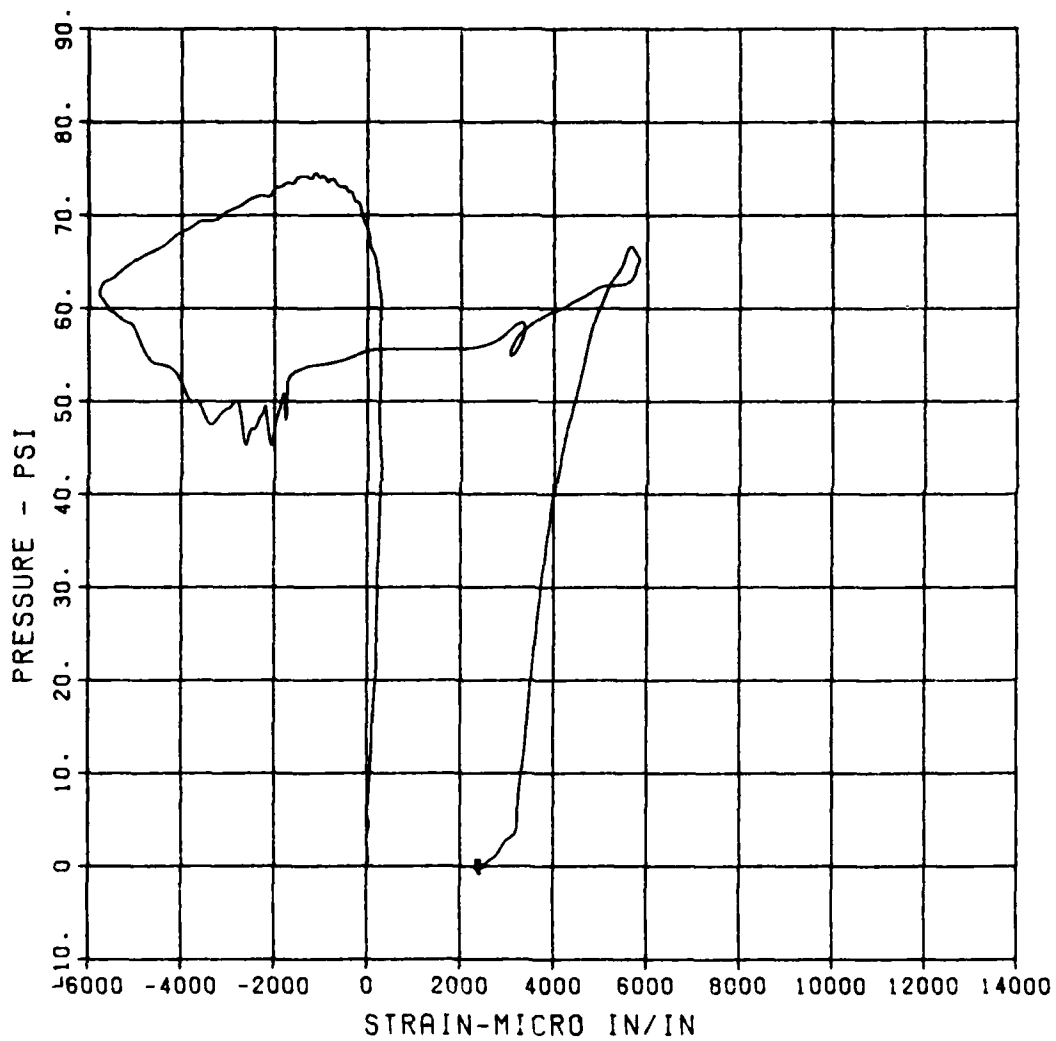
ST-1

MAXIMUM 5855.7036 SIGMA CAL 2.7605 CAL VAL 11666.7

F2

CHANNEL NO. 4 13701 1

08/17/84 R0181



STIRRUP SLAB 5B

SB-1

MAXIMUM
2640.2470

SIGMA CAL
2.4200

CAL VAL
11666.7

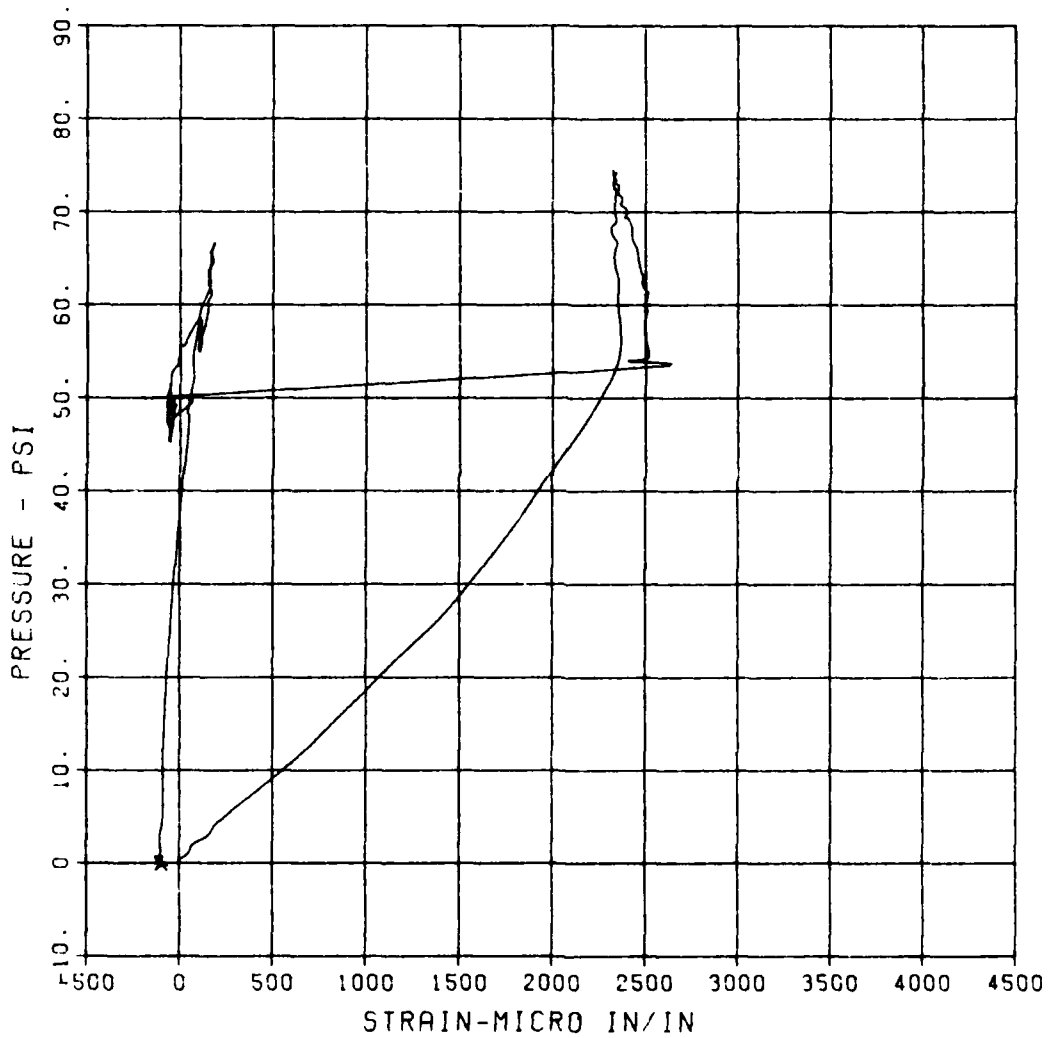
F2

CHANNEL NO. 5

13701 1

08/17/84

R0181



STIRRUP SLAB 5B

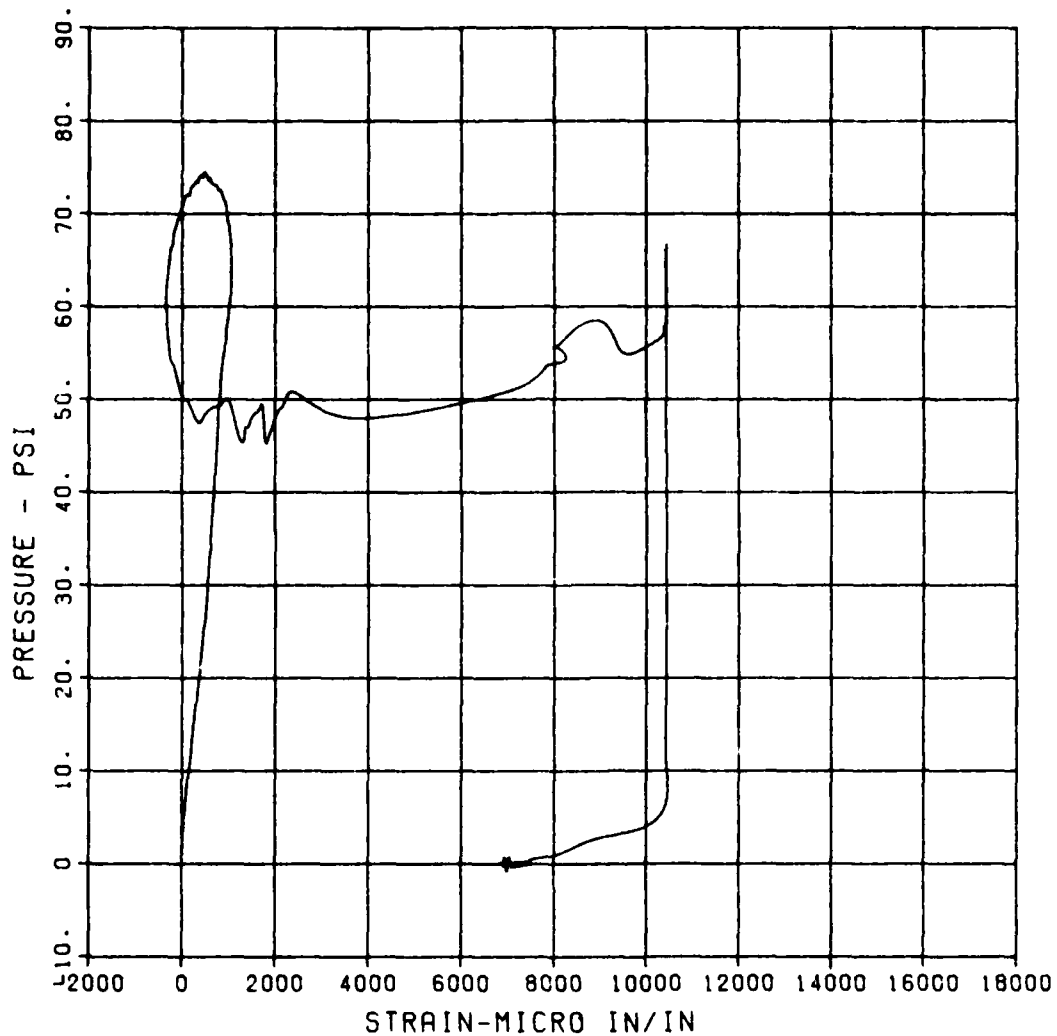
ST-2

MAXIMUM	SIGMA CAL	CAL VAL
10471.4495	3.0541	5766.1

F2

CHANNEL NO.	6	13701	1
-------------	---	-------	---

08/17/84	RO181
----------	-------



STIRRUP SLAB 5B

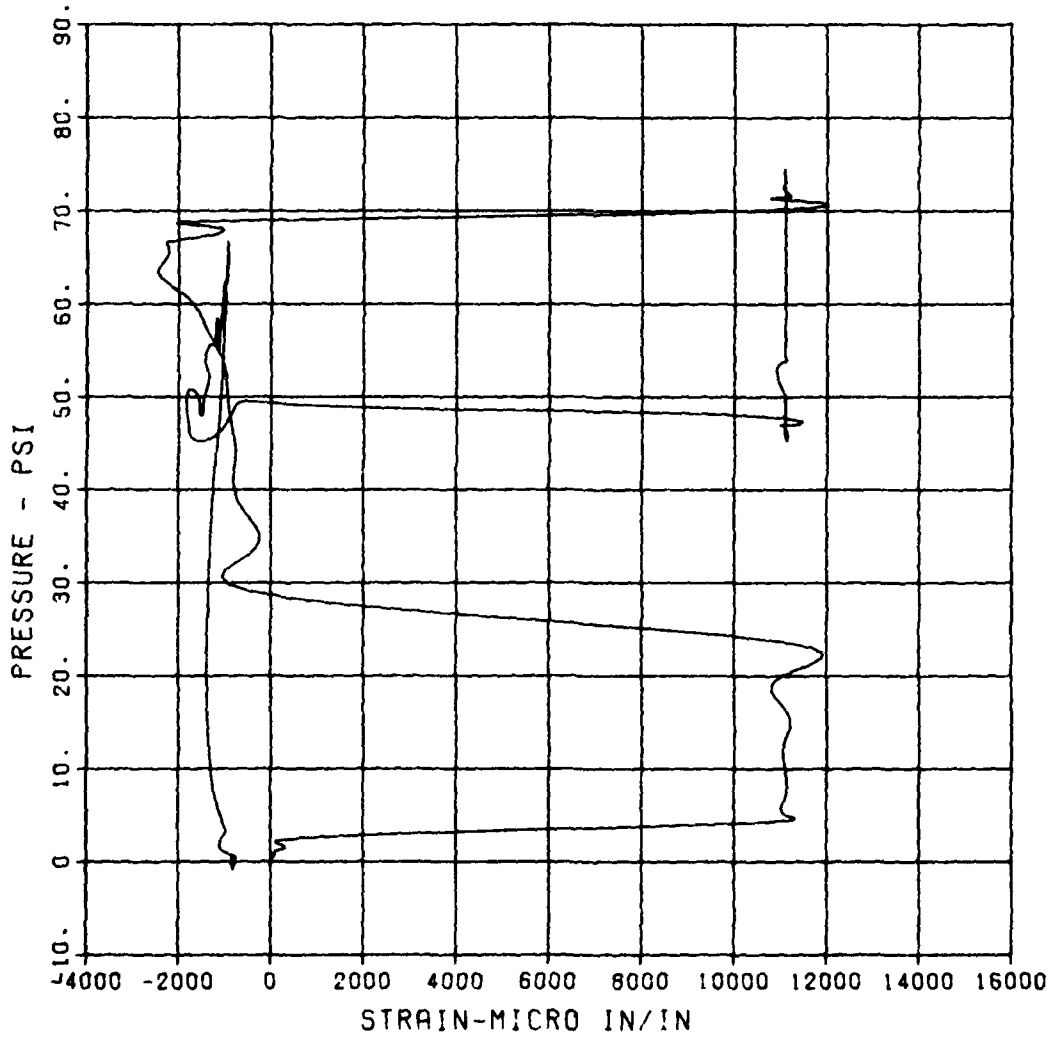
SB-2

MAXIMUM 12033.3612 SIGMA_CAL 3.0177 CAL_VAL 5766.1

F2

CHANNEL NO. 7 13701 1

08/17/84 R0181



STIRRUP SLAB 5B

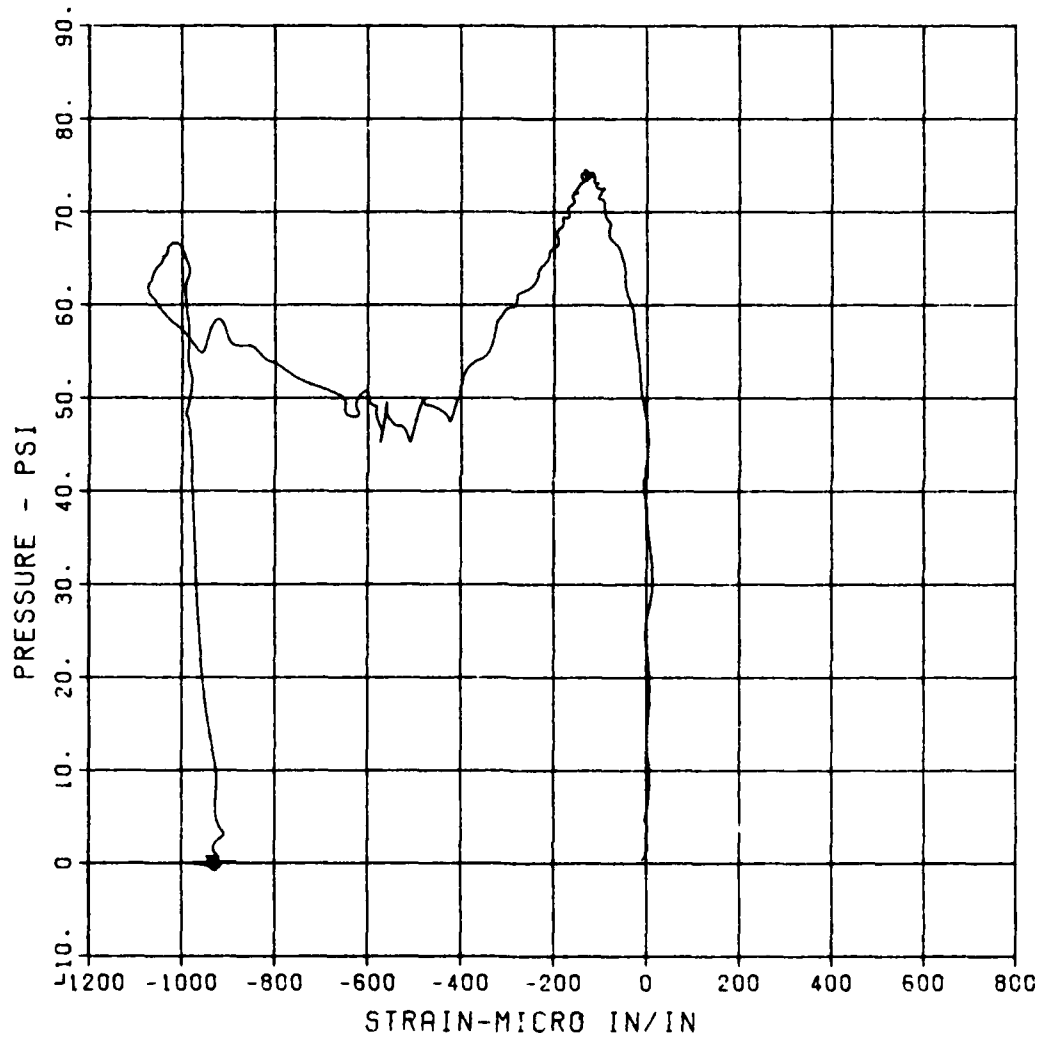
S-3

MAXIMUM -1074.8645 SIGMA CAL 2.7431 CAL VAL 5766.1

F2

CHANNEL NO. 8 13701 1

08/17/84 R0181



STIRRUP SLAB 5B

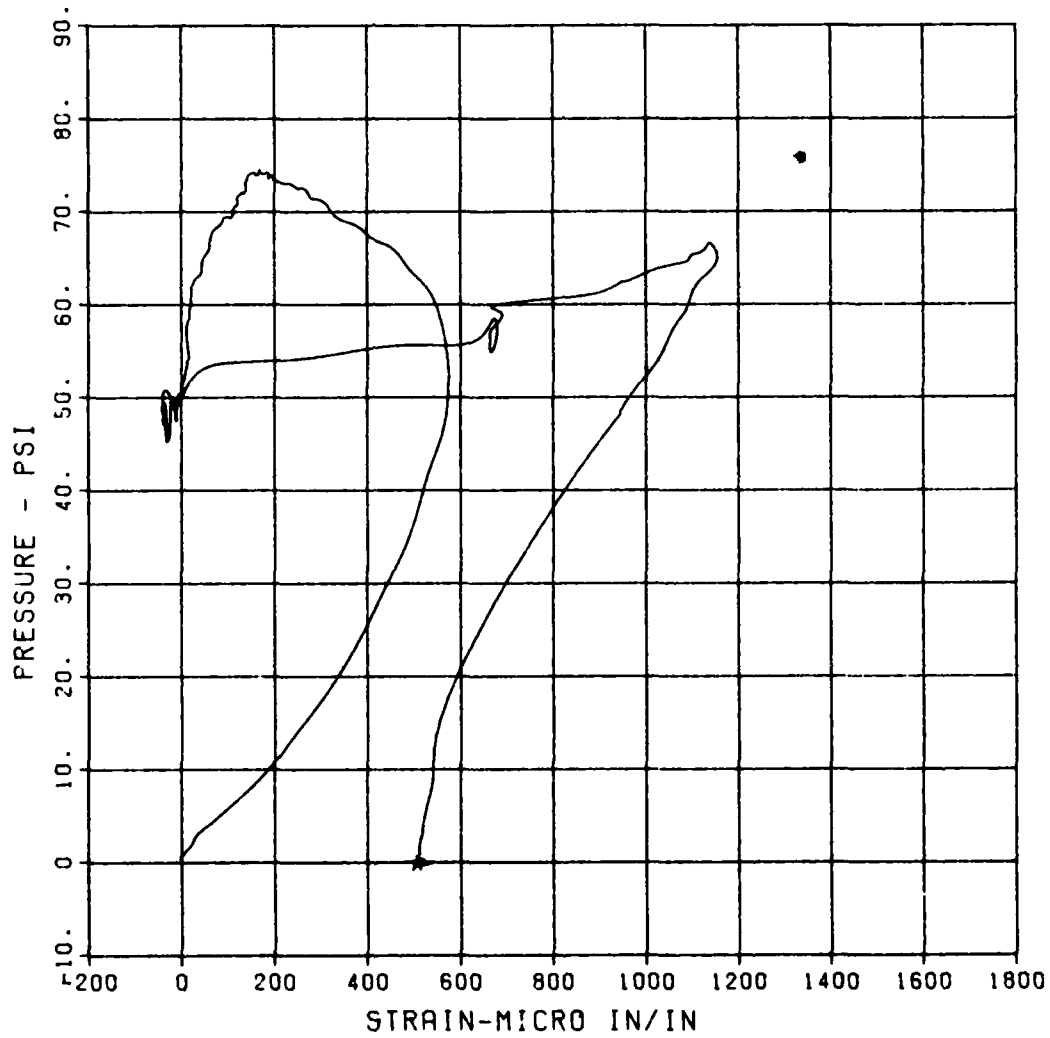
S-4

MAXIMUM	SICMA CAL	CAL VAL
1155.0916	2.7508	2899.8

F2

CHANNEL NO.	9	13701	1
-------------	---	-------	---

08/17/84	R0181
----------	-------



STIRRUP SLAB 5B

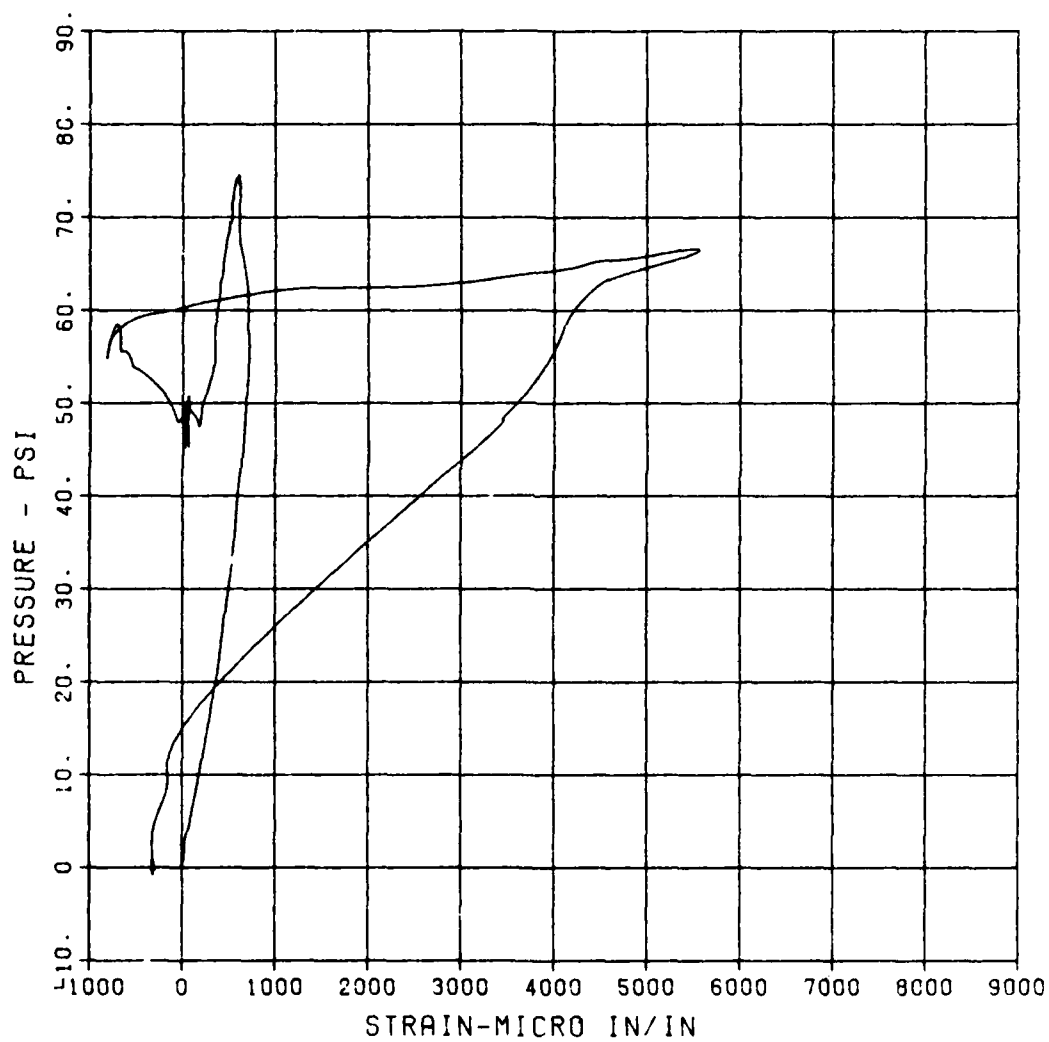
S-5

MAXIMUM	SIGMA CAL	CAL VAL
5564.8565	2.7177	5766.1

F2

CHANNEL NO. 10 13701 1

08/17/84 R0181



FEMA STIRRUP SLAB 5

P-1

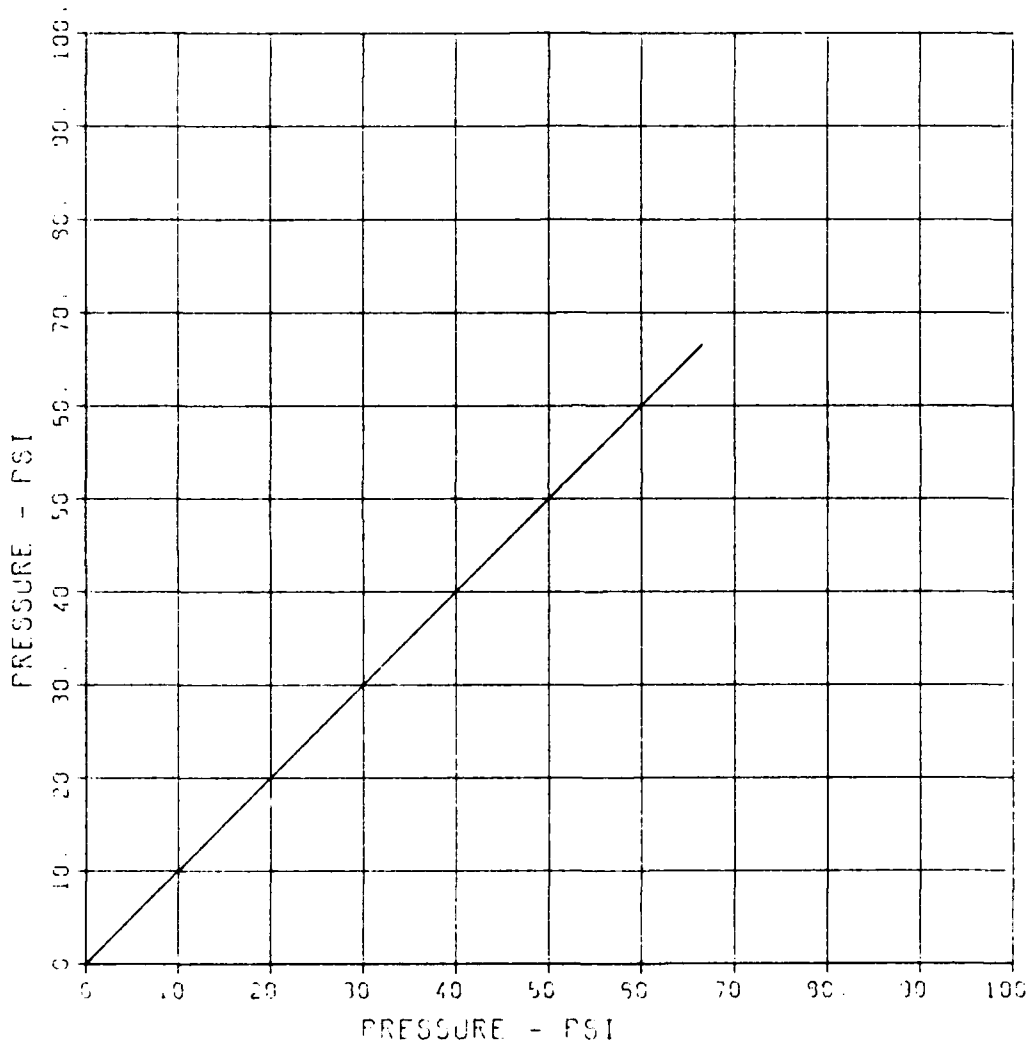
MAXIMUM
55.5554

SIGMA CAL
2.2325

CAL VAL
135.0

CHANNEL NO. 1 9216 1

04/25/84 R0432



FEMA STIRRUP SLAB 6

D-1

MAXIMUM
0.1753

SIGMA CAL
2.7010

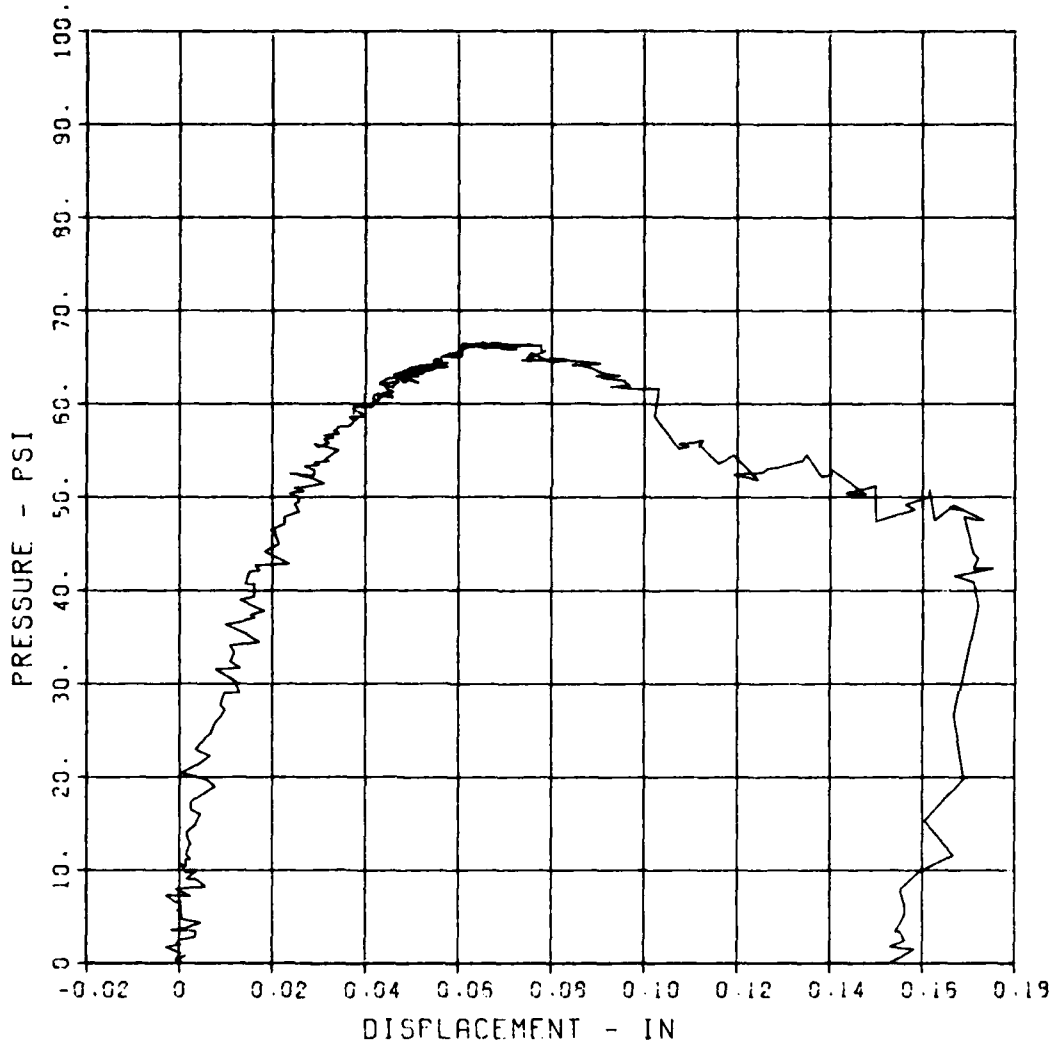
CAL VAL
1.1

CHANNEL NO. 2

9215 1

04/25/94

R0432



FEMA STIRRUP SLAB 5

D-2

MAXIMUM
3.1172

SICMA CAL
2.5541

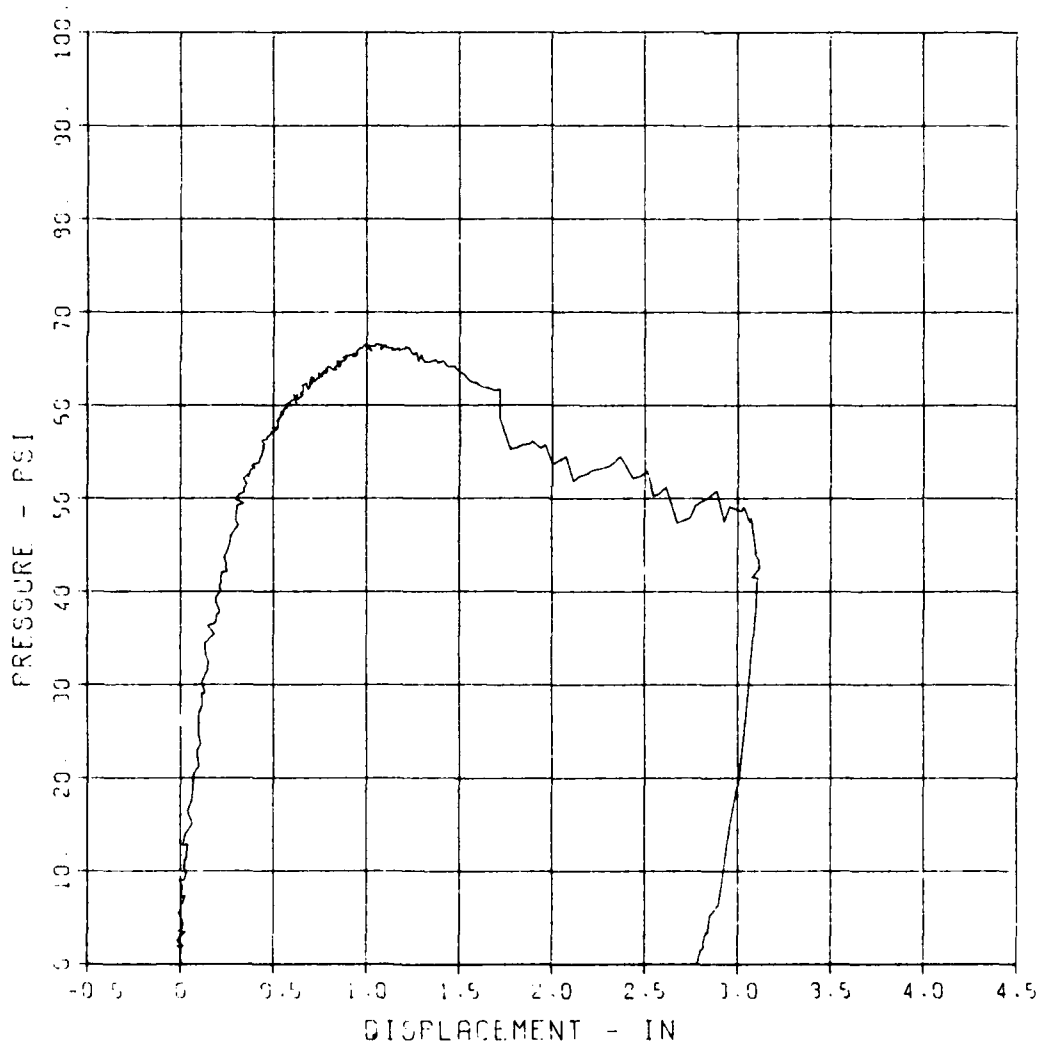
CAL. VAL
5.2

CHANNEL NO. 4

9215 1

04/25/94

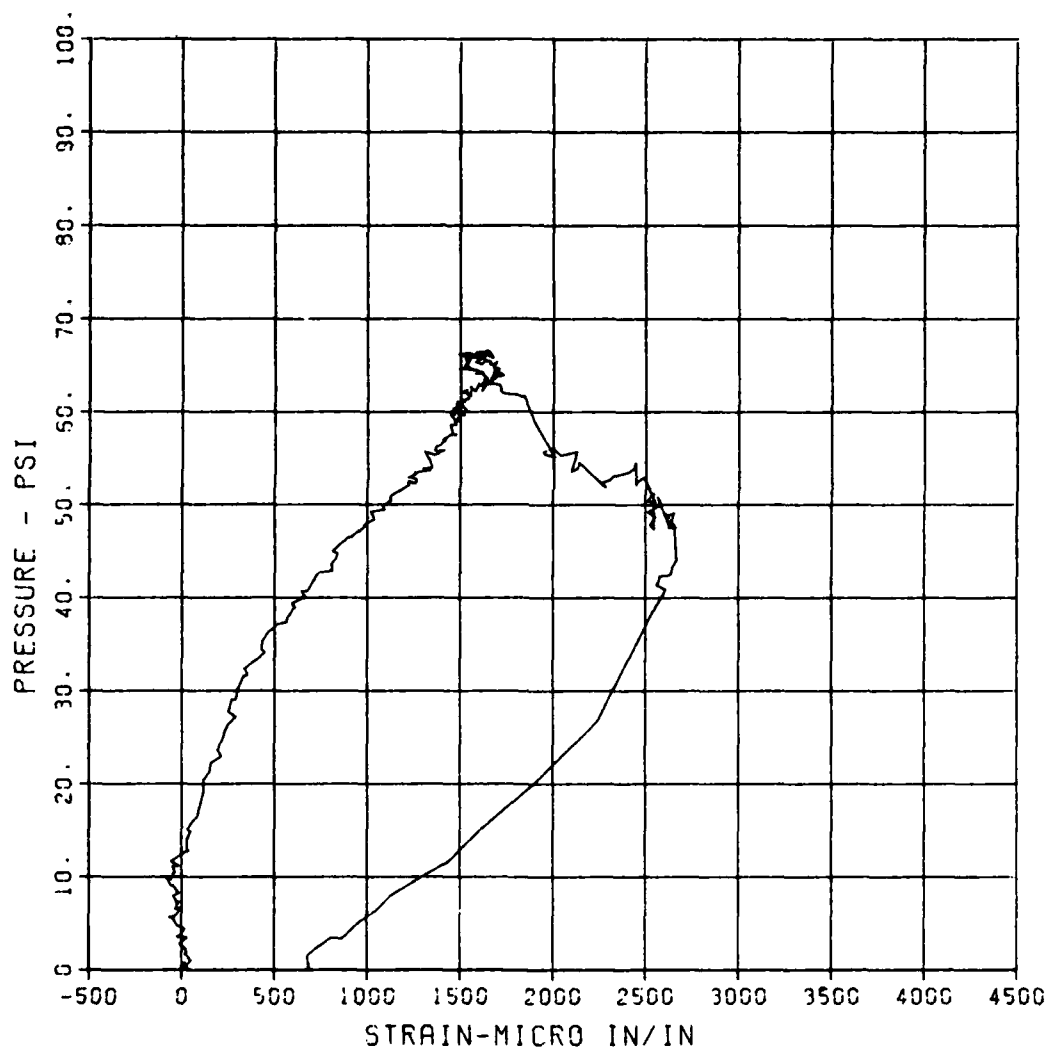
R0432



FEMA STIRRUP SLAB 6
ST-1

MAXIMUM SIGMA CAL CAL VAL
2665.9489 2.9417 11666.7

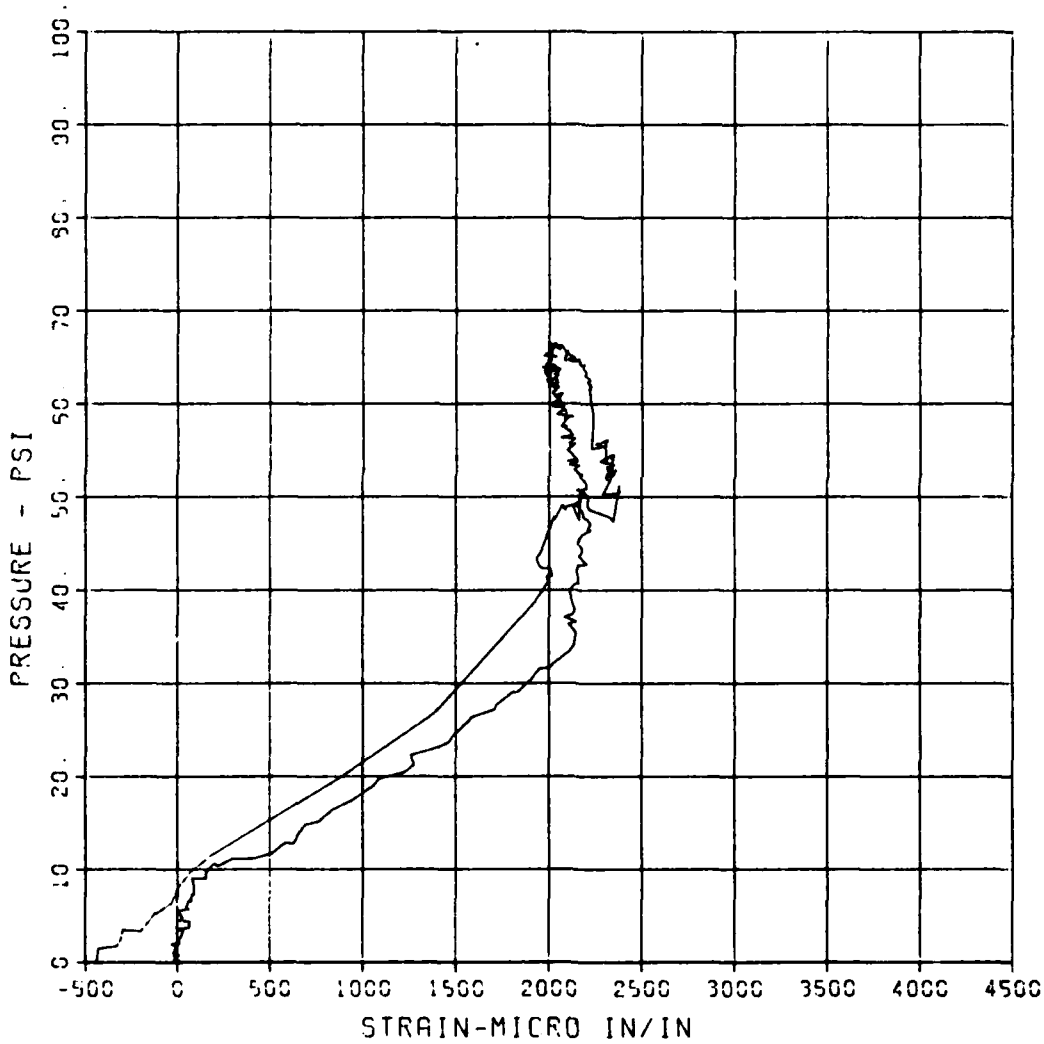
CHANNEL NO. 5 9216 1
04/25/94 R0432



FEMA STIRRUP SLAB 6
SB-1

MAXIMUM	SICMA CAL	CAL VAL
2390.4110	2.9005	11555.7

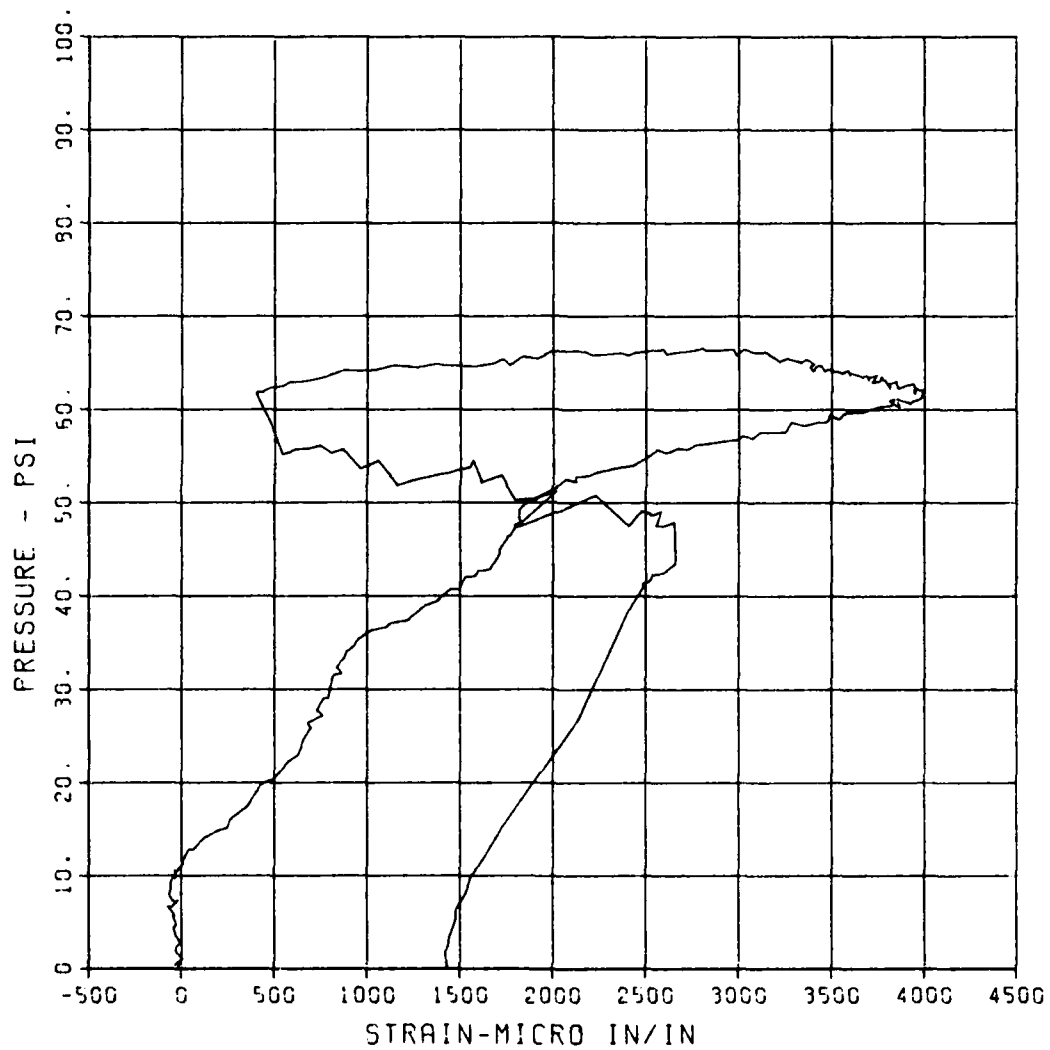
CHANNEL NO.	7	9215	1
04/19/94	R0347		



FEMA STIRRUP SLAB 6
ST-2

MAXIMUM SIGMA CAL CAL VAL
3930.7357 3.5547 5766.1

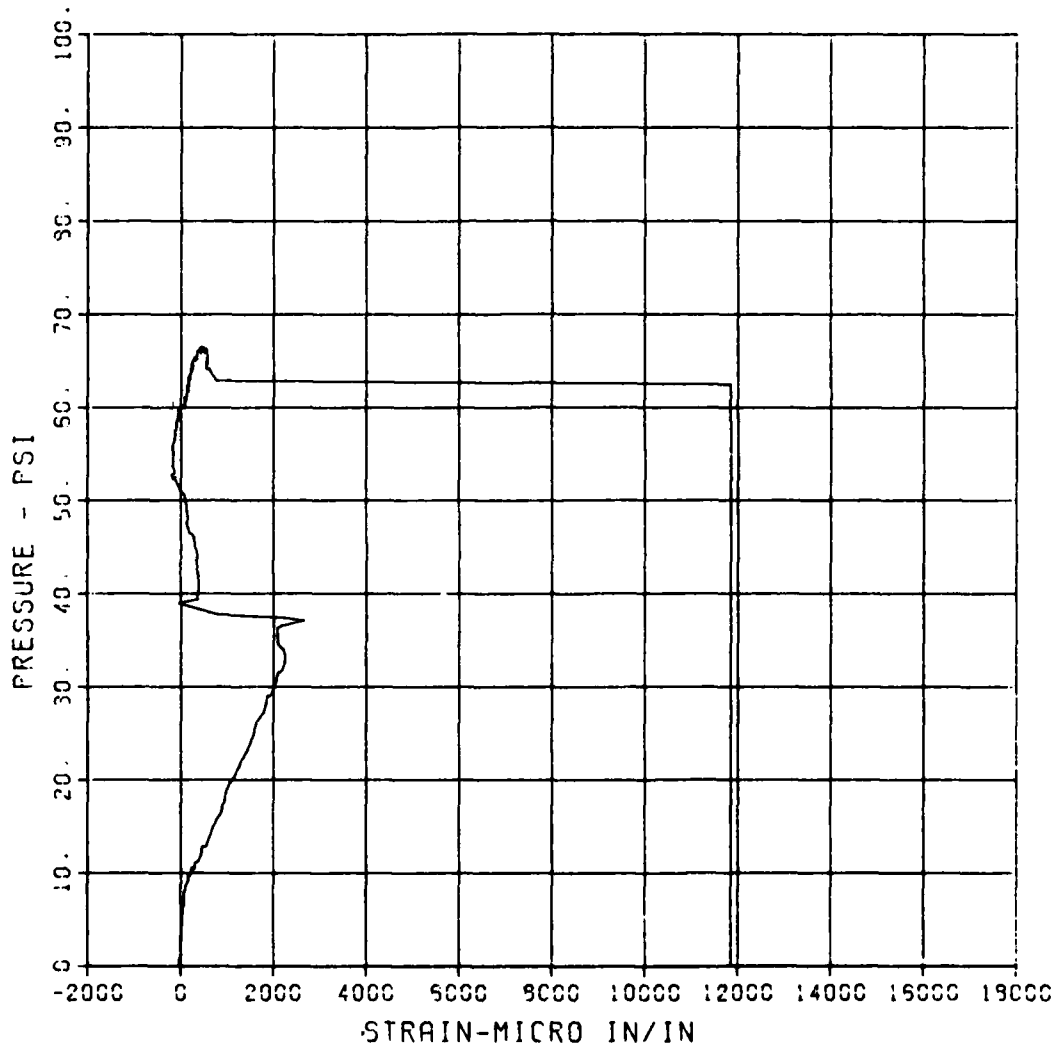
CHANNEL NO. 9 9216 1
04/25/84 R0432



FEMA STIRRUP SLAB 6
SB-2

MAXIMUM SIGMA CAL CAL VAL
11849-9512 3.3005 5766.1

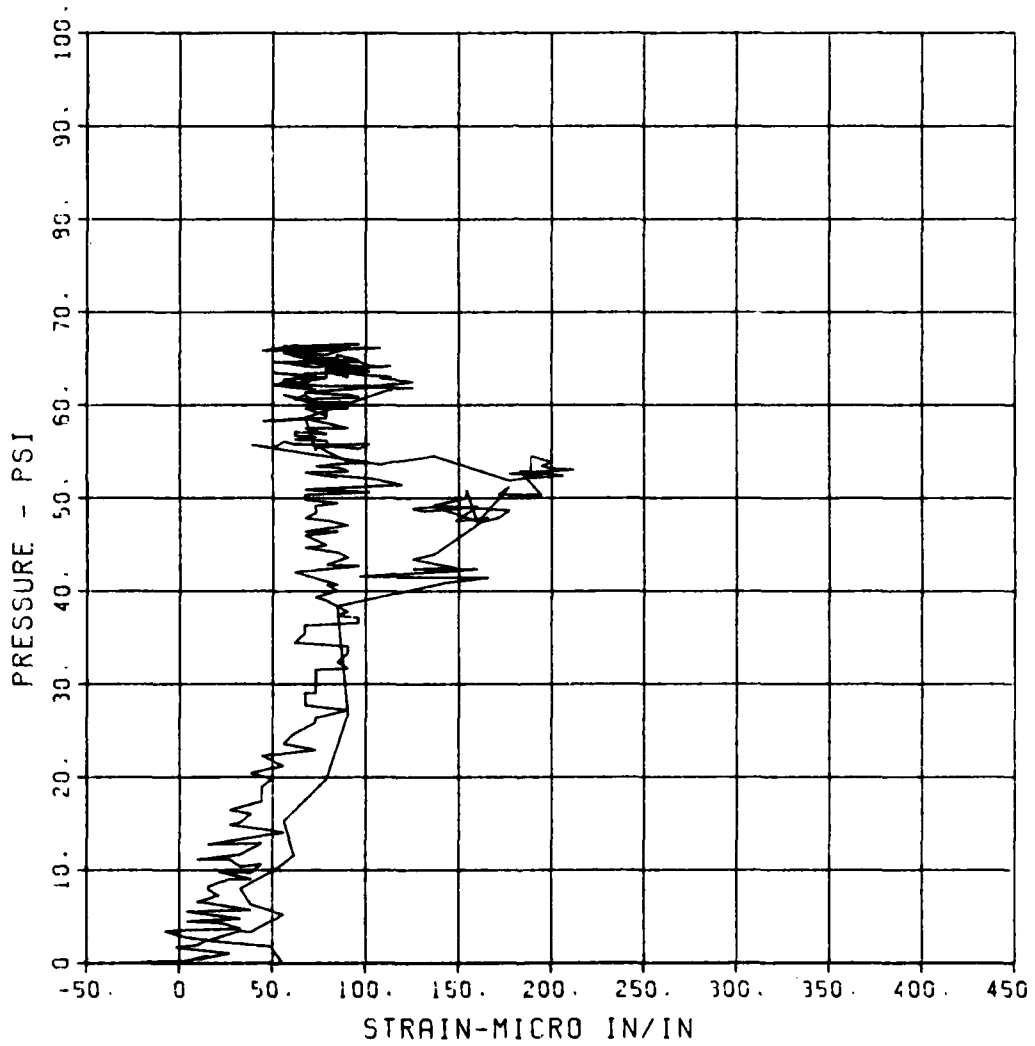
CHANNEL NO 9 8215 1
04/19/84 R0347



FEMA STIRRUP SLAB 6
S-3

MAXIMUM SIGMA CAL CAL VAL
211.7422 2.6894 5755.1

CHANNEL NO. 10 9215 1
04/25/84 R0432



FEMA STIRRUP SLAB 6

S-4

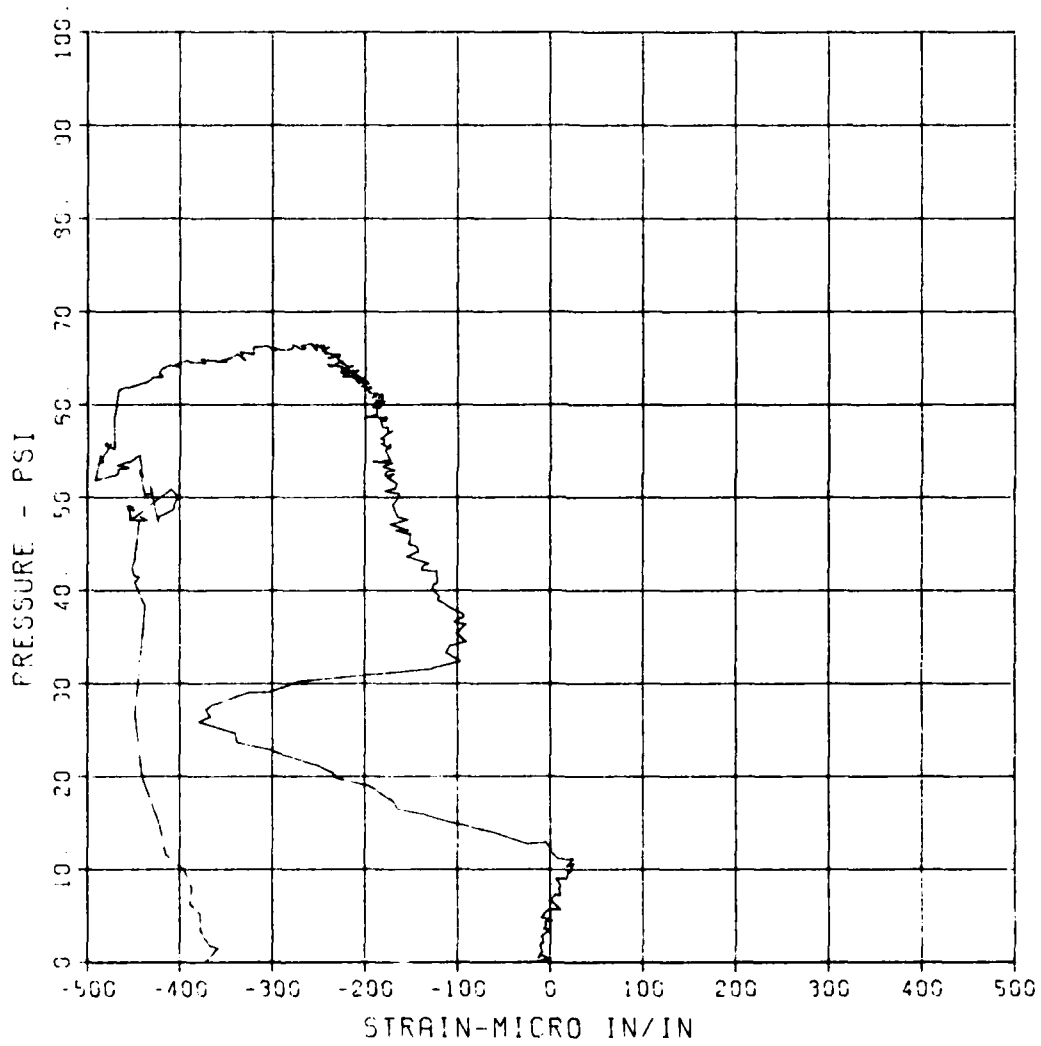
MAXIMUM
-431.5330

SICMA CAL
3.4014

CAL VAL
2933.8

CHANNEL NO. 11 8216 1

04/25/94 R0432



FEMA STIRRUP SLAB 6

S-5

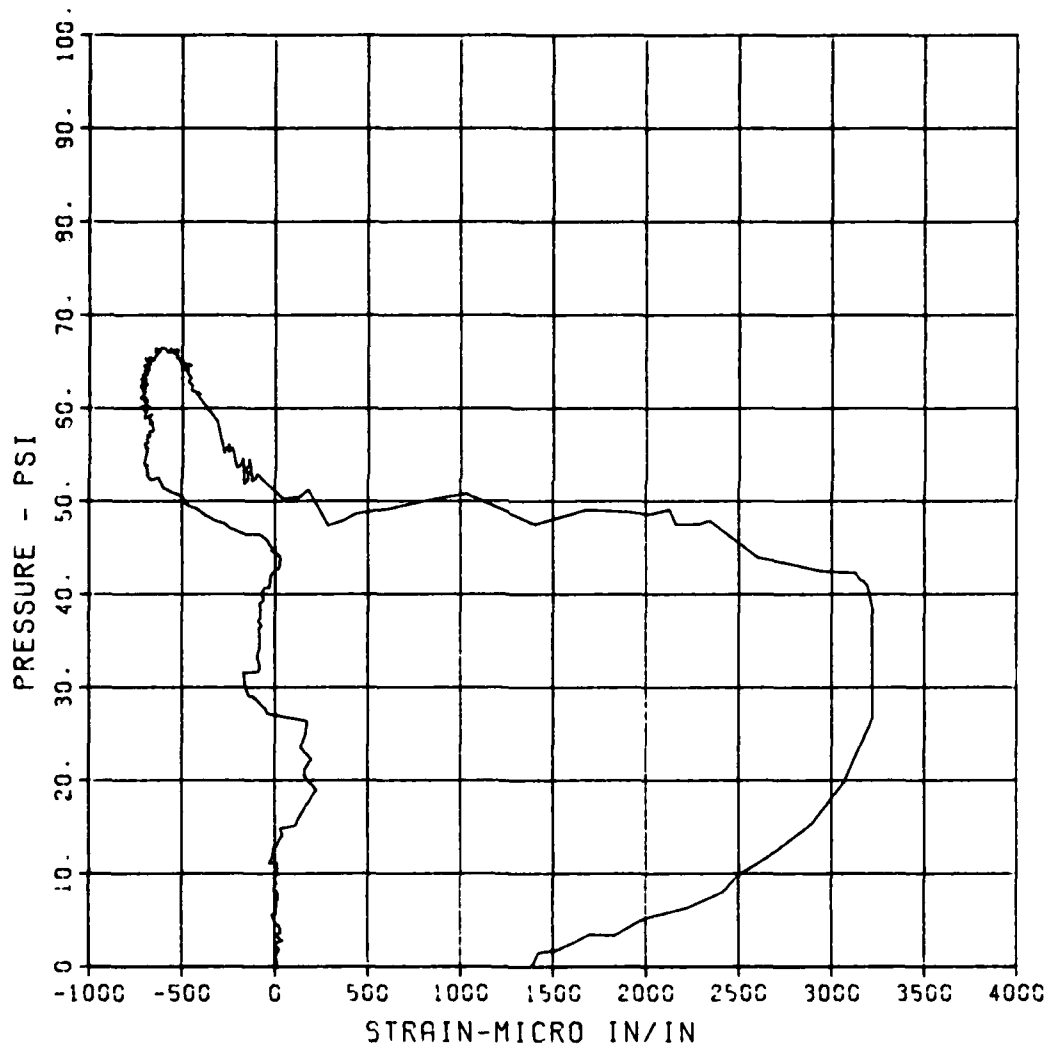
MAXIMUM
3220.1750

SIGMA CAL
2.6497

CAL VAL
5766.1

CHANNEL NO. 12 9216 1

04/19/84 R0347



FEMA STIRRUP SLAB 7

P-1

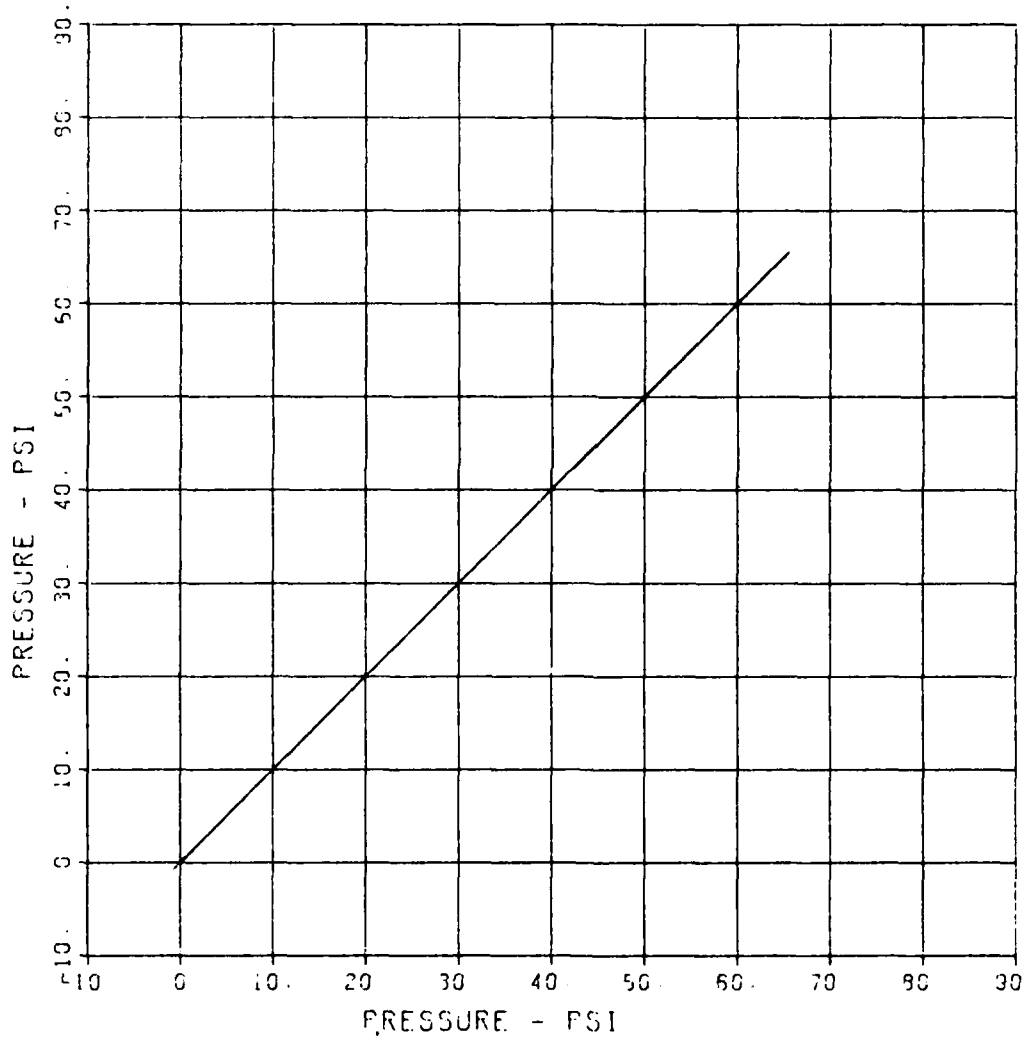
MAXIMUM
65.4336

SIGMA CAL
2.3334

CAL VAL
135.9

CHANNEL NO. 1 19442 1

05/04/94 R0618



FEMA STIRRUP SLAB 7

D-1

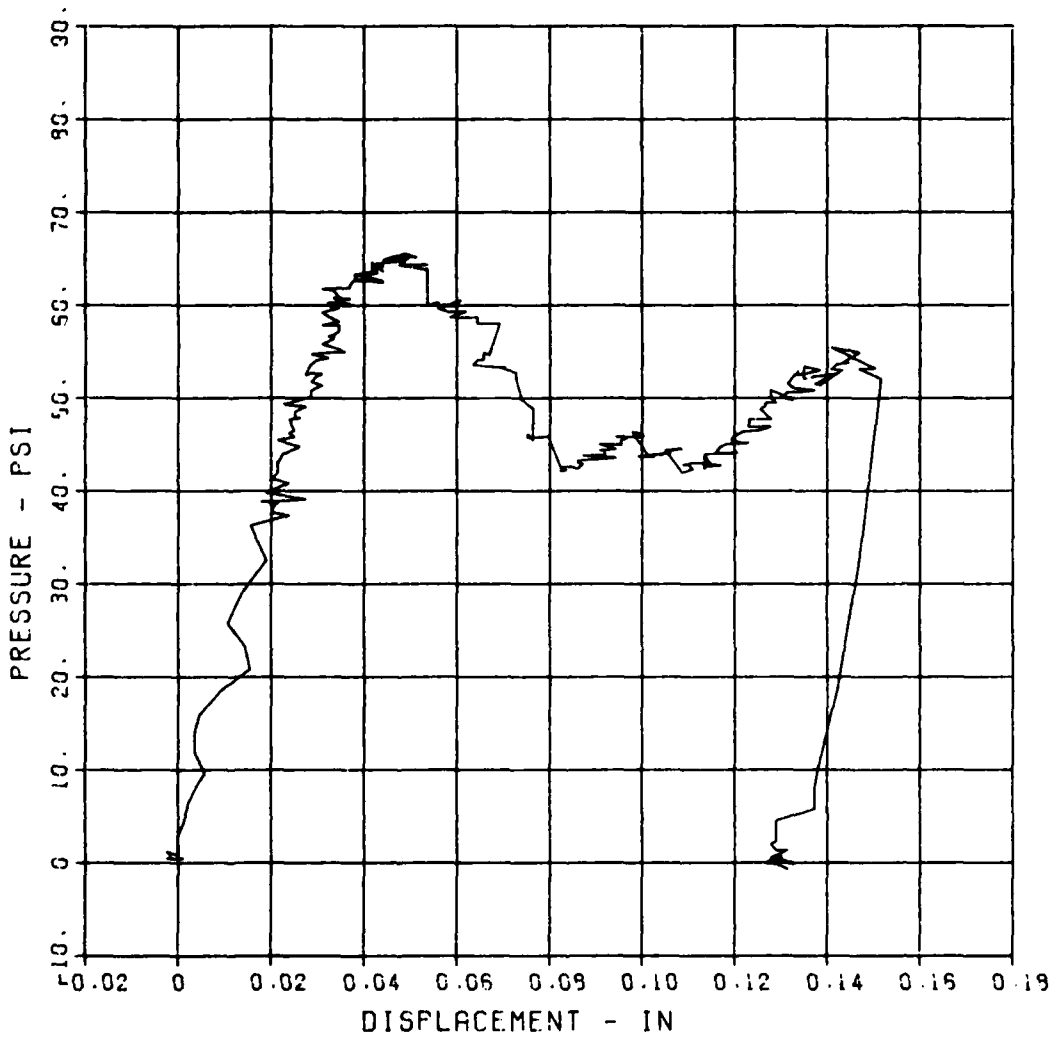
MAXIMUM
0.1515

SIGMA CAL
2.5139

CAL VAL
1.1

CHANNEL NO. 2 19442 1

05/04/84 R0619



FEMA STIRRUP SLAB 7

D-2

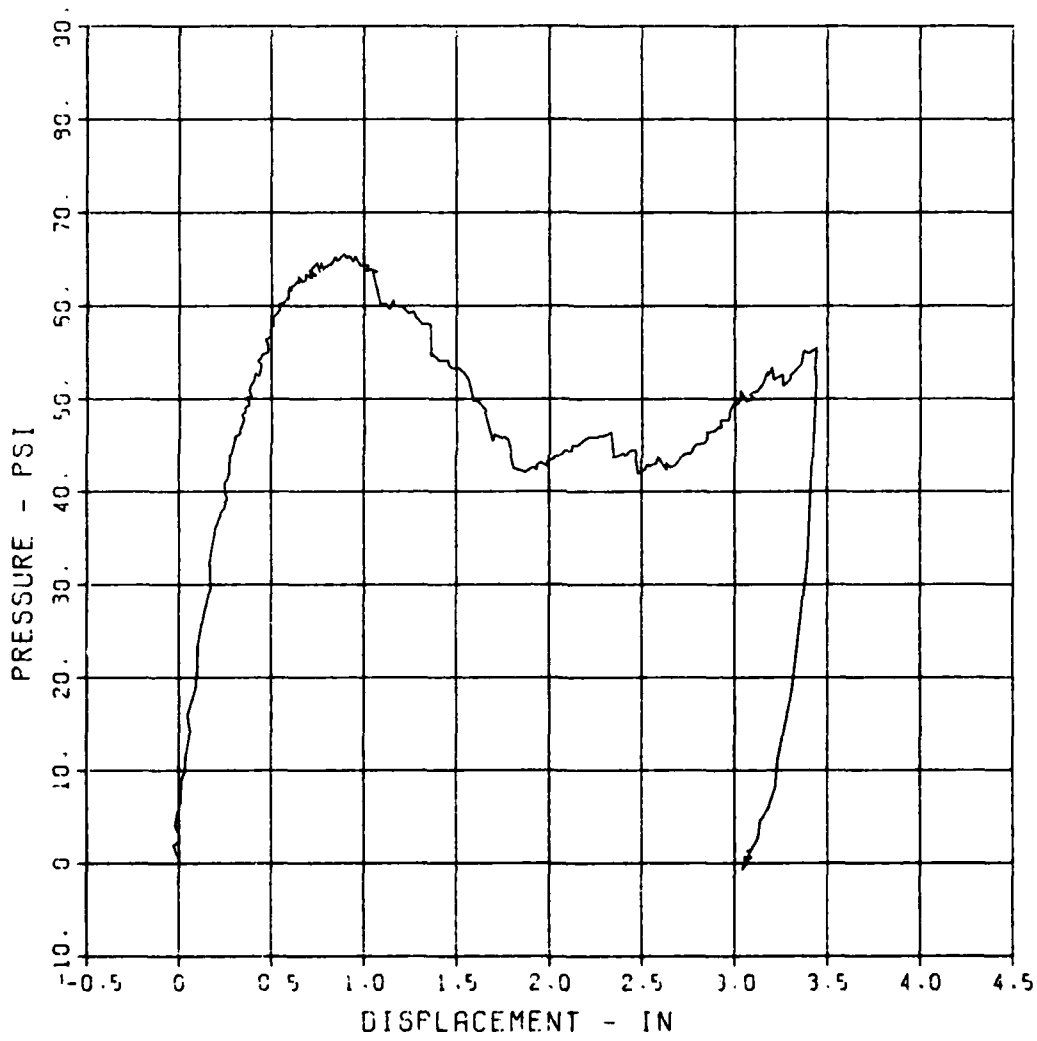
MAXIMUM
3.4423

SIGMA CAL
2.7792

CAL VAL
5.2

CHANNEL NO 3 19442 1

05/04/94 R0518



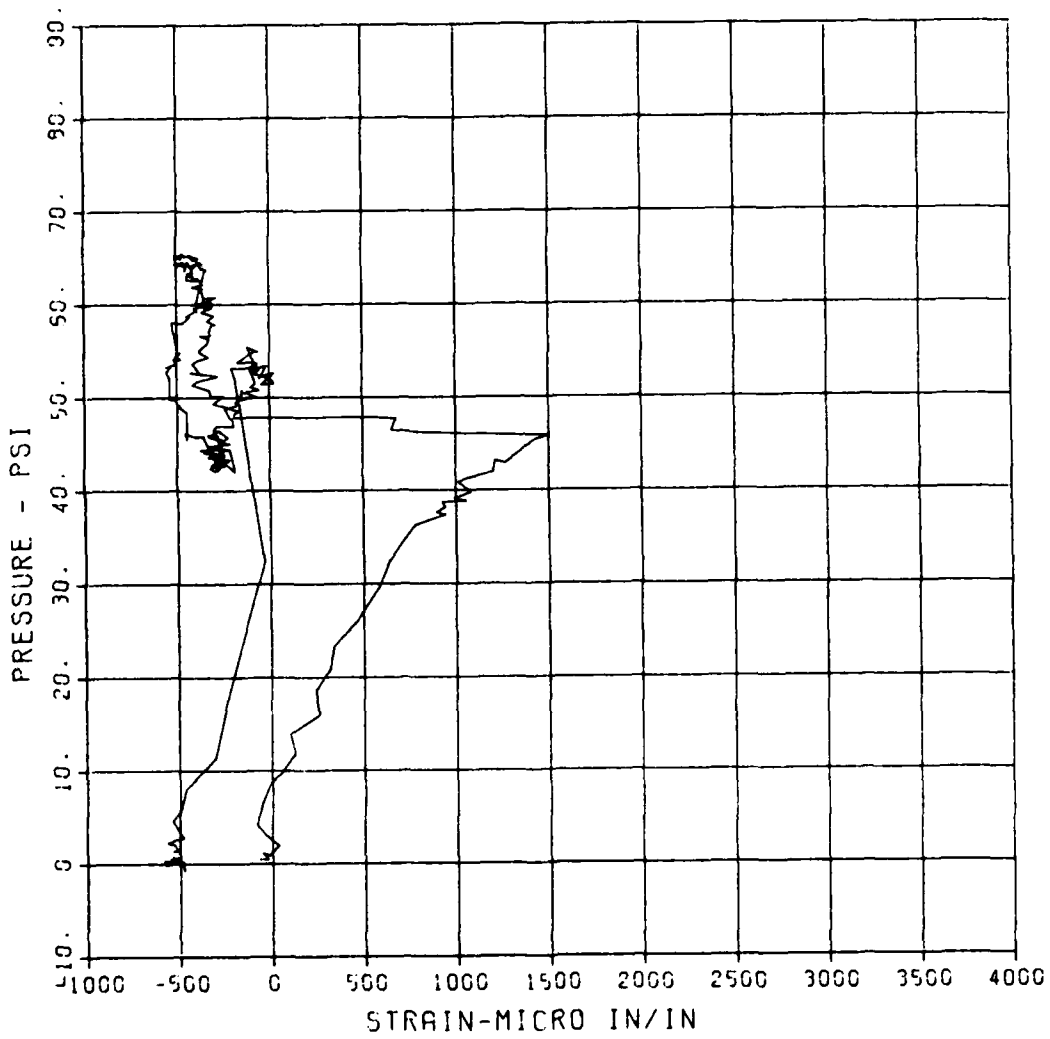
FEMA STIRRUP SLAB 7

ST-1

MAXIMUM	SIGMA CAL	CAL. VAL
1505.3246	3.5764	11555.7

CHANNEL NO. 4 19442 1

05/04/94 R0619



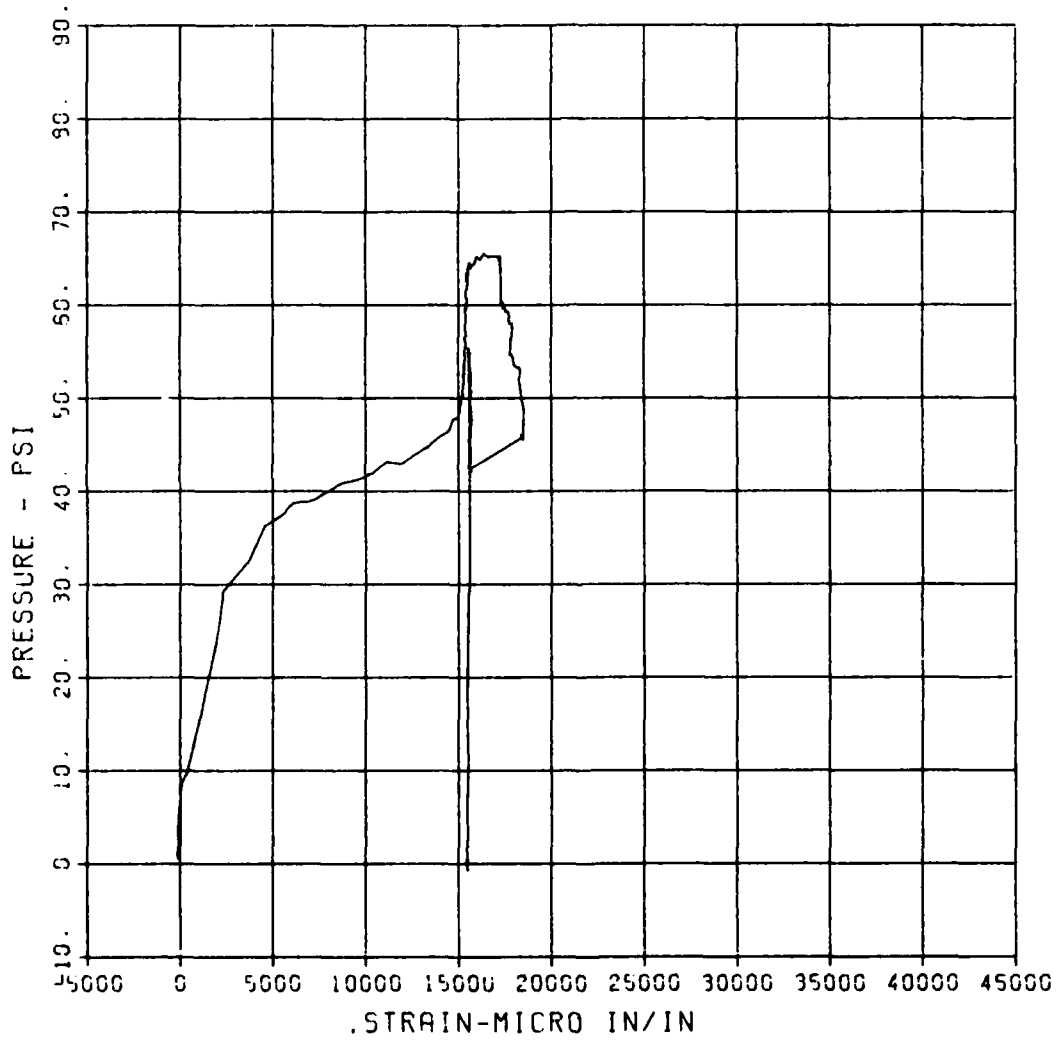
FEMA STIRRUP SLAB 7

SB-1

MAXIMUM	SICMA CAL	CAL VAL
19523.5543	2.7195	11556.7

CHANNEL NO. 5 19442 1

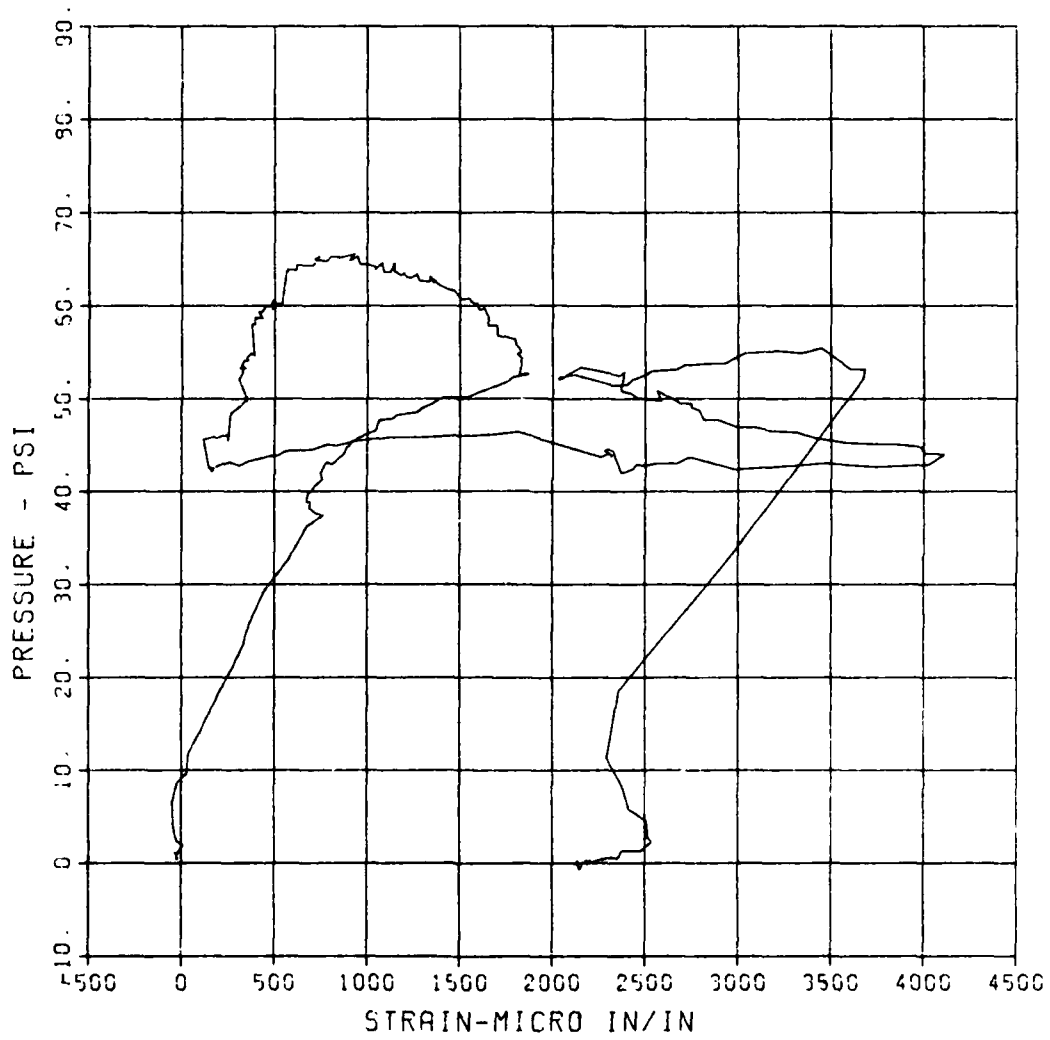
05/04/94 R0619



FEMA STIRRUP SLAB 7
ST-2

MAXIMUM SIGMA CAL CAL VAL
4111.6787 4.3576 5765.1

CHANNEL NO. 6 18442 1
05/04/94 R0519



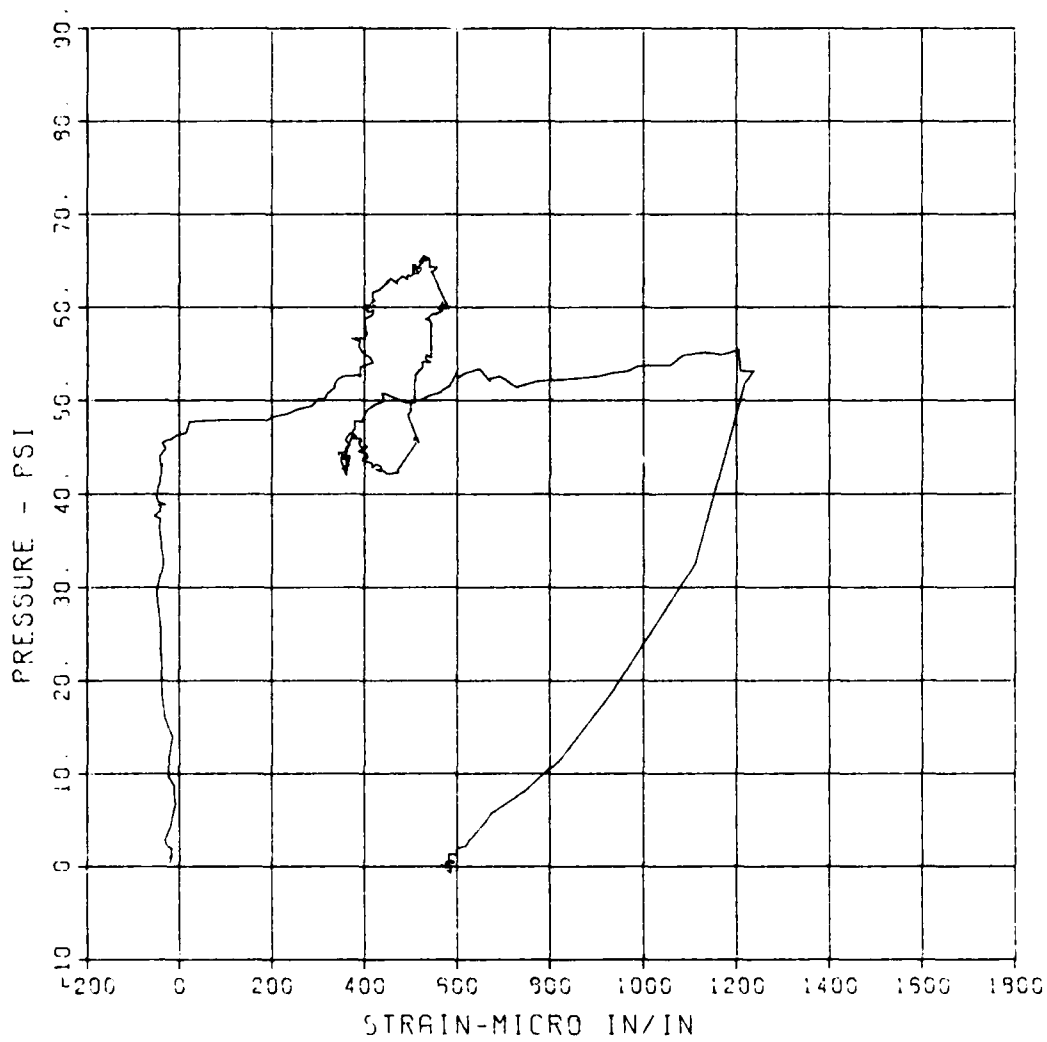
FEMA STIRRUP SLAB 7

S-4

MAXIMUM	SICMA CAL	CAL VAL
1237.3428	3.3959	2933.9

CHANNEL NO. 9 19442 1

05/04/94 R0619



FEMA STIRRUP SLAB 7

S-5

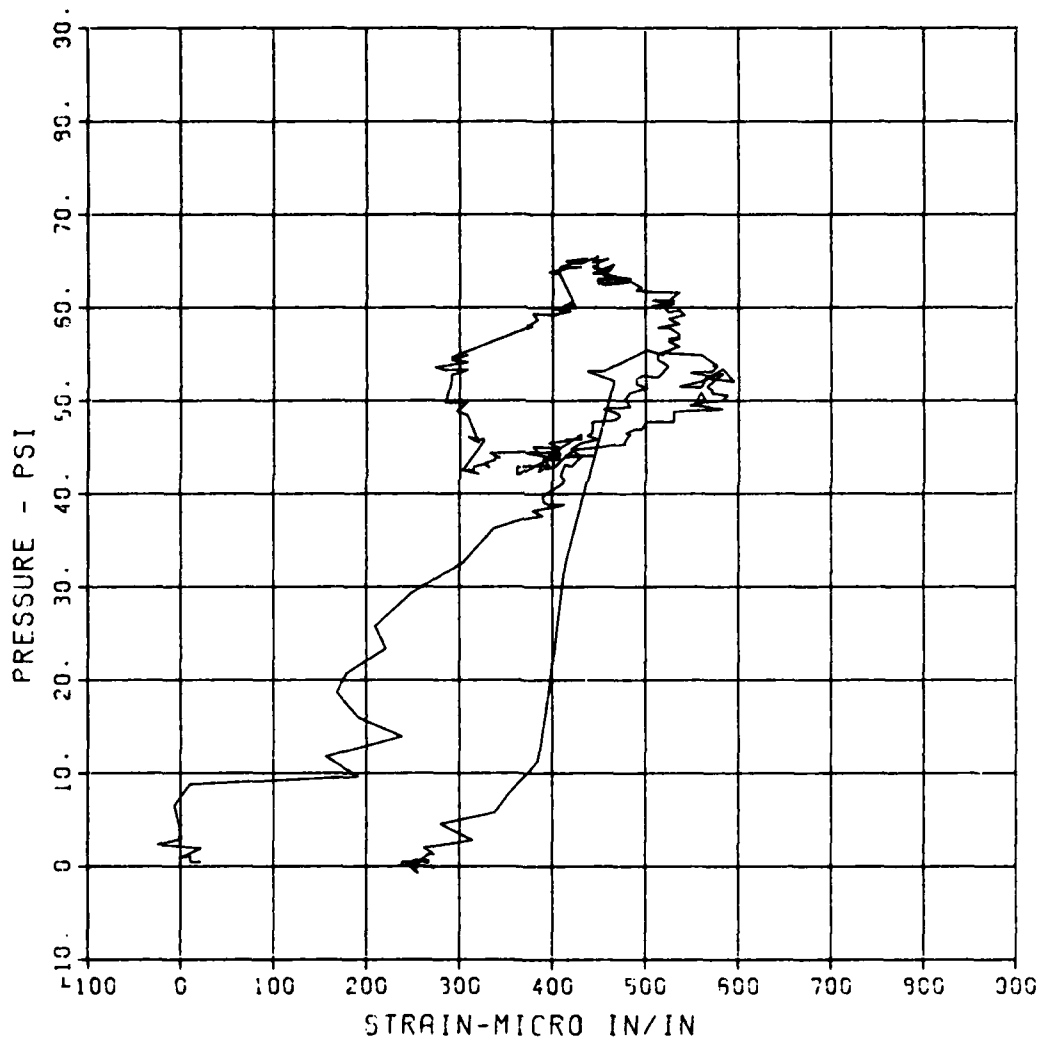
MAXIMUM
594.3943

SIGMA CAL
2.5425

CAL VAL
5756.1

CHANNEL NO. 10 19442 1

05/04/94 R0618



FEMA STIRRUP SLAB 8

P-1

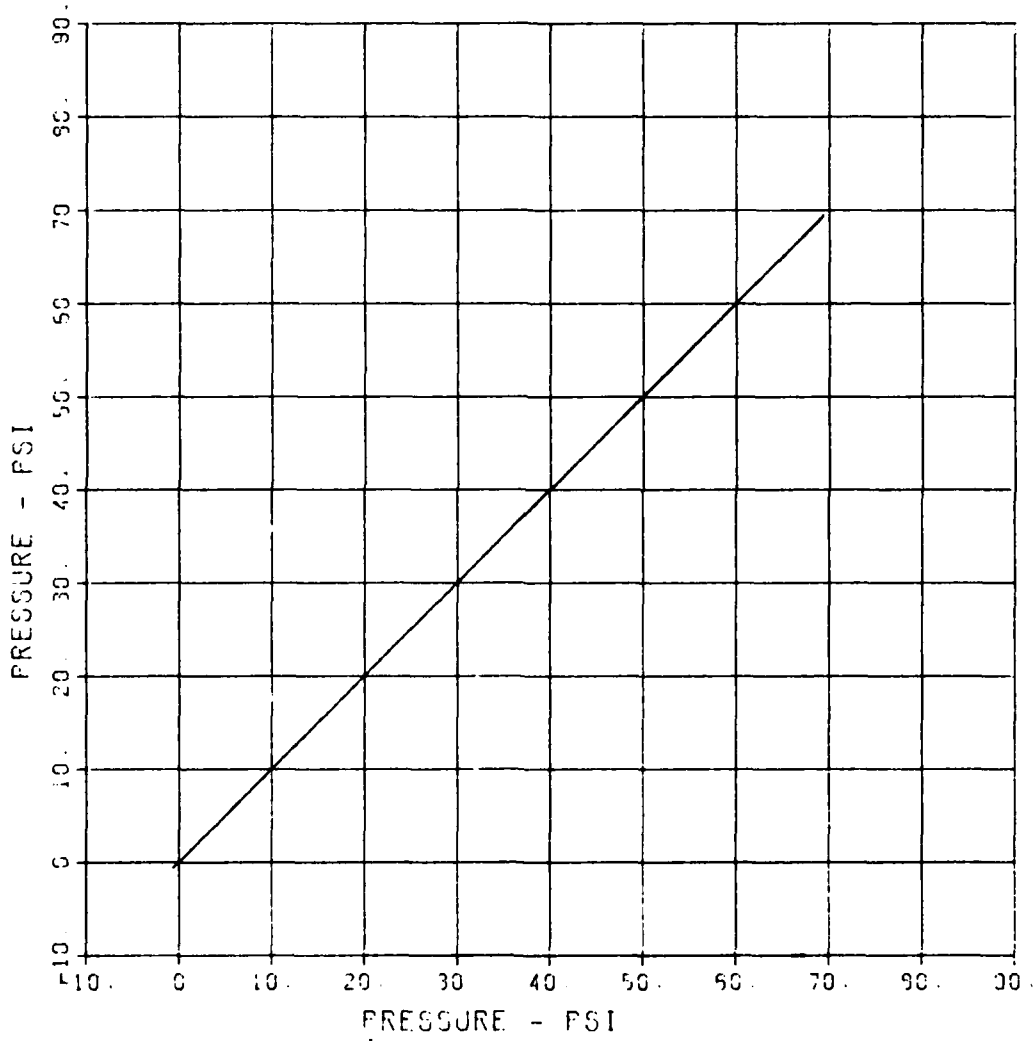
MAXIMUM
60.4462

SIGMA CAL
2.5919

CAL VAL
135.0

CHANNEL NO. 1 14730 1

04/24/94 R0409



FEMA STIRRUP SLAB 8

D-1

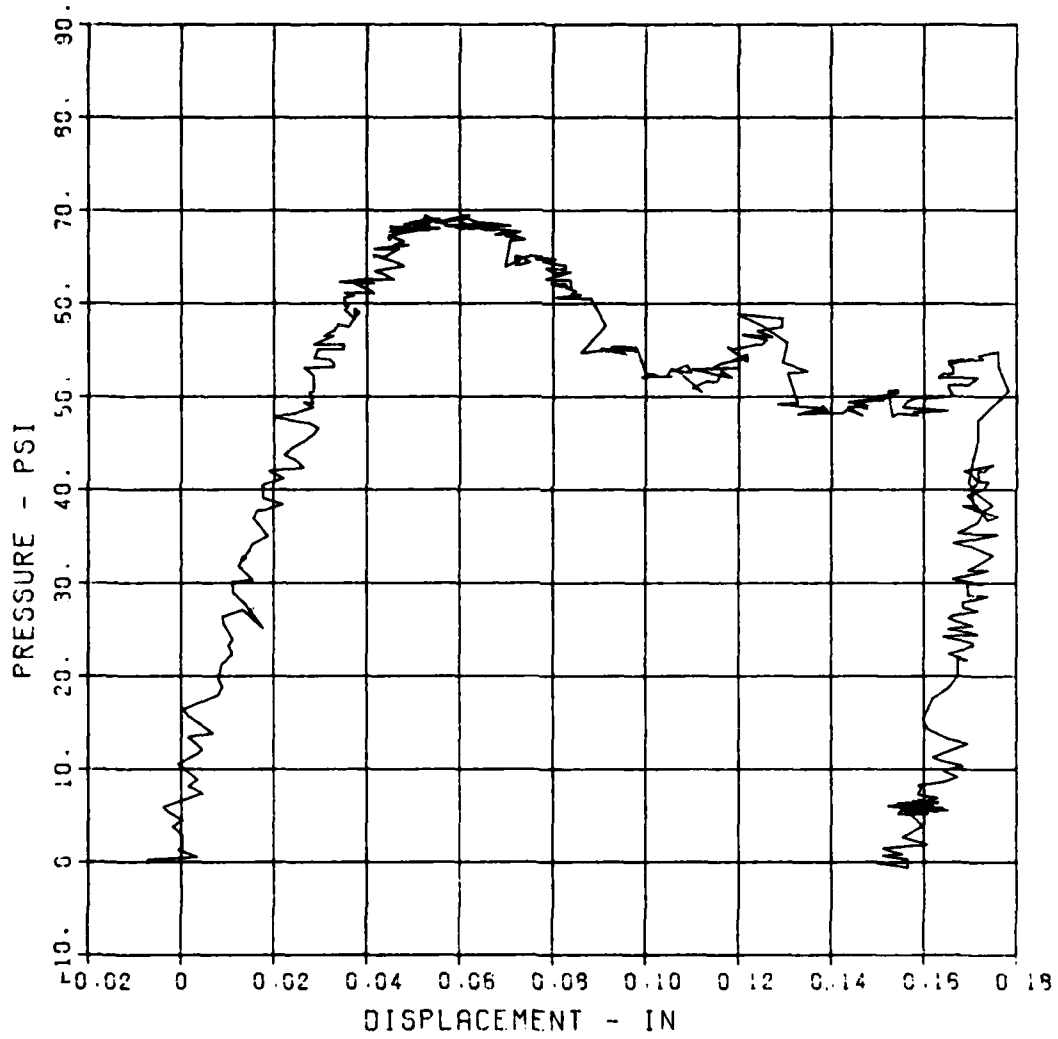
MAXIMUM
0.1792

SIGMA CAL
2.5631

CAL. VAL
1.1

CHANNEL NO. 2 14790 1

04/24/94 R0408



FEMA STIRRUP SLAB 8

D-2

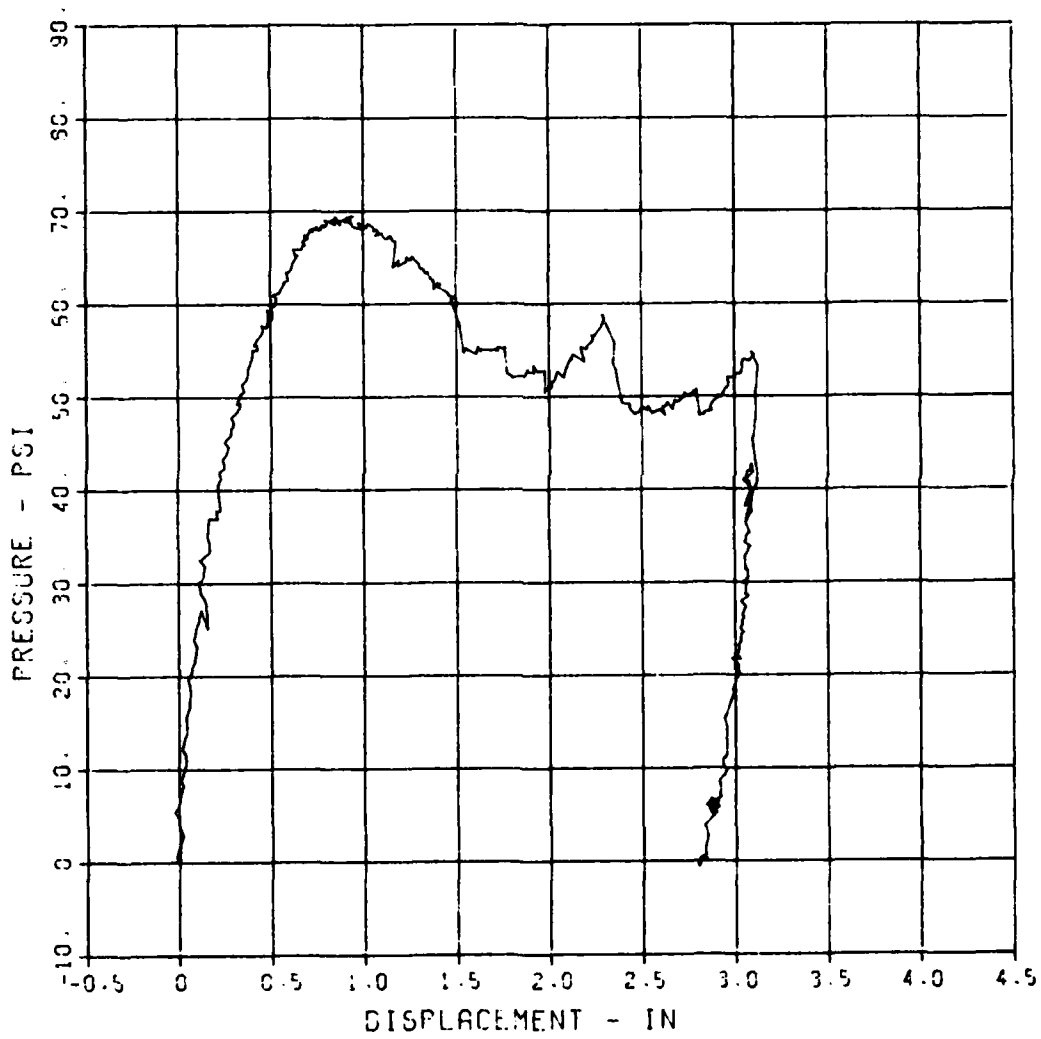
MAXIMUM
3.1264

SIGMA CAL
2.7255

CAL /AL
5.2

CHANNEL NO. 4 14700 :

04/10/84 R0346



FEMA STIRRUP SLAB 8

S-1

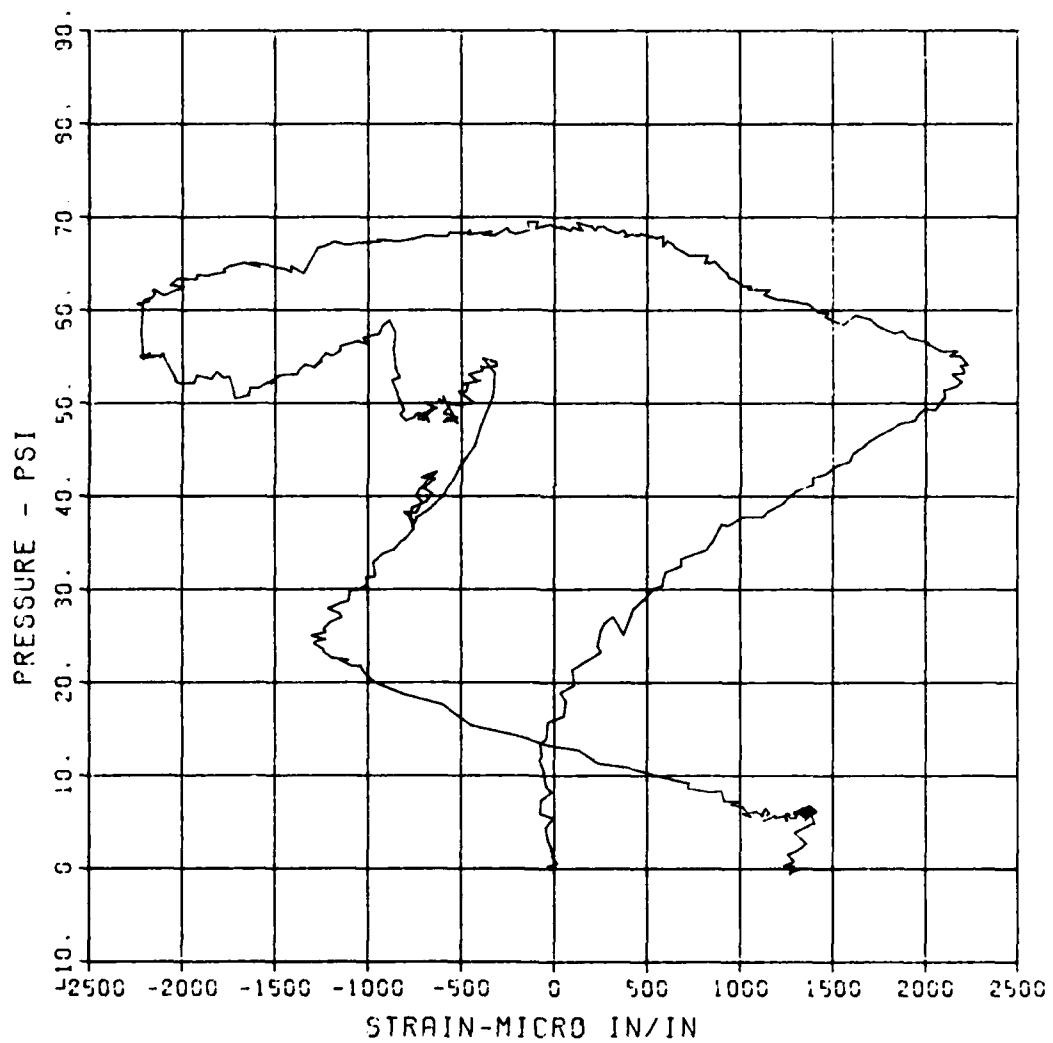
MAXIMUM
-2244.3274

SIGMA CAL
2.7493

CAL VAL
11555.7

CHANNEL NO. 5 14790 :

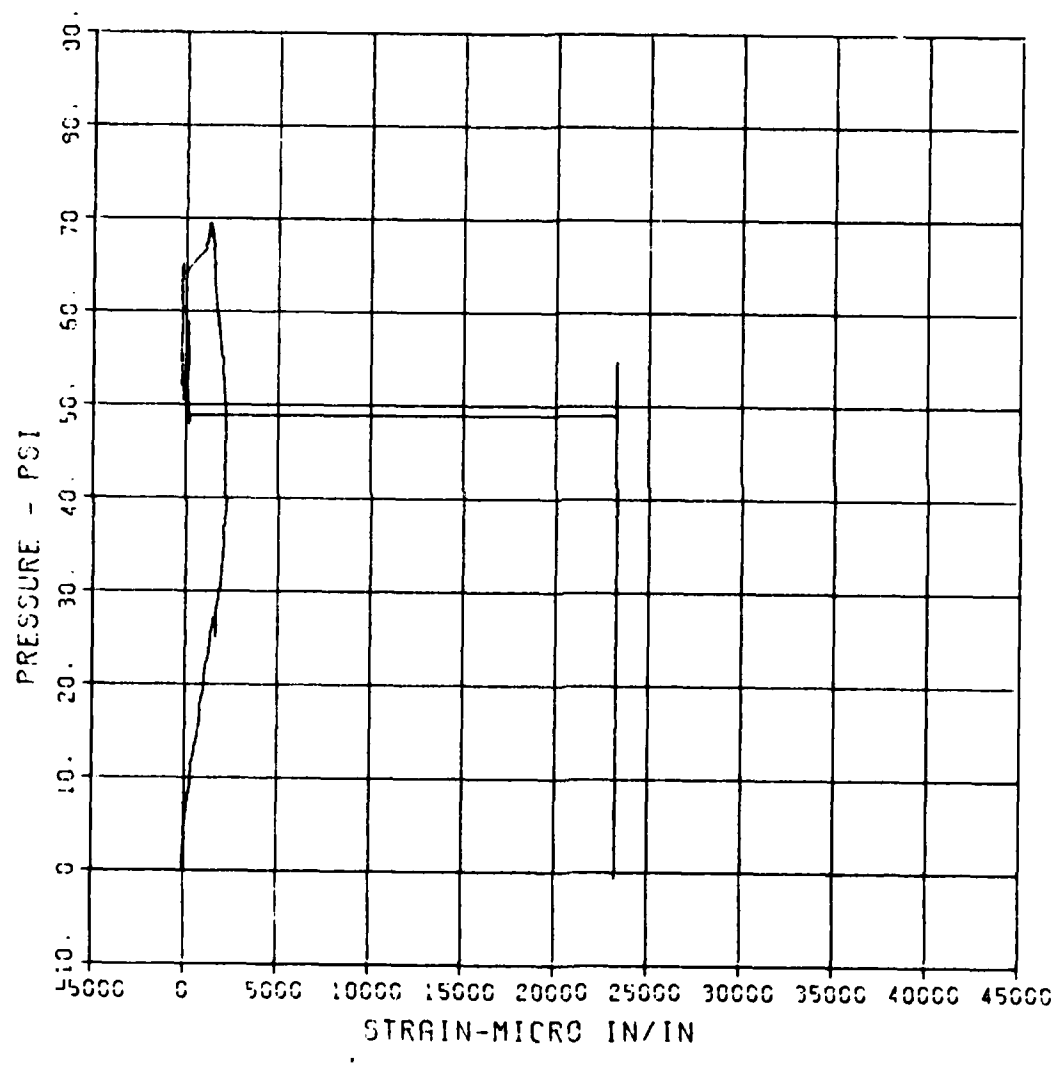
04/24/94 R0409



FEMA STIRRUP SLAB 8
SB-1

MAXIMUM SIGMA CAL CAL VAL
23265.0068 3.2043 11665.7

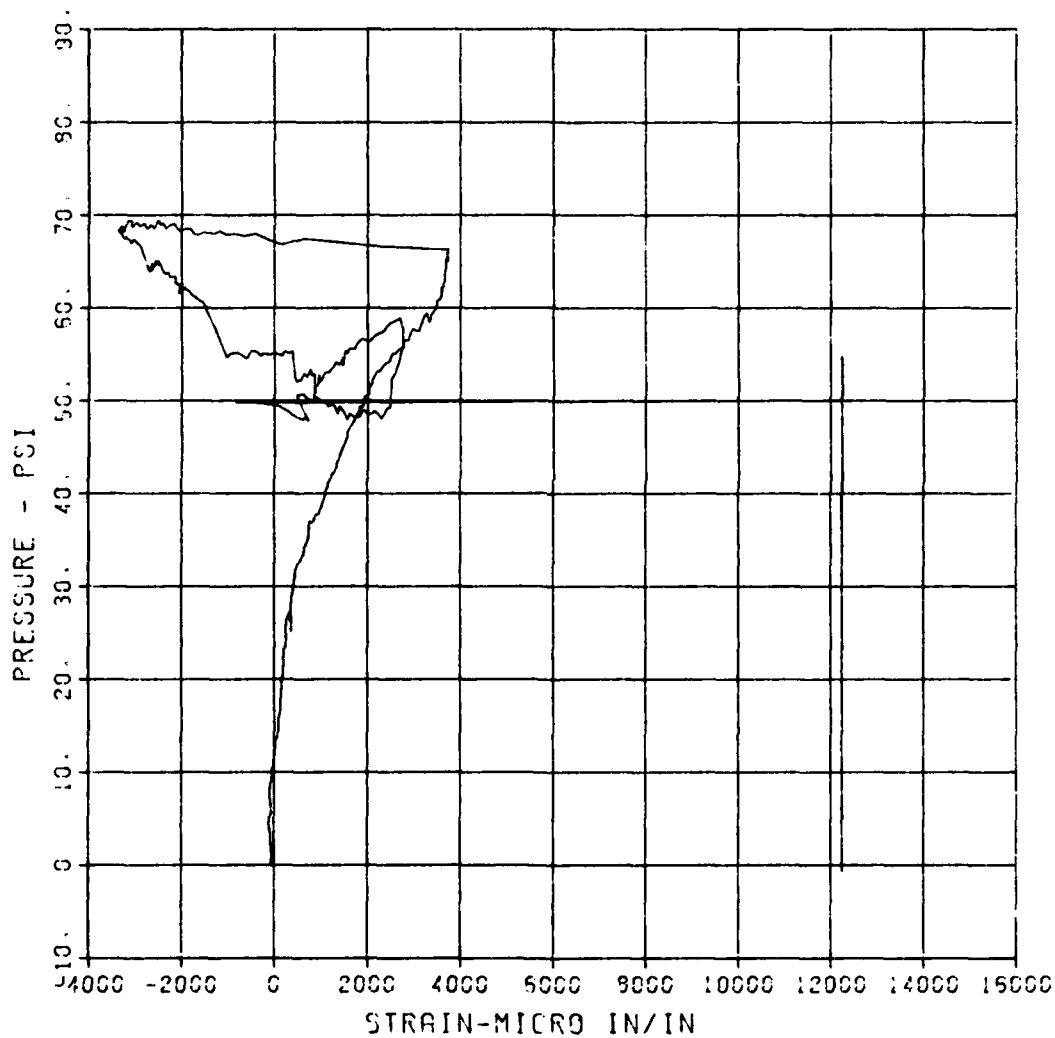
CHANNEL NO. 7 14700
04/10/84 R0346



FEMA STIRRUP SLAB 8
ST-2

MAXIMUM SIGMA CAL CAL VAL
12239.0773 3.5307 5755.1

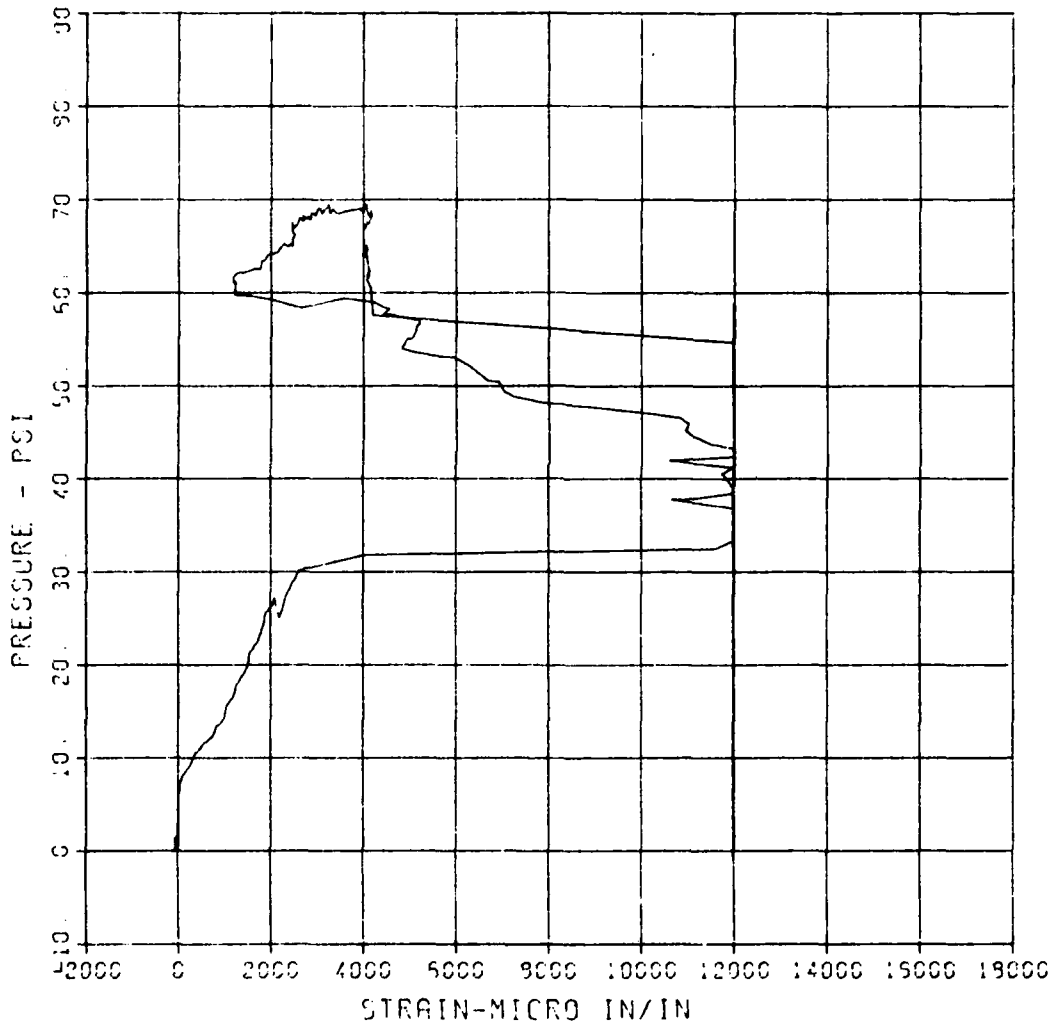
CHANNEL NO. 9 14730 1
04/10/94 R0346



FEMA STIRRUP SLAB 8
SB-2

MAXIMUM SIGMA CAL CAL VAL
11973.7534 3.5846 5766.7

CHANNEL NO 0 14730 1
04/10/84 R0346



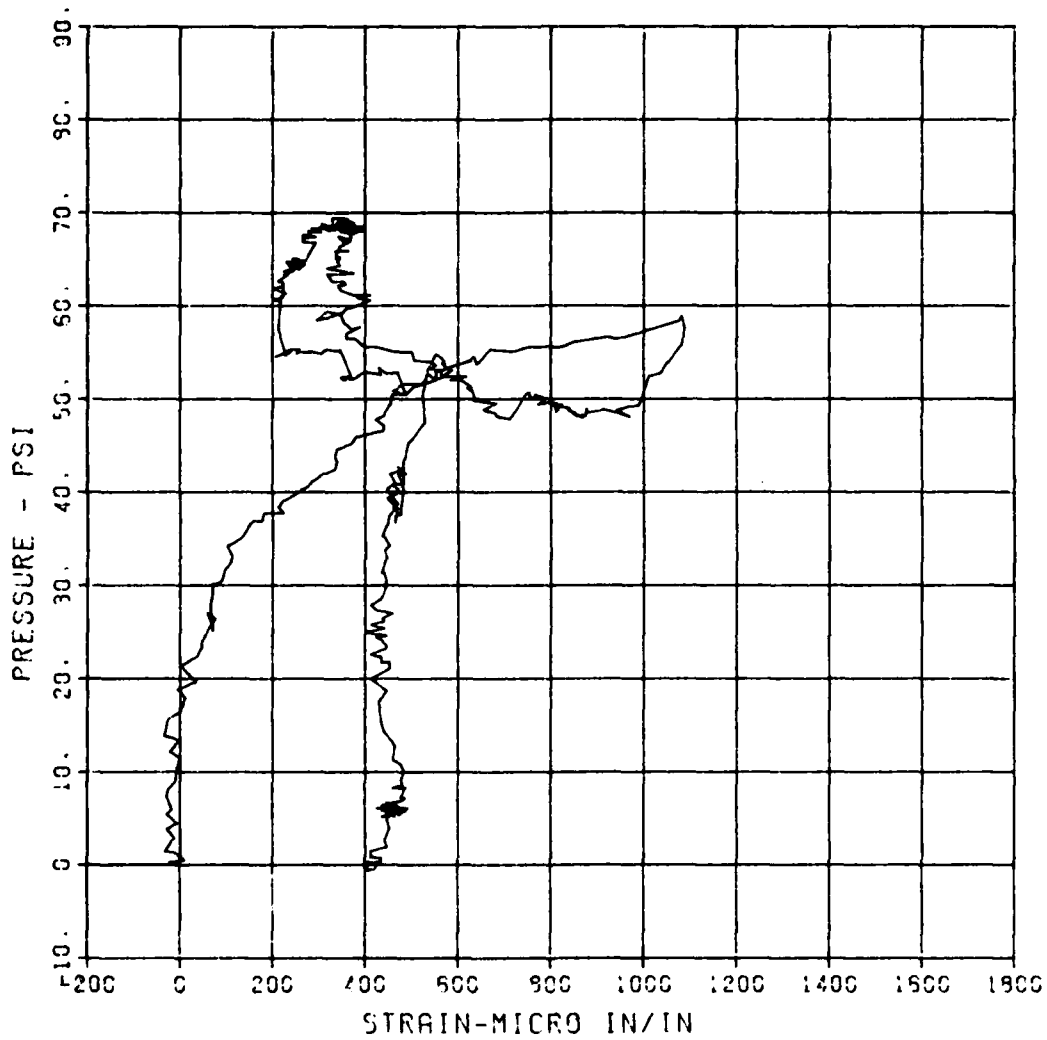
FEMA STIRRUP SLAB 8

S-3

MAXIMUM SIGMA CAL CAL VAL
1097.9550 2.7061 5766.1

CHANNEL NO. 10 14700 :

04/10/94 R0346



FEMA STIRRUP SLAB 8

S-4

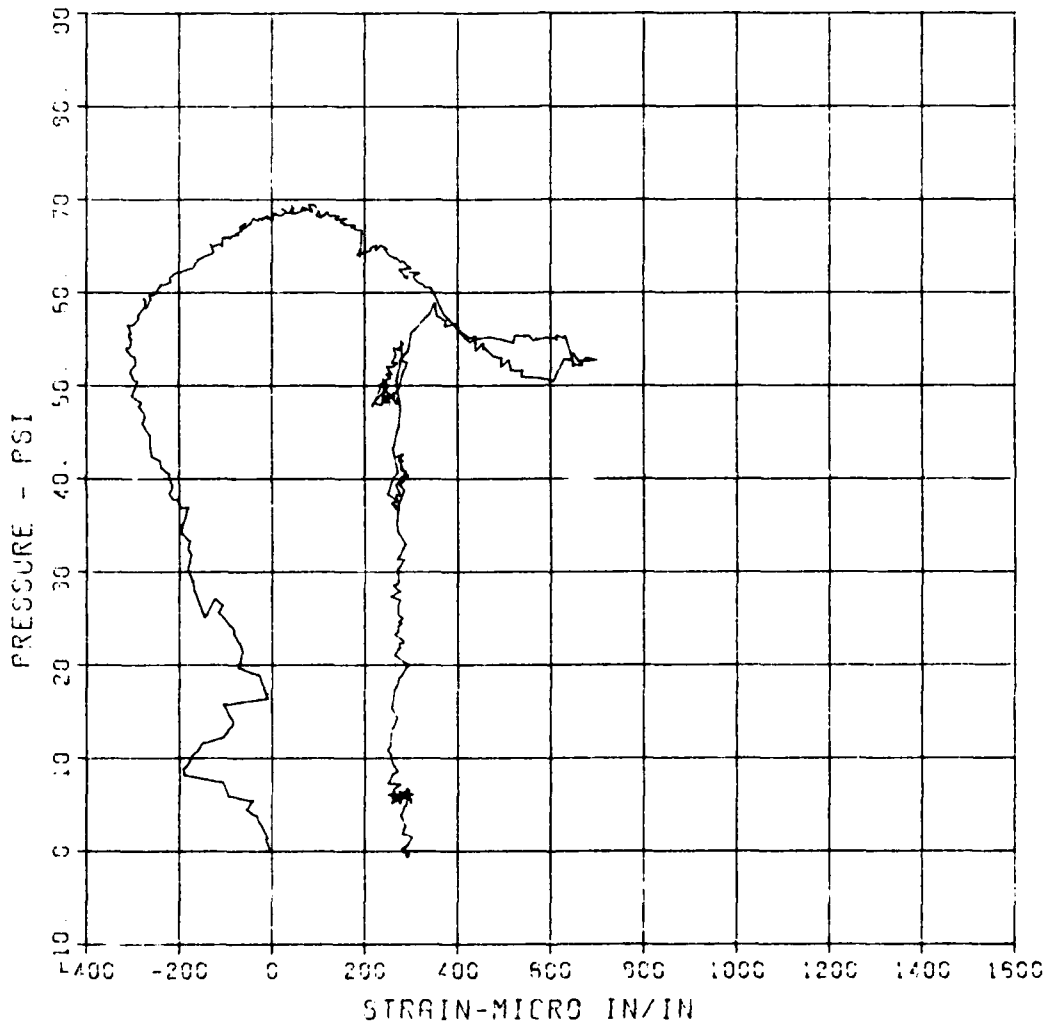
MAXIMUM
699.5553

SIGMA CAL
4.1590

CAL /AL
2990.9

CHANNEL NO. 11 14790 :

04/24/84 R0409



FEMA STIRRUP SLAB 8

S-5

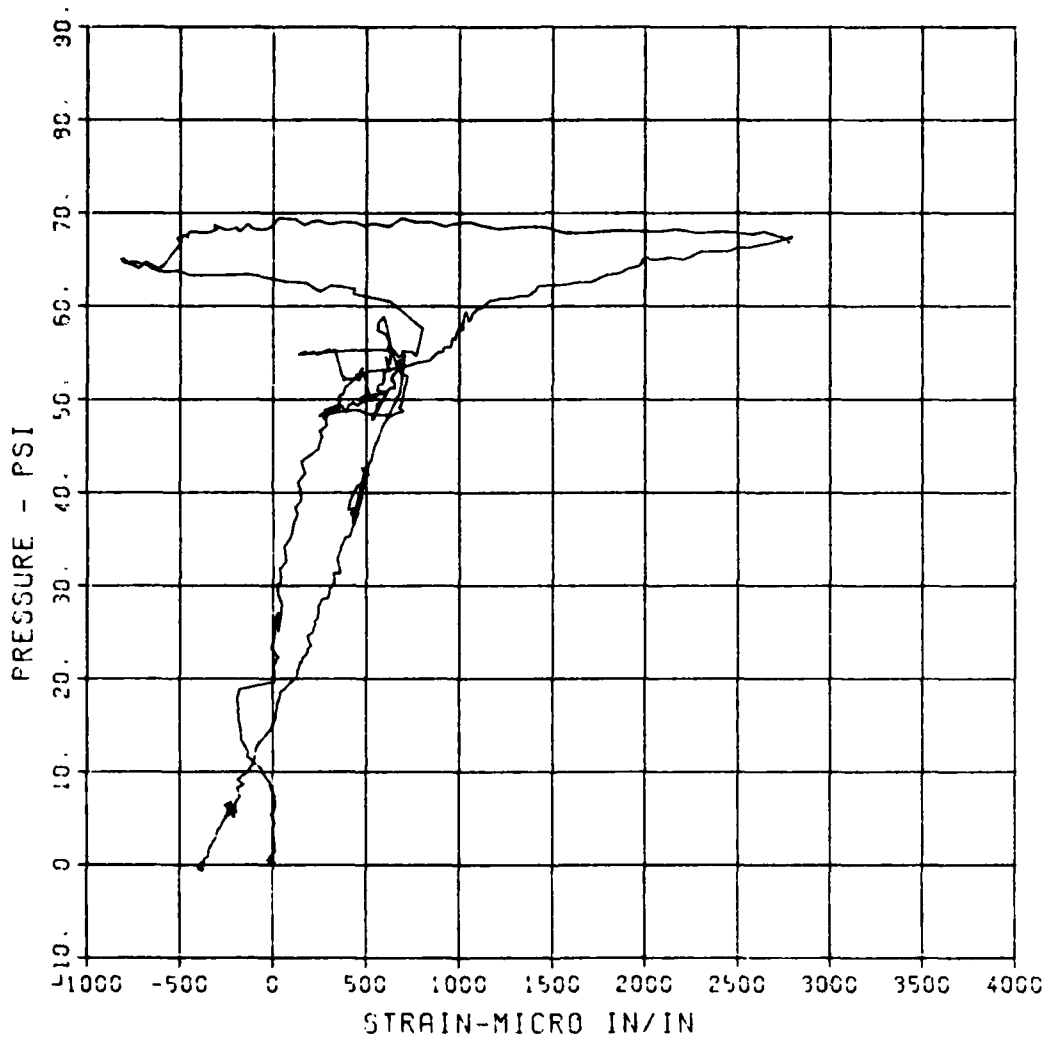
MAXIMUM
2734.4005

SIGMA CAL
2.7915

CAL VAL
5765.1

CHANNEL NO. 12 14730 1

04/24/84 R0409

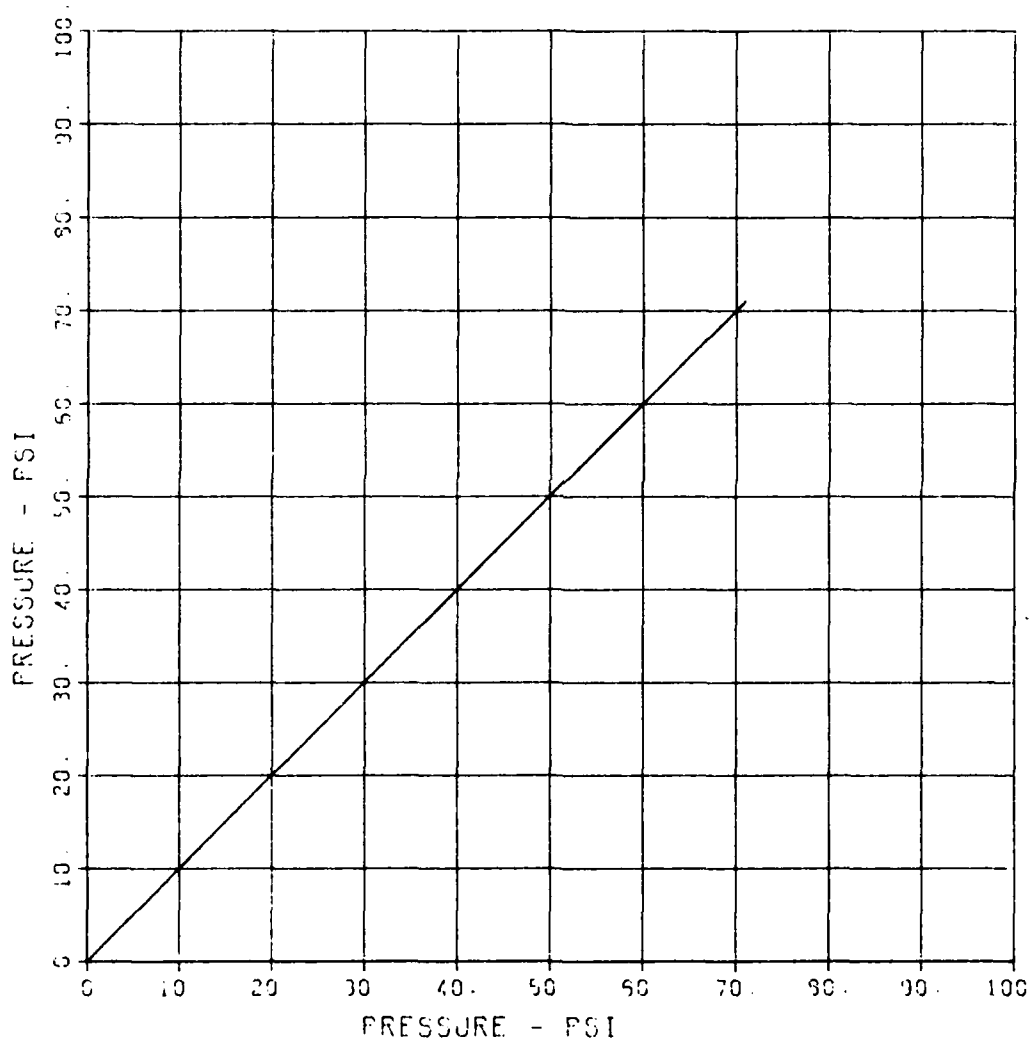


FEMA STIRRUP SLAB 9

P-1

MAXIMUM	SIGMA CAL	CAL VAL
71.0197	4.6556	135.9

CHANNEL NO. :	9715 :
04/26/94	50440



FEMA STIRRUP SLAB 3

D-1

MAXIMUM
0.1630

SICMA CAL
2.9350

CAL VAL
1.1

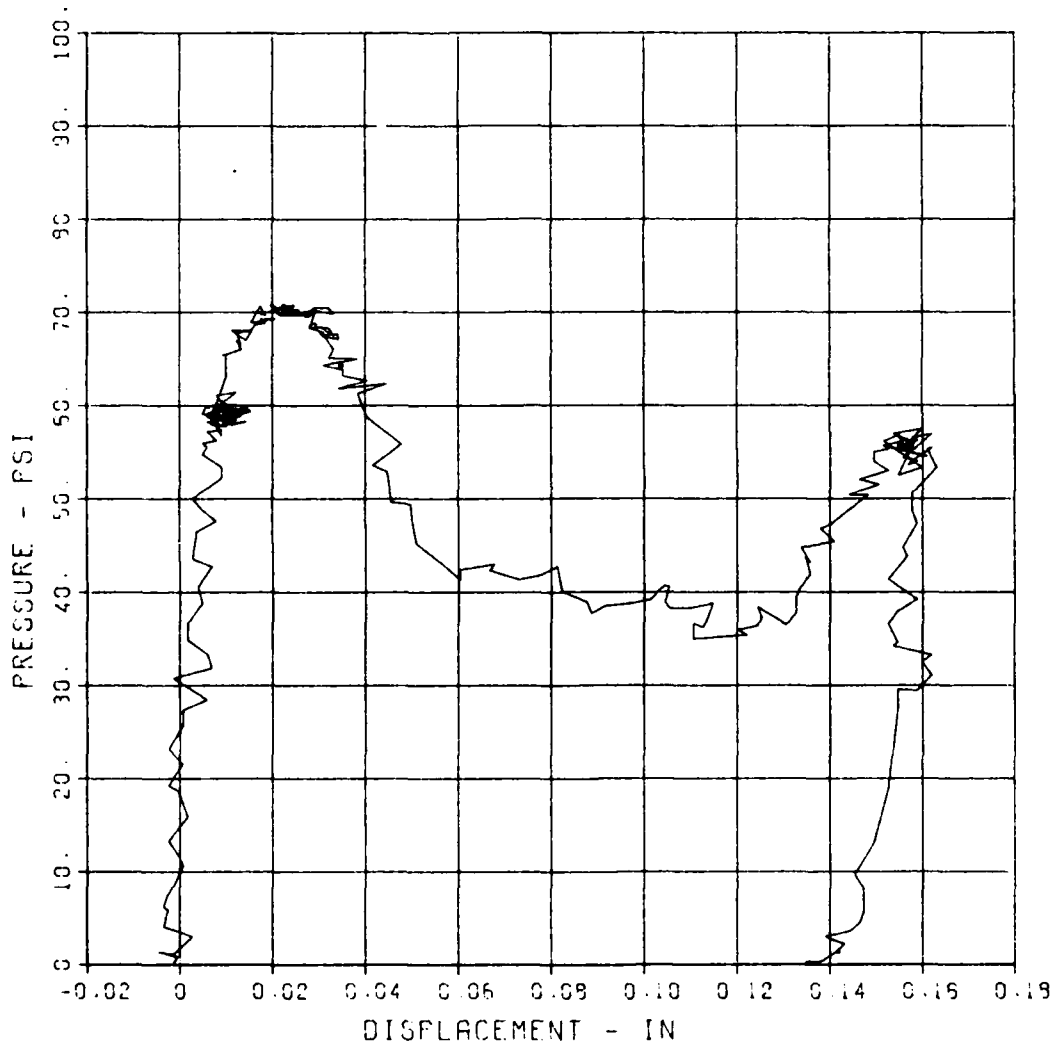
CHANNEL NO 2

2

9715 1

04/26/94

R0440



FEMA STIRRUP SLAB 9

D-2

MAXIMUM
3.4230

SIGMA CAL
2.3400

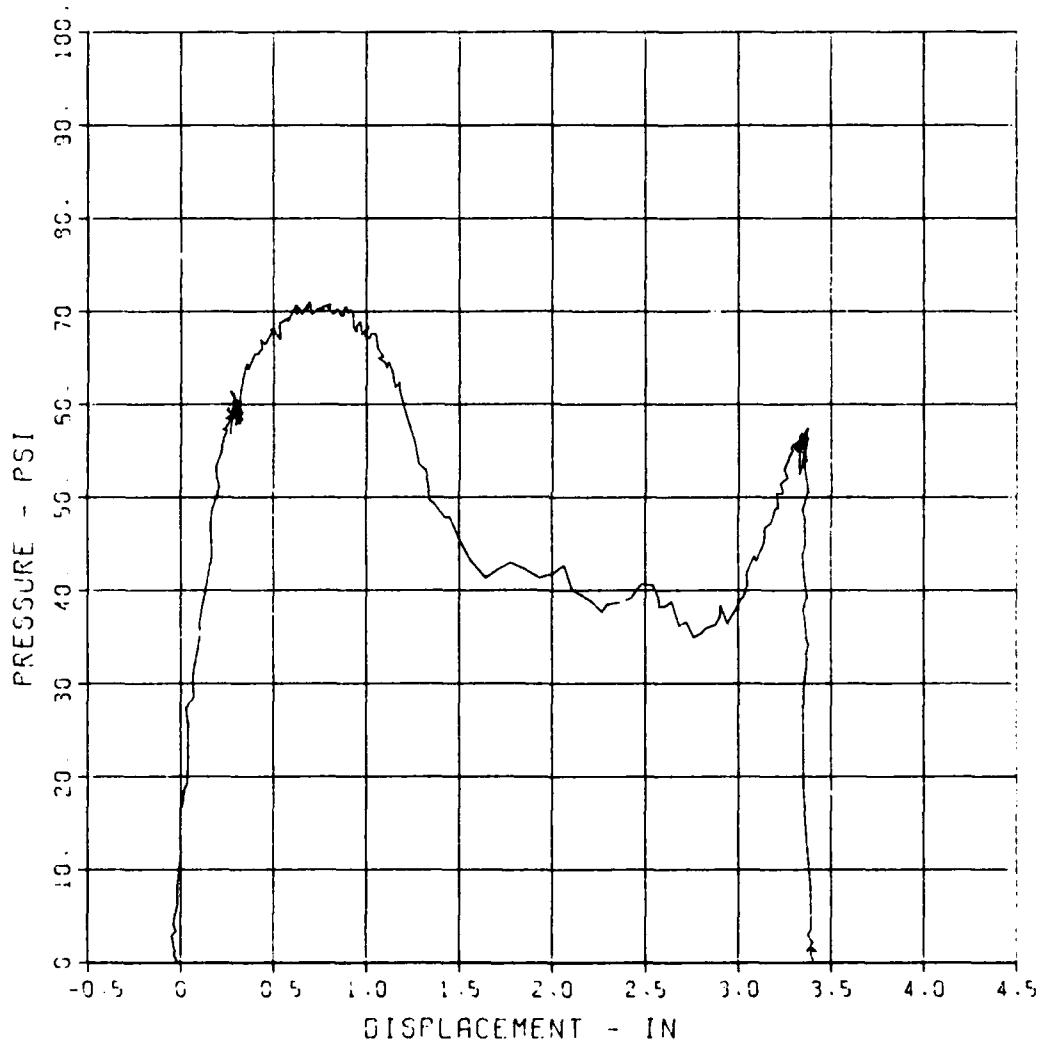
CAL VAL
5.2

CHANNEL NO. 3

9715 1

04/19/84

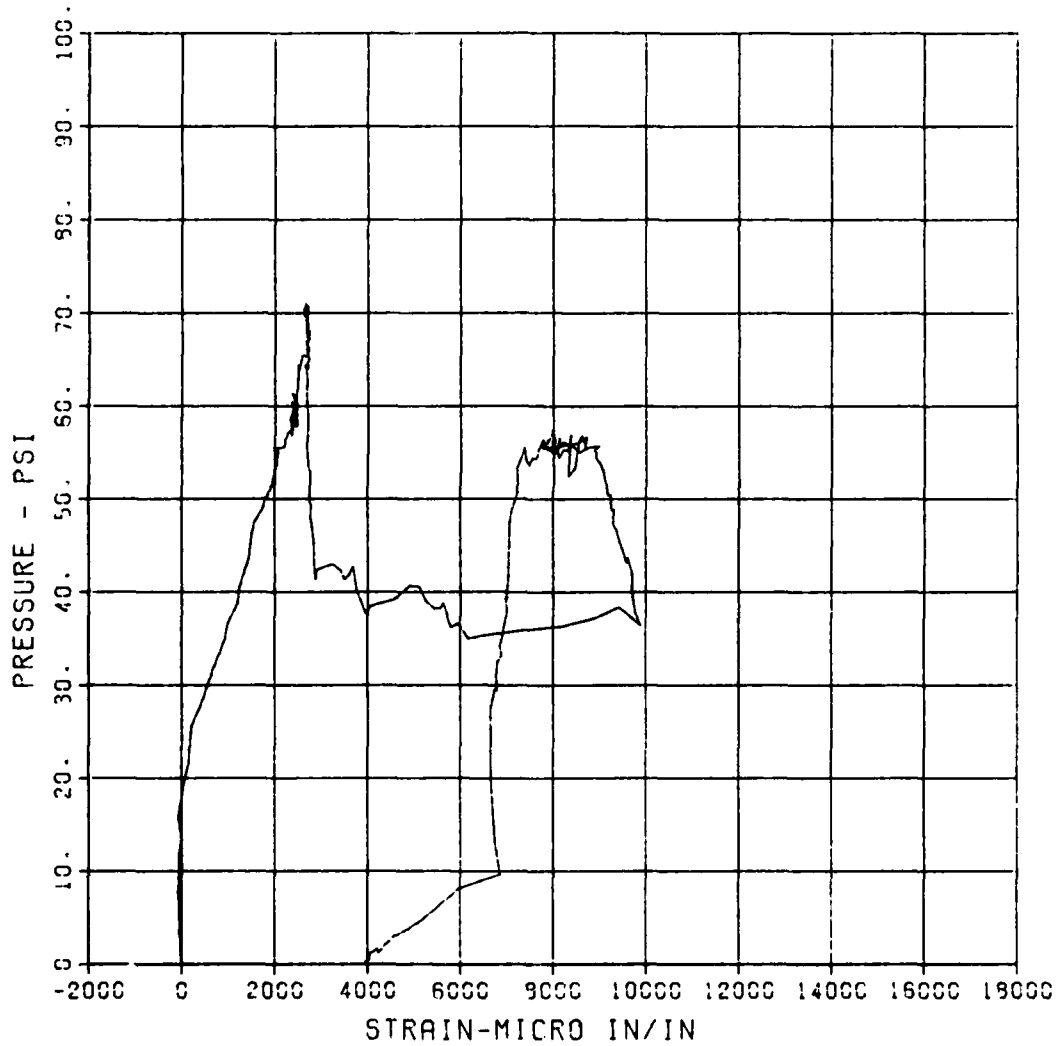
R0348



FEMA STIRRUP SLAB 9
ST-1

MAXIMUM SIGMA CAL CAL VAL
9992.2843 3.2336 11556.7

CHANNEL NO. 4 9715
04/19/84 R0348



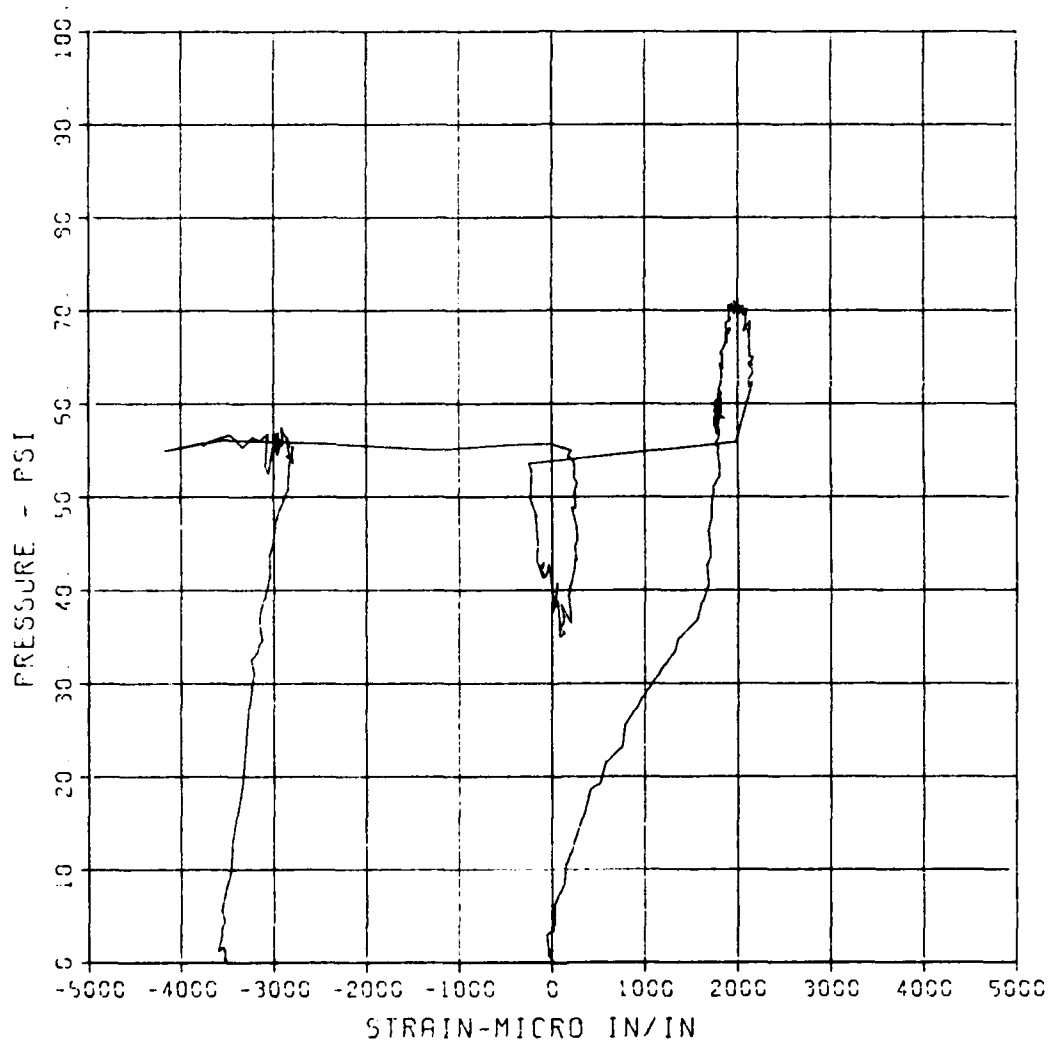
FEMA STIRRUP SLAB 9

SB-1

MAXIMUM SIGMA CAL CAL VAL
-4190.4077 3.0300 11666.7

CHANNEL NO. 5 9715 :

04/10/94 R0349



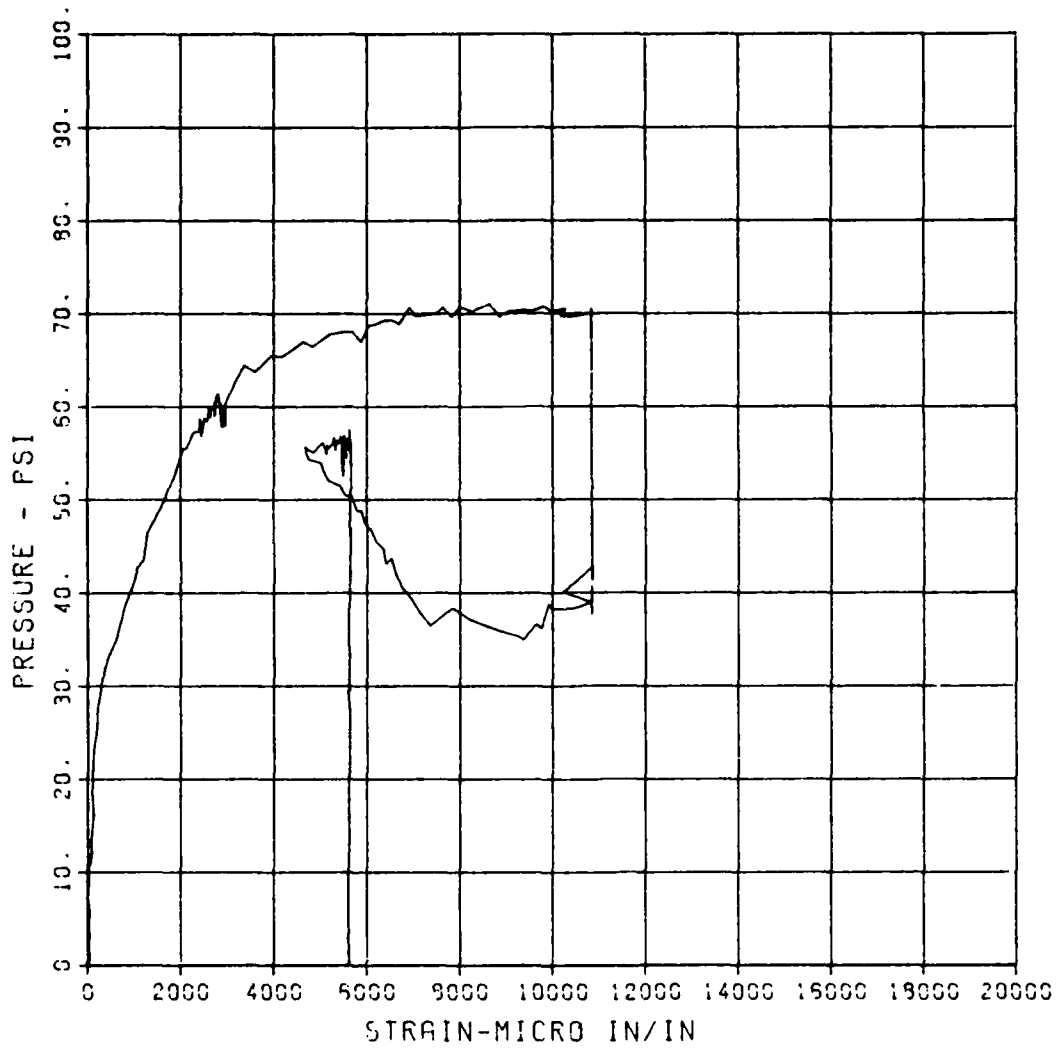
FEMA STIRRUP SLAB 9

ST-2

MAXIMUM 10847.4356 SIGMA CAL 3.7912 CAL VAL 5766.1

CHANNEL NO. 6 8715 1

04/26/94 R0440



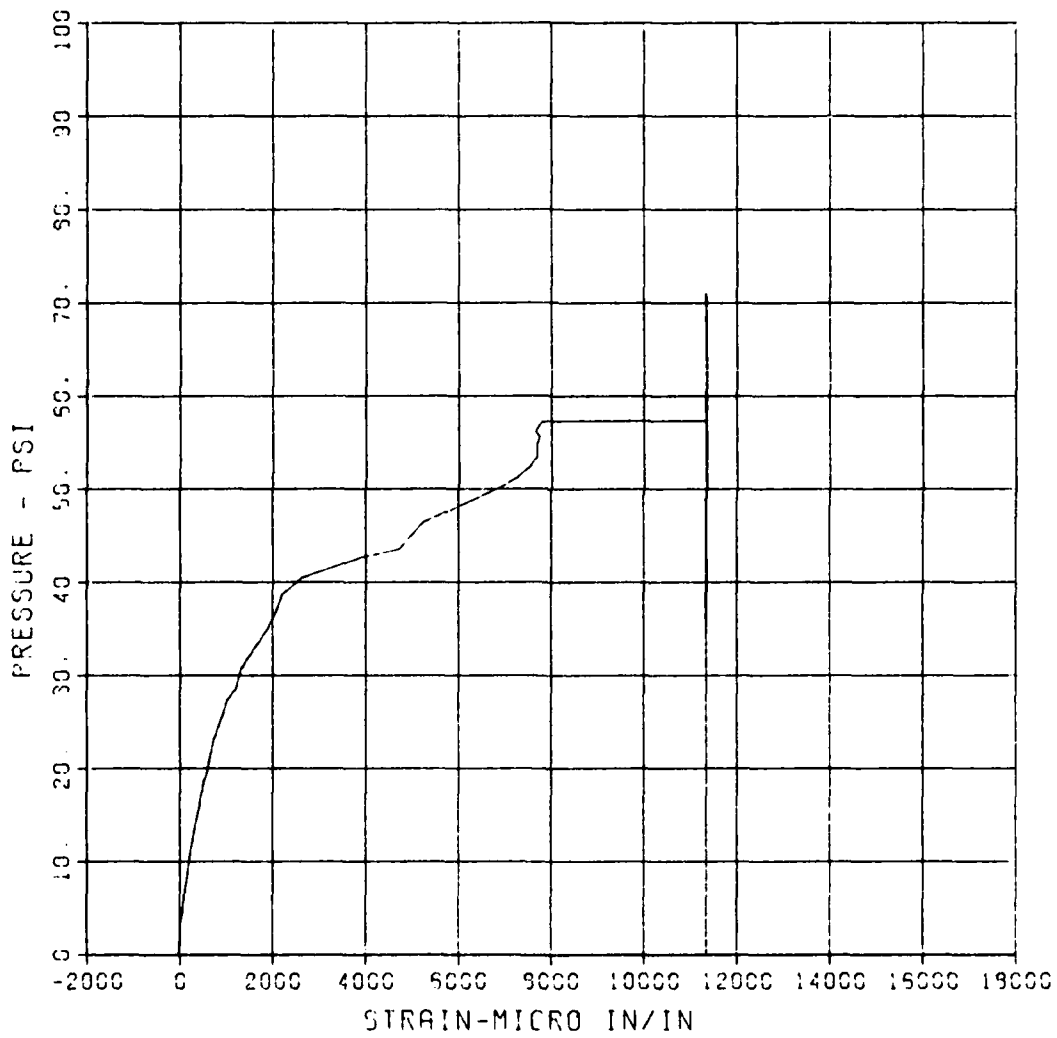
FEMA STIRRUP SLAB 3

SB-2

MAXIMUM	SICMA CAL	CAL VAL
11345.3331	3.0495	5765.1

CHANNEL NO. 7 9715 1

04/19/94 R0349



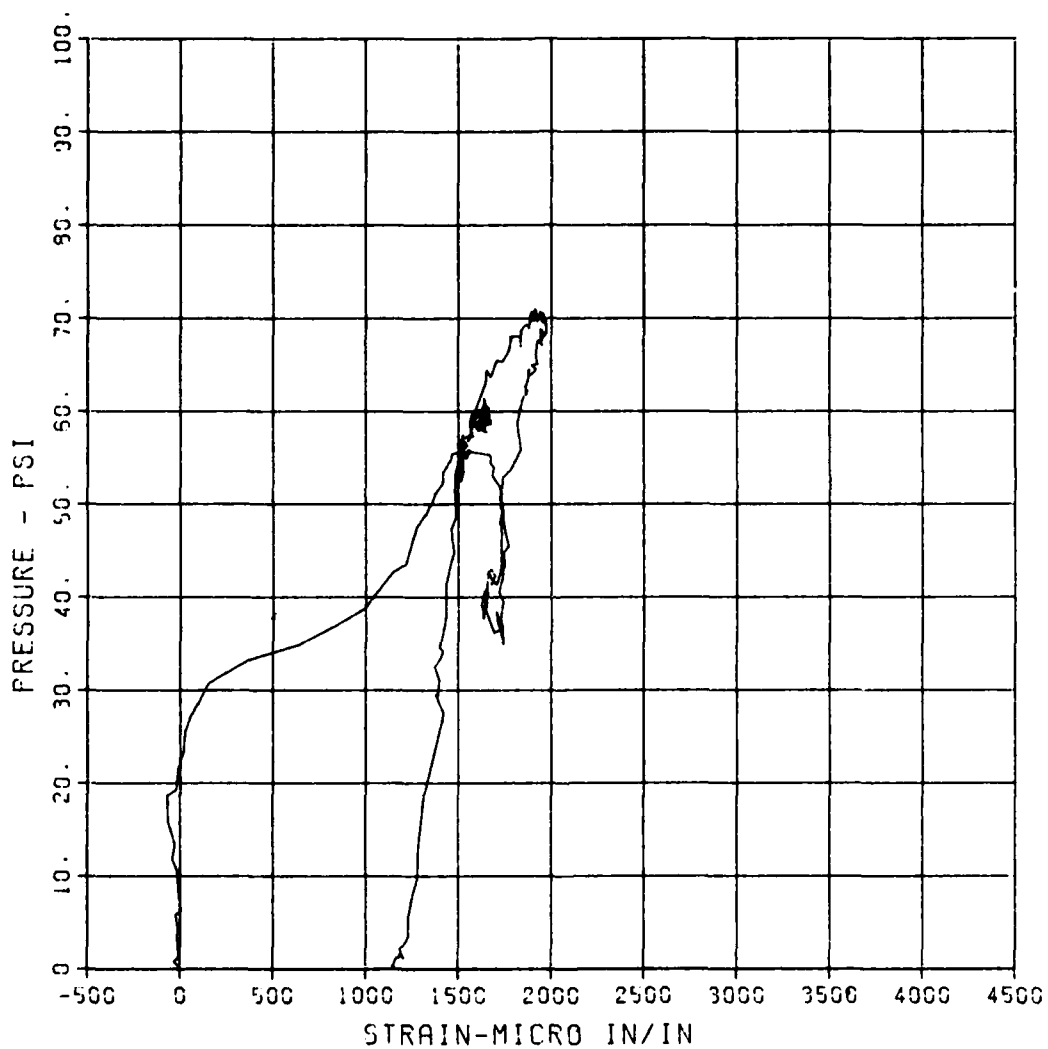
FEMA STIRRUP SLAB 9

S-3

MAXIMUM	SICMA CAL	CAL VAL
1970.1340	2.8333	5756.1

CHANNEL NO. 9 9715 1

04/25/94 R0440



FEMA STIRRUP SLAB 9

S-4

MAXIMUM
-594.0274

SIGMA CAL
5.0348

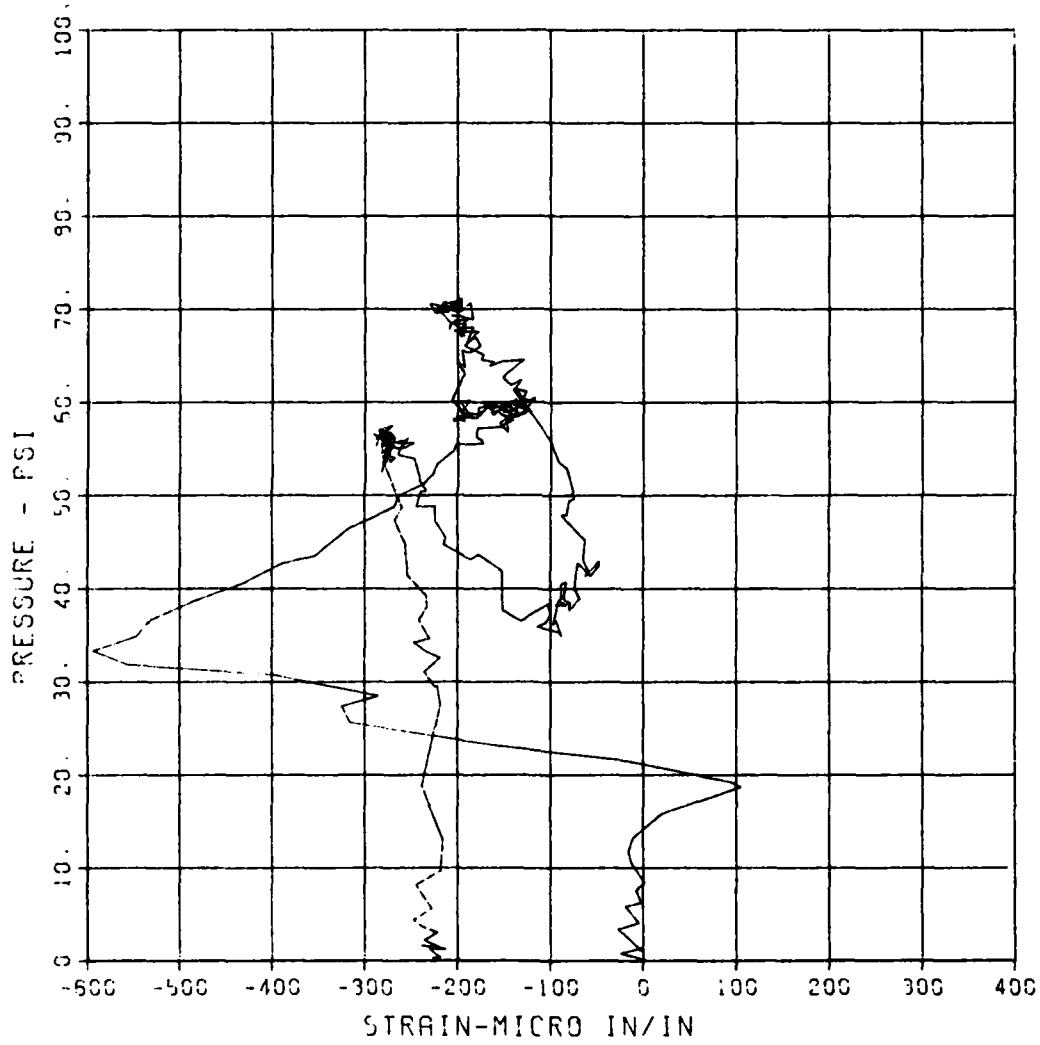
CAL VAL
2900.9

CHANNEL NO. 9

8715 1

04/25/94

R0440



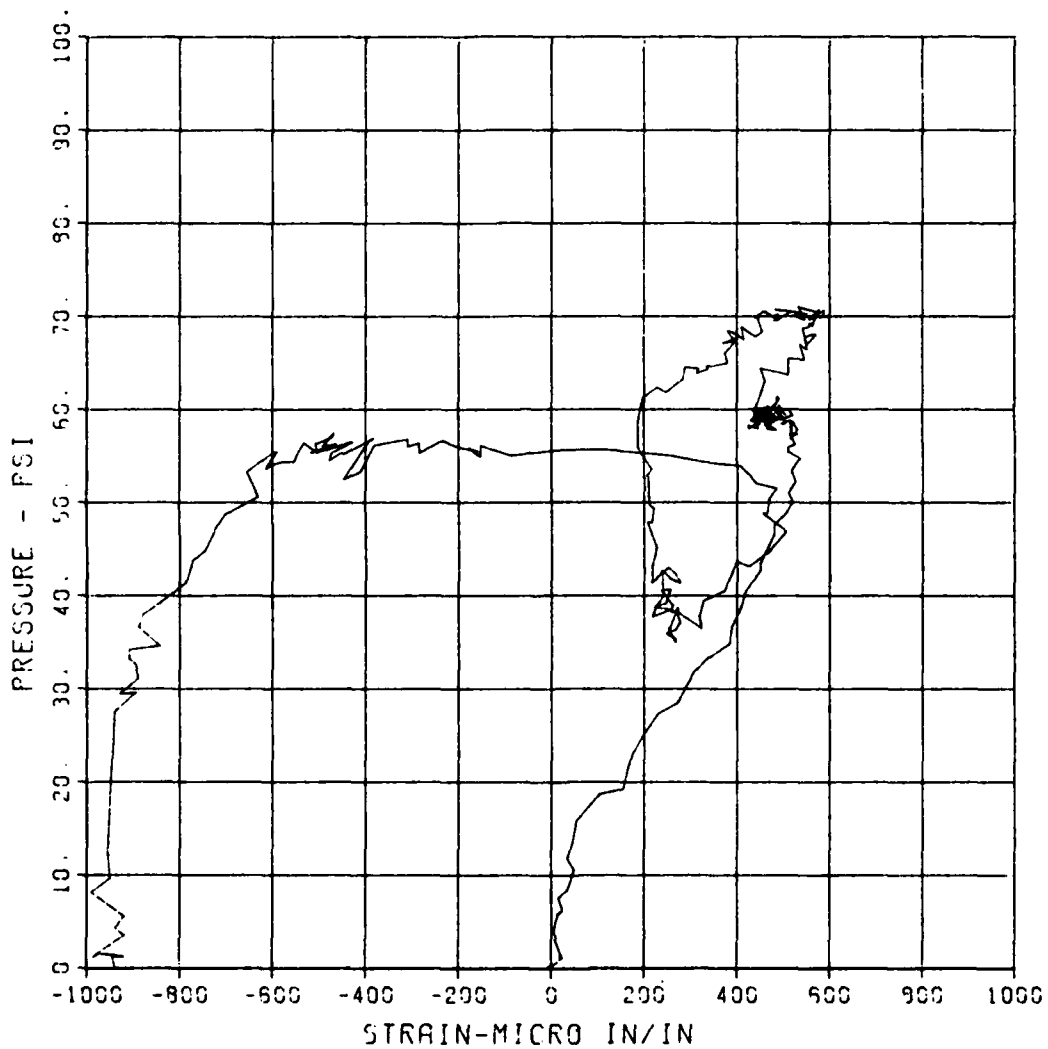
FEMA STIRRUP SLAB 3

S-5

MAXIMUM	SIGMA CAL	CAL VAL
-999.2223	3.3359	5766.1

CHANNEL NO 10 9715 :

04/25/94 R0440



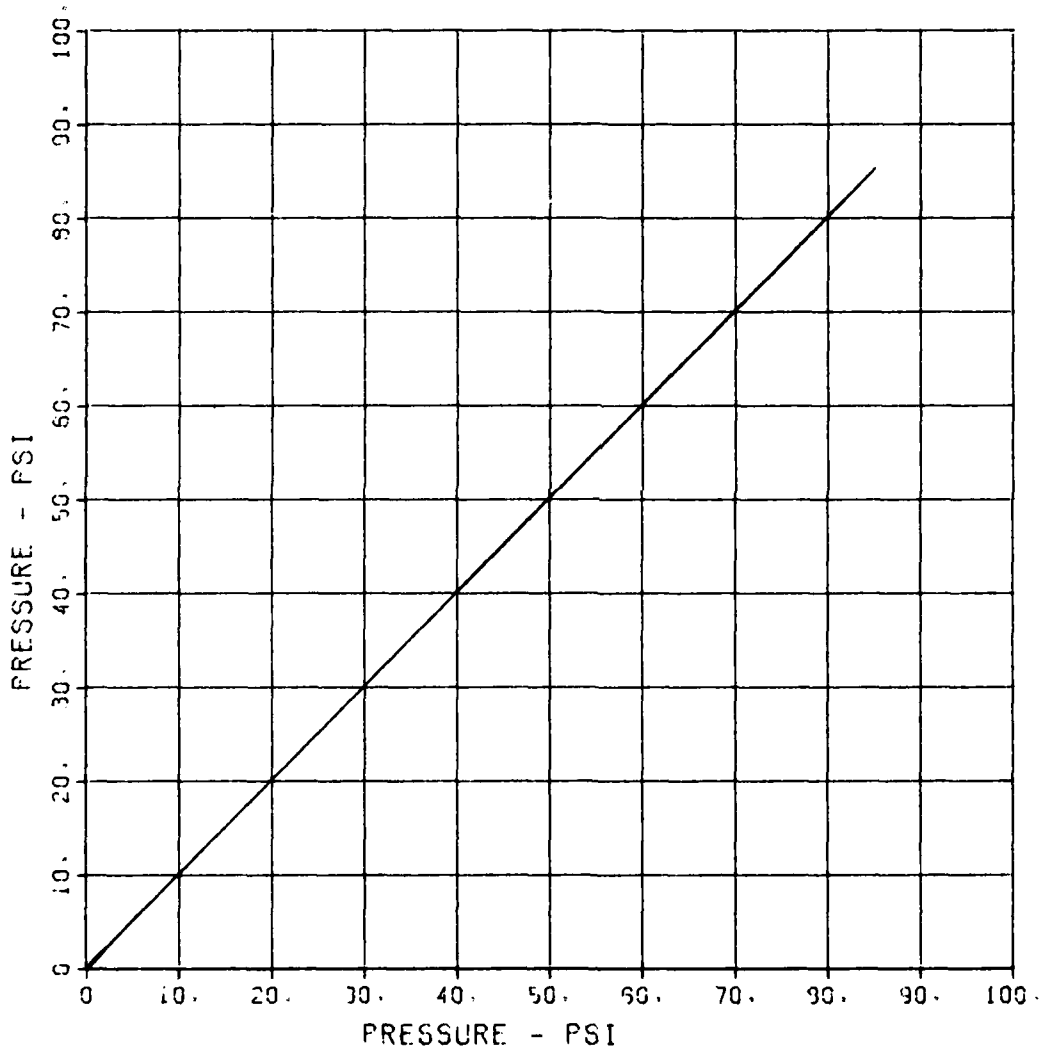
FEMA STIRRUP SLAB 10

P-1

MAXIMUM	SIGMA CAL	CAL VAL
95.0995	4.4741	135.3

CHANNEL NO. 1 16030 1

05/03/54 R0597



FEMA STIRRUP SLAB 10

D-2

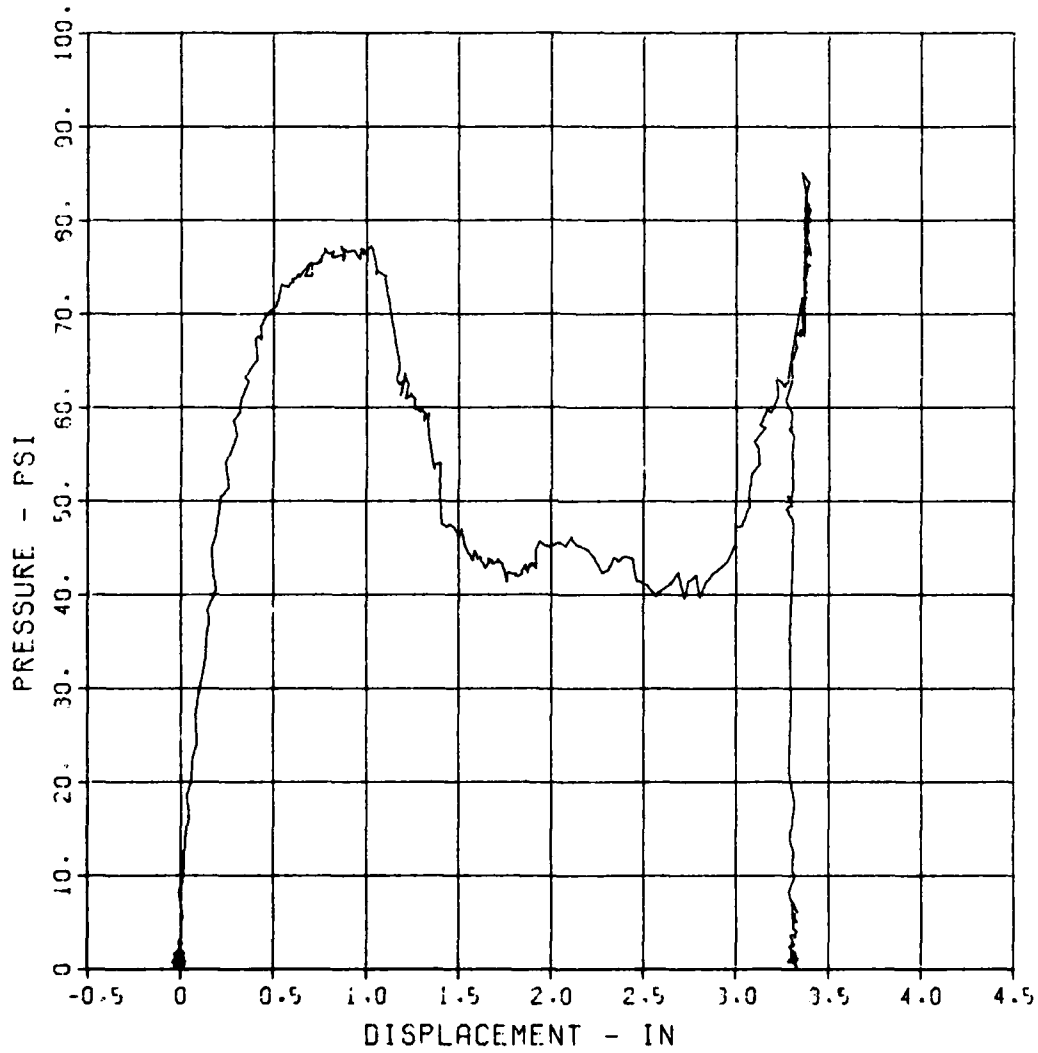
MAXIMUM
3.3991

SIGMA CAL
2.5232

CAL VAL
5.2

CHANNEL NO. 3 16030 1

05/03/94 R0597



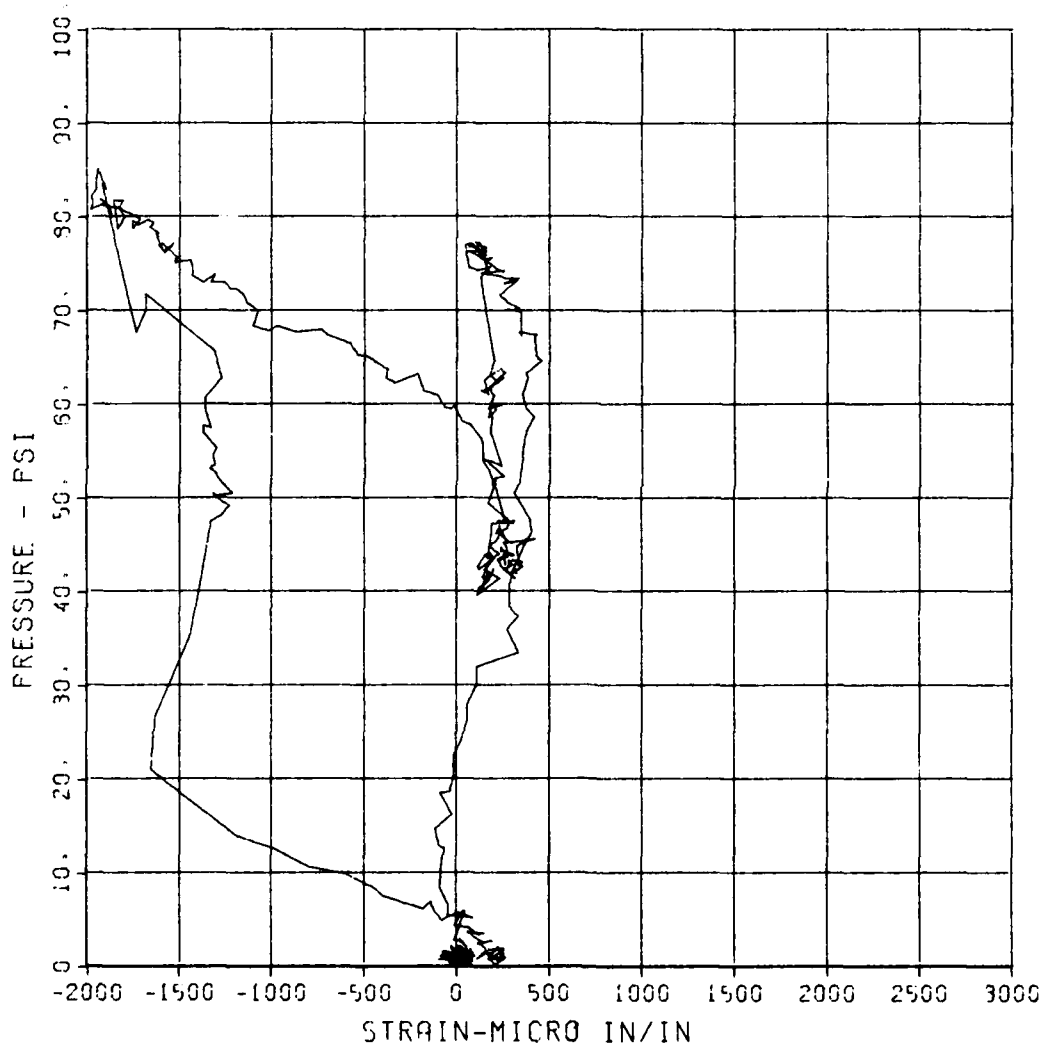
FEMA STIRRUP SLAB 10

ST-1

MAXIMUM	SIGMA CAL	CAL VAL
-1393.9722	2.9193	11665.7

CHANNEL NO. 4 15030 1

05/03/94 R0597



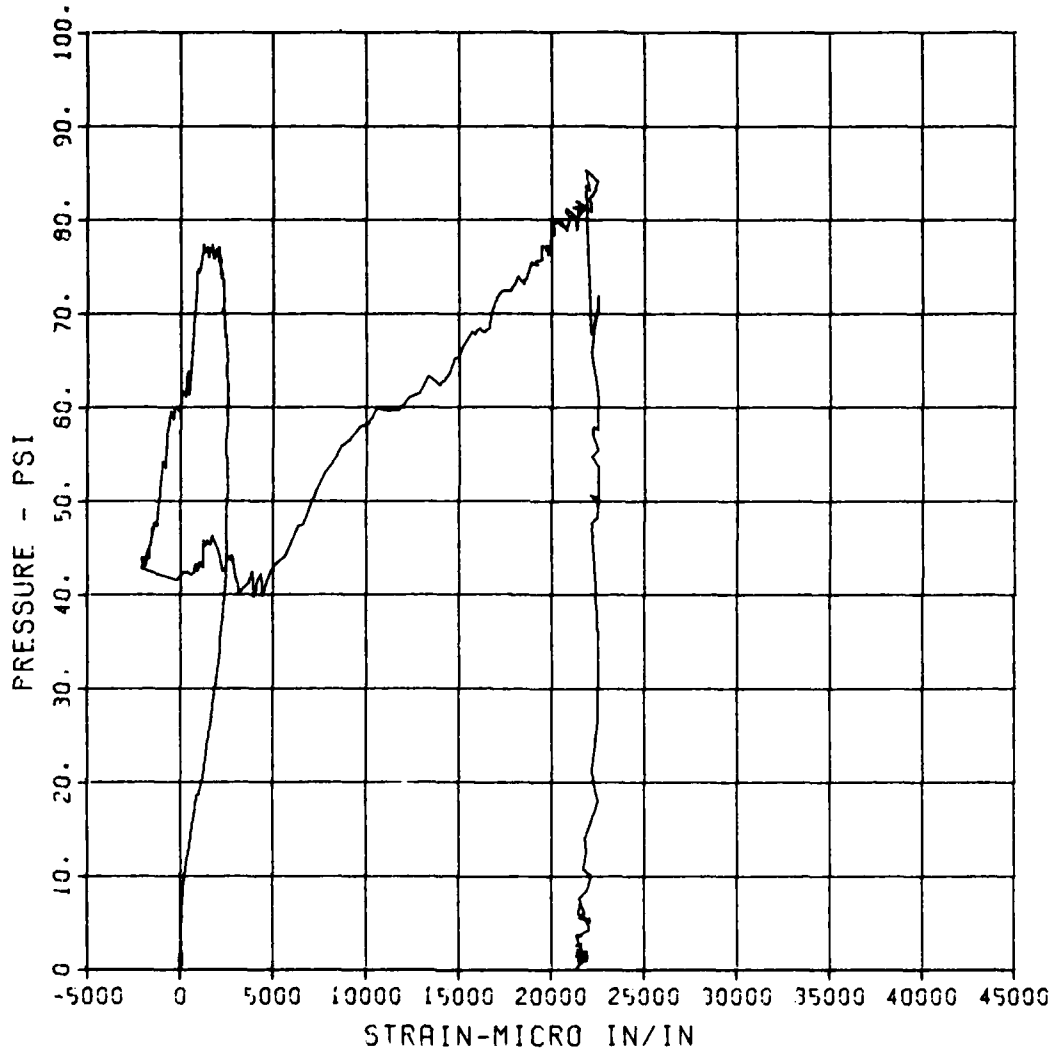
FEMA STIRRUP SLAB 10

SB-1

MAXIMUM SIGMA CAL CAL VAL
22524.5705 2.2750 11666.7

CHANNEL NO. 5 16030 1

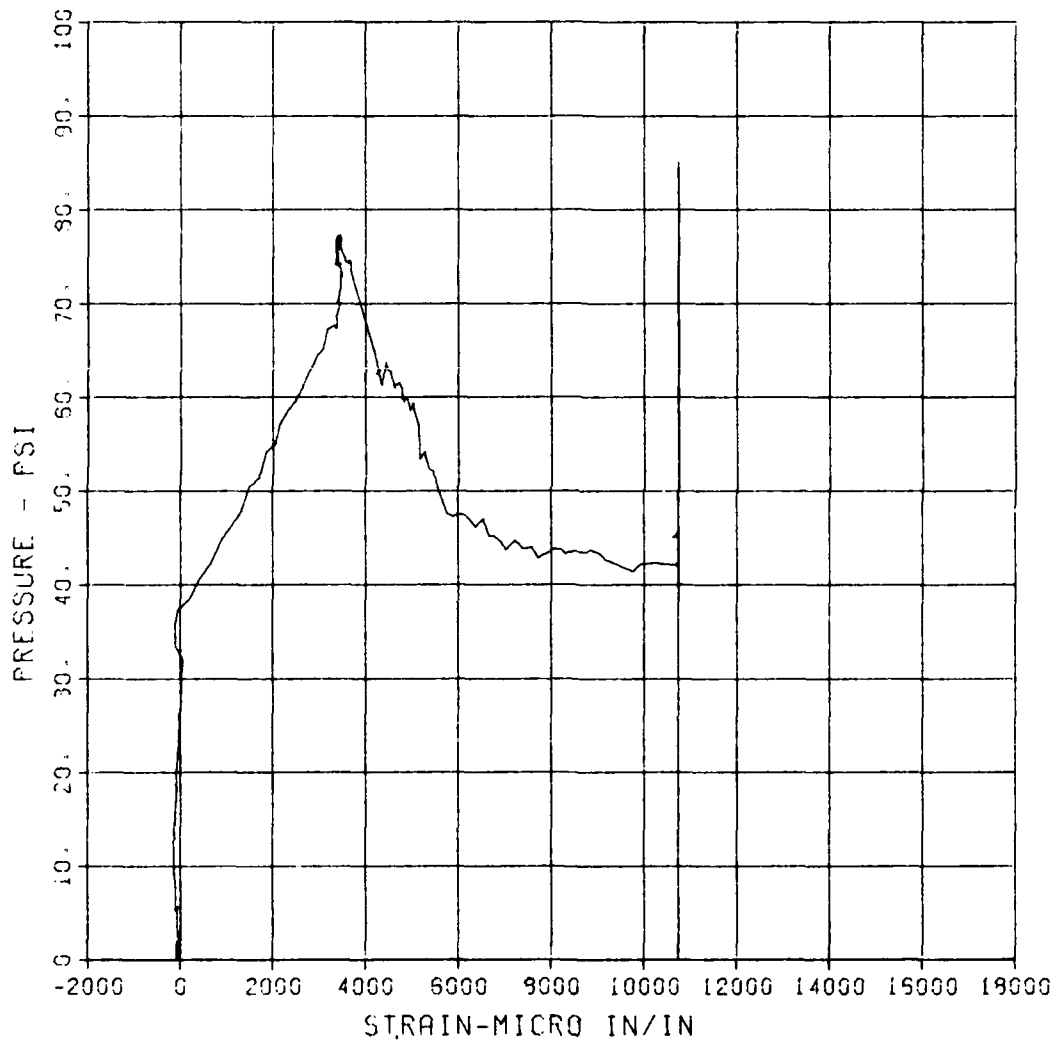
05/03/84 R0587



FEMA STIRRUP SLAB 10
ST-2

MAXIMUM SIGMA CAL CAL VAL
10740 9450 3.9531 5766.1

CHANNEL NO. 6 16030 1
05/03/94 R0597



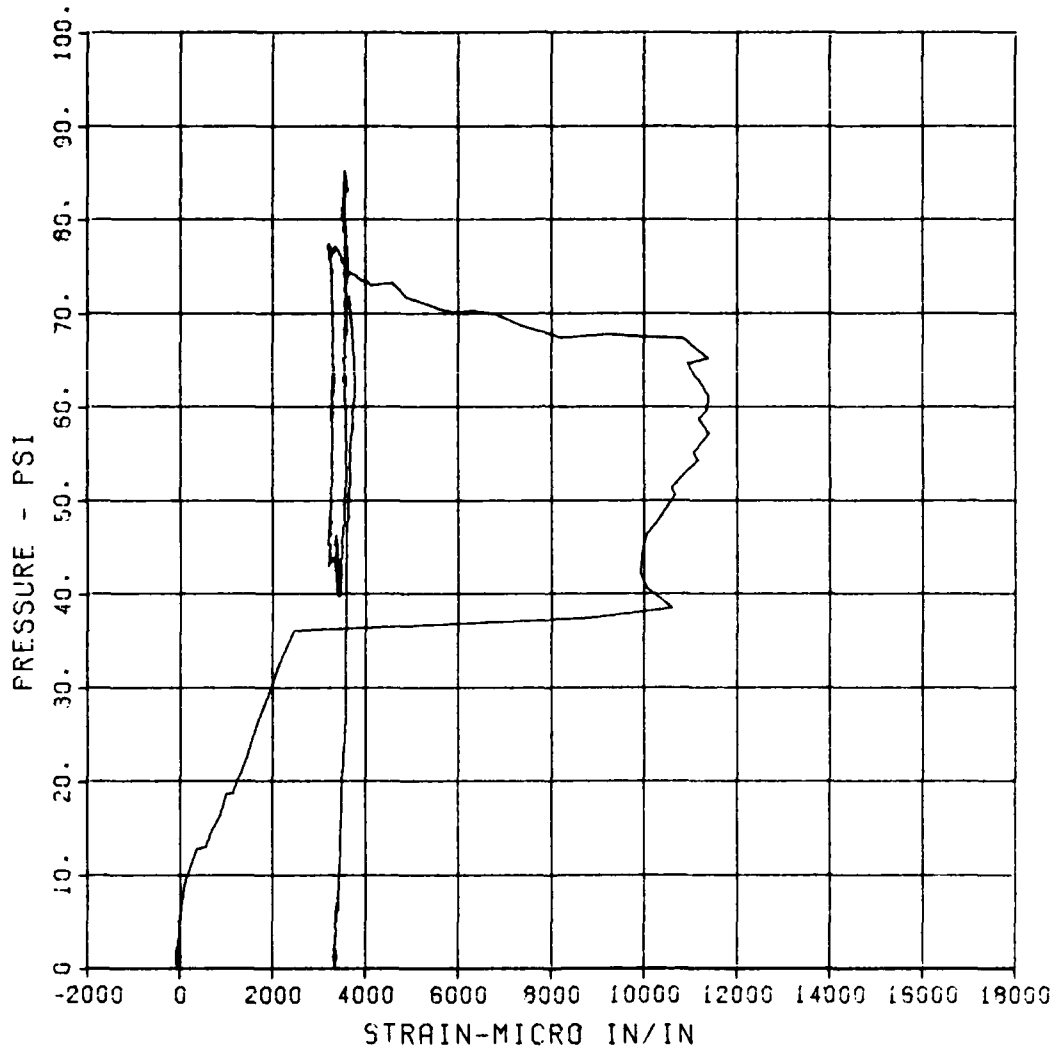
FEMA STIRRUP SLAB 10

SB-2

MAXIMUM 11395.9559 SIGMA CAL 2.9515 CAL_VAL 5766.1

CHANNEL NO. 7 15030 1

05/03/84 R0597



FEMA STIRRUP SLAB 10

S-3

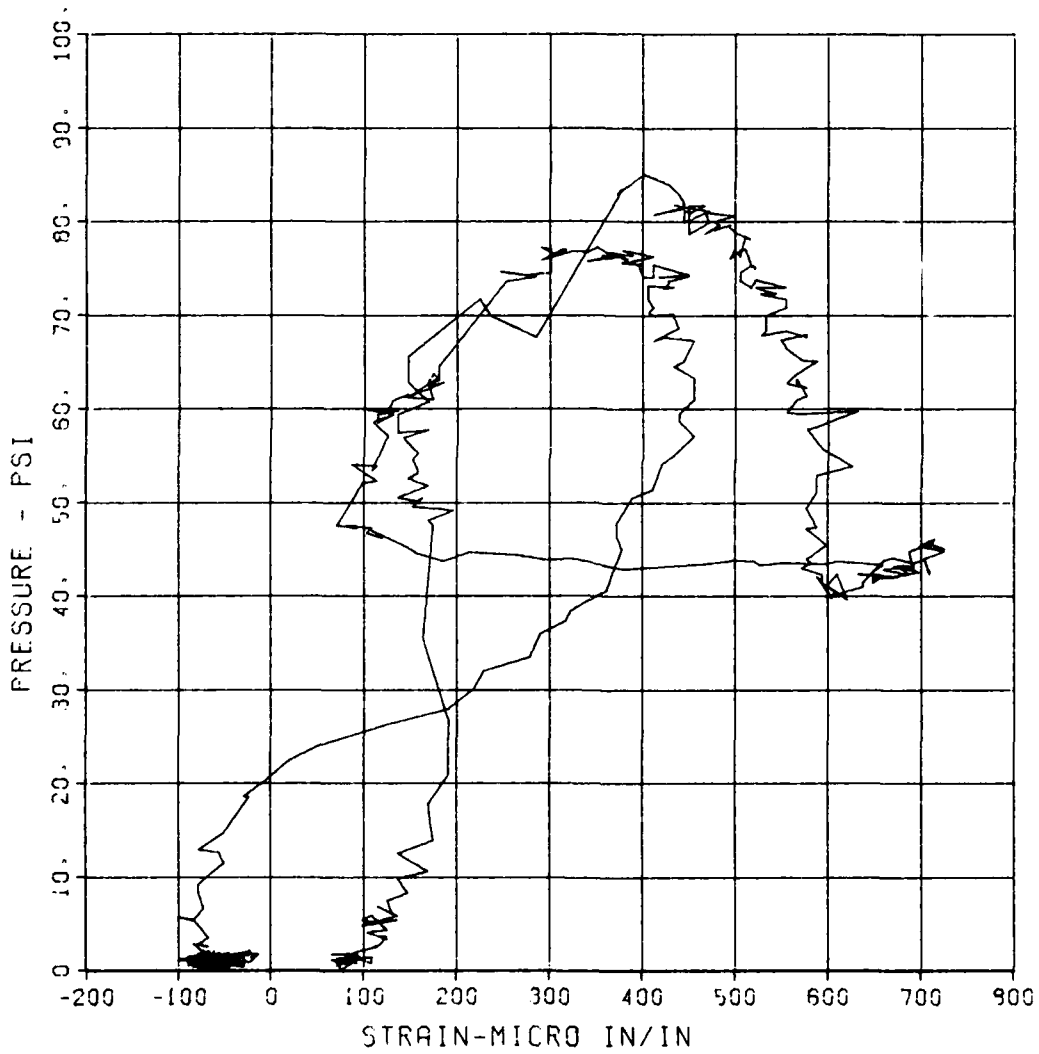
MAXIMUM
725.7725

SIGMA CAL
2.7764

CAL_VAL
5766.1

CHANNEL NO. 9 16030 1

05/03/94 R0597



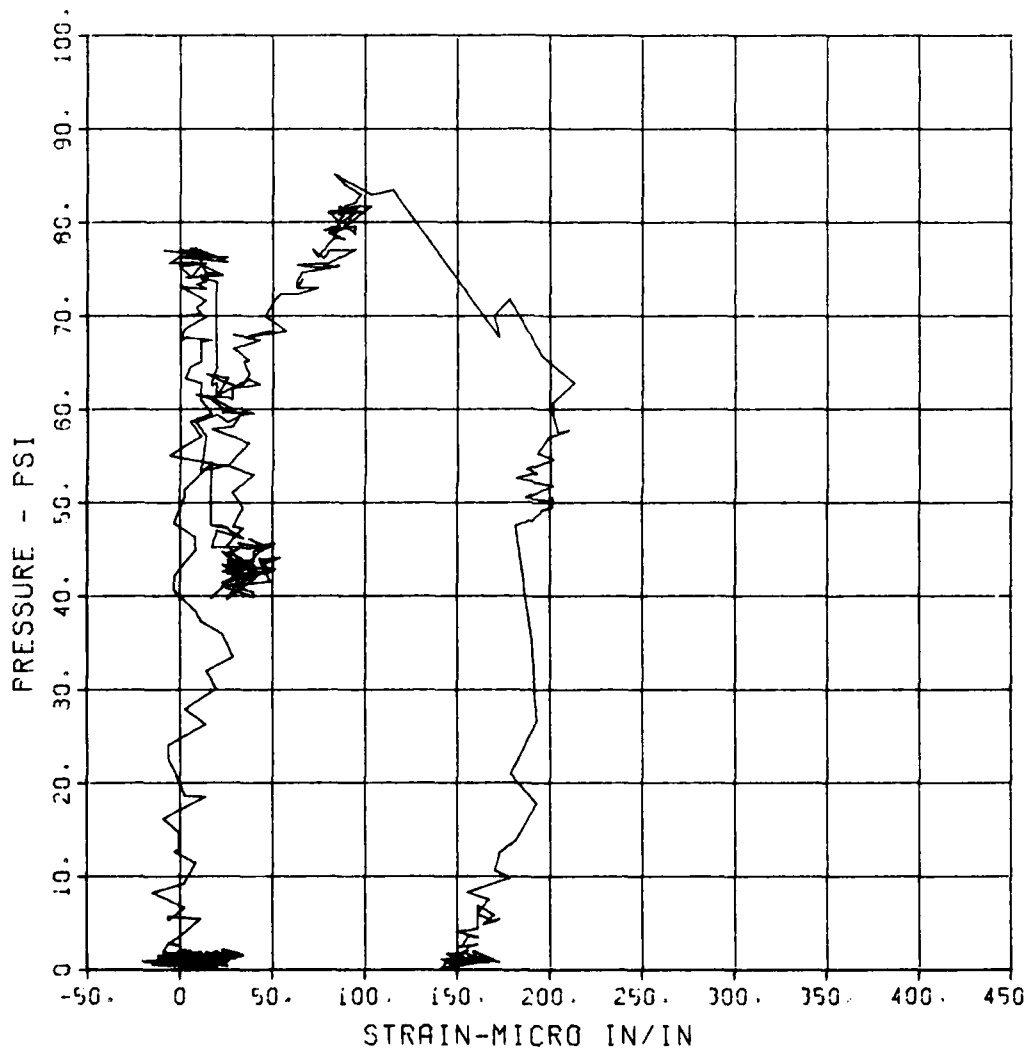
FEMA STIRRUP SLAB 10

S-4

MAXIMUM	SIGMA CAL	CAL VAL
213.1095	2.6541	2933.8

CHANNEL NO. 9 16030 1

05/03/84 R0597



APPENDIX C

NOTATION

c Neutral axis depth at the ultimate moment
 b Beam width
 d Depth from the compression face of the slab to the centroid of the tension steel (effective depth)
 d_b Diameter of reinforcement bar
 E Modulus of elasticity
 f'_c Compressive strength of concrete
 f_y Yield strength of steel
 f'_y Yield strength of compression steel
 l_p Equivalent plastic hinge length
 L Clear span length
 M Posttest measured deflection
 M_m Moment capacity at midspan
 M_s Moment capacity at the support
 P Applied overpressure
 q Reinforcing index
 R Electronically recorded maximum deflection
 t Slab thickness
 T Yield force of reinforcement per unit width
 W Uniform load
 Z Distance from critical section to point of contraflexure
 Δ Deflection at midspan
 ϵ_c Concrete strain
 θ_p Plastic hinge rotation to one side of the critical section
 ν Poisson's ratio
 ρ Tension steel ratio
 ρ' Compression steel ratio
 ρ_b Balanced reinforcement ratio
 ρ_s Ratio of volume of confining steel to volume of concrete core
 ϕ_u Ultimate curvature of the section
 ϕ_y Yield curvature of the section

DISTRIBUTION LIST

Director, Federal Emergency Management Agency
ATTN: Mr. Tom Provenzano (25 cys)
500 C St. SW
Washington, DC 20472

Commander, US Army Engineer District, Wilmington
ATTN: Pat Burns/Library
PO Box 1890
Wilmington, N. C. 28402

Headquarters, Department of Energy
ATTN: Library/G-049 MA-232.2/GTN
Washington, DC 20545

National Bureau of Standards
ATTN: Mr. Samuel Kramer
Dr. Lewis V. Spencer
Washington, DC 20234

Associate Director, Natural Resources and
Commercial Services
Office of Science & Technology
ATTN: Mr. Phillip M. Smith
Executive Office Building
Washington, DC 20500

Director, Office of Administration
Program Planning and Control
Department of Housing and Urban Development
ATTN: Mr. Bert Greenglass
Washington, DC 20410

Director, Defense Nuclear Agency
ATTN: SPTD/Mr. Tom Kennedy
STTL/Technical Library
Washington, DC 20305

Director, Defense Intelligence Agency
ATTN: Mr. Carl Wiehle (DB-4C2)
Washington, DC 20301

Assistant Secretary of the Army (R&D)
ATTN: Assistant for Research
Washington, DC 20301

Office, Chief of Engineers,
Department of the Army
ATTN: DAEN-RDZ-A
DAEN-ECE-D
Washington, DC 20314

Sandia Corporation
ATTN: Dr. Clarence R. Mehl
Dept. 5230
Box 5800, Sandia Base
Albuquerque, N. Mex. 87115

Director, US Army Engineer Waterways
Experiment Station
ATTN: Dr. S. A. Kiger
Mr. Bill Huff
Mr. Stan Woodson
3 cys
Library
P. O. Box 631
Vicksburg, Miss. 39180

Defense Technical Information Center
12 cy ATTN: (DTIC-DBAB/Mr. Myer H. Kahn)
Cameron Station
Alexandria, Va. 22314

Commander, US Army Materials and Mechanics
Research Center
ATTN: Technical Library
Watertown, Mass. 02172

Command and Control Technical Center
Department of Defense
Room 2E312 Pentagon
Washington, DC 20301

Los Alamos Scientific Laboratory
ATTN: Report Library MS-364
PO Box 1663
Los Alamos, N. Mex. 87544

Director, Ballistic Research Laboratory
ATTN: (DRXBR-TBD/Mr. George Coulter)
Aberdeen Proving Ground, Md. 21005

Commanding Officer, Office of Naval Research
Department of the Navy
Washington, DC 20390

Commanding Officer
US Naval Civil Engineering Laboratory
Naval Construction Battalion Center
ATTN: Library (Code LO8A)
Port Hueneme, Calif. 93043

Commander, Air Force Weapons Laboratory/SML
ATTN: Technical Library
Kirtland Air Force Base, N. Mex. 87117

Civil Engineering Center
AF/PRECET
Tyndall AFB, Fla. 32403

University of Florida
Civil Defense Technical Services
College of Engineering
Department of Engineering
Gainesville, Fla. 32601

Technical Reports Library
Kurt F. Wendt Library
College of Engineering
University of Wisconsin
Madison, Wisc. 53706

Agabian Associates
250 N. Nash Street
El Segundo, Calif. 90245

AT&T Bell Laboratories
ATTN: Mr. E. Witt
Whippany, N. J. 07081

James F. Beck & Associates
4216 Los Palos Avenue
Palo Alto, Calif. 94306

Chamberlain Manufacturing Corp.
GARD, Inc.
7449 N. Natchez Avenue
Niles, Ill. 60648

ITT Research Institute
ATTN: Mr. A. Longinow
10 West 35th Street
Chicago, Ill. 60616

H. L. Murphy Associates
Box 1727
San Mateo, Calif. 94401

HANI Corporation
ATTN: Document Library
1700 Main Street
Santa Monica, Calif. 90401

Research Triangle Institute
ATTN: Mr. Edward L. Hill
PO Box 12194
Research Triangle Park, N. C. 27709

Scientific Services, Inc.
517 East Bayshore Drive
Redwood City, Calif. 94060

US Army Engineer Division, Huntsville
ATTN: Mr. Paul Lahoud (10 cys)
PO Box 1600, West Station
Huntsville, AL 35807

EFFECTS OF SHEAR STIRRUP DETAILS ON ULTIMATE CAPACITY AND TENSILE MEMBRANE BEHAVIOR OF REINFORCED CONCRETE SLABS, Unclassified, US Army Engineer Waterways Experiment Station, August 1985, 177 pp.

At the time this study was initiated, civil defense planning in the United States called for the evacuation of nonessential personnel to safe host areas when a nuclear attack is probable, requiring the construction of blast shelters to protect the keyworkers remaining in the risk areas. The placement of shear stirrups in the one-way reinforced concrete roof slabs of the shelters will contribute significantly to project costs. Ten one-way reinforced concrete slabs were statically and uniformly loaded with water pressure, primarily to investigate the effect of stirrups and stirrup details on the load-response behavior of the slabs. The slabs had clear spans of 24.0 inches, span to effective depth ratios of 12.4, tensile reinforcement of 0.75 percent, and concrete strengths of approximately 5,000 psi.

The test series significantly increased the data base for uniformly loaded one-way slabs. Support rotations between 13.1 and 20.6 degrees were observed. A more ductile behavior was observed in slabs with construction details, implying better concrete confinement due to more confining steel (i.e., closely spaced stirrups, double-leg stirrups, and closely spaced principal reinforcing bars). The parameters investigated did not appear to have a significant effect on ultimate load capacity.

In the case of the Keyworker Shelter, the test series resulted in the recommendation of construction details which reduce construction costs to a level less than the preliminary shelter design.

EFFECTS OF SHEAR STIRRUP DETAILS ON ULTIMATE CAPACITY AND TENSILE MEMBRANE BEHAVIOR OF REINFORCED CONCRETE SLABS, Unclassified, US Army Engineer Waterways Experiment Station, August 1985, 177 pp.

At the time this study was initiated, civil defense planning in the United States called for the evacuation of nonessential personnel to safe host areas when a nuclear attack is probable, requiring the construction of blast shelters to protect the keyworkers remaining in the risk areas. The placement of shear stirrups in the one-way reinforced concrete roof slabs of the shelters will contribute significantly to project costs. Ten one-way reinforced concrete slabs were statically and uniformly loaded with water pressure, primarily to investigate the effect of stirrups and stirrup details on the load-response behavior of the slabs. The slabs had clear spans of 24.0 inches, span to effective depth ratios of 12.4, tensile reinforcement of 0.75 percent, and concrete strengths of approximately 5,000 psi.

The test series significantly increased the data base for uniformly loaded one-way slabs. Support rotations between 13.1 and 20.6 degrees were observed. A more ductile behavior was observed in slabs with construction details, implying better concrete confinement due to more confining steel (i.e., closely spaced stirrups, double-leg stirrups, and closely spaced principal reinforcing bars). The parameters investigated did not appear to have a significant effect on ultimate load capacity.

In the case of the Keyworker Shelter, the test series resulted in the recommendation of construction details which reduce construction costs to a level less than the preliminary shelter design.

EFFECTS OF SHEAR STIRRUP DETAILS ON ULTIMATE CAPACITY AND TENSILE MEMBRANE BEHAVIOR OF REINFORCED CONCRETE SLABS, Unclassified, US Army Engineer Waterways Experiment Station, August 1985, 177 pp.

At the time this study was initiated, civil defense planning in the United States called for the evacuation of nonessential personnel to safe host areas when a nuclear attack is probable, requiring the construction of blast shelters to protect the keyworkers remaining in the risk areas. The placement of shear stirrups in the one-way reinforced concrete roof slabs of the shelters will contribute significantly to project costs. Ten one-way reinforced concrete slabs were statically and uniformly loaded with water pressure, primarily to investigate the effect of stirrups and stirrup details on the load-response behavior of the slabs. The slabs had clear spans of 24.0 inches, span to effective depth ratios of 12.4, tensile reinforcement of 0.75 percent, and concrete strengths of approximately 5,000 psi.

The test series significantly increased the data base for uniformly loaded one-way slabs. Support rotations between 13.1 and 20.6 degrees were observed. A more ductile behavior was observed in slabs with construction details, implying better concrete confinement due to more confining steel (i.e., closely spaced stirrups, double-leg stirrups, and closely spaced principal reinforcing bars). The parameters investigated did not appear to have a significant effect on ultimate load capacity.

In the case of the Keyworker Shelter, the test series resulted in the recommendation of construction details which reduce construction costs to a level less than the preliminary shelter design.

EFFECTS OF SHEAR STIRRUP DETAILS ON ULTIMATE CAPACITY AND TENSILE MEMBRANE BEHAVIOR OF REINFORCED CONCRETE SLABS, Unclassified, US Army Engineer Waterways Experiment Station, August 1985, 177 pp.

At the time this study was initiated, civil defense planning in the United States called for the evacuation of nonessential personnel to safe host areas when a nuclear attack is probable, requiring the construction of blast shelters to protect the keyworkers remaining in the risk areas. The placement of shear stirrups in the one-way reinforced concrete roof slabs of the shelters will contribute significantly to project costs. Ten one-way reinforced concrete slabs were statically and uniformly loaded with water pressure, primarily to investigate the effect of stirrups and stirrup details on the load-response behavior of the slabs. The slabs had clear spans of 24.0 inches, span to effective depth ratios of 12.4, tensile reinforcement of 0.75 percent, and concrete strengths of approximately 5,000 psi.

The test series significantly increased the data base for uniformly loaded one-way slabs. Support rotations between 13.1 and 20.6 degrees were observed. A more ductile behavior was observed in slabs with construction details, implying better concrete confinement due to more confining steel (i.e., closely spaced stirrups, double-leg stirrups, and closely spaced principal reinforcing bars). The parameters investigated did not appear to have a significant effect on ultimate load capacity.

In the case of the Keyworker Shelter, the test series resulted in the recommendation of construction details which reduce construction costs to a level less than the preliminary shelter design.